



Miscellaneous Paper CERC-94-1
January 1994

AD-A277 170

2

Revere Beach and Point of Pines, Massachusetts, Shore Front Study

*by W. Gray Smith, Julie D. Rosati, Stephen A. Bratos, John McCormick
Coastal Engineering Research Center*

DTIC
ELECTE
MAR 22 1994
S B D

№	Наименование	Единица измерения	Количество	Стоимость, руб.	Средняя стоимость, руб.
1	Материалы	кг	100	10000	100
2	Работы	шт	10	10000	1000
3	Услуги	шт	10	10000	1000
4	Транспорт	шт	10	10000	1000
5	Прочие	шт	10	10000	1000
6	Итого				
7	Материалы	кг	100	10000	100
8	Работы	шт	10	10000	1000
9	Услуги	шт	10	10000	1000
10	Транспорт	шт	10	10000	1000
11	Прочие	шт	10	10000	1000
12	Итого				
13	Материалы	кг	100	10000	100
14	Работы	шт	10	10000	1000
15	Услуги	шт	10	10000	1000
16	Транспорт	шт	10	10000	1000
17	Прочие	шт	10	10000	1000
18	Итого				
19	Материалы	кг	100	10000	100
20	Работы	шт	10	10000	1000
21	Услуги	шт	10	10000	1000
22	Транспорт	шт	10	10000	1000
23	Прочие	шт	10	10000	1000
24	Итого				
25	Материалы	кг	100	10000	100
26	Работы	шт	10	10000	1000
27	Услуги	шт	10	10000	1000
28	Транспорт	шт	10	10000	1000
29	Прочие	шт	10	10000	1000
30	Итого				

Approved For Public Release; Distribution Is Unlimited

30728 94-08968

1970-1971

94 3 21 050

The contents of this report are not to be used for advertising, publication, or promotional purposes. Citation of trade names does not constitute an official endorsement or approval of the use of such commercial products.

Accession For	
NTIS GRA&I	<input checked="checked" type="checkbox"/>
DTIC TAB	<input type="checkbox"/>
Unannounced	<input type="checkbox"/>
Justification	
By	
Distribution	
Availability Codes	
Dist	Avail and/or Special
A-1	



PRINTED ON RECYCLED PAPER

Revere Beach and Point of Pines, Massachusetts, Shore Front Study

by W. Gray Smith, Julie D. Rosati, Stephen A. Bratos, John McCormick
Coastal Engineering Research Center

U.S. Army Corps of Engineers
Waterways Experiment Station
3909 Halls Ferry Road
Vicksburg, MS 39180-6199

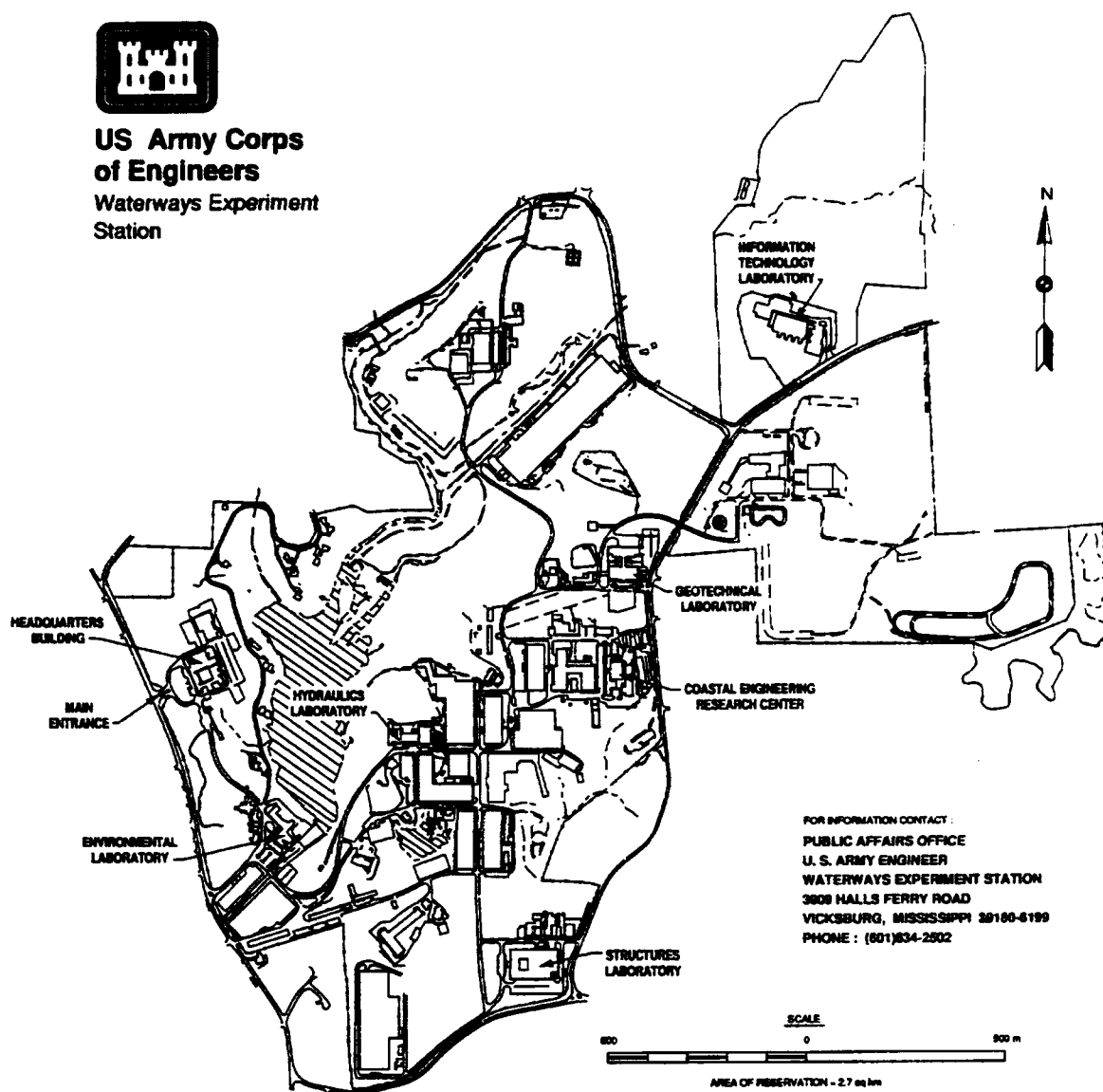
Final report

Approved for public release; distribution is unlimited

Prepared for U.S. Army Engineer Division, New England
Waltham, MA 02254-9149



**US Army Corps
of Engineers**
Waterways Experiment
Station



Waterways Experiment Station Cataloging-in-Publication Data

Revere Beach and Point of Pines, Massachusetts, shore front study /
by W. Gray Smith ... [et al.], Coastal Engineering Research Center ; pre-
pared for U.S. Army Engineer Division, New England.

306 p. : ill. ; 28 cm. -- (Miscellaneous paper ; CERC-94-1)

Includes bibliographical references.

1. Beach erosion -- Massachusetts -- Mathematical models. 2. Shore
protection -- Massachusetts -- Revere Beach. 3. Coast changes -- Mas-
sachusetts -- Mathematical models. 4. Coastal engineering -- Massa-
chusetts. I. Smith, W. Gray. II. United States. Army. Corps of
Engineers. New England Division. III. Coastal Engineering Research
Center (U.S.) IV. U.S. Army Engineer Waterways Experiment Station.
V. Series: Miscellaneous paper (U.S. Army Engineer Waterways Experi-
ment Station) ; CERC-94-1.
TA7 W34m no.CERC-94-1

Contents

Preface	xiii
Conversion Factors, Non-SI To SI Units Of Measurement	xv
Summary	xvi
1 Introduction	1
Study Area	1
Study Area History	1
Flood Protection Projects	2
CERC Project Overview	4
Objectives of Report	5
2 Nearshore Wave and Water Level Database	6
Overview	6
Description of Models	8
Methodology and Results - Part I	11
1991 Halloween Storm - Part II	27
Halloween Storm Input Data Set	39
3 Calibration and Verification of SBEACH with Halloween Storm Data ..	47
Overview	47
Halloween Storm Data Set	47
SBEACH Applications with Halloween Storm Data	55
SBEACH Sensitivity Analyses	65
Role of Longshore Processes	76
Profile Response Simulations at POP	77
4 Development of Runup and Overtopping Module	78
Overview	78

Initial ROTM Development	79
Physical Model Tests	92
5 Assessment of Storm-Induced Overtopping	101
Overview	101
Application of Runup and Overtopping Methods	101
6 Summary and Conclusions	130
References	134
Appendix A: Physical Model Testing of Overtopping	A1
Overview	A1
Facility	A2
Testing	A2
Development of Regression Equations	A8
Discussion	A10
Appendix B: Overtopping Calculations	B1
Appendix C: Revetment/Dune Overtopping Options	C1
Appendix D: Alternative Overtopping Simulations	D1
Appendix E: Overtopping Volumes at Peak Storm Conditions	E1
Appendix F: Profile Response Simulations	F1
Appendix G: Maximum Wave Parameters at the Seaward Terminus of Each Profile	G1

List of Figures

Figure 1. Location map	2
Figure 2. Location of coastal structures at Revere Beach and POP	3
Figure 3. SHALWV grid with locations of WIS stations and the NDBC buoy	12
Figure 4. Wave height comparison of SHALWV Station 2 and NDBC 44013	14

Figure 5.	REF/DIF grid with Broad Sound bathymetry	15
Figure 6.	Water level time series - November 1945 storm	18
Figure 7.	Water level time series - November 1945 storm	18
Figure 8.	Water level time series - February 1958 storm	19
Figure 9.	Water level time series - March 1958 storm	19
Figure 10.	Water level time series - January 1961 storm	20
Figure 11.	Water level time series - April 1961 storm	20
Figure 12.	Water level time series - December 1962 storm	21
Figure 13.	Water level time series - February 1964 storm	21
Figure 14.	Water level time series - February 1969 storm	22
Figure 15.	Water level time series - February 1972 storm	22
Figure 16.	Water level time series - November 1972 storm	23
Figure 17.	Water level time series - February 1978 storm	23
Figure 18.	Storm wave heights versus time, 1945-1961	24
Figure 19.	Storm wave heights versus time, 1961-1969	25
Figure 20.	Storm wave heights versus time, 1972-1978	26
Figure 21.	Contour plot of normalized wave height, $T = 8$ sec, $H = 10$ ft, Dir = 20 deg, Tide = 10 ft	28
Figure 22.	Contour plot of normalized wave height, $T = 8$ sec, $H = 10$ ft, Dir = 10 deg, Tide = 10 ft	29
Figure 23.	Contour plot of normalized wave height, $T = 8$ sec, $H = 10$ ft, Dir = 0 deg, Tide = 10 ft	30
Figure 24.	Contour plot of normalized wave height, $T = 8$ sec, $H = 10$ ft, Dir = -10 deg, Tide = 10 ft	31
Figure 25.	Contour plot of normalized wave height, $T = 8$ sec, $H = 10$ ft, Dir = -20 deg, Tide = 10 ft	32
Figure 26.	Contour plot of normalized wave height, $T = 13$ sec, $H = 10$ ft, Dir = 20 deg, Tide = 10 ft	33

Figure 27. Contour plot of normalized wave height, $T = 15$ sec, $H = 20$ ft, Dir = 0 deg, Tide = 5 ft	34
Figure 28. Contour plot of normalized wave height, $T = 15$ sec, $H = 30$ ft, Dir = 0 deg, Tide = 5 ft	35
Figure 29. Contour plot of normalized wave height, $T = 15$ sec, $H = 20$ ft, Dir = 0 deg, Tide = 15 ft	36
Figure 30. Contour plot of normalized wave height, $T = 15$ sec, $H = 30$ ft, Dir = 0 deg, Tide = 15 ft	37
Figure 31. FNOC and 3GWAM comparisons to NDBC buoy 44013	40
Figure 32. SHALWV Station 2 wave height, period, and direction	41
Figure 33. SHALWV Station 2 and NDBC buoy 44013 wave height comparison	42
Figure 34. October 1991 storm water level time series	44
Figure 35. 1991 Halloween Storm wave height versus time	45
Figure 36. 1991 Halloween Storm wave height versus time with -15-deg adjustment to incident wave angle	45
Figure 37. 1991 Halloween Storm wave height versus time with +15-deg adjustment to incident wave direction	46
Figure 38. Measured pre- and post-Halloween Storm profiles	49
Figure 39. Halloween Storm Profile 1	50
Figure 40. Halloween Storm Profile 3	50
Figure 41. Pre-Halloween Storm Profile 4	53
Figure 42. Calibration iterations for Profile 2	58
Figure 43. Calibration iterations for Profile 5	60
Figure 44. Calibration iterations for Profile 7	62
Figure 45. Predicted SBEACH results for the Halloween storm (Profile 7)	65
Figure 46. Wave angle sensitivity testing	68
Figure 47. Wave height sensitivity testing	70

Figure 48. Grain size sensitivity testing	72
Figure 49. Overtopping conditions expected at vertical seawall	81
Figure 50. Definition sketch for the hypothesis $B_{max} = \bar{q}T$	83
Figure 51. Weir flow overtopping condition	85
Figure 52. Broken waves overtopping condition	86
Figure 53. Dimensionless overtopping versus dimensionless freeboard graph	87
Figure 54. Bore runup overtopping conditions	88
Figure 55. Graphical presentation of hybrid method proposed for bore runup overtopping condition	89
Figure 56. Schematic of the ROTM	90
Figure 57. $K = 2.5 \times 10^6$ and $Eps = 0.003$ (Profile 6)	104
Figure 58. $K = 2.0 \times 10^6$ and $Eps = 0.003$ (Profile 6)	105
Figure 59. $K = 0.5 \times 10^6$ and $Eps = 0.001$ (Profile 6)	106
Figure 60. $K = 2.5 \times 10^6$ and $Eps = 0.003$ (Profile 7)	107
Figure 61. $K = 2.0 \times 10^6$ and $Eps = 0.003$ (Profile 7)	108
Figure 62. $K = 0.5 \times 10^6$ and $Eps = 0.001$ (Profile 7)	109
Figure 63. $K = 2.5 \times 10^6$ and $Eps = 0.003$ (Profile 8)	110
Figure 64. $K = 2.0 \times 10^6$ and $Eps = 0.003$ (Profile 8)	111
Figure 65. $K = 0.5 \times 10^6$ and $Eps = 0.001$ (Profile 8)	112
Figure 66. Revetment design at Profile 6	115
Figure 67. Revetment design at Profile 7	115
Figure 68. Revetment design at Profile 8	116
Figure 69. November 1945 (50- and 100-yr): Water levels and predicted overtopping rates	121
Figure 70. February 1978 (50- and 100-yr): Water levels and predicted overtopping rates	121

Figure 71. Predicted overtopping confidence intervals (Tidal Flood Zone 1)	123
Figure 72. Predicted overtopping confidence intervals (Tidal Flood Zone 2A)	123
Figure 73. Predicted overtopping confidence intervals (Tidal Flood Zone 4A)	124
Figure 74. Predicted overtopping confidence intervals (Tidal Flood Zone 5B)	124
Figure 75. Predicted overtopping confidence intervals (Tidal Flood Zone PP)	125
Figure A1. Plan and profile views of 18-in. wave flume	A12
Figure A2. Plan and profile views of 3-ft wave flume	A13
Figure A3. Great Blizzard storm profile	A14
Figure A4. Profile 2 (1978) as reproduced in physical model	A14
Figure A5. Standard Project Northeaster storm profile	A15
Figure A6. Profile 1 (November 1991) as reproduced in physical model	A15
Figure A7. Profile 3 (November 1991) as reproduced in physical model	A16
Figure A8. Profile 4 (November 1991) as reproduced in physical model	A16
Figure A9. Profile 5 (November 1991) as reproduced in physical model	A17
Figure A10. Profile 2 (November 1991) as reproduced in physical model	A17

List of Tables

Table 1. Historic and Synthetic Storms	7
Table 2. WIS Phase II Stations	13
Table 3. Wave and Water Level Database Storm Parameters	17

Table 4.	Revere Beach Profile Locations	48
Table 5.	Volumetric Profile Changes (Halloween Storm)	51
Table 6.	Error Calculations Associated with SBEACH Calibration Sequence	64
Table 7.	Sensitivity Analysis Results	67
Table 8.	Predicted Relative Longshore Transport Rates (Halloween Storm)	76
Table 9.	Site Configurations for Overtopping Calculations	80
Table 10.	Overtopping Predictions for Original ROTM	92
Table 11.	Predicted and Measured Overtopping Volumes for Great Blizzard (Original ROTM)	92
Table 12.	Physical Model Verification Input Data (Profile 2)	94
Table 13.	Worst Case/Bore Runup Physical Model Input	95
Table 14.	Storms Used in Development of Broken Wave Submodule	97
Table 15.	Broken Waves Physical Model Input (Profile 2)	98
Table 16.	Dune Optimization Results	113
Table 17.	Revetment Optimization Results	116
Table A1.	Wave Data from SBEACH and Interpolated Wave Conditions Physical Model Verification (First Test Series)	A18
Table A2.	Wave Data from SBEACH and Interpolated Wave Conditions Physical Model Verification (Second Test Series)	A19
Table A3.	Verification of Physical Model Results (Second Test Series)	A20
Table A4.	Wave Data from SBEACH and Interpolated Wave Conditions Bore Runup Study	A21
Table A5.	Representative Seawall Crest Elevations	A23
Table A6.	Physical Model Results for Bore Runup Study	A24
Table A7.	Input Conditions for Broken Waves Study	A26
Table A8.	Input Conditions for Worst-Case Study	A27

Table A9. Bore Runup Regression Input	A28
Table A10. Broken Waves and Worst-Case Regression Input	A31
Table A11. Bore Runup Parameter Ranges	A35
Table A12. Broken Wave Parameter Ranges	A35
Table A13. Worst-Case Parameter Ranges	A36
Table B1. Total Overtopping Calculations	B3
Table B2. Storm: NV45SPN	B4
Table B3. Storm: NV45500	B5
Table B4. Storm: NV45100	B6
Table B5. Storm: NV4550	B7
Table B6. Storm: NV4520	B8
Table B7. Storm: NV4510	B9
Table B8. Storm: FB5850	B10
Table B9. Storm: FB5820	B11
Table B10. Storm: FB5810	B12
Table B11. Storm: FB585	B13
Table B12. Storm: FB582	B14
Table B13. Storm: MR5850	B15
Table B14. Storm: MR5820	B16
Table B15. Storm: MR5810	B17
Table B16. Storm: MR585	B18
Table B17. Storm: MR582	B19
Table B18. Storm: JN61100	B20
Table B19. Storm: JN6150	B21
Table B20. Storm: JN6120	B22

Table B21. Storm: JN6110	B23
Table B22. Storm: JN615	B24
Table B23. Storm: JN612	B25
Table B24. Storm: AP61100	B26
Table B25. Storm: AP6150	B27
Table B26. Storm: AP6120	B28
Table B27. Storm: AP6110	B29
Table B28. Storm: DC6250	B30
Table B29. Storm: DC6220	B31
Table B30. Storm: DC6210	B32
Table B31. Storm: DC625	B33
Table B32. Storm: DC622	B34
Table B33. Storm: FB645	B35
Table B34. Storm: FB642	B36
Table B35. Storm: FB6920	B37
Table B36. Storm: FB6910	B38
Table B37. Storm: FB695	B39
Table B38. Storm: FB7250	B40
Table B39. Storm: FB7220	B41
Table B40. Storm: FB7210	B42
Table B41. Storm: NV7250	B43
Table B42. Storm: NV7220	B44
Table B43. Storm: NV7210	B45
Table B44. Storm: NV725	B46
Table B45. Storm: NV722	B47

Table B46. Storm: FB78100	B48
Table B47. Storm: FB7850	B49
Table B48. Storm: FB7820	B50
Table B49. Storm: FB7810	B51
Table B50. Storm: FB785	B52
Table B51. Storm: FB782	B53
Table C1. Dune Overtopping (23-ft Dune Crest)	C2
Table C2. Revetment Overtopping (Without Beach Fill)	C3
Table D1. Storm: Halloween, Profile Data: 30 October 1991	D2
Table D2. Storm: Halloween, Profile Data: 30 October 1991, "Relaxed" ROT M	D3
Table D3. Storm: Great Blizzard, Profile Data: 1978	D4
Table D4. Storm: Great Blizzard, Profile Data: 1978, "Relaxed" ROT M	D5
Table D5. Storm: Halloween, Profile Data: 27 November 1991	D6
Table D6. Worst-Case Simulation (Pre-Physical Model Study of Worst-Case) (1978 Profile and November 1945 SPN)	D7
Table D7. Worst-Case Simulation (Post-Physical Model Study of Worst-Case) (1978 Profile and November 1945 SPN)	D8
Table E1. Overtopping Volumes Over Peak Storm Condition (Peak Tidal Cycle) Tidal Flood Zone 1	E2
Table E2. Overtopping Volumes Over Peak Storm Condition (Peak Tidal Cycle) Tidal Flood Zone 2A	E3
Table E3. Overtopping Volumes Over Peak Storm Condition (Peak Tidal Cycle) Tidal Flood Zone 4A	E4
Table E4. Overtopping Volumes Over Peak Storm Condition (Peak Tidal Cycle) Tidal Flood Zone 4C	E5
Table E5. Overtopping Volumes Over Peak Storm Condition (Peak Tidal Cycle) Tidal Flood Zone 5B	E6

Table E6.	Overtopping Volumes Over Peak Storm Condition (Peak Tidal Cycle) Tidal Flood Zone PP	E7
Table G1.	Maximum Wave Parameters at Seaward Terminus of Each Profile	G2

Preface

The coastal processes study at Revere Beach and Point of Pines (POP), Massachusetts, reported herein was requested by the U.S. Army Engineer Division, New England (CENED), as part of the Saugus River and Tributaries Flood Damage Reduction Project. The investigation was conducted in two parts by personnel of the U.S. Army Engineer Waterways Experiment Station (WES), Coastal Engineering Research Center (CERC) during the period November 1990 to December 1991 for Part I and from December 1992 to July 1993 for Part II. Part I focused on storm-induced beach profile response at Revere Beach and POP to aid in the design of flood mitigation structures at the site. Results of Part I and availability of pre- and post-Halloween storm (October 1992) profile data prompted Part II of the study. Part II was designed to improve upon and augment information generated during Part I of the study.

This report presents work conducted during Part II of the study with pertinent information from Part I included as required for explanation of Part II tasks. Part II was designed with four components: (a) validate application of the Storm-Induced BEAch CHange (SBEACH) numerical model, which is a numerical simulation model used to evaluate beach profile change and coastal process parameters in response to varying storm conditions; (b) test sensitivity of SBEACH to variations in median grain size, wave height, and angle; (c) develop a runup and overtopping module (ROTM), which uses SBEACH output to predict overtopping volumes; and (d) predict profile response and overtopping volumes due to the nearshore wave and water level database developed in Part I. Based on interim results of Part II, a physical model study of overtopping was added to provide data with which to further refine the ROTM.

Part I of the study described was conducted by Messrs. David B. Driver and Stephen A. Bratos, Coastal Oceanography Branch (COB), and Ms. Julie D. Rosati, Coastal Processes Branch (CPB), Research Division (RD), CERC. Part II of the study was conducted by Messrs. W. Gray Smith (CPB), Stephan A. Bratos (COB) and John McCormick, Engineering Applications Unit, Engineering Development Division, and Ms. Julie D. Rosati (CPB). Mr. Donald L. Ward, Wave Research Branch, Wave Dynamics Division,

conducted the physical model testing described in Appendix A, and further documentation of this task can be found in Ward (1993). This investigation was performed under the general supervision of Dr. James R. Houston, Director, CERC; Mr. Charles C. Calhoun, Jr., Assistant Director, CERC; Mr. H. Lee Butler, Chief, RD, CERC; and Mr. Bruce A. Ebersole, Chief, CPB, CERC. Mr. Albert Lemire was the CENED Technical Monitor for this study.

Technical Monitor for Headquarters, U.S. Army Corps of Engineers was Mr. John H. Lockhart. Director of WES during this study was Dr. Robert W. Whalin. Commander was COL Bruce K. Howard, EN.

Conversion Factors, Non-SI To SI Units Of Measurement

Non-SI units of measurement used in this report can be converted to SI units as follows:

Multiply	By	To Obtain
acre-feet	1,233.489	cubic meters
cubic feet	0.02831685	cubic meters
cubic yards	0.7645549	cubic meters
degrees (angle)	0.01745329	radians
feet	0.3048	meters
inches	2.54	centimeters
knots (international)	0.5144444	meters per second
miles (U.S. nautical)	1.852	kilometers
miles (U.S. statute)	1.609347	kilometers
square feet	0.09290304	square meters
yards	0.9144	meters

Summary

The U.S. Army Engineer Division, New England (CENED) requested assistance from the U.S. Army Engineer Waterways Experiment Station, Coastal Engineering Research Center in quantifying storm-induced coastal processes, including beach erosion and overtopping along the Revere Beach and Point of Pines (POP) coastal reach. Specifically, CERC was asked by CENED to evaluate the degree of protection provided by a coarse-grained beach fill at Revere Beach, as well as to assess the benefits and optimize the design of a revetment and/or beach fill and dune system at POP. Wave and water level conditions associated with a set of 50 storms were defined using measured water level data and hindcast wave data. The cross-shore profile response model Storm-Induced BEach CHange (SBEACH) was applied to evaluate beach profile change. A runup and overtopping module was developed and revised during the course of the study, and was applied to each storm event. This summary gives a brief overview of the project.

The coastal reach from Revere Beach to POP, Massachusetts, is located approximately 6 miles northeast of Boston, and 7 miles north of the main entrance channel to Boston Harbor. The 2.8-mile reach forms a littoral cell, bounded to the southwest by Roughans Point headland, and by the Saugus River estuary to the northeast. Overall, the site behaves as a classic spit, with littoral material transported from the southwest to northeast, depositing at POP. Storms causing significant beach erosion and upland flooding in the New England area are typically "northeasters." The most severe event in recent history was the 6 and 7 February 1978 "Great Blizzard," which provided impetus for the communities to request the CENED to develop the Saugus River and Tributaries Flood Damage Reduction Plan (SRTFDRP). Included in this plan are a dike and ponding area at Revere Beach, beach/dune system and possibly revetment at POP, floodgates at the entrance to the Saugus River, and a series of walls, dikes, and revetments along Lynn Harbor. Furthermore, acquisition and management of the Saugus and Pines River tidal estuary for flood water storage was included. Goals of the project were reduction and containment of flooding at Revere Beach, reduction of dune overwash and back beach inundation of POP, prevention of storm surges and flooding up the Saugus and Pines Rivers, and reduction of wave overwash flooding Lynn.

In conjunction with the CENED, the Metropolitan District Commission (MDC) sponsored placement of approximately 600,000 cu yd of beach fill along Revere Beach. The project was intended to provide erosion protection for the existing seawalls along Revere Beach for approximately a 2-year return storm tide. Relatively coarse beach fill material (median grain size 0.49 mm) was used, which mixed with finer native materials (median grain size 0.21 mm) after placement, resulting in notable longshore sorting of grain sizes.

The CERC study has been conducted in two parts. In Part I, CERC developed a nearshore wave and water level database using hindcast wind and wave data for 11 historical northeaster storms from which a suite of 50 synthetic storms was created. SBEACH was used to assess beach response at 8 profiles in the project area as a function of these storms. Results indicated that the existing coarse-grained beach fill at Revere Beach might provide unexpected flood protection due to its greater erosive resistance relative to the native material. This conclusion was substantiated with observations of beach response and overtopping rates during the 1991 "Halloween" storm, which impacted the area from 27 October - 1 November 1991. Additionally, Part I indicated that a sand dune/berm system might provide sufficient flood protection at POP.

Results of Part I and the availability of pre- and post-Halloween storm profile data prompted Part II of the study. Part II was designed with four components: (a) validate application of SBEACH to the project site using the Halloween storm data, (b) test sensitivity of SBEACH to variations in median grain size, and wave height and angle, (c) develop a runup and overtopping module (ROTM), which uses SBEACH output to predict overtopping volumes, and (d) predict profile response and overtopping volumes due to the nearshore wave and water level database developed in Part I. Based on interim results of Part II, a physical model study of overtopping was added to provide data with which to further refine the ROTM.

Investigation of coastal processes at Revere Beach and POP has proven to be a challenging endeavor due to varying wave, beach, and structural characteristics along the project site. Longshore variations present during the Halloween storm and presumably other storms limit the applicability of SBEACH to this site. Calibration and verification of the ROTM have also been limited by available data sets. However, some model results were substantiated with field data.

Despite the complexities of coastal processes at the project site, it is anticipated that design of flood protection structures will be greatly augmented by study findings. Results have strongly indicated potential flood protection benefits associated with a coarse-grained beach fill at Revere Beach and POP. Observations of beach stability and minimal overtopping during the Halloween storm substantiate modeling results at Revere Beach. Dune optimization and

profile response simulations with the storm database along POP have indicated potential benefits of a dune system for flood protection with minor predicted erosion and overtopping levels pointing to advantages over the proposed revetment. Project observations and SBEACH predictions indicate that the existing coarse beach fill provides a high level of flood protection at Revere Beach, and is possible at POP through implementation of either a coarse-grained dune/berm system or through construction of a combination revetment and beach fill.

1 Introduction

Study Area

The coastal reach from Revere Beach to Point of Pines (POP), Massachusetts, is located approximately 6 miles¹ northeast of Boston and 7 miles north of the main entrance channel to Boston Harbor (Figure 1). The 2.8-mile reach forms a littoral cell bordered to the southwest by Roughans Point headland and by the Saugus River estuary to the northeast. Exposure to waves from the southeast via Broad Sound and partial sheltering by Nahant Peninsula to the east combine to create a general southwest-to-northeast direction of sediment transport. Wave energy tends to focus at two locations: between Revere and Beach Streets, and at Carey Circle (Figure 2). Overall, the reach behaves as a classic spit with littoral material at the southwest end of Revere Beach moving northeast to deposit at POP. Native sediments are typically a light gray fine- to medium-sized sand (median grain size 0.21 mm) with an average coarse sand and gravel content of 5 percent.

Seawalls front the majority of Revere Beach and part of POP, as shown in Figure 2. The native beach widens northeast of Carey Circle to the end of the POP residential area, which is fronted by a beach and sand dunes.

Study Area History

Boundaries for Revere Beach, the oldest public beach in the nation, were established in 1895 when the high-water beach was substantially wider than the native pre-fill beach. Gradual erosion of the beach subjected beachfront establishments to progressively more wave action and flooding; thus, seawalls were constructed in the 1920's for protection. The mean high water (mhw) line at Revere Beach varied from 0 to 200 ft from the seawall, and normal high tides approached or reached the backshore seawalls. This daily wave action and frequent overtopping resulted in deterioration of the walls. The

¹ A table of factors for converting non-SI units of measurement to SI units is presented on page xv.

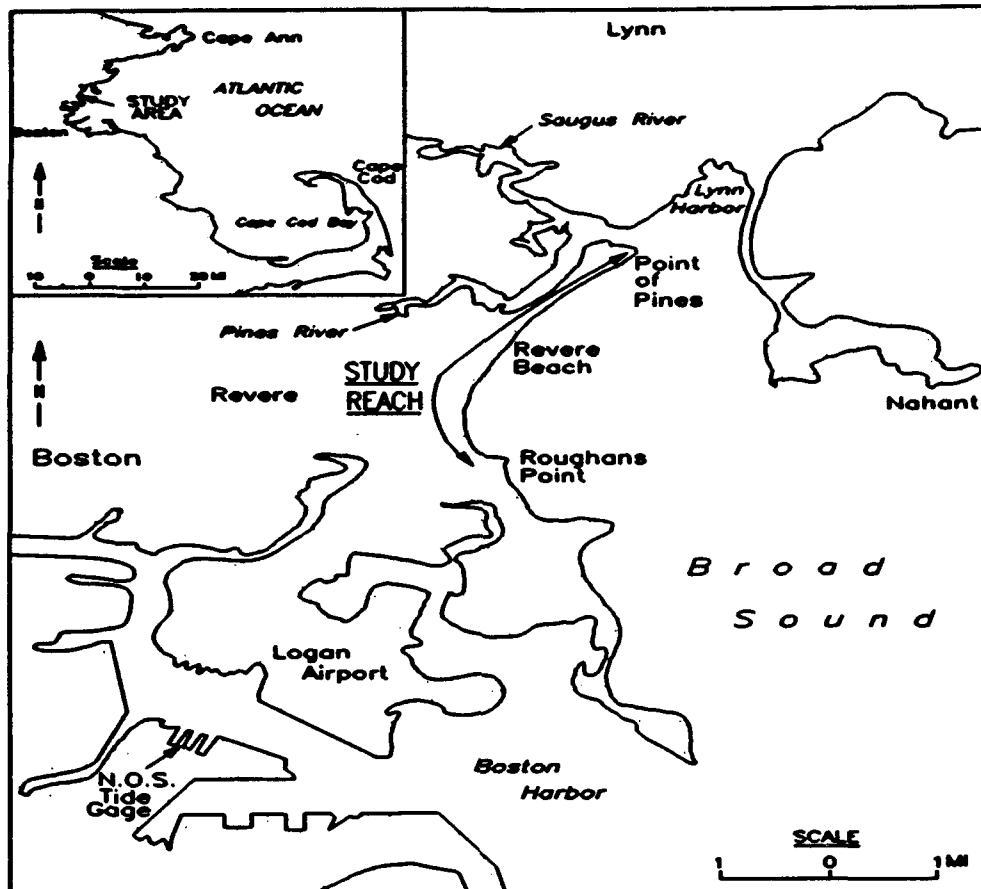


Figure 1. Location map

dunes at POP and seawalls along the rest of the reach were not sufficient to prevent severe flooding of the homes and businesses during storms.

Flood Protection Projects

Storms causing significant beach erosion and upland flooding in the New England area are typically "northeasters," occurring during winter months. The most severe storm event in recent history was the 6-7 February 1978 "Great Blizzard," which had a peak surge coinciding with a spring tide to create a 100-year water level (14.9 ft mean low water (mlw) at the National Ocean Survey (NOS) Boston Harbor gauge (see Figure 1)). This storm caused extensive flooding in the project area, damaged 25 percent of the city of Revere's homes, left 3,000 people homeless, and flooded over 3,000 buildings in the Revere, Lynn, Malden, and Saugus project area (Camp, Dresser, and McKee 1978). The Great Blizzard provided impetus for the communities to request the U.S. Army Engineer Division, New England (CENED) to develop the Saugus River and Tributaries Flood Damage Reduction Project (SRTFDRP). Included in this plan are a dike and ponding area at Revere

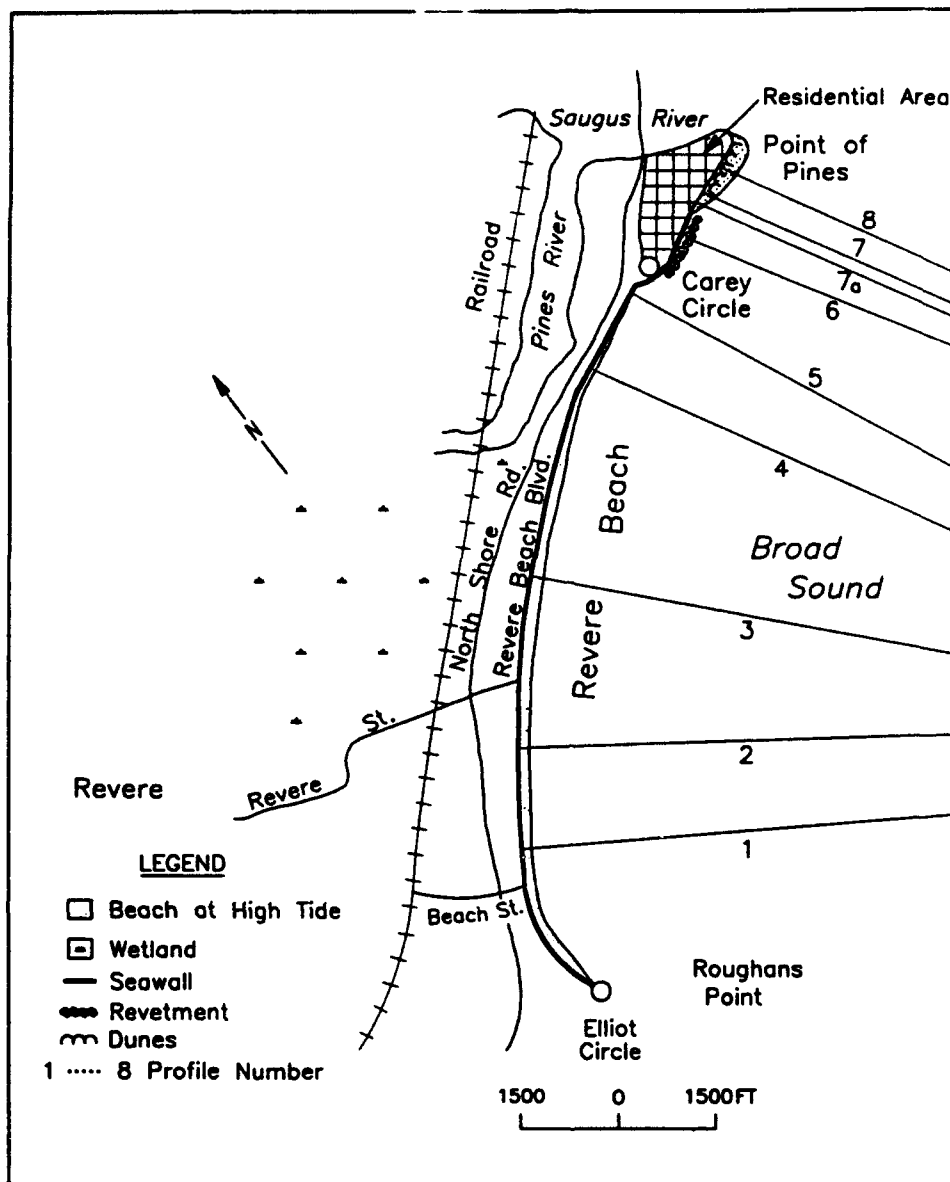


Figure 2. Location of coastal structures at Revere Beach and POP

Beach, beach/dune system and possible revetment at POP, floodgates at the Saugus River entrance, and a series of walls, dikes, and revetments along Lynn Harbor. Furthermore, acquisition and management of the Saugus and Pines River tidal estuary for flood water storage is included in the plan. Goals of the project are reduction and containment of flooding at Revere Beach, reduction of dune overwash and back beach inundation at POP, prevention of storm surges and flooding up the Saugus and Pines Rivers, and reduction of wave overwash flooding Lynn.

In conjunction with the CENED, the Metropolitan District Commission (MDC) sponsored placement of approximately 600,000 cu yd of beach fill

along Revere Beach from the fall of 1990 through the summer of 1991. The fill was designed for a 50-ft-wide beach berm at 18 ft mhw with a 1:15 seaward slope to existing grade. The beach fill was part of the Revere Beach Erosion Control Project authorized in 1970, and was separate from the proposed SRTFDRP. The project was intended to provide erosion protection for the existing seawalls along Revere Beach for approximately a 2-year return storm tide. Incidental flood protection benefits were expected, but not quantified. Relatively coarse beach fill material (median grain size 0.49 mm) was obtained from an abandoned Interstate 95 embankment. Since placement, the coarse fill has mixed with finer native materials, and experienced notable longshore sorting of grain sizes.

CERC Project Overview

In the fall of 1990, as part of the SRTFDRP, the CENED requested that the U.S. Army Engineer Waterways Experiment Station (WES), Coastal Engineering Research Center (CERC) assist in evaluating the flood protection provided to Revere Beach by the newly placed beach fill. This effort was conducted to consider the beach fill in the design of the SRTFDRP. In addition, CERC was asked to evaluate the potential protection provided to homes at POP with and without a beach fill and/or stone revetment. In this part of the project (hereafter referred to as Part I), CERC developed a nearshore wave and water level database using hindcast wind and wave data for 11 historical northeaster storms from which a suite of 50 synthetic storms was created. The Storm-Induced BEACH CHange (SBEACH) model (Larson and Kraus 1989a; Larson, Kraus, and Byrnes 1990) was used to assess beach response at eight profiles in the project area as a function of storm intensity. SBEACH simulates cross-shore (two-dimensional) beach, berm, and dune erosion due to storm waves and water levels. Longshore sediment transport along the project reach is assumed to be uniform during the storm event. SBEACH was modified for the study to allow refractive and diffractive effects of Nahant Peninsula to be included in wave transformation calculations. In the absence of calibration and verification data, typical calibration parameters were used with SBEACH for Part I. Results indicated that the existing coarse-grained Revere Beach fill might provide unexpected flood protection due to its greater erosive resistance relative to the native material. This conclusion was substantiated by observations of beach response and overtopping rates during the 1991 "Halloween" storm, which impacted the study area from 27 October - 1 November 1991. Additionally, Part I indicated that a sand dune/berm system might provide sufficient flood protection at POP, possibly resulting in significant cost savings by eliminating the proposed revetment. Part I was completed in the fall of 1991.

Results of Part I and the availability of pre- and post-Halloween storm profile data prompted Part II of the study, initiated in the winter of 1992. Part II was designed with four components:

- a. Validate application of SBEACH using the Halloween storm data.
- b. Test sensitivity of SBEACH to variations in median grain size, and wave height and angle.
- c. Develop a runup and overtopping module (ROTM), which uses SBEACH output, to predict overtopping volumes.
- d. Predict profile response and overtopping volumes due to the nearshore wave and water level database developed in Part I.

Based on interim Part II results, a fifth component was added.

- e. Physical model study of overtopping to provide data with which to further refine the ROTM.

The CENED required overtopping rates as a function of storm intensity to design the park dike, ponding area, and storage acquisition limits for the Saugus and Pines Rivers Estuary. At POP, information about the stability of various improvement designs (dunes, revetment, and dune with underlying revetment) as a function of beach grain size and storm intensity was necessary for design. Part II was completed in the spring of 1993.

Objectives of Report

The purpose of this report is to provide a concise document presenting methodologies and results of the CERC study. Information and results pertaining to Part I will be presented as relevant to final study results (e.g., development of the nearshore wave and water level database); however, Part I results that have been superseded by Part II calculations (e.g., cross-shore beach response modeling in the absence of calibration/verification data) will not be detailed.

The report is organized into six main chapters, and six appendices. Chapter 2 discusses development of the nearshore wave and water level database in Part I of the study, and hindcast of the 1991 Halloween storm (Part II). Storm-induced beach erosion modeling is presented in Chapter 3, and Chapter 4 discusses development of the ROTM. Chapter 5 assesses results of the storm-induced overtopping results, and Chapter 6 summarizes the study and presents major findings. Appendix A is included to detail the methodology in the physical model tests of overtopping. Appendices B-F contain results of overtopping predictions and profile response simulations.

2 Nearshore Wave and Water Level Database

Chapter 2 describes the procedures and results of the nearshore wave and water level database task of this study. Included is an overview presenting the scope of this task, a general description of the Massachusetts Bay and Broad Sound wave climate, a review of available information, and a brief description of the numerical wave models used in this task. The process used to develop the nearshore wave and water level database is followed by a discussion of the results of the wave and storm simulations.

Overview

The purpose of this task was to develop nearshore wave and water level conditions representing significant storms within the Wave Information Study (WIS) 20-year hindcast period as well as two storms of record outside the WIS hindcast. Eleven historical storms were selected from a set developed by Hardy and Crawford (1986) which includes nine storms within the WIS hindcast and two other storms, occurring on 30 November 1945 and 6-7 February 1978. Table 1 lists the eleven historical storms used in this part of the study. The synthetic storms, derived using the historical storms, listed in this table are discussed in detail in later sections of this chapter. These storm conditions provided input to the beach erosion model SBEACH. Another objective of this task was to develop a nearshore wave database representing wave conditions in Broad Sound for the entire 20-year WIS hindcasting period. A wave hindcast was also performed for the 1991 Halloween storm and is described in the section "1991 Halloween Storm - Part II."

The principal cause of waves and storm surge in Broad Sound and at Revere Beach is extratropical storms known as "northeasters." These storms usually travel northeast along the Atlantic coast and produce highest winds from between east and north. As northeasters pass Cape Cod, fetch lengths over the Atlantic Ocean and Massachusetts Bay of as much as 200 n.m. may exist. This fetch, when combined with a duration of 54 hr and the 50-knot

Table 1
Historic and Synthetic Storms

Historical Storm Date	Synthetic Storm Return Period (yr)	Historical Storm Date	Synthetic Storm Return Period (yr)
30 November 1945	SPN,500,100,50,20,10	19 February 1964	5,2
16 February 1958	50,20,10,5,2	9 February 1969	20,10,5
20 March 1958	50,20,10,5,2	18 February 1972	50,20,10
2 January 1961	100,50,20,10,5,2	8 November 1972	50,20,10,5,2
12 April 1961	100,50,20,10	6 February 1978	100,50,20,10,5,2
5 December 1962	50,20,10,5,2		

maximum wind speed associated with the 6-7 February 1978 storm (100-year event), caused wave heights in excess of 20 ft just outside Broad Sound. Waves entering Broad Sound encounter Nahant Peninsula, which shelters the northern reach of Revere Beach and POP. Sheltering by Nahant significantly reduces wave heights along Revere Beach from southwest to northeast. Wave propagation within Broad Sound is characterized by complex refraction and diffraction processes due to Nahant, the Winthrop Heights headland, and irregular bathymetry.

A few studies concerning the wave climate in Massachusetts Bay and Broad Sound have been published. The Raytheon Company (1974) published a report for the Massachusetts Port Authority, which includes wave statistics developed from 6 years of shipboard observations and U.S. Air Force (USAF) wind data for Massachusetts Bay. Also included in the report are wave measurements taken during a 2-week period in March and April 1974 in Massachusetts Bay at latitude 42°26' and longitude 70°43'. The maximum hourly significant wave height was 8.9 ft. With only 308 measurements, this is a limited data set, which also lacks information about wave direction.

Bohlen (1978) presents a set of refraction diagrams for Massachusetts Bay and Broad Sound using characteristic wave periods of 6 and 12 sec, several directions from offshore, and various water levels.

The best available data source for Massachusetts Bay is the deepwater buoys operated by the National Oceanic and Atmospheric Administration's National Data Buoy Center (NDBC). Climatological information in the Massachusetts Bay is available from two buoys, stations 44005 and 44013 (Gilhousen et al. 1986). Hourly measurements include wind speed and direction, and wave height and period from 1978 to 1988 and 1984 to 1988 for stations 44005 and 44013, respectively. The actual period in which

complete wave data are available for 44013 is less than the reported period. These wave measurements also lack wave direction information.

The WIS hindcast for the Atlantic Coast Phase II includes five stations in the Massachusetts Bay area (Corson et al. 1982). The 20-year hindcast provides wave height, period and direction, and wind speed and direction at 3-hr intervals.

The WIS Phase III hindcast for the Atlantic Coast includes a station near Nahant Peninsula (Jensen 1983). Phase III wave data were generated by transforming Phase II wave data into shallow water. In generating Phase III data, straight and parallel contours were assumed and no additional energy sources, such as winds, were added to the existing Phase II wave conditions.

Because the 1945 and 1978 storm events are outside the WIS 20-year hindcast, data for these storms were taken from another source. The 1945 storm was part of a 1981 analysis of six extratropical storms, along the eastern U.S. coast, performed by Oceanweather Inc. for WIS. The analysis involved construction of pressure fields from ship observations, buoy data, and historical weather maps. The wind fields were produced from the pressure fields using a boundary layer model and were corrected based on manual kinematic analysis of the critical area of the storm wind field. The wind fields were produced for a domain ranging from approximately latitude 25-50° N and longitude 50-80° W and lasted the duration of the storm with data at 6-hr intervals. A similar wind field analysis was performed as part of this study for the 1978 storm because of its significance (100-year return period) and the lack of adequate data. The standard deepwater wave hindcasting model WISWAVE was used with these wind fields to generate wind and wave data at the Phase II stations used in this study.

The wind and wave information at the Phase II stations was used to drive the SHALlow Water WaVe Model (SHALWV) in the Massachusetts Bay area. SHALWV output wave information near the tip of Nahant Peninsula was then used as input to the nearshore Refraction/Diffraction model REF/DIF. No measured wave data from Broad Sound are available. Therefore, the nearshore wave propagation and transformation model, REF/DIF, could not be calibrated or verified.

Description of Models

SHALWV

The numerical wave hindcasting model SHALWV was used to produce wave data in Massachusetts Bay and the surrounding area. SHALWV

numerically simulates growth, decay, propagation, shoaling, refraction, and sheltering of a directional wave spectrum over arbitrary bathymetry. The spectrum is represented two-dimensionally in discrete frequency and direction bands. The model is time dependent and simulates time-varying wave and wind conditions during storms such as northeasters.

The model is based on the solution of the inhomogeneous energy balance equation solved with finite difference methods using square grid cells. The field equation represents wind wave growth, refraction, shoaling, nonlinear wave-wave interactions, high frequency energy dissipation, wave bottom interactions and decomposition of the energy into wind-sea and swell wave components. The model bases time-steps on the Courant number stability criterion

$$\frac{\Delta L}{\Delta t} > C_g(f^*) \quad (1)$$

where

ΔL = length of grid cell

Δt = computational time-step

C_g = group velocity associated with lowest frequency
at the deepest grid point

f^* = lowest spectral frequency

The Courant number criterion ensures that wave energy does not propagate more than one grid cell during a time-step.

REF/DIF

Originally the time-independent spectral model STWAVE (Steady State WAVE Model) was proposed to simulate nearshore wave transformation in Broad Sound. Since STWAVE does not have the capability to diffract waves around features such as Nahant Peninsula, and given that this feature significantly influences the wave energy along Revere Beach and Point of Pines, it was necessary to select a different model. The numerical model REF/DIF was selected to transform waves within the Broad Sound area. REF/DIF is a combined refraction/diffraction model based on Kirby and Dalrymple's (1983) parabolic approximation for Berkhoff's (1972) mild slope equation, where reflected waves are neglected. The model is valid for waves propagating within 60 deg of the input direction. The mild slope equation, in terms of the horizontal gradient operator, is given by

$$\nabla \cdot CC_g \nabla A + \sigma^2 \frac{C_g}{C} A = 0 \quad (2)$$

where

C = wave celerity

C_g = group velocity

σ = angular frequency ($2\pi/T$ where T = period)

A = wave amplitude

and the linear dispersion relationship is $\sigma^2 = gk \tanh(kh)$ where g is the gravitational constant, k is the wave number ($2\pi/L$ where L = wave length), and h is the water depth.

The model is based on Stokes perturbation expansion. In order to have a model that is valid in shallow water outside the Stokes range of validity, a dispersion relationship that accounts for the nonlinear effects of amplitude is provided. This relationship, developed by Hedges (1976), is

$$\sigma^2 = gk \tanh(kh(1 + |A|/h)) \quad (3)$$

The Hedges form is fit with the Stokes relationship to form a model valid in shallow and deep water. The model can be operated in three different modes: (a) linear, (b) Stokes-to-Hedges nonlinear model, and (c) Stokes weakly nonlinear.

Broken wave propagation is based on Kirby and Dalrymple's (1986) implementation of the dissipation scheme proposed by Dally, Dean, and Dalrymple (1985a,b) given by

$$\omega = \frac{KC_g(1 - (\gamma h/H)^2)}{h} \quad (4)$$

where ω is the dissipation factor, K and γ are empirical constants, determined to be 0.15 and 0.4, respectively, by Dally, Dean, and Dalrymple (1985a,b), and H and h are the wave height and water depth, respectively. Wave breaking is initiated using the breaking index $H > 0.78h$. Once the wave height exceeds $0.78h$, the wave breaking scheme is used.

Land boundaries such as coastlines and islands are modeled using the thin film approximation where surface piercing features are replaced by shoals with very shallow depth (less than 0.1 depth units). Kirby and Dalrymple

(1986) and Dalrymple, Kirby, and Hwang (1984) describe applications of REF/DIF.

A disadvantage in using REF/DIF over STWAVE is that REF/DIF is a monochromatic wave model. It is possible to represent spectral wave information by superposition of linear monochromatic waves but this requires many model runs to represent the frequency and direction bands and therefore is labor intensive. For waves generated by storms which are removed from the Massachusetts Bay area, the directional spread becomes more narrow. This is generally referred to as swell. When swell exists, the locally generated sea can be considered relatively negligible.

Methodology and Results - Part I

Offshore hindcast

As mentioned in the overview, the purpose of this task was to develop nearshore wave conditions along Revere Beach and Point of Pines for significant storm events as well as for the entire WIS 20-year hindcast period, 1956 to 1975. Because no long-term wave measurements are available for Massachusetts Bay, the WIS Phase II wave data and hindcast techniques were used to generate wave conditions for input into the nearshore model REF/DIF. Two storms selected for this study, which occurred in November 1945 and February 1978, were outside the WIS 20-year hindcast period (1956-1975). For these two storms, it was necessary to generate Phase II wind and wave data using WIS Phase I to Phase II analysis.

WIS Phase II wind and wave time series data for the time period 1956 to 1975, and including the two storms in 1945 and 1978, were input into the wave hindcasting model SHALWV to produce wave information near the existing Phase III station. This represents an improvement in modeling technique since, in contrast to the existing Phase III station data, wind energy was input to the model and actual bathymetry was represented.

Wind-field input was generated from WIS Phase II stations 8, 9, 13, 16, and 17, shown in Figure 3. Table 2 shows each station's latitude, longitude, and depth. Station 16 wave data were used for the model's offshore input boundary.

A 12 x 15 grid with square cells of 10 n.m. on each side was chosen to resolve the bathymetry of Massachusetts Bay and the sheltering effects created by the irregular coastline. Figure 3 shows the orientation of the grid with the study site. For this application the directional wave spectrum was divided into 20 frequency and 16 direction bands.

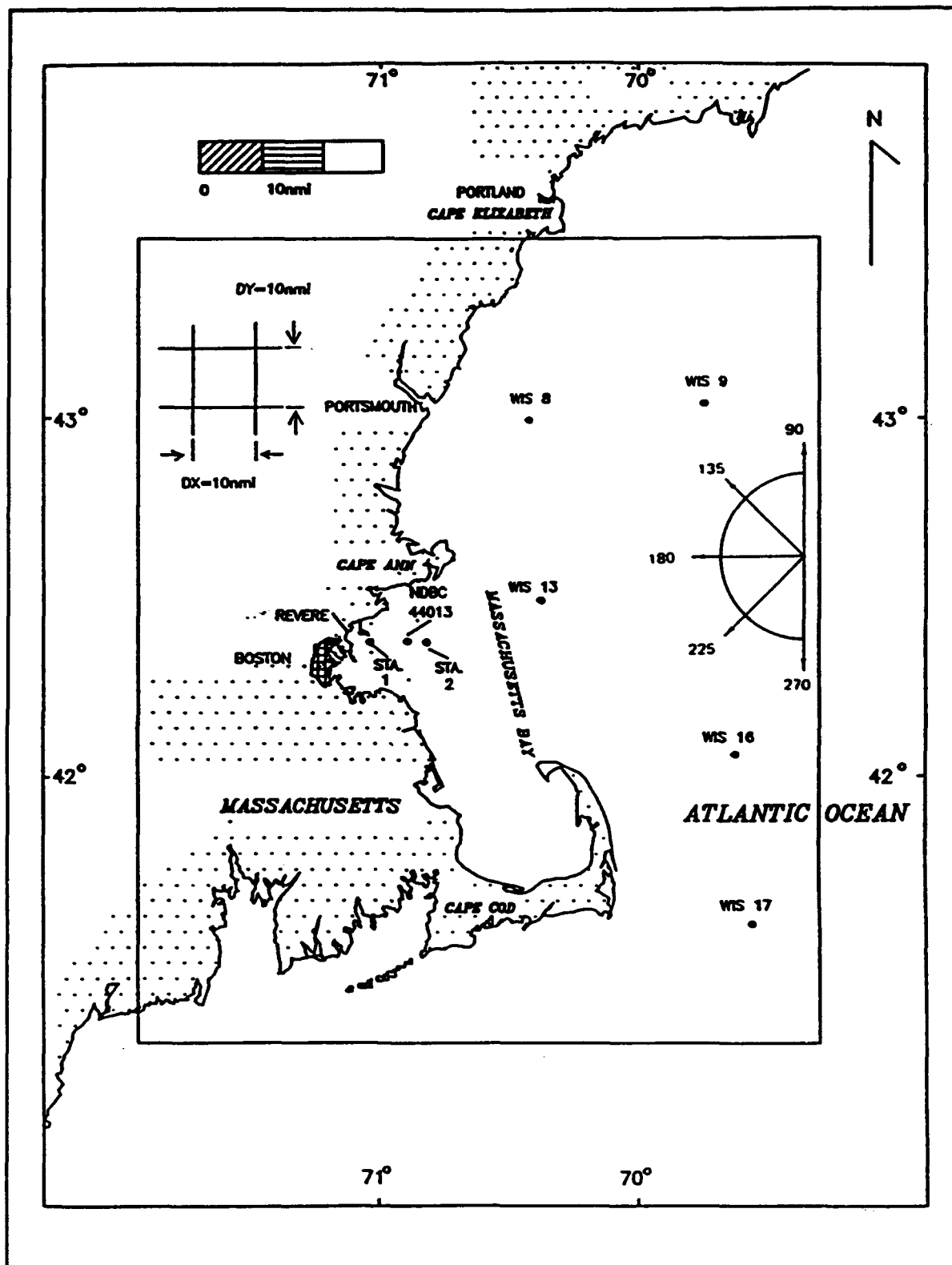


Figure 3. SHALWV grid with locations of WIS stations and the NDBC buoy

Table 2 WIS Phase II Stations			
Station Number	Latitude	Longitude	Depth (meters)
8	43.03 N	70.31 W	92
9	43.09 N	69.63 W	110
13	42.54 N	70.23 W	128
16	42.11 N	69.48 W	220
17	41.61 N	69.40 W	37

Figure 4 shows a comparison of wave heights between SHALWV Station 2 and NDBC 44013, in water depths of 138 and 100 ft, respectively. The buoy and station are separated by approximately 3 n.m. The station observations (58435) are at 3-hr intervals while the buoy has hourly observations (26106). The buoy represents less than 3 years of measured data and the station represents 20 years of hindcast data. In order to compare the model results to the buoy measurements, a wave height distribution plot is presented in Figure 4. The horizontal axis represents the percent occurrence of each wave height interval, defined on the vertical axis, based on the total number of observations for each data set. For example, approximately 46 percent of the 26106 wave heights measured by the buoy were less than 1.5 ft. The buoy measured a higher percentage of waves between 1.5 and 2.9 ft and less than 1.5-ft height intervals than the numerical model generated. For height intervals 3 ft and above, the buoy measured a lower percentage of waves than the model generated. This indicates that the wave conditions during the measurement period may have been somewhat milder than during the 20-year hindcast period.

Nearshore wave analysis

The wave model REF/DIF was used to generate wave information in Broad Sound for both the significant storm events as well as the 20-year hindcast. A 165 X 176 grid with square cells of 200 ft on each side was chosen in order to resolve bathymetric features in Broad Sound. Figure 5 shows the REF/DIF grid and the bathymetry of Broad Sound. The input boundary for this grid is along the y-axis. The x-axis is directed due west and the y-axis points due south. North is toward the bottom of the page in the negative y-direction.

The grid covers an area much larger than the study area in order to ensure that diffractive and sheltering effects due to Nahant Peninsula are adequately modeled, as well as to move any side boundary effects out of the study area.

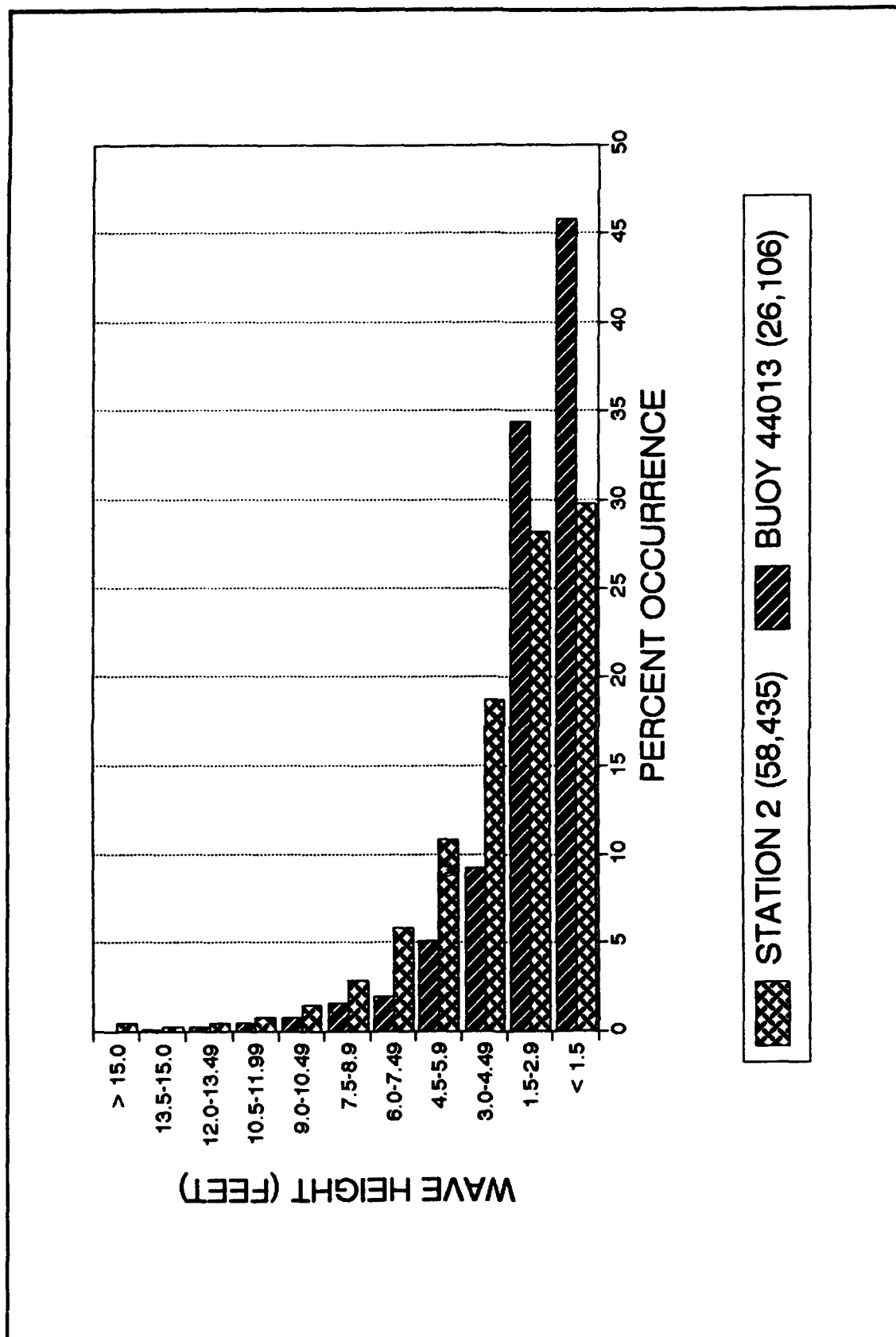


Figure 4. Wave height comparison of SHALWV Station 2 and NDBC 44013

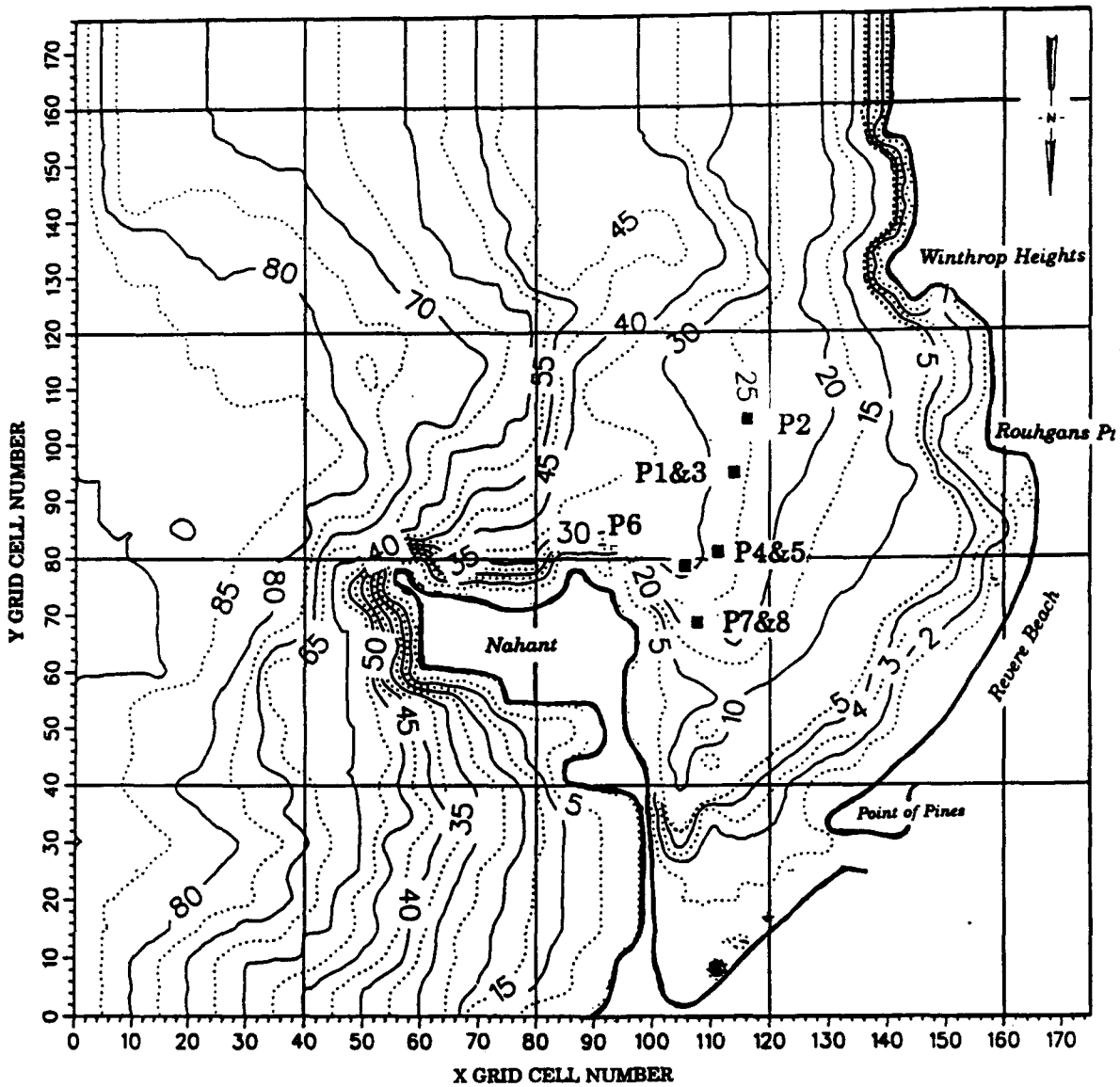


Figure 5. REF/DIF grid with Broad Sound bathymetry (depth in ft, mlw)

For some wave conditions the southern side boundary of the model caused an increase in wave heights due to inaccuracies in the lateral boundary conditions. In order to remove this boundary effect from the area of interest, the last 17 columns (161 to 176) along the y-axis were added. The depths for column 160 are repeated in columns 161 to 176 and do not represent the actual bathymetry.

Storm events were simulated using actual wave conditions (height, period, and direction) and water levels. The spectral significant wave height H_{ms} was used as the monochromatic wave height and the peak spectral wave period T_p was the representative wave period for REF/DIF simulations. REF/DIF was used in the Stokes to Hedges nonlinear mode in order to better represent the nonlinearities present in long period storm waves in Broad Sound. In order to represent a range of return periods (2, 5, 10, 20, 50, 100, and 500 years), synthetic storms were produced from each historic storm by adjusting the phasing of the tidal time series and storm surge records to obtain various maximum water levels for each historical storm. A Standard Project Northeaster (SPN) was created with the November 1945 storm by adding an extra 1 ft of surge throughout the storm. Table 3 shows the maximum water level for each event modeled. The relationship between the water level and return period was taken from the stage-frequency curves for Point of Pines and Revere Beach presented by Hardy and Crawford (1986). The return periods associated with these storms are based on total water level only. Table 1 shows each historical storm date and the return periods of each synthetic storm. One exception to the synthetic events is the 100-year storm for the February 1978 historical storm. This storm was modeled with actual tide conditions and represents the actual storm. Water level time series for each storm event are presented in Figures 6-17.

Storm parameters for each of these synthetic storms were saved near the beginning of each SBEACH profile shown in Figure 5 as P1-P8. The number for each output point corresponds to a profile number. Figures 18-20 show plots of wave height versus time at each output point for select storms. Different return periods corresponding to a given historical storm did not produce significantly different values at the output points (P1-P8), because the variation between each synthetic storm is the water level only. The depths of the output P1-P8 range from approximately 25 to 30 ft, and this change in water level between synthetic storms is not enough to cause significant change in wave height. Since results for different return periods generated from each historical storm event are similar, only one synthetic event is plotted for each historical event. These plots show that the most severe event in terms of wave height is the November 1945 storm. The maximum wave height during this storm reached 28 ft at point P2. Also evident from these plots is the variation in maximum wave height and storm duration for different storms with the same return period. Note that the return period was defined only in terms of maximum water level.

Table 3
Wave and Water Level Database Storm Parameters

Storm	Peak Water Level (ft, MLW)	Peak Surge (ft)	Duration (hr)	Storm	Peak Water Level (ft, MLW)	Peak Surge (ft)	Duration (hr)
November 1945 SPN	16.6	5.0	72	April 1961 10-yr	13.8	4.2	51
November 1945 500-yr	15.8	5.0	72	December 1962 50-yr	14.6	3.4	66
November 1945 100-yr	14.9	5.0	72	December 1962 20-yr	14.2	3.4	66
November 1945 50-yr	14.6	5.0	72	December 1962 10-yr	13.8	3.4	66
November 1945 20-yr	14.2	5.0	72	December 1962 5-yr	13.4	3.4	66
November 1945 10-yr	13.8	5.0	72	December 1962 2-yr	12.8	3.4	66
February 1958 50-yr	14.6	3.4	21	February 1964 5-yr	13.4	2.8	45
February 1958 20-yr	14.2	3.4	21	February 1964 2-yr	12.8	2.8	45
February 1958 10-yr	13.8	3.4	21	February 1969 20-yr	14.2	3.5	36
February 1958 5-yr	13.4	3.4	21	February 1969 10-yr	13.8	3.5	36
February 1958 2-yr	12.8	3.4	21	February 1969 5-yr	13.4	3.5	36
March 1958 50-yr	14.6	3.0	45	February 1972 50-yr	14.6	4.0	59
March 1958 20-yr	14.2	3.0	45	February 1972 20-yr	14.2	4.0	59
March 1958 10-yr	13.8	3.0	45	February 1972 10-yr	13.8	4.0	59
March 1958 5-yr	13.4	3.0	45	November 1972 50-yr	14.6	3.1	81
March 1958 2-yr	12.8	3.0	45	November 1972 20-yr	14.2	3.1	81
January 1961 100-yr	14.9	3.6	30	November 1972 10-yr	13.8	3.1	81
January 1961 50-yr	14.6	3.6	30	November 1972 5-yr	13.4	3.1	81
January 1961 20-yr	14.2	3.6	30	November 1972 2-yr	12.8	3.1	81
January 1961 10-yr	13.8	3.6	30	February 1978 100-yr	14.9	5.1	54
January 1961 5-yr	13.4	3.6	30	February 1978 50-yr	14.6	5.1	54
January 1961 2-yr	12.8	3.6	30	February 1978 20-yr	14.2	5.1	54
April 1961 100-yr	14.9	4.2	51	February 1978 10-yr	13.8	5.1	54
April 1961 50-yr	14.6	4.2	51	February 1978 5-yr	13.4	5.1	54
April 1961 20-yr	14.2	4.2	51	February 1978 2-yr	12.8	5.1	54

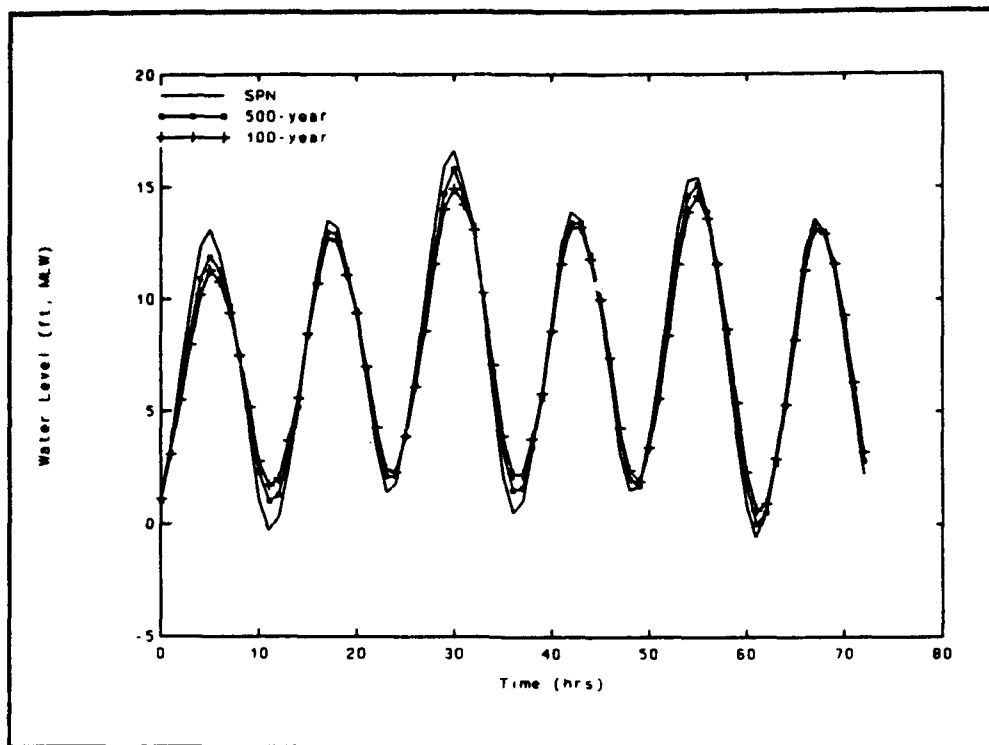


Figure 6. Water level time series - November 1945 storm

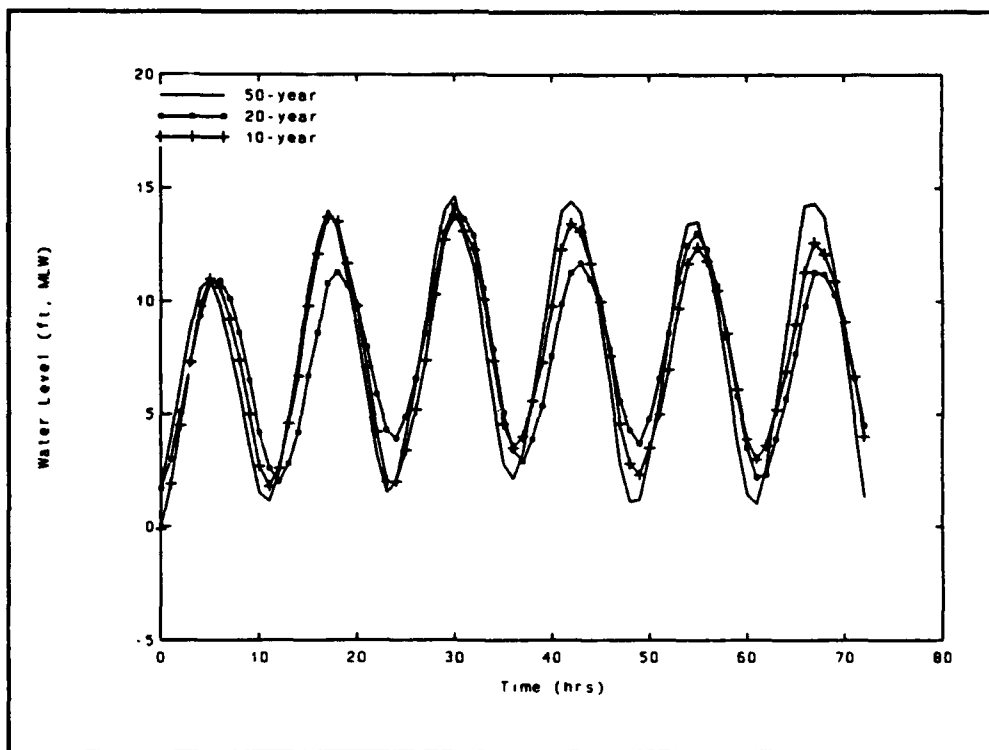


Figure 7. Water level time series - November 1945 storm

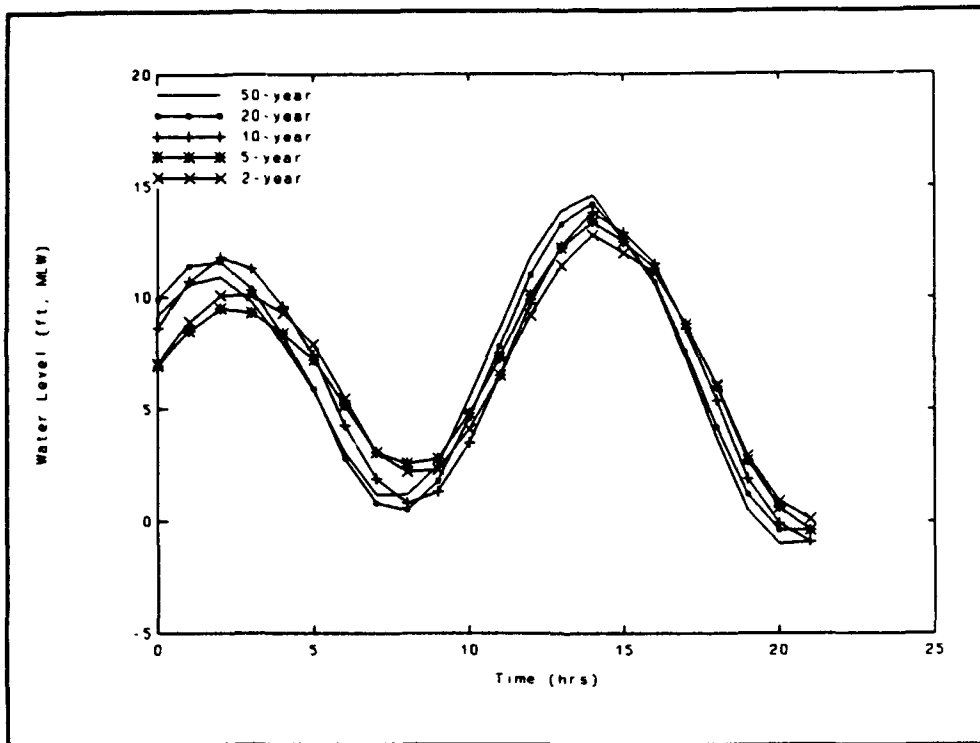


Figure 8. Water level time series - February 1958 storm

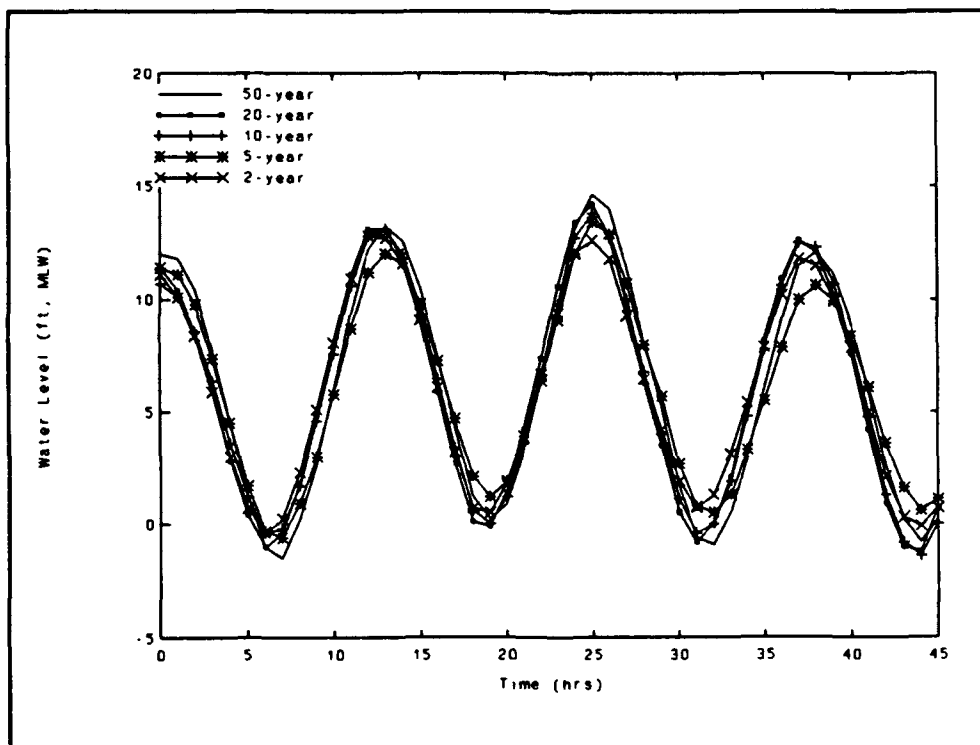


Figure 9. Water level time series - March 1958 storm

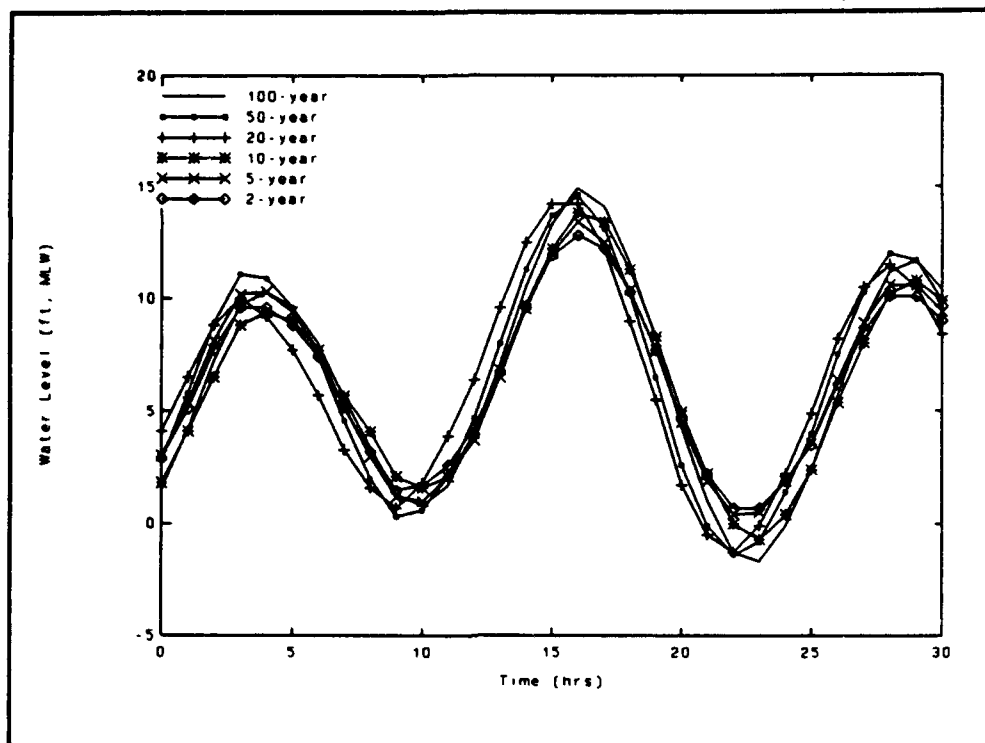


Figure 10. Water level time series - January 1961 storm

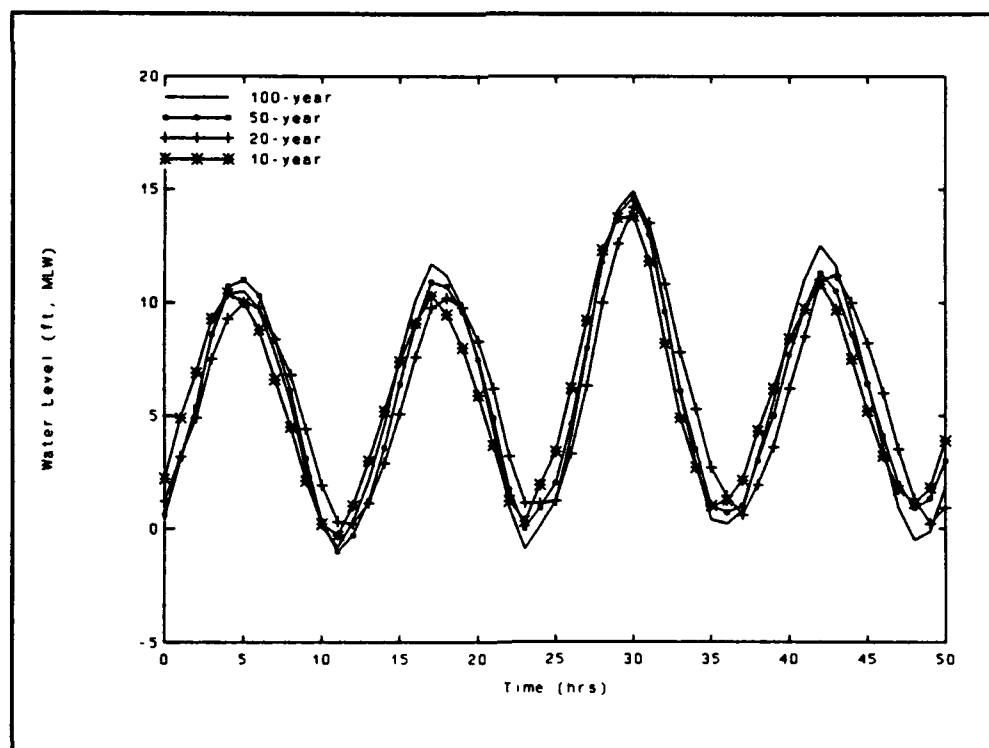


Figure 11. Water level time series - April 1961 storm

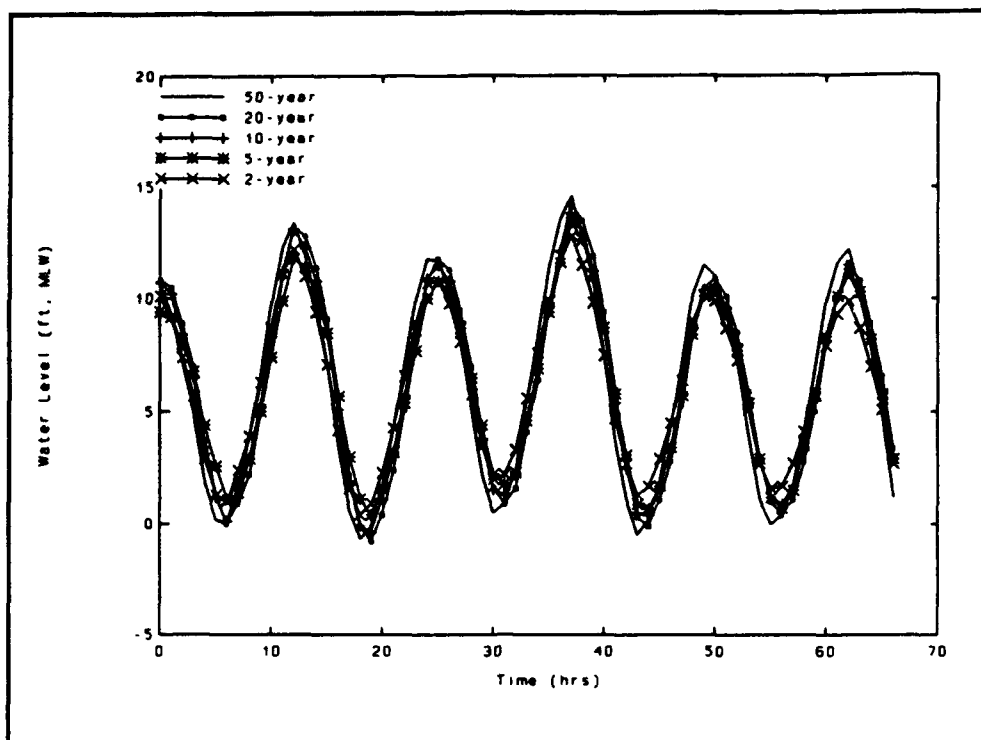


Figure 12. Water level time series - December 1962 storm

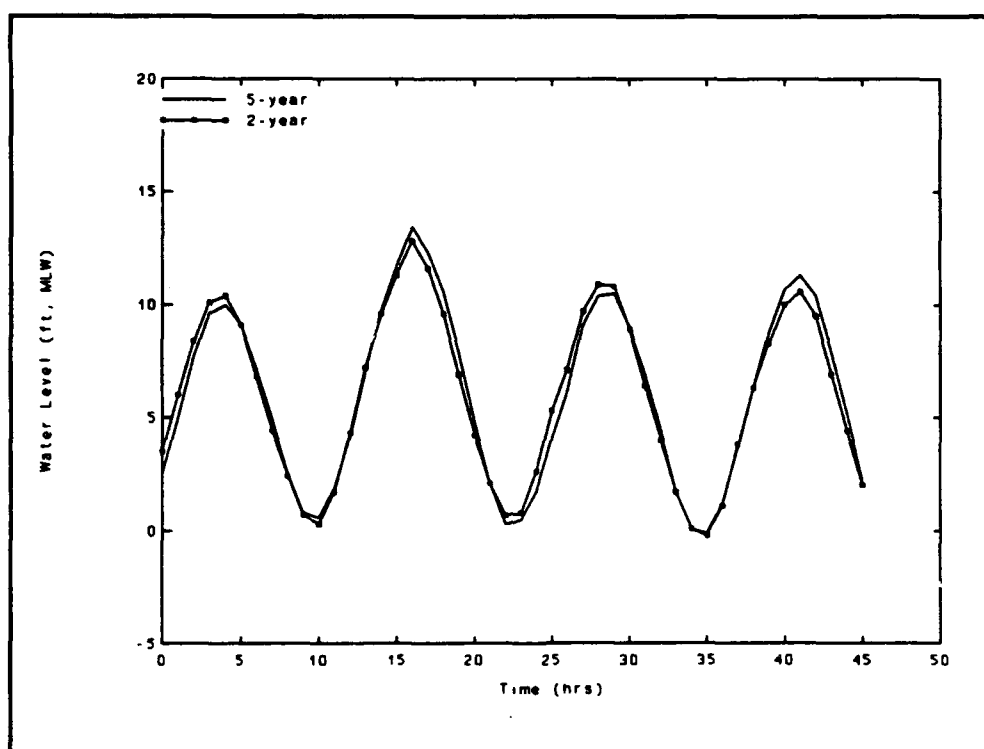


Figure 13. Water level time series - February 1964 storm

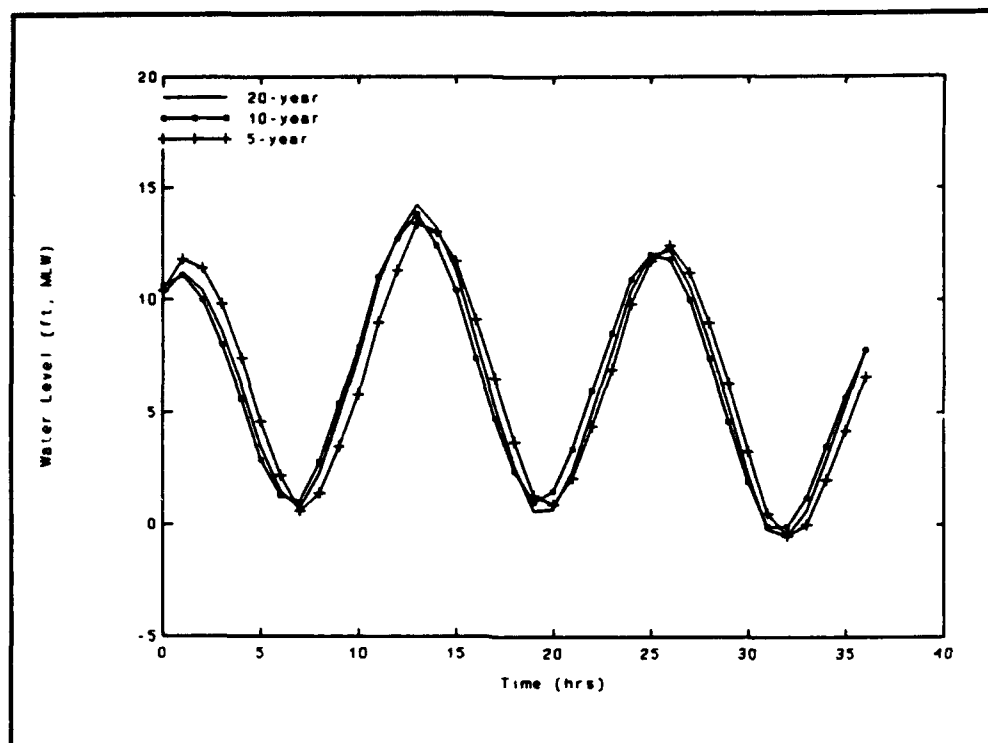


Figure 14. Water level time series - February 1969 storm

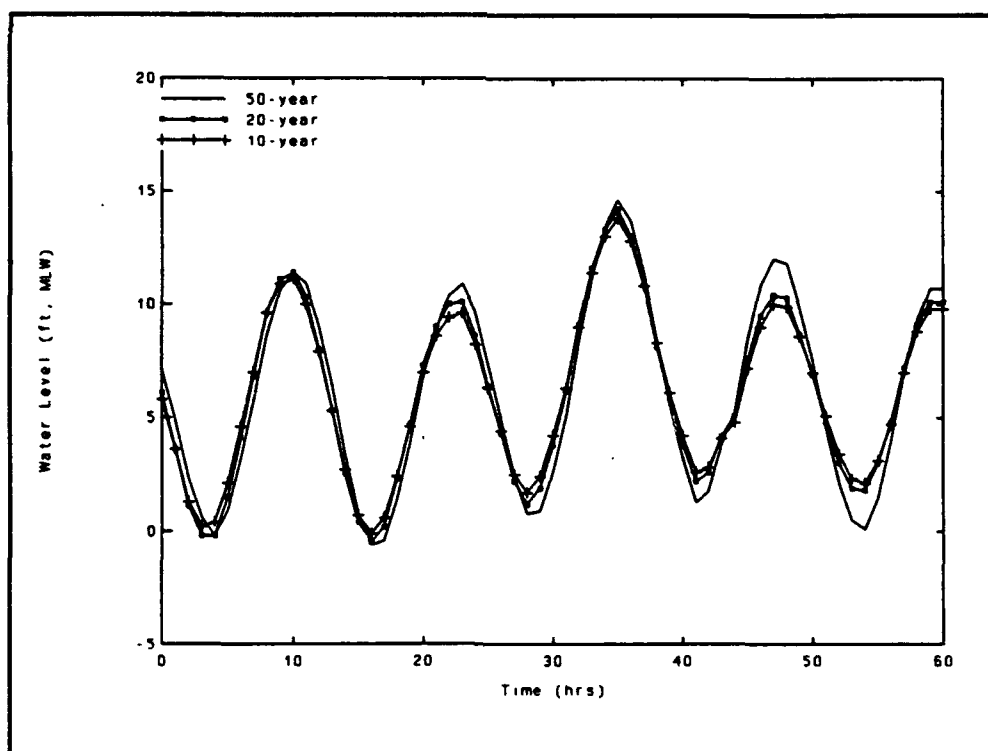


Figure 15. Water level time series - February 1972 storm

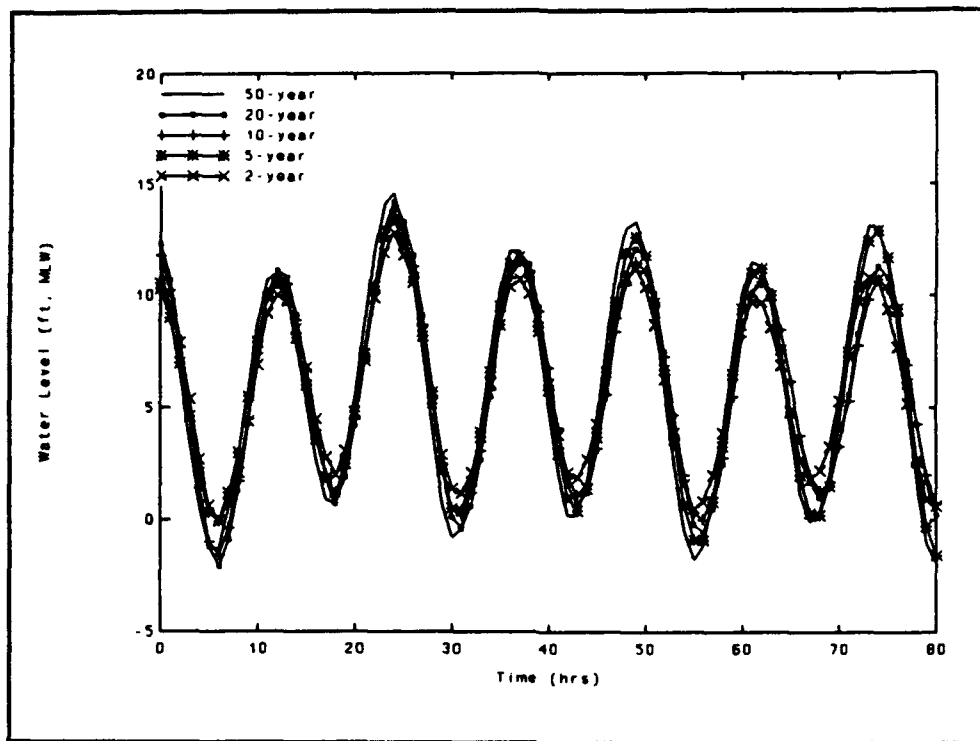


Figure 16. Water level time series - November 1972 storm

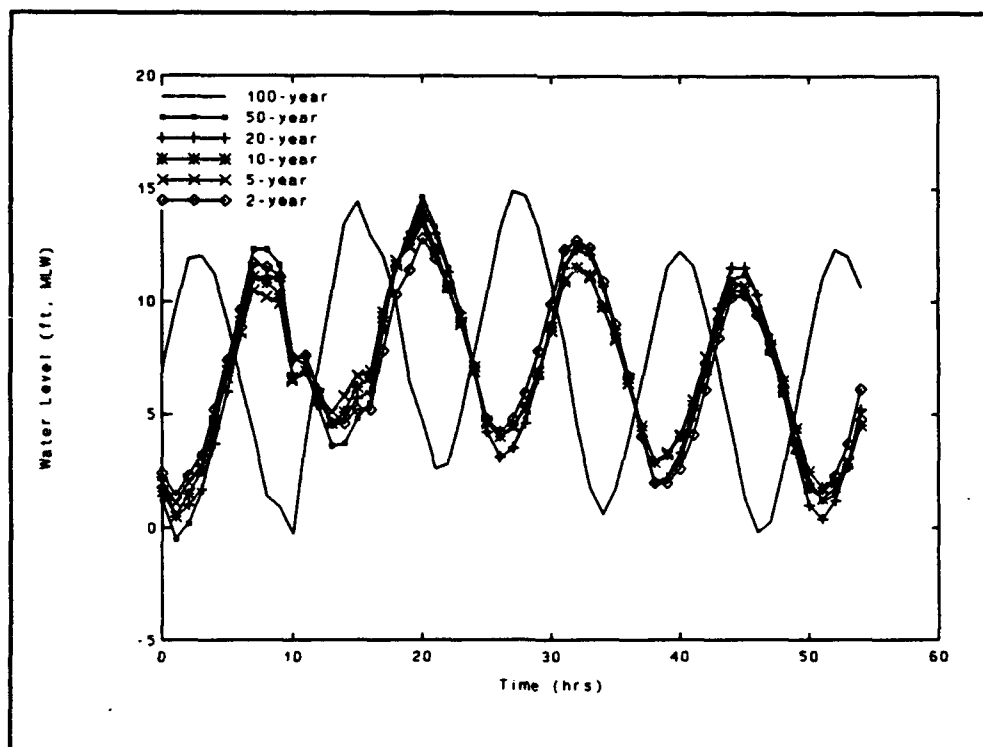
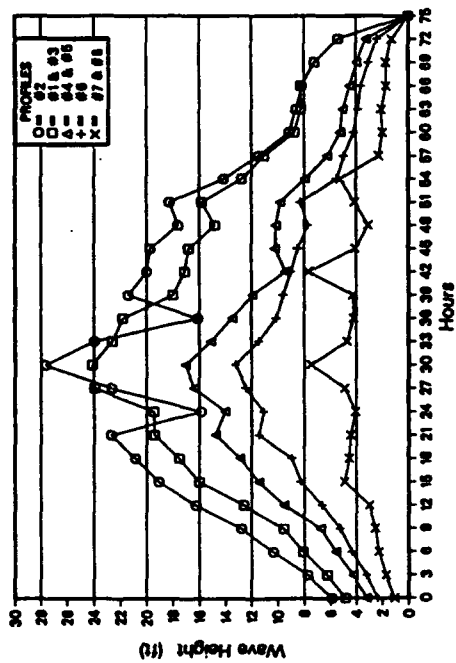
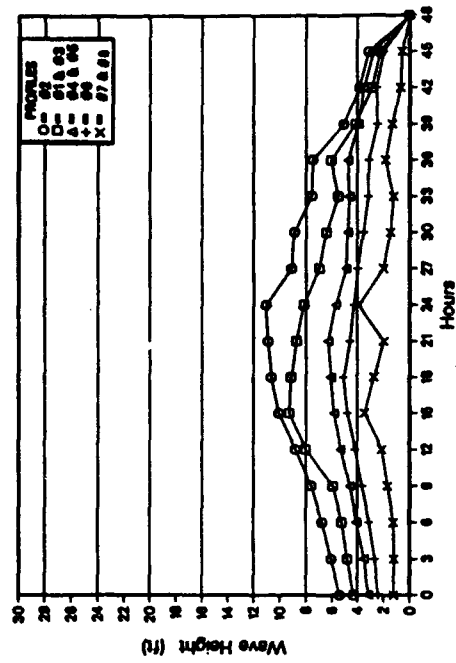


Figure 17. Water level time series - February 1978 storm

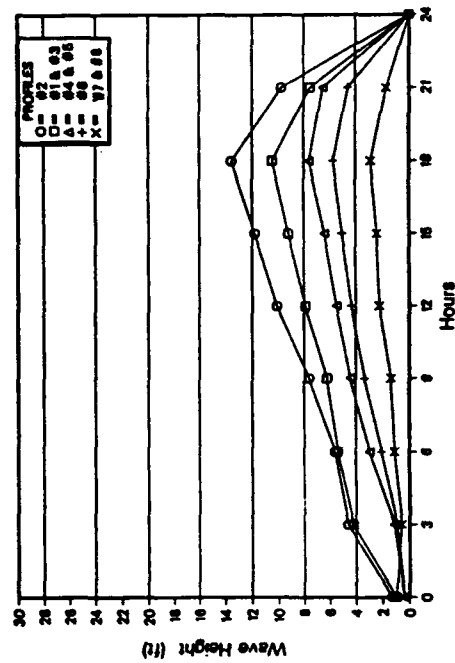
NOVEMBER 1945
50 Year Water Level



MARCH 1953
10 Year Water Level



FEBRUARY 1958
10 Year Water Level



APRIL 1961
50 Year Water Level

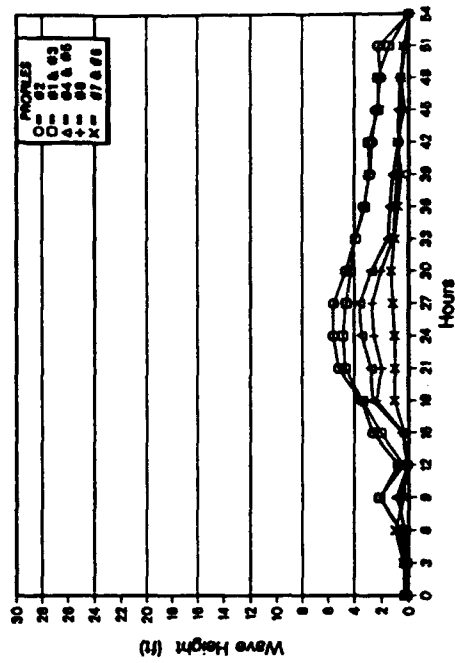
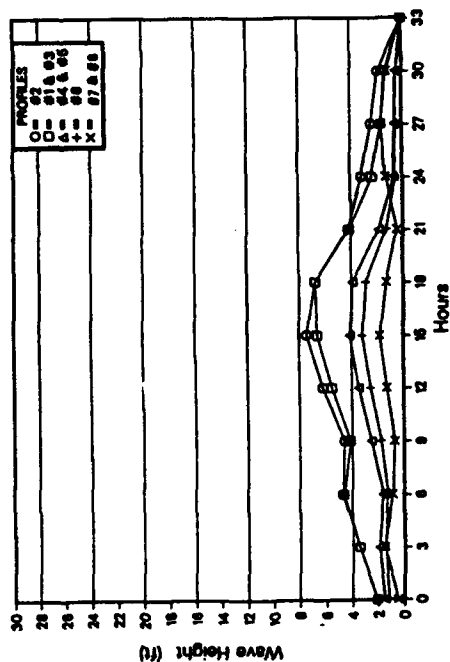
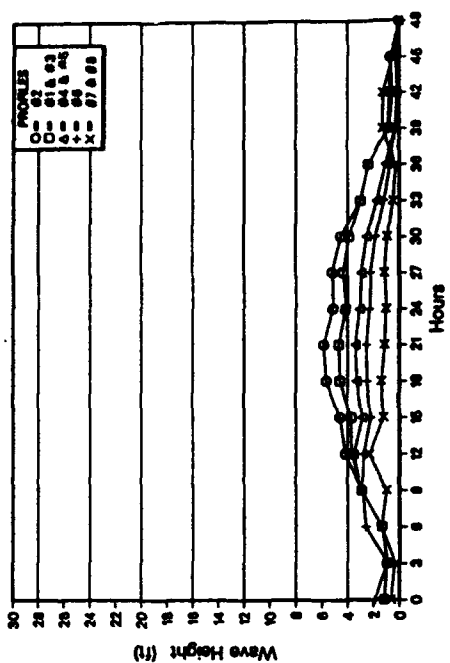


Figure 18. Storm wave heights versus time, 1945-1961

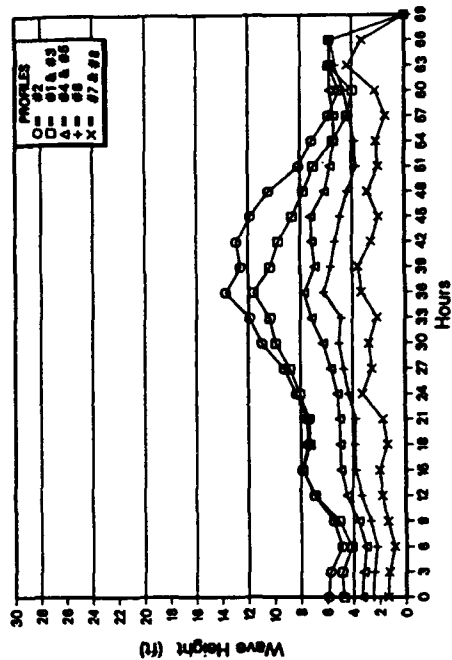
JANUARY 1961
20 Year Water Level



FEBRUARY 1964
5 Year Water Level



DECEMBER 1962
10 Year Water Level



FEBRUARY 1969
10 Year Water Level

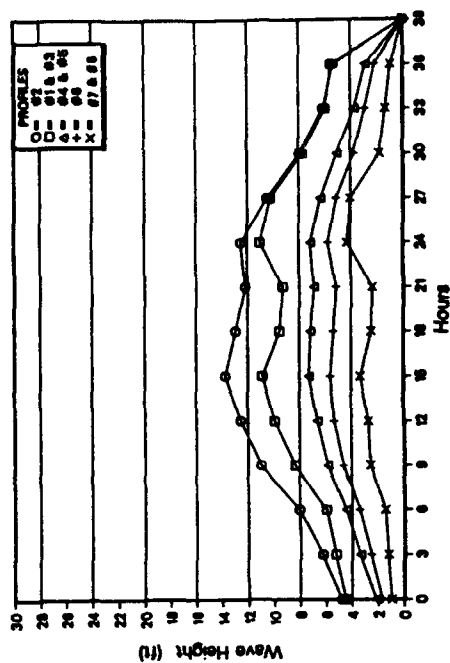
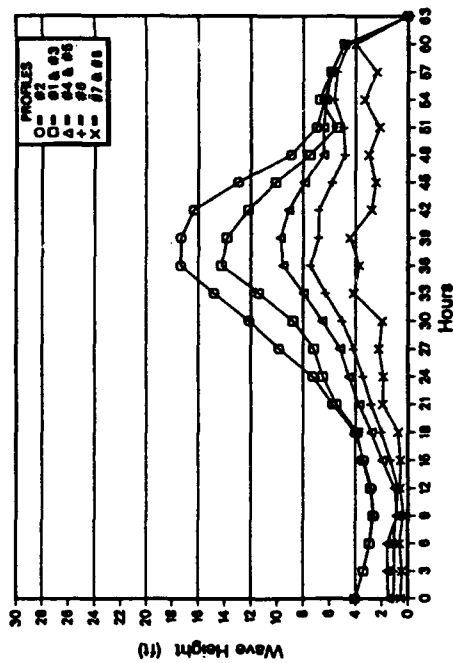
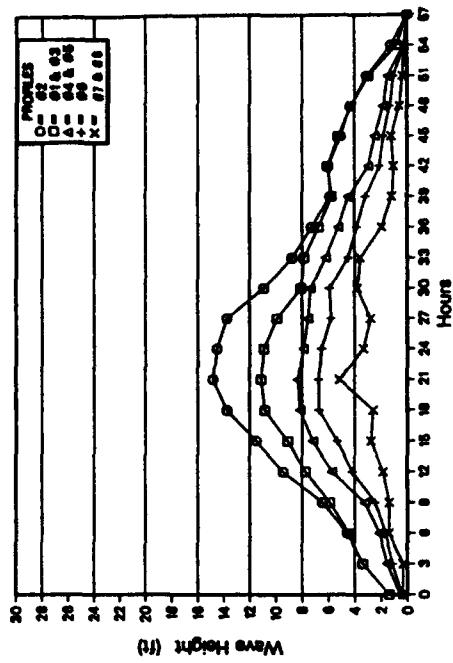


Figure 19. Storm wave heights versus time, 1961-1969

FEBRUARY 1972
20 Year Water Level



FEBRUARY 1978
20 Year Water Level



NOVEMBER 1972
10 Year Water Level

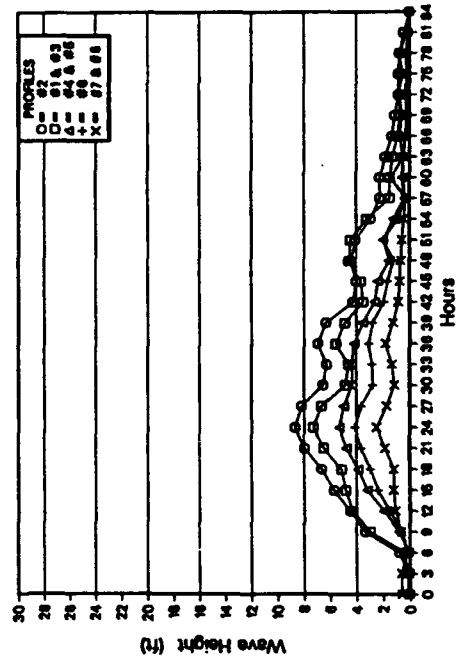


Figure 20. Storm wave heights versus time, 1972-1978

Contour plots of normalized wave heights are shown in Figures 21-30. The plots in Figures 21-26 are representative of storm conditions. The characteristic wave period is 8 sec and the water level is approximately 10 ft (mlw). All tides or water levels are referenced from mean low water. The incident wave height for these plots is 10 ft. The incident direction ranges from +20 to -20 deg in 10-deg increments. Incident direction is measured positive counterclockwise from the x-axis. The plots show the general decrease in wave height from southwest to northeast along Revere Beach and a dramatic decrease in the lee of Nahant Peninsula.

The plots in Figures 27-30 represent conditions during extreme storm events. The predominant wave direction during storms is due east (positive x-direction) or 0 deg. The wave period ranges from 12 to 15 sec and the water level ranges from below the mean tide level (which is approximately 4.5 ft) to about 15 or 16 ft mlw during extreme storms such as the 100-year event. Low water levels, coupled with storm waves of 20 and 30 ft, limit the amount of wave energy that reaches Revere Beach. This can be seen by comparing Figures 27 and 28 with Figures 29 and 30.

The 20-year hindcast for Broad Sound was performed in Part I of the study. Refer to the Part I draft report, "Storm-Induced Beach Erosion and Flooding at Revere Beach and Point of Pines, Massachusetts" (Driver, Bratos, and Rosati; in preparation) for a detailed discussion and summary tables of the hindcast.

1991 Halloween Storm - Part II

Part II presents the numerical wave hindcast for the 1991 Halloween storm. The purpose of this task was to develop nearshore wave and water level conditions simulating the 1991 Halloween storm. An overview of the Halloween storm, and the modeling procedure and the wave models used, are given. This is followed by a discussion of the input data set and a comparison to measured wind and wave data. Offshore and nearshore wave simulations are then discussed as well as sensitivity testing. Finally, the results of the simulation are presented.

The 1991 Halloween storm is particularly noteworthy because of its long duration, long peak wave periods, and high energy levels. The large North Atlantic extratropical storm developed when a low pressure system formed on the eastern seaboard. The storm gained energy when it absorbed Hurricane Grace around 27 October. The storm significantly impacted the east coast from about 27 October to 3 November 1991. During the storm, peak periods were recorded as high as 20 sec and 12-m maximum significant wave heights were measured at the NDBC Georges Bank buoy. The maximum water level measured at the NOS Boston gauge was approximately 14.0 ft mlw with an estimated surge of 4 ft.

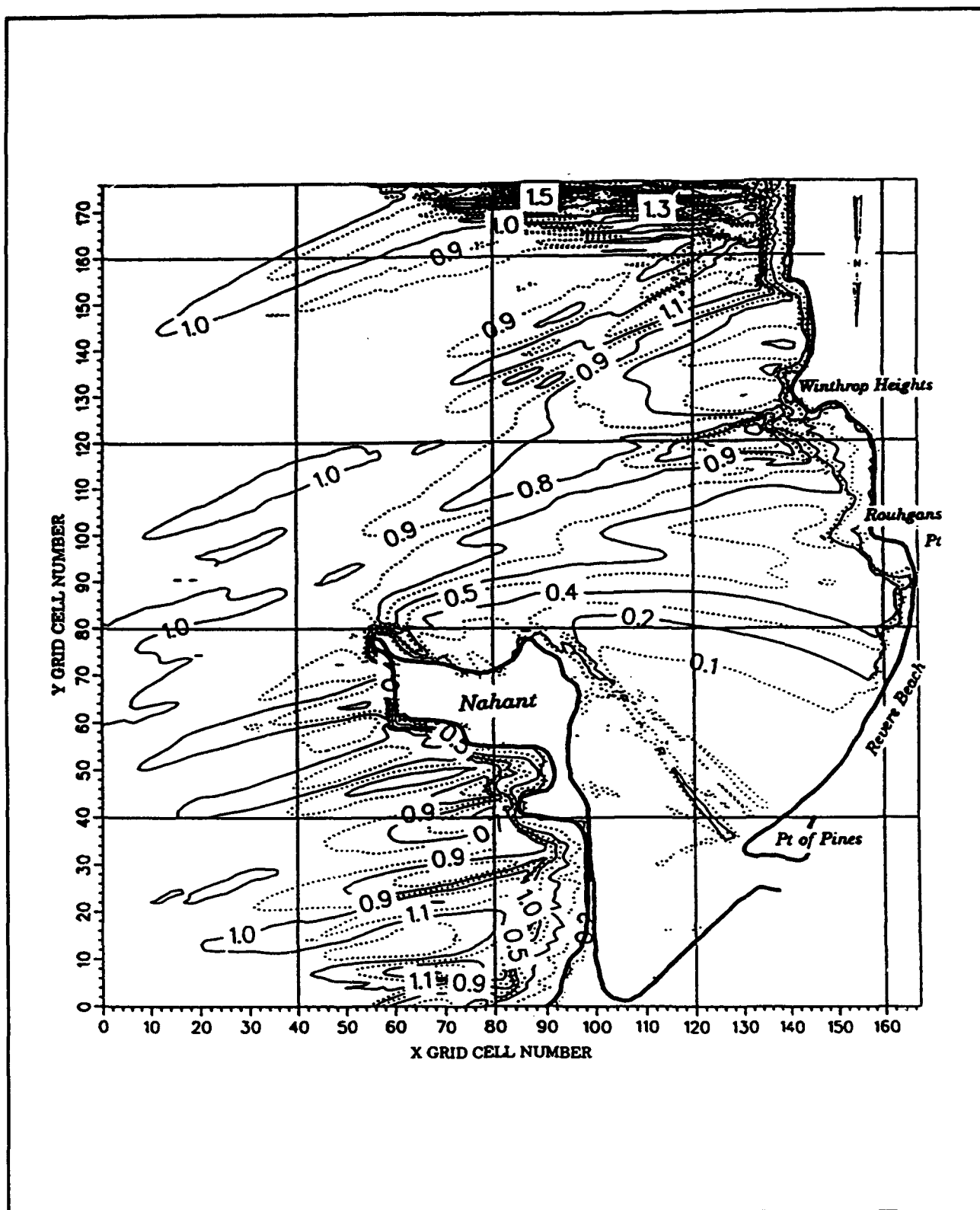


Figure 21. Contour plot of normalized wave height, $T = 8$ sec, $H = 10$ ft, $Dir = 20$ deg, Tide = 10 ft

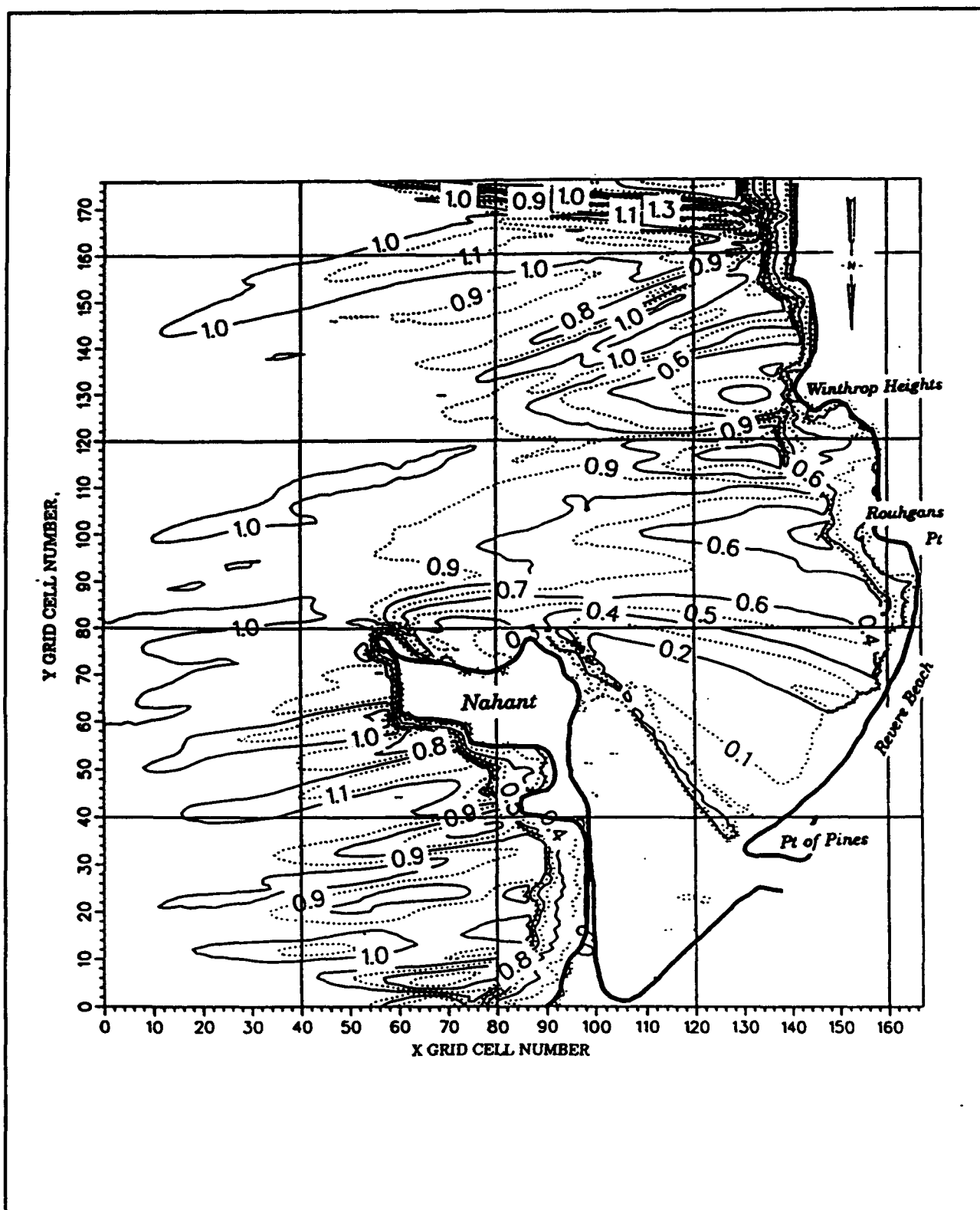


Figure 22. Contour plot of normalized wave height, $T = 8$ sec, $H = 10$ ft, $Dir = 10$ deg, Tide = 10 ft

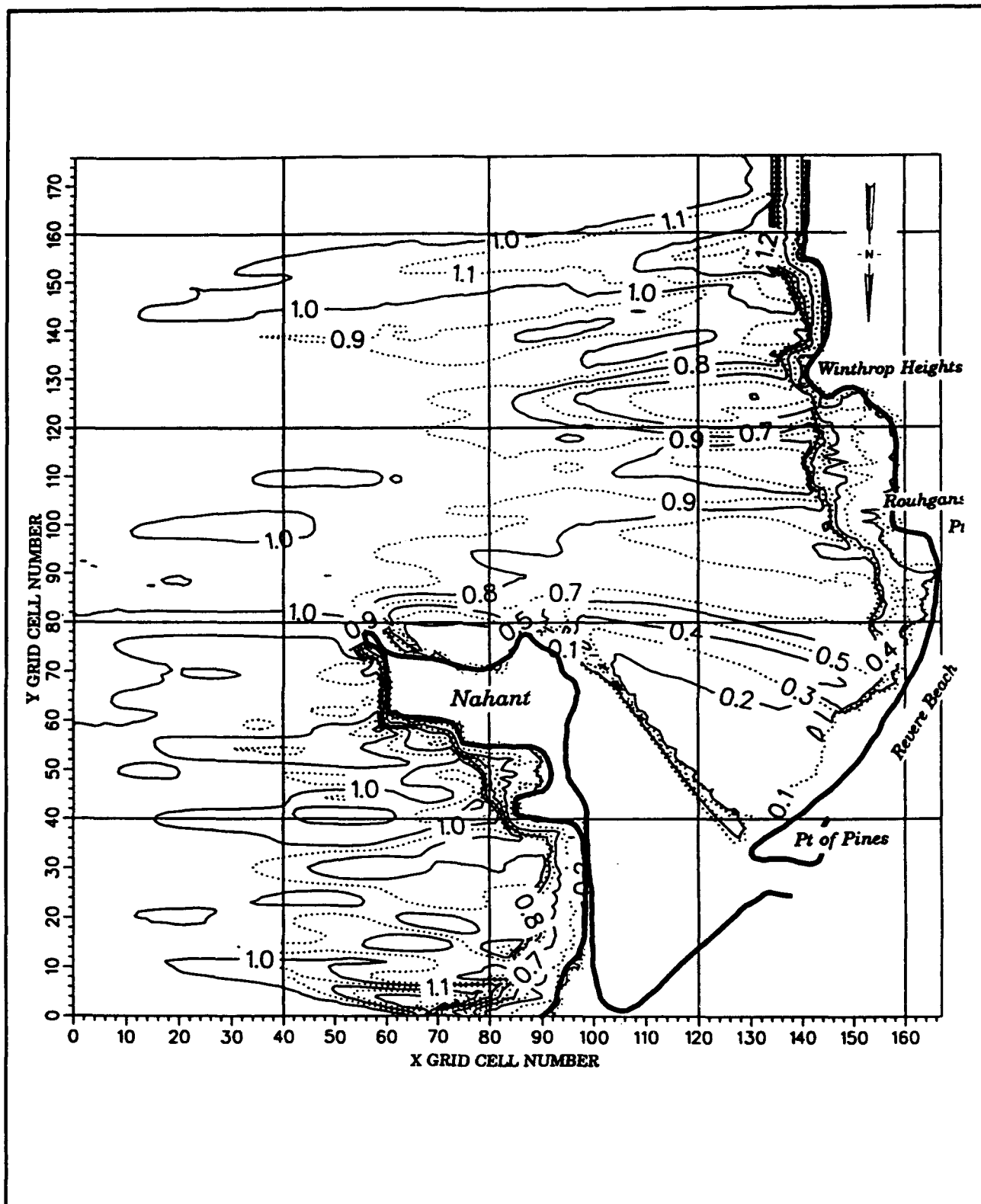


Figure 23. Contour plot of normalized wave height, $T = 8$ sec, $H = 10$ ft, $\text{Dir} = 0$ deg, Tide = 10 ft

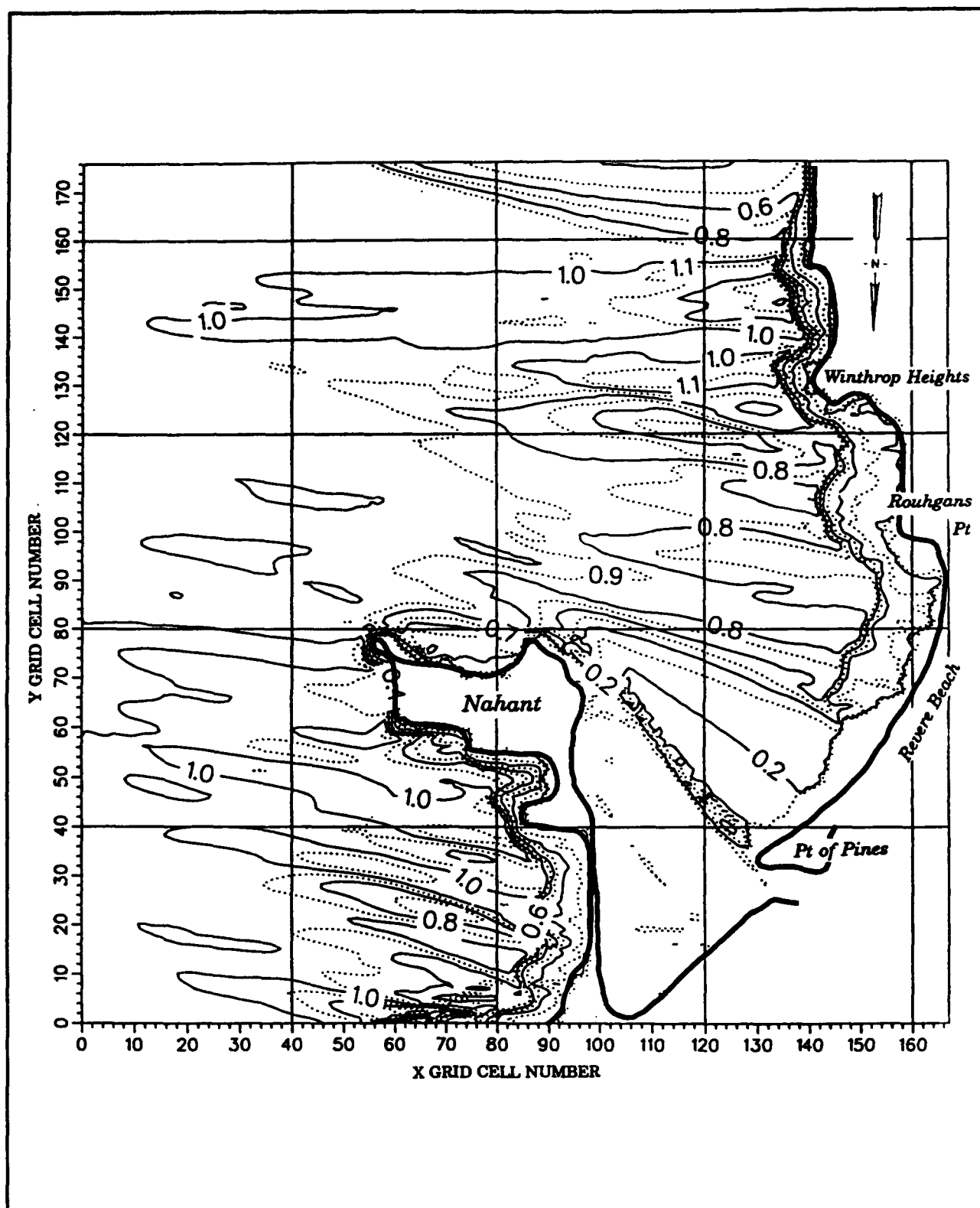


Figure 24. Contour plot of normalized wave height, $T = 8$ sec, $H = 10$ ft, $Dir = -10$ deg, Tide = 10 ft

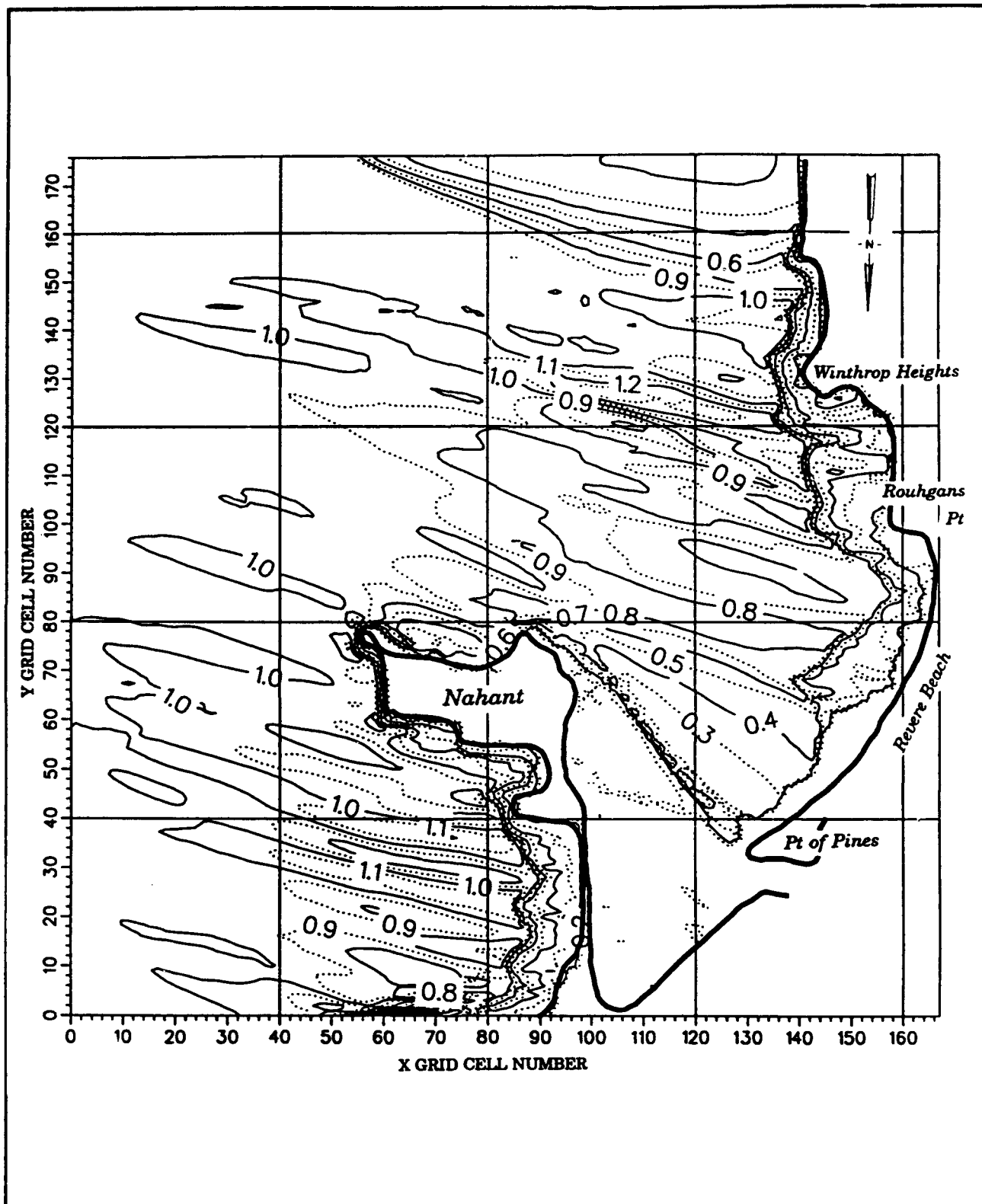


Figure 25. Contour plot of normalized wave height, $T = 8$ sec, $H = 10$ ft, $Dir = -20$ deg, Tide = 10 ft

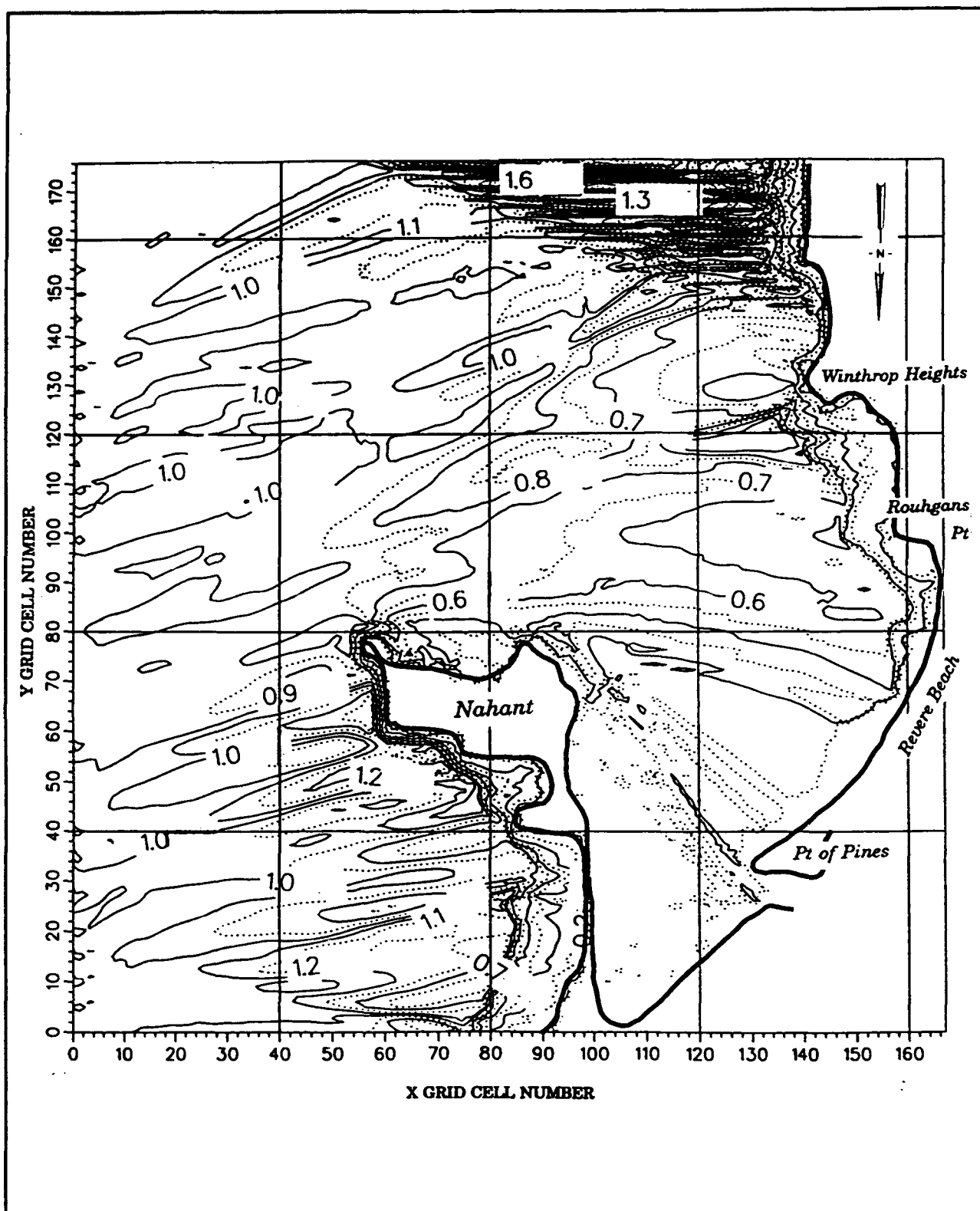


Figure 26. Contour plot of normalized wave height, $T = 13$ sec, $H = 10$ ft, $Dir = 20$ deg, Tide = 10 ft

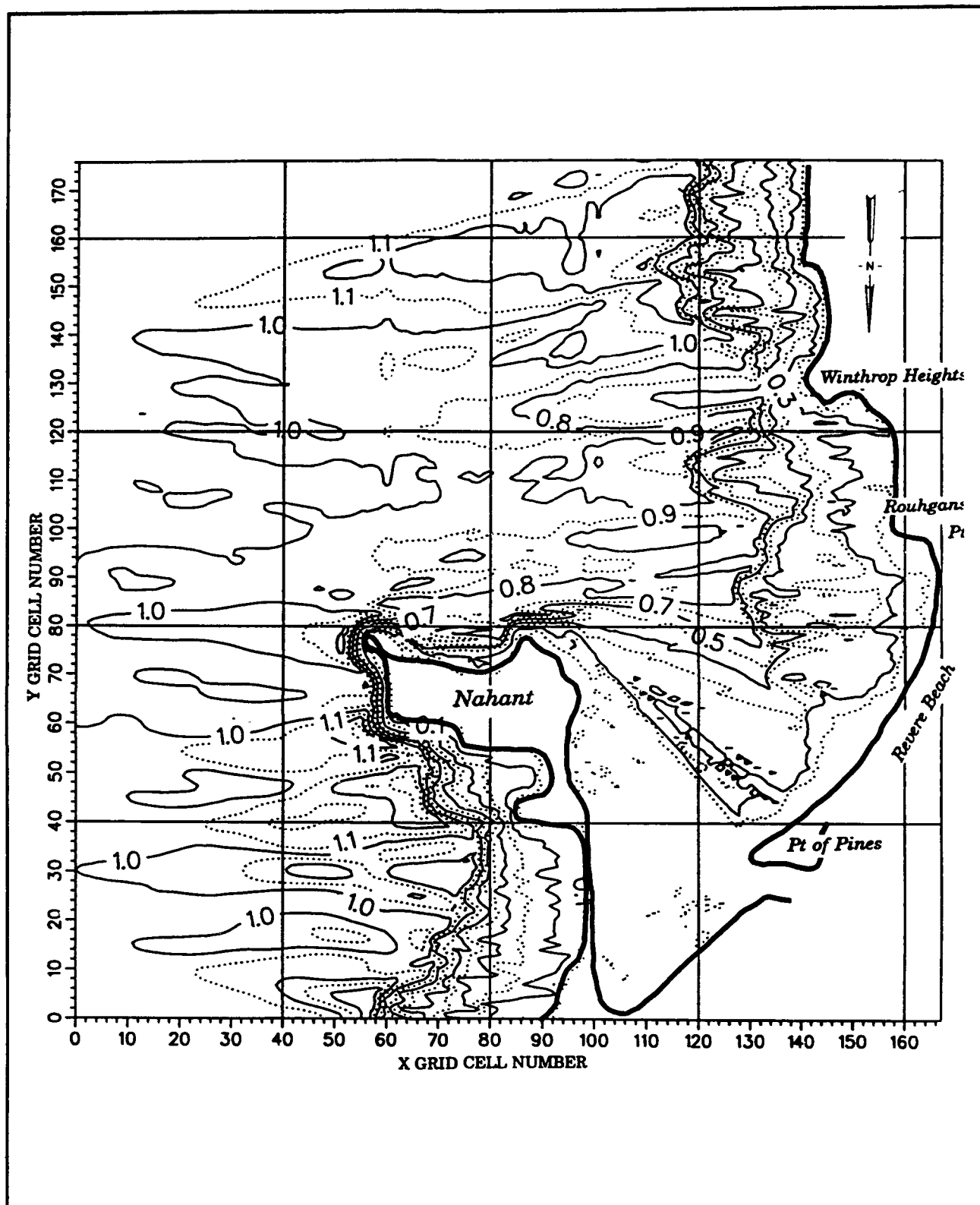


Figure 27. Contour plot of normalized wave height, $T = 15$ sec, $H = 20$ ft, $Dir = 0$ deg, Tide = 5 ft

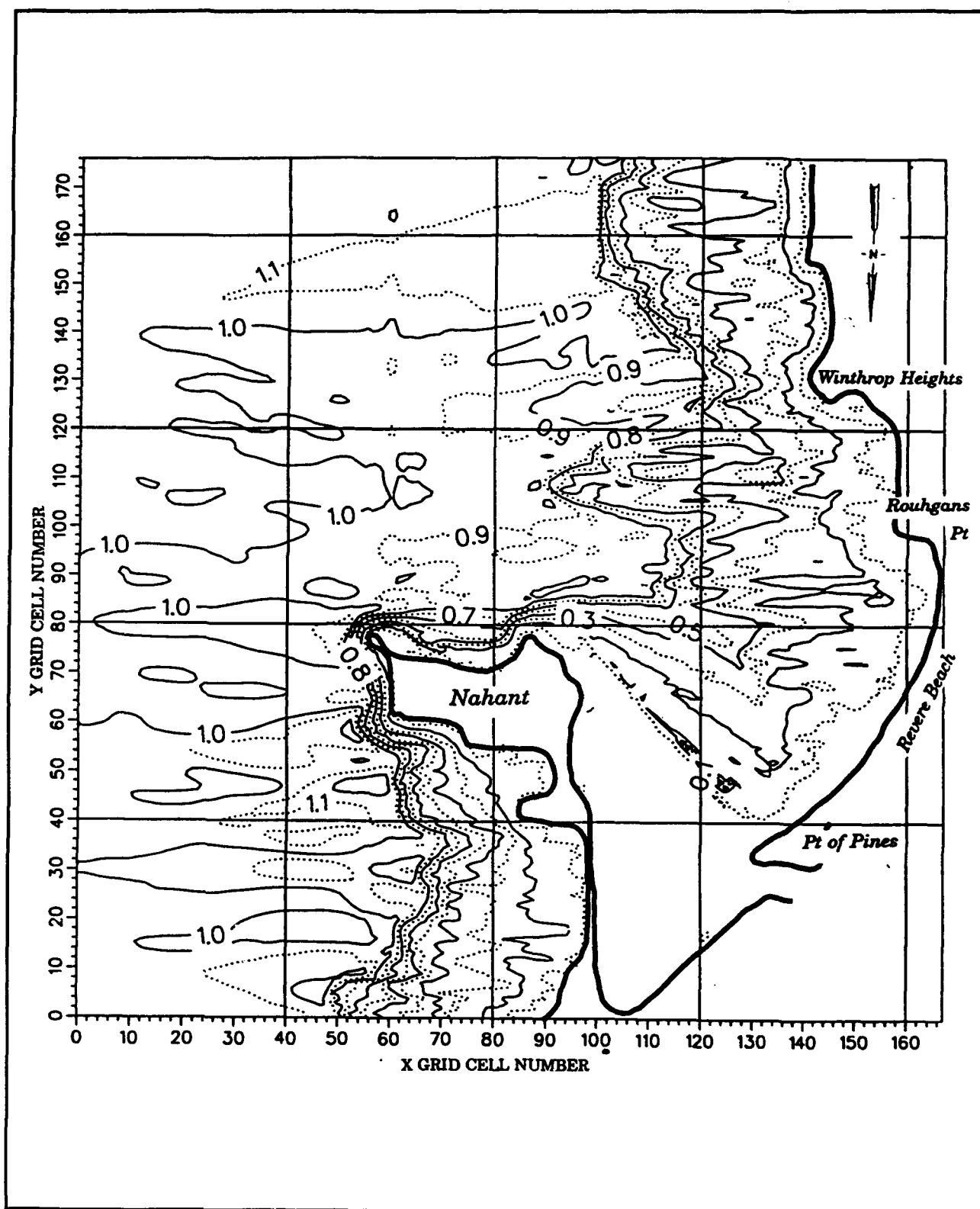


Figure 28. Contour plot of normalized wave height, $T = 15$ sec, $H = 30$ ft, $Dir = 0$ deg, Tide = 5 ft

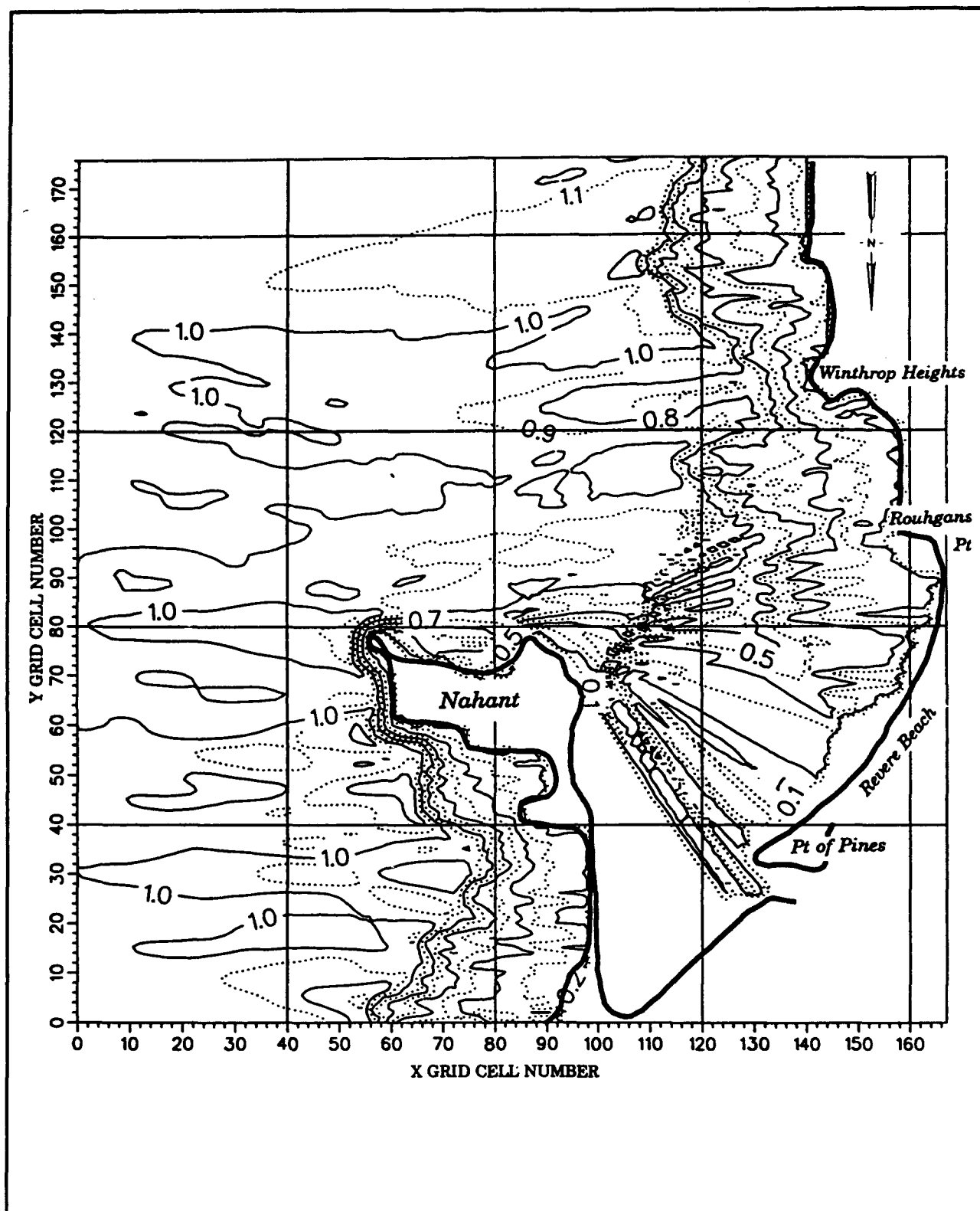


Figure 30. Contour plot of normalized wave height, $T = 15$ sec, $H = 30$ ft, $Dir = 0$ deg, Tide = 15 ft

The modeling procedure for this task includes the use of wind and wave output from the Third Generation wind Wave Model (3GWAM) and wave simulations using the second generation wind wave model SHALWV and the refraction/diffraction model REF/DIF. The best data set available for the Halloween storm was a by-product of the Surface Wave Dynamics Experiment (SWADE). For this comprehensive experiment, the model 3GWAM was used to simulate wind wave growth and dissipation. 3GWAM is a third-generation model that integrates the basic transport equation describing the evolution of a two-dimensional wave spectrum without any ad hoc assumptions about the spectral shape. The source functions describing the wind input, nonlinear transfer, and white-capping dissipation are explicit. Refraction terms and an additional bottom dissipation source function are included. The model runs on a spherical latitude-longitude grid for an arbitrary region of the ocean. *The WAM Model - A Third Generation Ocean Wave Prediction Model* (WAMDI 1988), gives more detail about the 3GWAM model. Grids for this model covered the entire Atlantic Ocean Basin and included a regional grid which covered the east coast from the southern tip of Florida to Nova Scotia. The resolution of the regional grid was 0.25 deg or about 15 n.m. Hourly wind and wave output from 3GWAM was used as input to SHALWV. Wind input for SHALWV coincided with the locations of the WIS stations used in Part I of the Revere Beach study.

SHALWV is a wave hindcasting model which simulates time-varying wind and wave conditions during storms. The model is based on the inhomogeneous energy balance equation solved with finite difference methods using square grid cells. The SHALWV grid used for the Halloween storm is the same as that used in Part I of the study. Figure 3 in Chapter 2 section shows the SHALWV grid. The grid is 12 by 15 with 10-n.m. cells, and the directional wave spectrum is divided into 20 frequency and 16 direction bands. Refer to the "Description of Models" and "Methodology and Results - Part I" sections of Chapter 2 for detailed descriptions of SHALWV and its application.

The wave model REF/DIF used SHALWV output of significant wave height and peak period and direction to generate wave conditions in Broad Sound for the Halloween storm. The wave model REF/DIF is a combined refraction/diffraction model based on Kirby and Dalrymple's (1983) parabolic approximation for Berkhoff's (1972) mild slope equation, where reflected waves are neglected. For the Broad Sound application, the nonlinear mode of the model was used. The same grid as that used in Part I of the study was used for the Halloween storm simulation. It is a 165 by 176 grid with square cells of 200 ft on each side. Figure 5 in Chapter 2 shows the REF/DIF grid and the bathymetry of Broad Sound. The input boundary for this grid is along the y-axis. The x-axis is directed due west and the y-axis points due south.

Halloween Storm Input Data Set

Input to the 3GWAM model was wind stresses produced by the Fleet Numerical Oceanography Center (FNOC) global model. In order to compare the FNOC winds to NDBC buoy 44013, the FNOC wind stresses were converted to wind speed using Wu's (1980) drag law. The first two plots in Figure 31 show a comparison between the FNOC wind speed and direction to the wind speed and direction of buoy 44013. The wind speed plot shows good comparison between model-derived and measured winds, although the FNOC winds overpredict the buoy winds by as much as 3 m/sec during the peak of the storm. It should be noted that no single widely accepted method to convert the FNOC wind stresses to wind speeds exists and the choice of the method used could have a significant impact on the comparison. This uncertainty exists only in the comparison of the data to the buoy. The 3GWAM model operates with wind stresses. The next two plots in Figure 31 show the 3GWAM model results of significant wave height and peak period compared to buoy 44013 data.

The comparison between model and buoy wave heights is particularly good, even though the model underpredicts the measured wave height by less than 0.5 m at the peak of the storm and overpredicts the wave height by about 1.5 m at the beginning of the storm. The comparison between wave periods is also good where the maximum measured peak period of 20 sec is represented in the model results as well. The plots in Figure 31 also show that the peak of the storm occurred at about the beginning of the 304th Julian day or October 31.

Even though wave data were available from 3GWAM simulations, SHALWV was run for simulations in the Massachusetts Bay area for consistency with Part I of the study. Because input data from 3GWAM were available on an hourly basis, SHALWV simulations were run with input and output every hour. In order to include all the significant wave action occurring during the storm, the SHALWV simulation began on 27 October at 0100 hr and ended on 3 November at 2200 hr. The plot in Figure 32 shows wave height, period, and direction output from SHALWV Station 2. SHALWV stations are shown in Figure 3 of the Part I section. Similarities between the SHALWV simulation and the 3GWAM simulation can be seen in the 9.5-m maximum wave height, the 20-sec peak period, and wave direction ranging from 225 deg at the beginning of the storm to 175 deg at the end of the storm. Figure 33 shows a wave height plot comparing the SHALWV height of 9.5 m about 6 hr before the buoy's maximum wave height of 9.0 m. These differences in magnitude and timing of the storm are considered to be inaccuracies in the FNOC wind field. Note that the unusually low buoy wave height at about 120 hr into the simulation is probably due to measurement error.

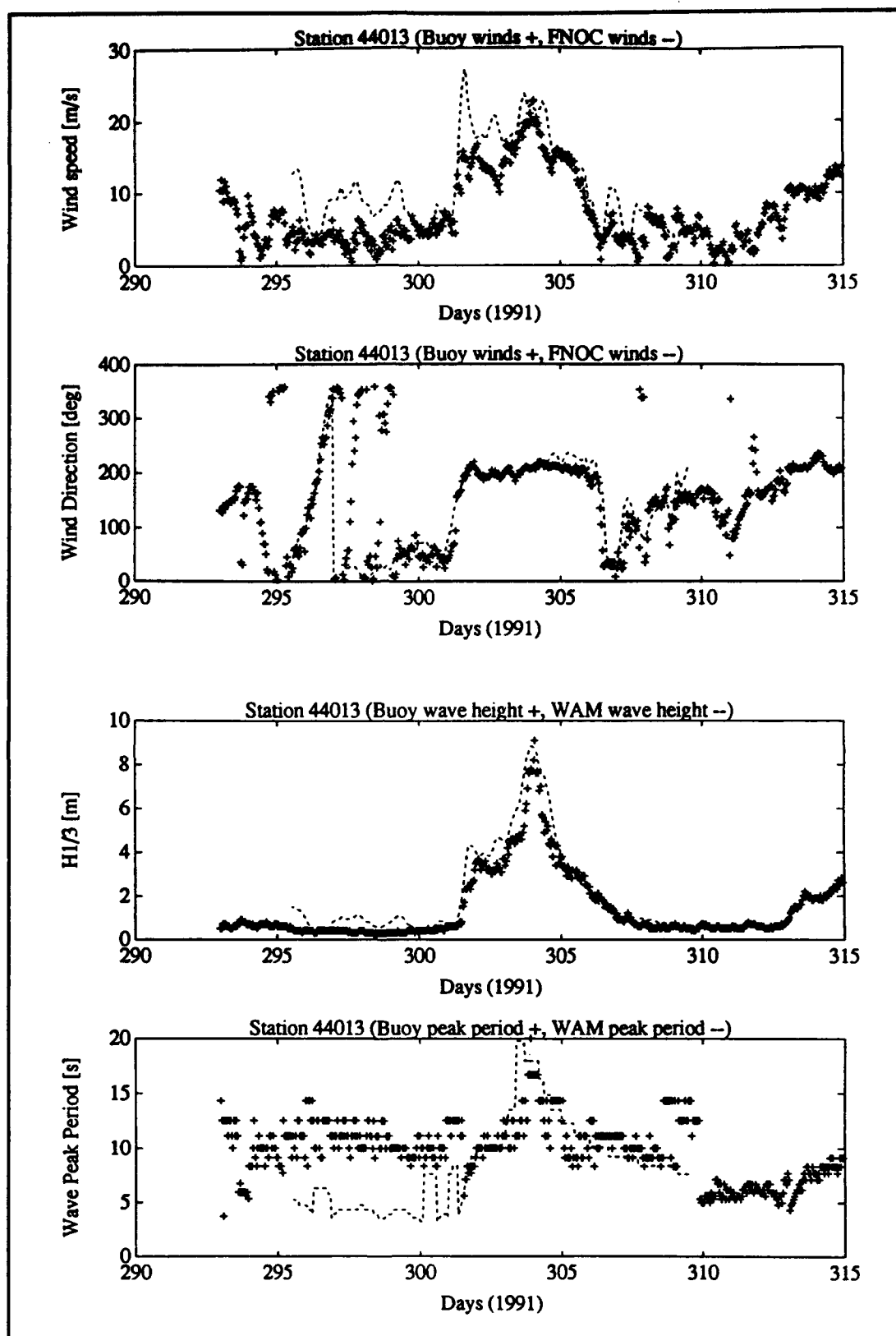


Figure 31. FNOC and 3GWAM comparisons to NDBC buoy 44013

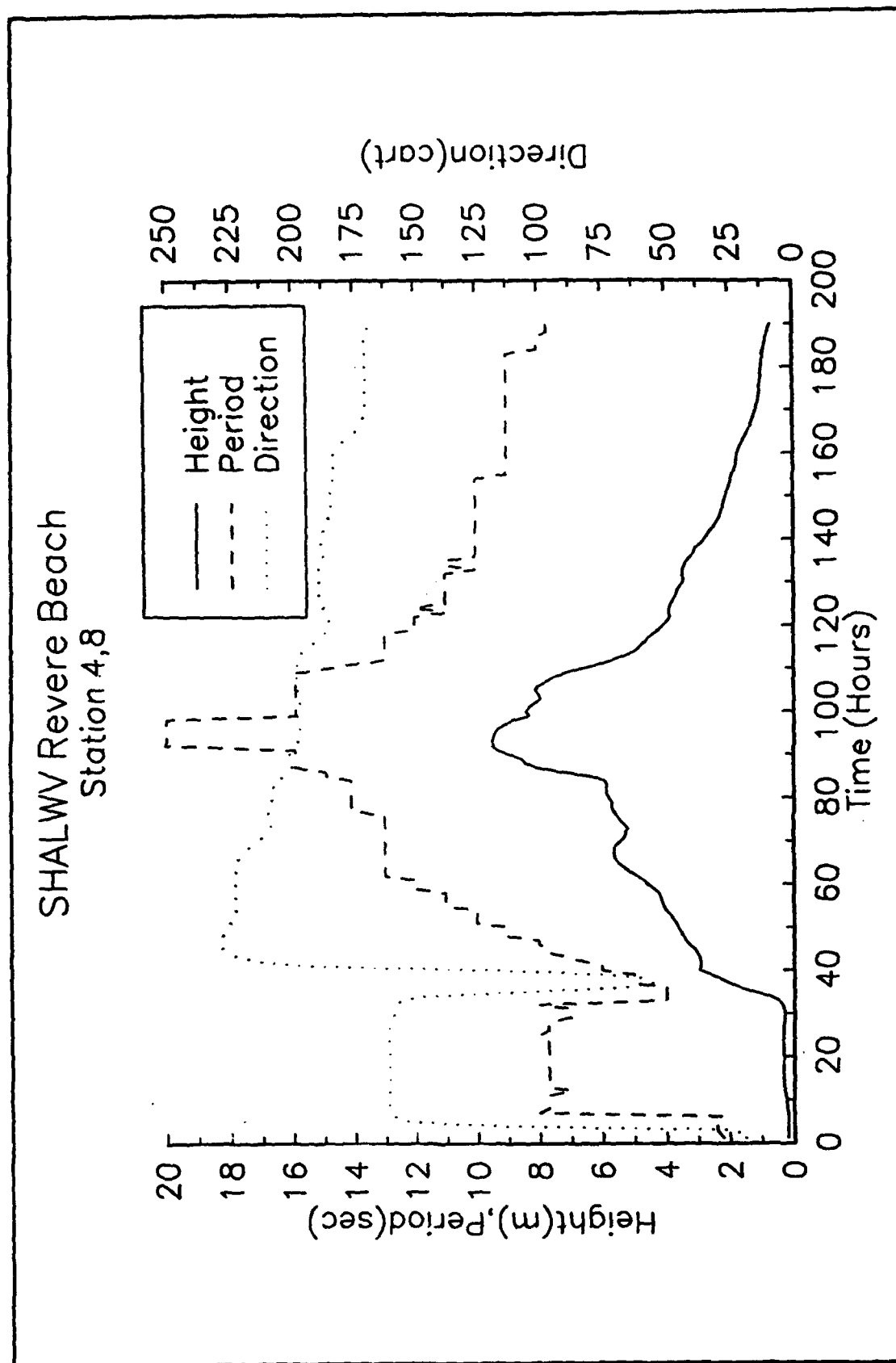


Figure 32. SHALWV Station 2 wave height, period, and direction

SHALWV – Halloween Storm Model Station 2 – Buoy 44013

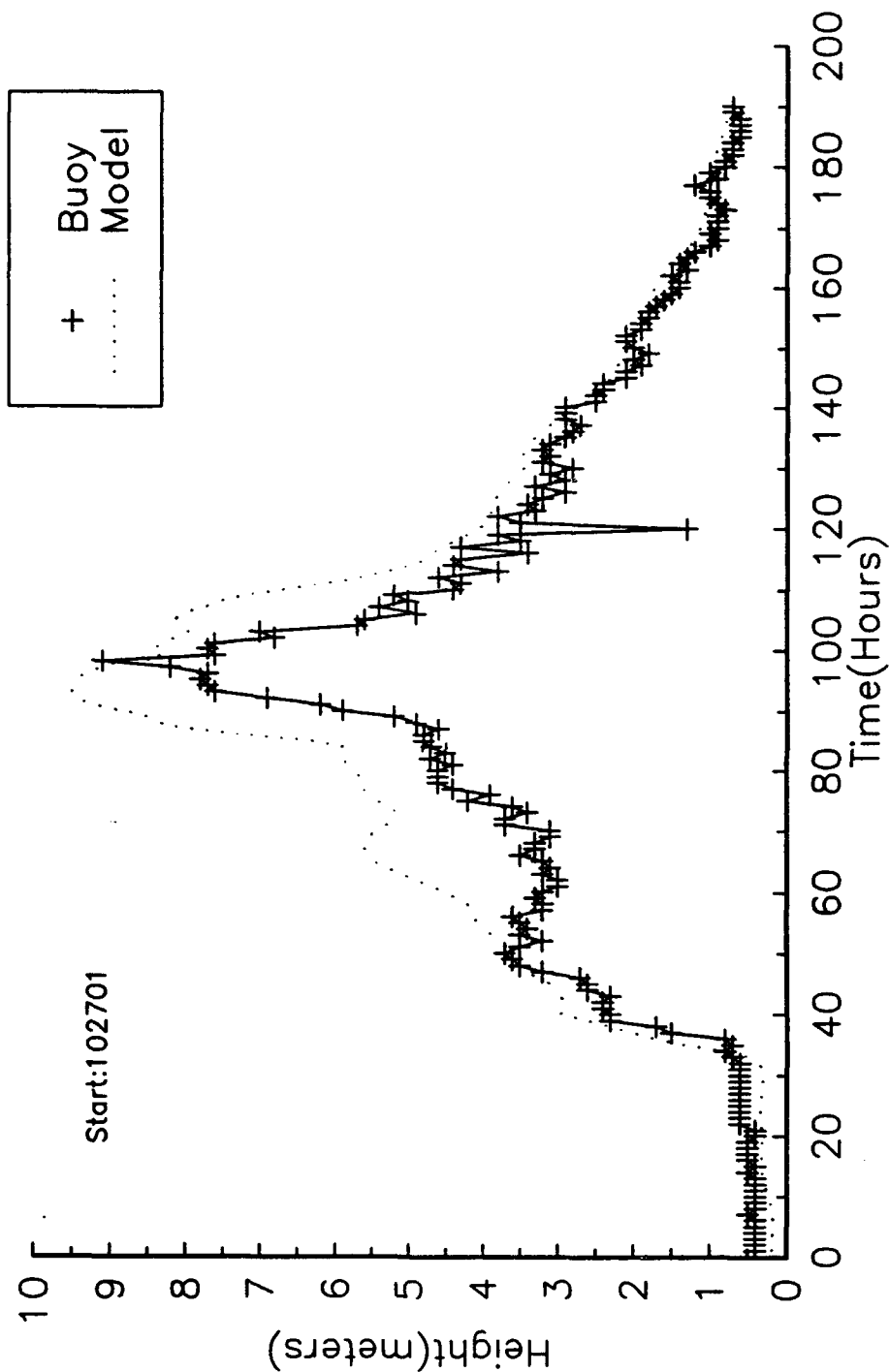


Figure 33. SHALWV Station 2 and NDBC buoy 44013 wave height comparison

For the REF/DIF simulation of Broad Sound, SHALWV wave conditions at 3-hr intervals were input to the REF/DIF model. For accuracy in the nearshore areas and consistency with the rest of the study, water level information from the NOS Boston gauge was obtained. Figure 34 shows the water level time series with a maximum water level of 14.0 ft mlw occurring around 30 October at 2000. The time period chosen for REF/DIF simulations starts on 28 October at 0600 and ends on 2 November at 2200. For each wave condition simulated by REF/DIF, wave height, period, and direction were saved at the offshore terminus of each SBEACH profile. Refer to Figure 5 in the Part I section for the location of these points. Figure 35 shows wave height time series during the storm at the offshore terminus of each profile. A maximum wave height of 22 ft occurs at the beginning of Profile 2. Comparing this plot to the plots in Figures 18-20 of Chapter 2, it is seen that the Halloween storm has the longest duration of the storms simulated. The 22-ft maximum wave height for the Halloween storm is exceeded only by a 28-ft occurrence during the November 1945 storm. Sensitivity tests were run for the REF/DIF simulation by adjusting each of the incident wave directions from the actual storm time series by ± 15 deg. From Figures 36 and 37, it can be seen that, in general, as the incident wave direction moves from east to southeast, the resulting wave height increases by approximately 2 to 4 ft for all but Profile 8. As the incident wave direction moves from east to northeast, the resulting wave height decreases 4 to 6 ft for all but Profile 8.

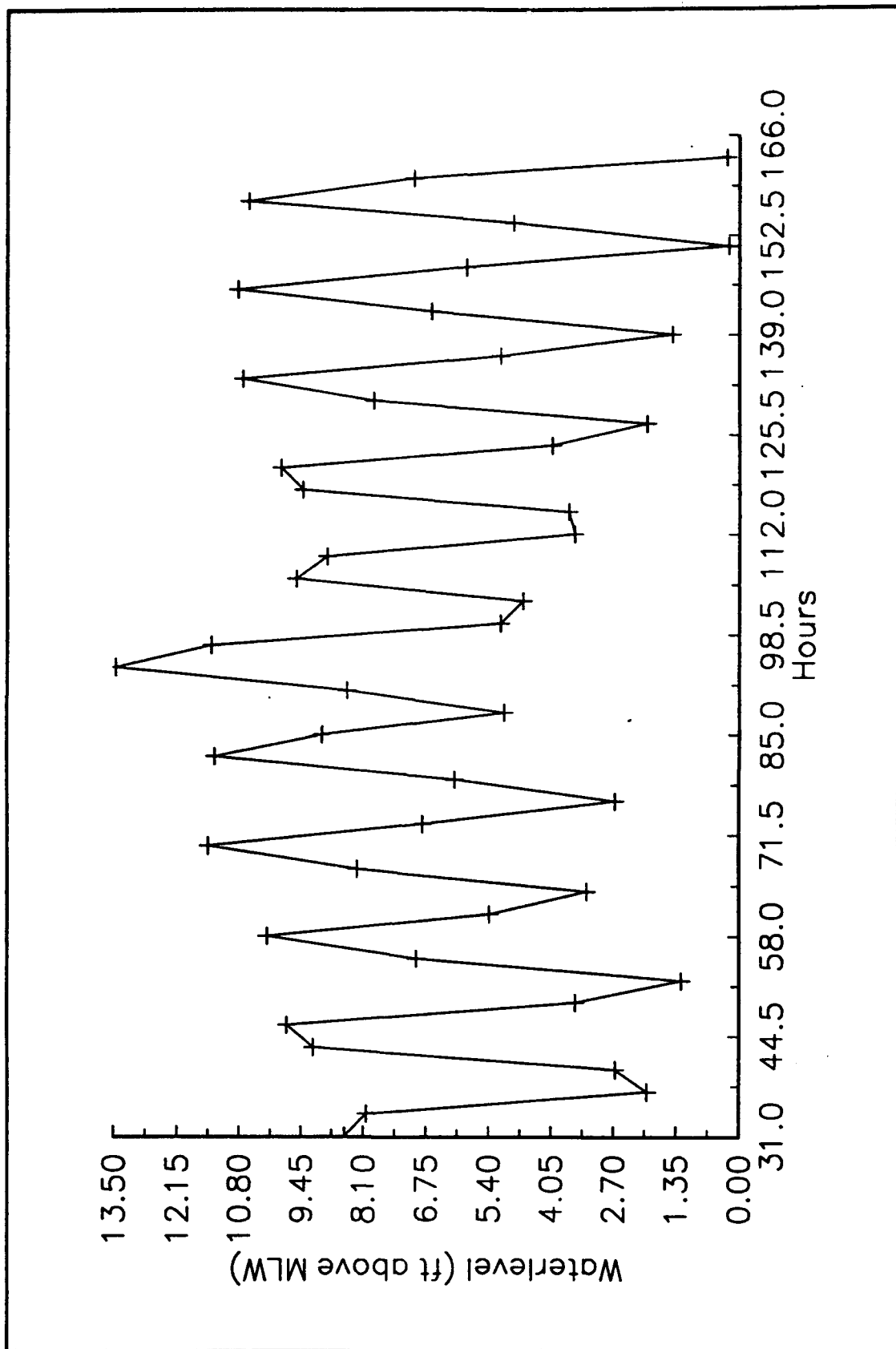


Figure 34. October 1991 storm water level time series

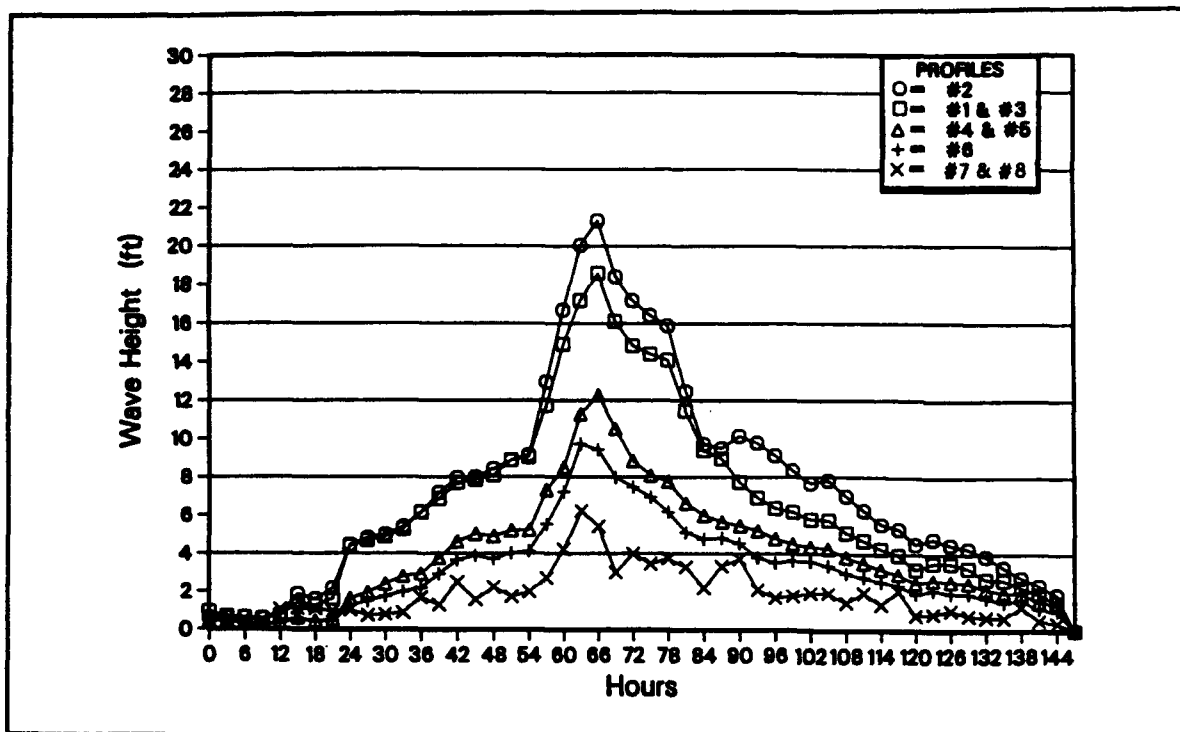


Figure 35. 1991 Halloween storm wave height versus time

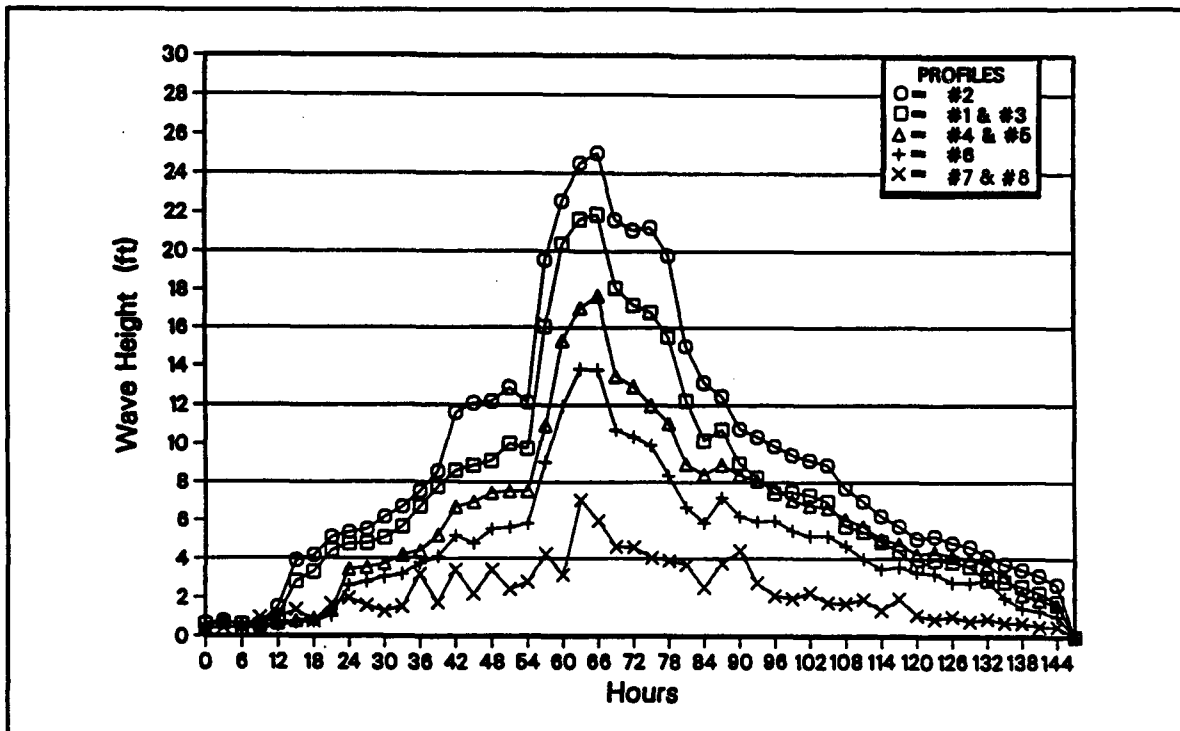


Figure 36. 1991 Halloween storm wave height versus time with -15-deg adjustment to incident wave angle

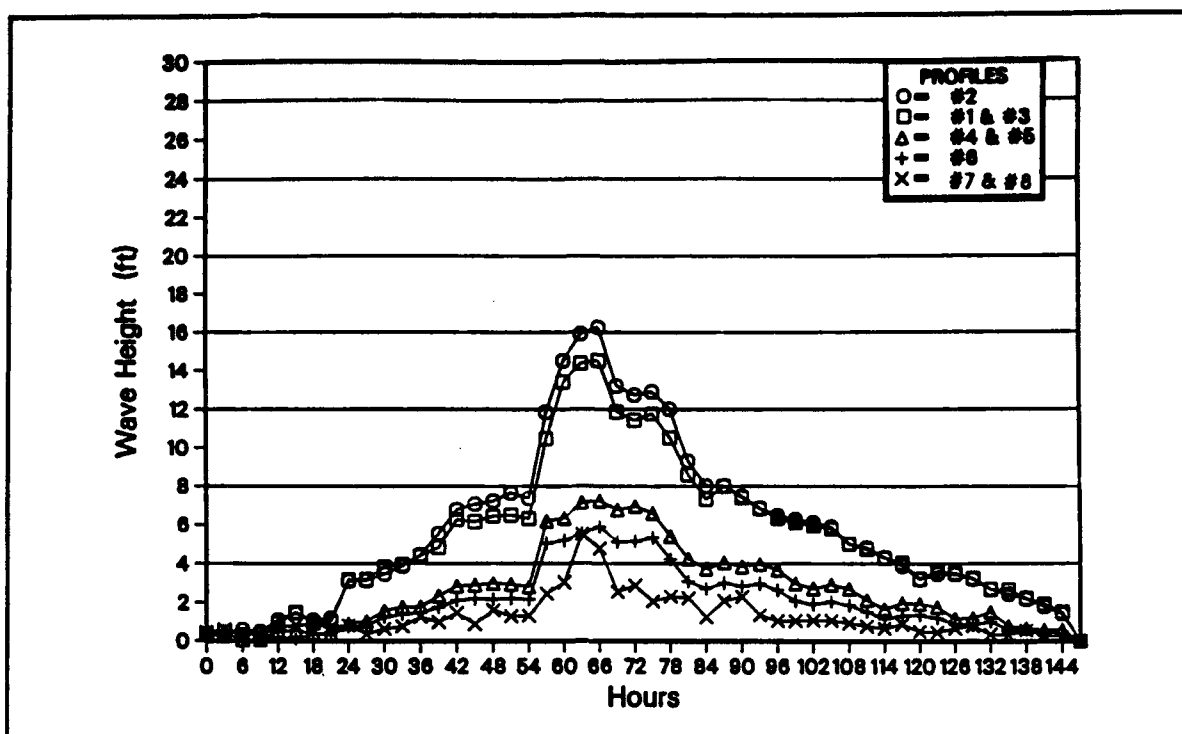


Figure 37. 1991 Halloween storm wave height versus time with + 15-deg adjustment to incident wave direction

3 Calibration and Verification of SBEACH with Halloween Storm Data

Overview

The cross-shore profile response model SBEACH was applied to evaluate beach profile change at Revere Beach and POP. Beach profile data acquired from the 1991 Halloween storm were used along with the transformed hind-cast wave data and measured water level data to calibrate and verify SBEACH. The model was calibrated using profile data measured at three locations along the study reach and applicability to the project site was investigated using various calibration parameters. Model calibration focused on optimizing foreshore erosion and dune response, while limiting overall differences between measured and predicted profiles, because overtopping predictions were of primary interest. Verification of the model for the Revere Beach and POP site was attempted using measured data, and an investigation of longshore and cross-shore processes was completed to analyze model results. A calibrated model was used to generate storm-induced profile response information, as well as profile and wave information to drive the ROTM. Sensitivity testing was conducted to evaluate the effects of varying wave direction and height, and beach grain size on relative profile response. Chapter 3 presents the results of this work and discusses effects of the results on work to follow.

Halloween Storm Data Set

Three profiles (Profiles 2, 5, and 7) shown in Figure 2 (Chapter 1) were available for evaluation of site response to the Halloween storm. Immediate pre- and post-Halloween storm profile response data were available, as was a later post-storm survey for Profiles 1-8. Surveys conducted on 30 October 1991 were taken during the initial stages of the storm and were used as pre-storm profiles for SBEACH calibration procedures. Post-storm profiles were

surveyed on 1 November 1991 and were used as final profiles for SBEACH calibration. The surveys described consisted only of the land-based portion of the profile and were augmented with hydrographic surveys taken during July 1991 (pre-storm) and December 1991 (post-storm).

Special attention was paid to Profile 7 data, since the pre-storm profile was reestablished due to the storm conditions present at the time of the survey. The reestablished Profile 7 was located approximately 150 ft northeast of Profile 7A, which refers to Profile 7 from previous work, renamed herein for convenience. Pre-storm survey data extended only 50 ft seaward of the dune; thus, the remainder of the profile was completed using December 1990 Broad Sound hydrographic survey data, photogrammetric maps from July 1991, and data from a Part I draft report (Driver, Bratos, and Rosati; in preparation).

Detailed information on the location of the profiles is shown in Figure 2 and Table 4. It is noted that all references made to the Revere Beach reach refer to Profiles 1-5 and all references to the Point of Pines reach refer to Profiles 6-8.

Table 4 Revere Beach Profile Locations				
Profile Number	Profile Starting Location		Station or Reach	Profile Length (ft)
1	737,490 ¹	514,340 ²	30 + 55 ³	10,302
2	737,930	516,040	48 + 21	10,422
3	739,290	519,000	80 + 84	9,882
4	741,510	522,090	119 + 10	9,271
5	742,950	523,380	138 + 70	9,516
6	743,750	524,100	Reach C	10,302
7	744,336	524,616	Reach E	8,944
7A	744,250	524,500	Reach E	8,944
8	744,750	524,900	Reach E	8,686
¹ Easting (ft) ² Northing (ft) ³ Station with respect to Elliot Circle (ft)				

An assessment of beach response to the Halloween storm was conducted using Profiles 2, 5, and 7, and additional profile data taken on 1 July 1991 and 27 November 1991 at Profiles 1 and 3. All profiles taken at the time of the Halloween storm (Profiles 2, 5, and 7) exhibit a loss of material during the storm (Figure 38). Profiles 1 and 3 (Figures 39 and 40) exhibit a gain

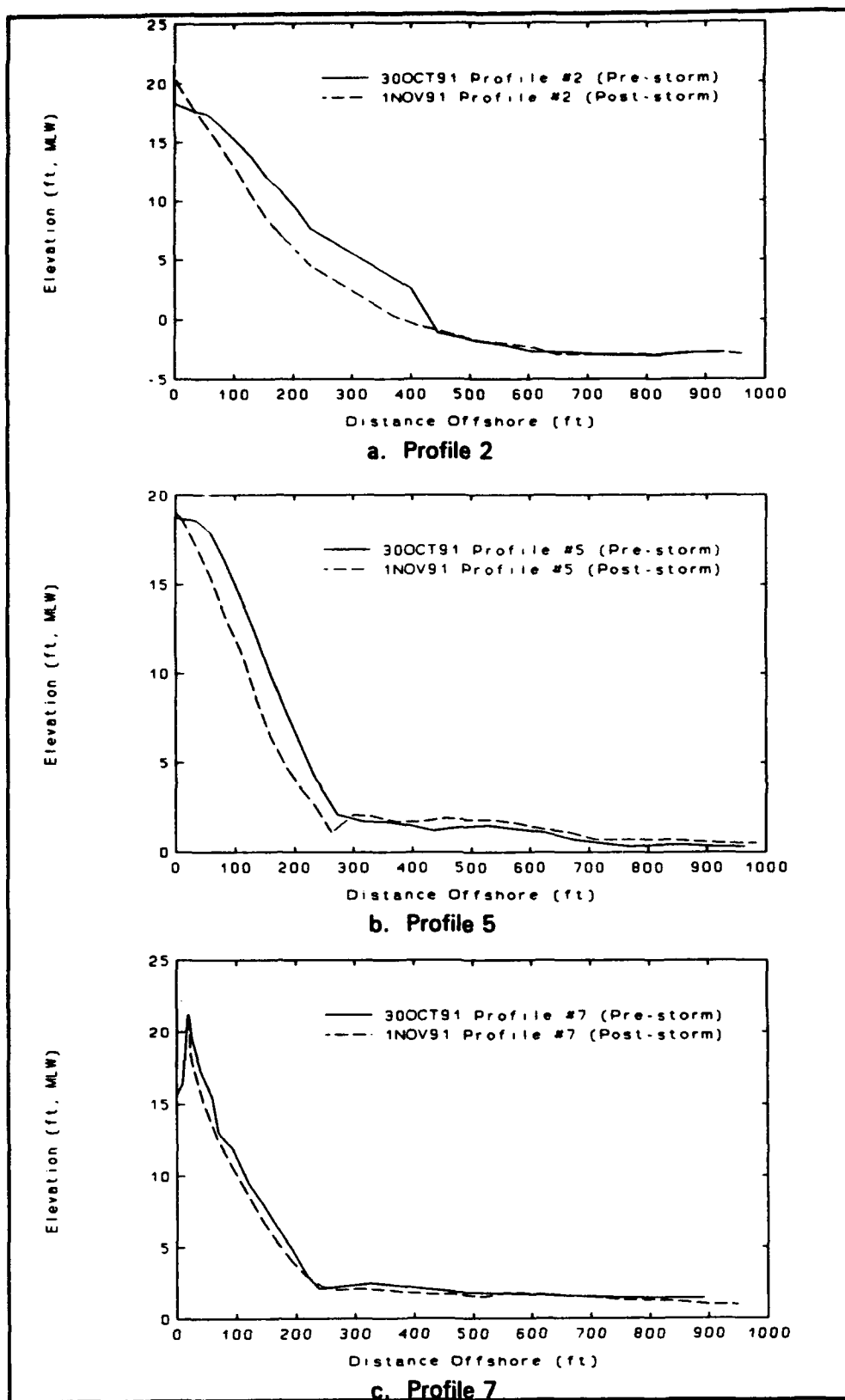


Figure 38. Measured pre- and post-Halloween storm profiles

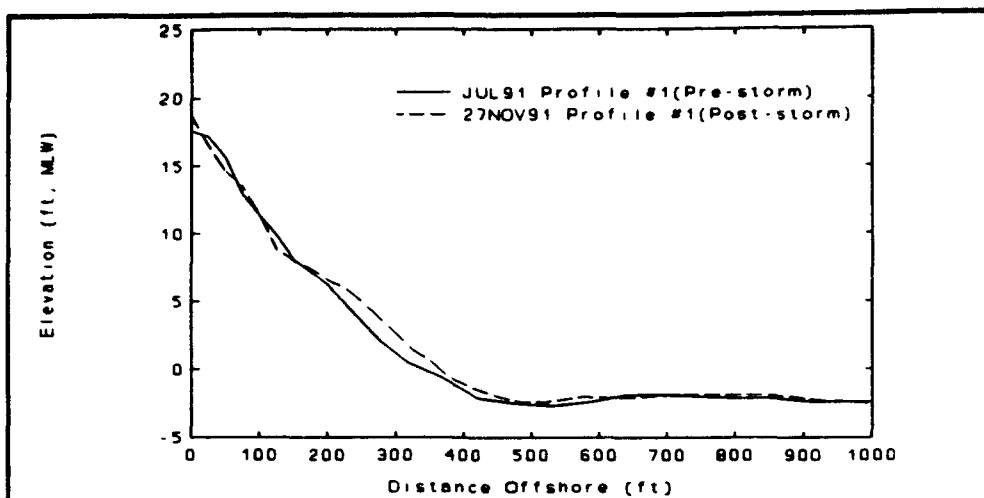


Figure 39. Halloween storm Profile 1

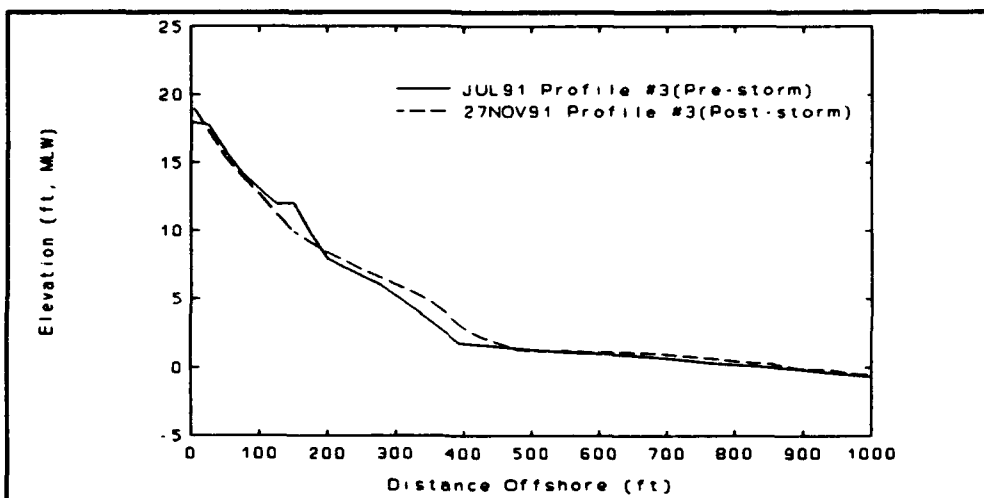


Figure 40. Halloween storm Profile 3

of beach material. It is noted that Profiles 1 and 3 were surveyed nearly 4 weeks after the storm, and likely include some post-storm recovery.

Comparison of pre- (30 October) and post-Halloween storm (1 November) profiles indicated a homogeneous stripping of material across each profile (Figure 38), with no bar formation as should normally be expected for a storm event. (Note that survey error is thought to have resulted in an apparent accretion at the end of Profile 5. The uniformity of difference between the pre- and post-storm profiles and a discontinuity at the seaward end of the land-based survey approximately 280 ft offshore give credibility to this conclusion). Volumetric losses decreased from southwest to northeast, with volumetric losses at Profiles 5 and 7 approximately 40 and 35 percent of the loss measured at Profile 2, respectively. Differences in losses are likely due

to increased wave energy at Profile 2 relative to other profiles, as well as changes in the sand supply on updrift beaches at given locations. This trend and the absence of any major seaward movement of material beyond approximately 500 ft offshore indicated the influence of nonuniform longshore sediment transport during the storm.

Additional post-Halloween storm (27 November) profiles were available for Profiles 1-8. Only Profiles 1 and 3 will be discussed due to a lack of any reasonable pre-storm data for Profiles 4, 6, and 8. Data from Profiles 1, 2, 3, 5, and 7 indicate complex sediment transport patterns occurred during the Halloween storm. Erosion/accretion characteristics are quantified in Table 5, which lists the calculated cumulative volumetric profile change as a function of distance offshore. These values indicate the distribution of volumetric change across the profile, thus better depicting profile response to the Halloween storm. Additionally, the changes 1,000 ft offshore are normalized by the volumetric change at Profile 2 at the 1,000-ft distance, thus representing the relative magnitude of change between profiles along Revere Beach and POP. Note that 1,000 ft offshore was judged as representative, because no significant movement of material occurred offshore of this distance.

The sediment transport patterns depicted in Table 5 are due, in part, to project sheltering by Nahant Peninsula, shoreline orientation, impoundment characteristics of Roughans Point, partial profile recovery, and differences between beach fill and native beach grain sizes. Specifically, gains at Profiles 1 and 3 are likely a function of a number of the above explanations. Profile recovery plays a role in the profile response exhibited at Profiles 1 and 3, but it is unlikely that the strongly accretional characteristics displayed are totally a result of recovery. Additionally, reduced wave energy (Profile 3)

Table 5
Volumetric Profile Changes (Halloween Storm)

Profile Number	Volumetric Changes(yd ³ /yd) vs Distance Offshore(ft)				Magnitude of Relative Change	Survey Dates	Profile Response Type
	500	1000	1500	2000			
1	30.0	37.1	37.1	33.7	0.31	1JUL91-27NOV91	Accretive
2	-120.0	-119.0	-115.0	-126.7	1.0	30OCT91-1NOV91	Erosive
3	11.2	21.4	27.0	31.3	0.18	1JUL91-27NOV91	Accretive
5	-62.7	-48.5	-34.6	-22.9	0.41	30OCT91-1NOV91	Erosive
7	-32.2	-40.1	-43.5	-46.4	0.34	30OCT91-1NOV91	Erosive

and impoundment characteristics (Profile 1) would allow the deposition of material introduced from the Profile 2 reach, with a reversal in transport direction occurring from Profile 2 to Profile 1 due to shoreline orientation. Historically this pattern of erosion (Profiles 2, 5, and 7) and accretion (Profiles 1 and 3) is similar to that observed during the Halloween storm, with Profiles 1 and 3 proving more stable due to the processes described.

Profile 7 experienced the least volumetric loss. However, it was anticipated due to greatly decreased wave energy that losses at Profile 7 would be a lesser percentage of losses measured at Profile 2. Profile 7 losses are attributed to the more erosive characteristics of the finer native material at that location as compared to the fill material. Additionally, visual observations indicated an accretion of material in the vicinity of Profile 6, thus allowing for volumetric losses with little compensation of material from updrift beaches.

Collectively, the data indicate nonuniform sediment transport was influential in distributing material along the project site during the Halloween storm. The trend of volumetric loss (Profiles 2, 5, and 7), accretion (Profiles 1 and 3), and the absence of any movement of material beyond approximately 500 ft offshore all indicate variable longshore transport rates. Based on historical observations, these trends are representative of storm response at Revere Beach and POP.

Previous analysis of Revere Beach response to the Halloween storm was conducted by U.S. Army Engineer Division, New England (CENED) personnel, excluding POP. Their findings supported the existence of a variable response along the project reach. The methodology adapted by CENED staff was based upon the determination of relative volumetric changes between November 1991 surveys and a design template when compared with an assumed 1987 profile. This method is well-founded to the offshore limit of the design toe; however, beyond this point it is an absolute comparison between the assumed 1987 profile and the measured 1991 profile.

Two analyses of volumetric change were completed by the CENED, one using the design toe as the offshore limit and one using the limit of the assumed 1987 profile. Results proved significantly different with the latter method resulting in a large volume of material deposited offshore of the design toe as a result of the Halloween storm. This deposited material was not distributed evenly along the project reach and the profiles tended to be either strongly accretive or erosive with a majority of profiles failing to conserve material. From this analysis it was concluded that cross-shore and longshore mechanisms were prominent during the Halloween storm, with the majority of the material remaining within the Revere Beach limits. This result is at odds with the large volume of material deposited along reach C (Profile 6) which indicates more pronounced longshore movement and a larger loss of material from Revere Beach to POP. Additional data indicated that some of the large areas of accretion previously found by the CENED had

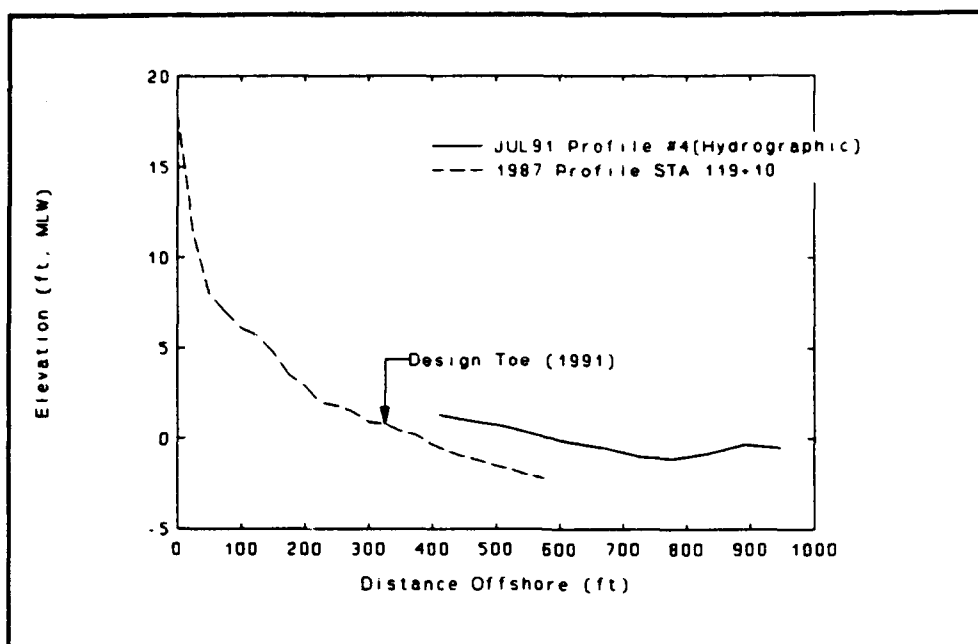


Figure 41. Pre-Halloween storm Profile 4

experienced a substantial amount of deposition prior to the storm. Figure 41 depicts Profile 4, which points to a large quantity of material depositing prior to the storm. This movement of material is an important fact and leads to the conclusion that the method using the design toe as the boundary is potentially more accurate. This analysis found a significantly higher volumetric loss for Revere Beach and would explain the source of material gained along reach C. It is evident, therefore, that losses at POP during the course of the storm were reduced through the introduction of material from the Revere Beach fill.

Project response to the Great Blizzard and December 1992 storms is qualitatively discussed for comparison with the Halloween storm to indicate effectiveness of the coarse fill, and clarify general site processes. The 1978 Great Blizzard had a peak water level of approximately 14.9 ft mlw measured at the Boston gauge, indicating a 100-year return period event. Peak wave height during the storm was approximately 20 ft just outside of Broad Sound, with a peak wave period of 12 sec and duration of 54 hr. As discussed, this storm caused extensive flooding and damage to Revere Beach and POP. The December 1992 storm, with a peak water level of approximately 13.9 ft mlw at the Boston gauge, was approximately a 17-year storm, similar to the Halloween storm. These northeasters, Halloween and December 1992, caused flooding at Roughans Point, and breaching of a dune at POP. However, at Revere Beach, the coarse beach fill provided protection of the seawall with little overtopping occurring. Despite water level differences between the Halloween and December 1992 storms, and the Great Blizzard, a comparison of storm effects on beach response indicates that the beach fill is very

effective in dissipating wave energy. Profile data indicate that little coarse material is lost offshore during extreme events.

Water levels and wind data

Water level data for SBEACH simulation of the Halloween storm were obtained from the NOS Boston gauge for the time period from 0600 on 28 October 1991 to 0600 on 11 November 1991. The peak water level observed during the storm was 14.0 ft mlw at 2200 on 30 October 1991, with a low-water level of 2.0-ft mlw at 0600 on 1 November 1991.

Wind speed and direction are used within SBEACH to calculate wind set-up effects on the water level. Wind input used in the simulations was obtained for Boston's Logan International Airport from the National Wind Data Index. Wind records showed a variation in wind speed from 13 to 32 knots with the origin of wind being consistently from the northeast. SBEACH proved to be insensitive to variations in wind speed and direction for this application. A constant wind speed and direction were chosen to represent the wind data for the duration of the Halloween storm. Winds were held constant as shore normal with a wind speed of 30 knots. These values were selected in order to account for maximum effects of wind setup on the water elevation.

Grain size

Calibration and verification of the SBEACH model were conducted along Revere Beach using the median grain size of the coarse-grained beach fill (0.49 mm). POP was modeled using the native sediment size of 0.21 mm.

It is noted that there is evidence from the 1 July 1991 beach surveys that some material redistributed prior to the Halloween storm. For instance, Profile 2 contained an accretional area that developed above mlw prior to the storm; thus, the composition of fill material had been altered. Other data indicate that sand had moved just offshore of the fill design toe before the storm, thus affecting the profile grain distribution. In addition, it is noted that beyond the toe of the fill, the profile consisted of 0.21-mm material with a portion of this possibly part of the active profile. The inclusion of the 0.21-mm material into the active profile would alter profile response relative to SBEACH results using 0.49-mm sand. One final consideration was the placement of an approximately 1-ft-thick aesthetic layer of 0.21-mm fill on the 0.49-mm material, potentially adjusting grain size characteristics and introducing an additional volume of material into the system. The data are insufficient to develop solid conclusions about the effects of these added factors, but it is necessary to consider the resulting effects on SBEACH output.

Waves

Wave data used in SBEACH simulations included wave height, period, and direction as computed using the REF/DIF nearshore wave refraction and diffraction model. Input wave conditions, computed using the procedures outlined in Chapter 2, correspond to the offshore boundary of each given profile and are input to SBEACH, which transforms the waves onshore. In addition, refraction/diffraction coefficients were generated by REF/DIF and used as input to an altered version of SBEACH, which implemented these coefficients to include the diffractive effects of Nahant Peninsula. These coefficients were interpolated over SBEACH profiles and allowed for more realistic modeling of wave transformation as affected by both refraction and diffraction. A detailed discussion of the methodology follows in a later section.

SBEACH Applications with Halloween Storm Data

SBEACH overview

SBEACH simulates cross-shore (two-dimensional) beach, berm, and dune erosion due to storm waves and water levels and was used to assess beach response at Revere Beach and POP as a function of the wave and water level database described in Chapter 2. The two-dimensionality of the model limits applications to locations where alongshore variations in wave, current, and transport processes can be neglected due to their uniformity. The model is driven by breaking waves and water levels that generate cross-shore sediment transport and beach profile change.

Version 2.0 of SBEACH was implemented in this study and has been updated to include variable cross-shore grid spacing, wind setup estimation, advanced breaking wave calculation methods, and a routine to simulate dune overwash (Rosati et al. 1993). SBEACH predicts the formation and movement of offshore bars, and is capable to a lesser extent of simulating beach recovery.

The model is founded on the calculation of cross-shore sediment transport, which is divided into four separate regions. The four regions across the beach profile are the pre-breaking zone extending to the offshore boundary from the breakpoint, the breaker transition zone extending from the breakpoint to the plunge point, the zone of broken waves, and the swash zone. Input to the model includes time-varying quantities such as wave heights, periods and angles; water levels; and wind speed and direction. Other input variables include water depth of input wave heights, median grain size, and initial beach profile characteristics. The empirical foundation and model formulation are described by Larson and Kraus (1989a). Sensitivity and verification of the

model using field data are discussed by Kraus and Larson (1988), Larson and Kraus (1989a), and Larson, Kraus, and Byrnes (1990). SBEACH Version 2.0 and the associated SBEACH PC interface are detailed by Rosati et al. (1993).

SBEACH modifications

Wave transformation within SBEACH is accomplished using linear Airy theory wave shoaling and refraction for pre-breaking waves. Shoreward of the breakpoint, wave transformation is described by a generalized form of the wave decay model of Dally, Dean, and Dalrymple (1985a,b). The standard version of the model does not account for diffraction, which is significant for the Revere Beach/POP study due to Nahant Peninsula. To account for these diffractive effects, SBEACH was modified and enhanced to make use of the refraction/diffraction coefficients computed by the REF/DIF nearshore wave model run in a linear mode. These coefficients were saved from each REF/DIF run and input to SBEACH, which enabled the model to better represent both pre- and post-breaking waves. The energy flux at each grid point was modified using the refraction/diffraction coefficients and used to compute the wave height at the next landward grid point. Use of this methodology allows SBEACH to better simulate wave transformation at the project site, thus improving model accuracy.

Calibration procedure

SBEACH was calibrated and verification attempted with Halloween storm beach profile data along with the transformed hindcast wave data and measured water level data. The model was calibrated using profile data measured at Profiles 2, 5, and 7, and applicability was investigated using various calibration parameters. The calibration parameters contained in SBEACH are an empirical transport rate coefficient K and a slope-dependent transport coefficient Eps . The transport rate coefficient K governs the time response of the profile to a given set of conditions with its effects seen in the foreshore erosion characteristics and dune erosion. Eps , the slope-dependent transport coefficient, affects the shape and volume of the offshore bar and adjusts the foreshore slope and erosive response dependent upon the bar shape.

Due to the necessity to estimate overtopping, model calibration was focused primarily on optimizing foreshore erosion (Revere Beach) and to a lesser degree dune response (POP), while limiting the differences between measured and predicted profiles. Prediction of correct foreshore recessions and dune elevations should yield more accurate wave, water level, and profile conditions at the shoreward boundary, thus resulting in more accurate overtopping estimates. Foreshore recessions are described as the recession of the beach face centered at approximately 10 ft mlw. The overall profile prediction error is defined as the sum of the squares of the difference between the predicted

profile elevations and the measured post-storm profile elevations at each grid cell.

Primary emphasis was initially placed on prediction of a correct foreshore recession. It was deemed necessary to select a method that would best represent the overtopping conditions at all three profiles along Revere Beach and POP. It was anticipated that the dune erosion at POP could be better predicted considering Profile 7 separately, but to best produce overtopping parameters for all three profiles the foreshore erosion was deemed most important. A number of calibration runs were completed and a final set of calibration parameters was chosen to best represent the foreshore erosion and to a lesser degree eliminate overall profile prediction error.

Calibration results

Calibration of the SBEACH model was conducted by varying the calibration parameters K and Eps . Each parameter has separate effects on the profile response, where K affects the cross-shore transport rates and Eps controls the depth of the trough shoreward of the offshore bar. K was varied from 0.5×10^{-6} to $2.5 \times 10^{-6} \text{ m}^4/\text{N}$ and Eps ranged from 0.001 to $0.003 \text{ m}^2/\text{sec}$. It was anticipated that the higher values of the parameters would best represent the profiles, for each measured profile experienced a relatively high amount of erosion in the nearshore region. The procedure began by selecting values of $K = 2.0 \times 10^{-6} \text{ m}^4/\text{N}$ and $Eps = 0.002 \text{ m}^2/\text{sec}$, with adjustment of the parameters dependent upon model results.

Figures 42-44 depict some calibration results for Profiles 2, 5, and 7. Calibration parameters are indicated adjacent to each figure. It is evident for Profiles 2 and 5 with higher amounts of erosion, that more erosive parameter sets yield better foreshore recession agreement, but agreement is still poor. Profile 7 experienced a lesser degree of erosion; thus, profile predictions using less erosive calibration parameters improved agreement. Table 6 lists errors associated with each predicted profile. Each error calculation is indicative of an individual profile and should not be used to infer accuracy of prediction relative to another profile. Figures 42-44, along with the error calculations, were used to select sets of calibration parameters.

Figures 42-44 depict poor agreement between SBEACH results and measured post-storm profiles. The lack of a conservation of material at each profile is the major problem for the model in this application. SBEACH assumes conservation of sand across the profile, but none of the measured profiles satisfy this criteria. It is evident that prediction improves for Profile 7 with the least measured volumetric loss. Profile 2 has minor profile response predicted where the only alteration is a slight foreshore erosion and an offshore movement of the fill material below 5 ft mhw. Response at Profile 5 is more severe at the seawall due to a steeper initial slope, which

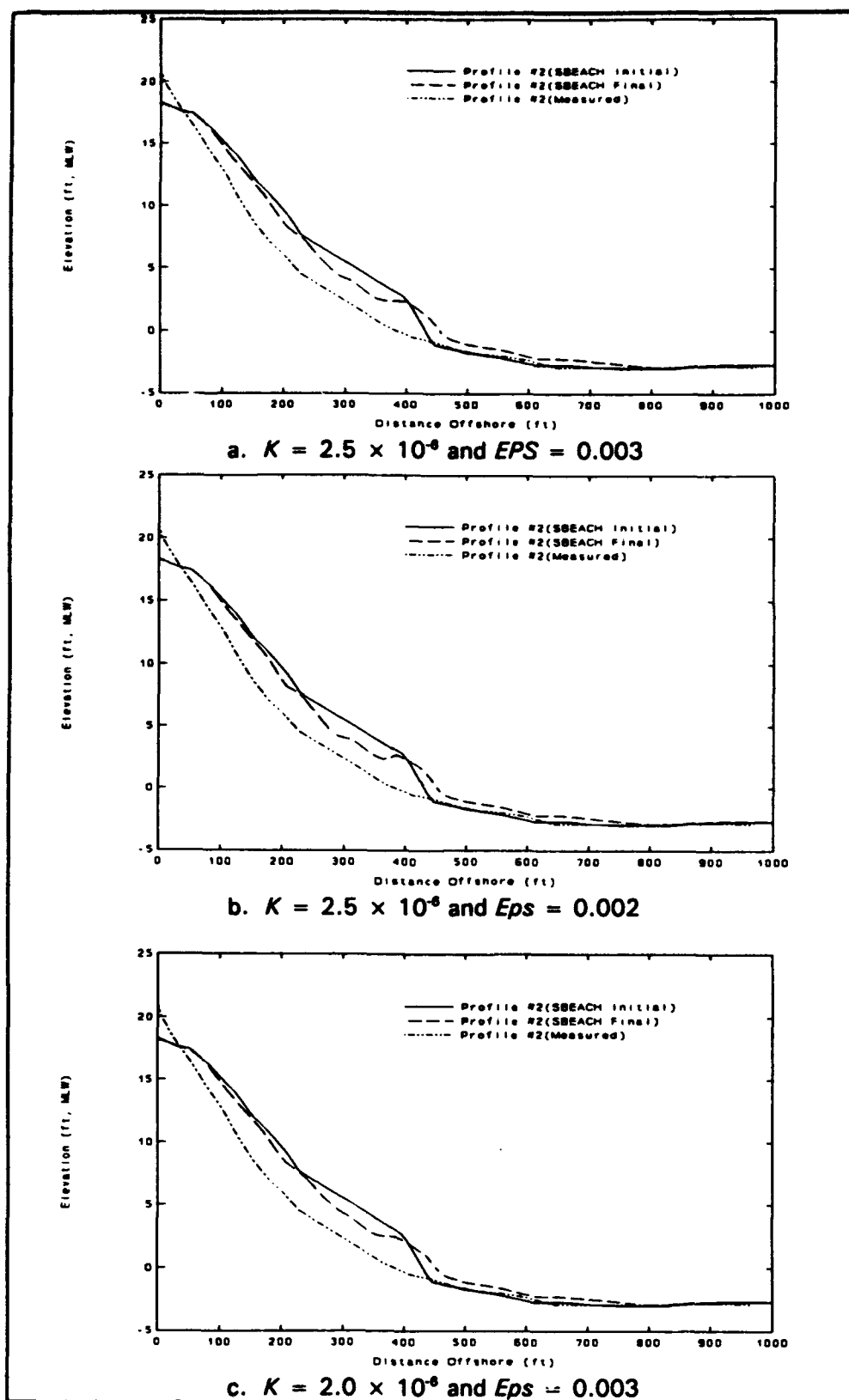


Figure 42. Calibration iterations for Profile 2 (Continued)

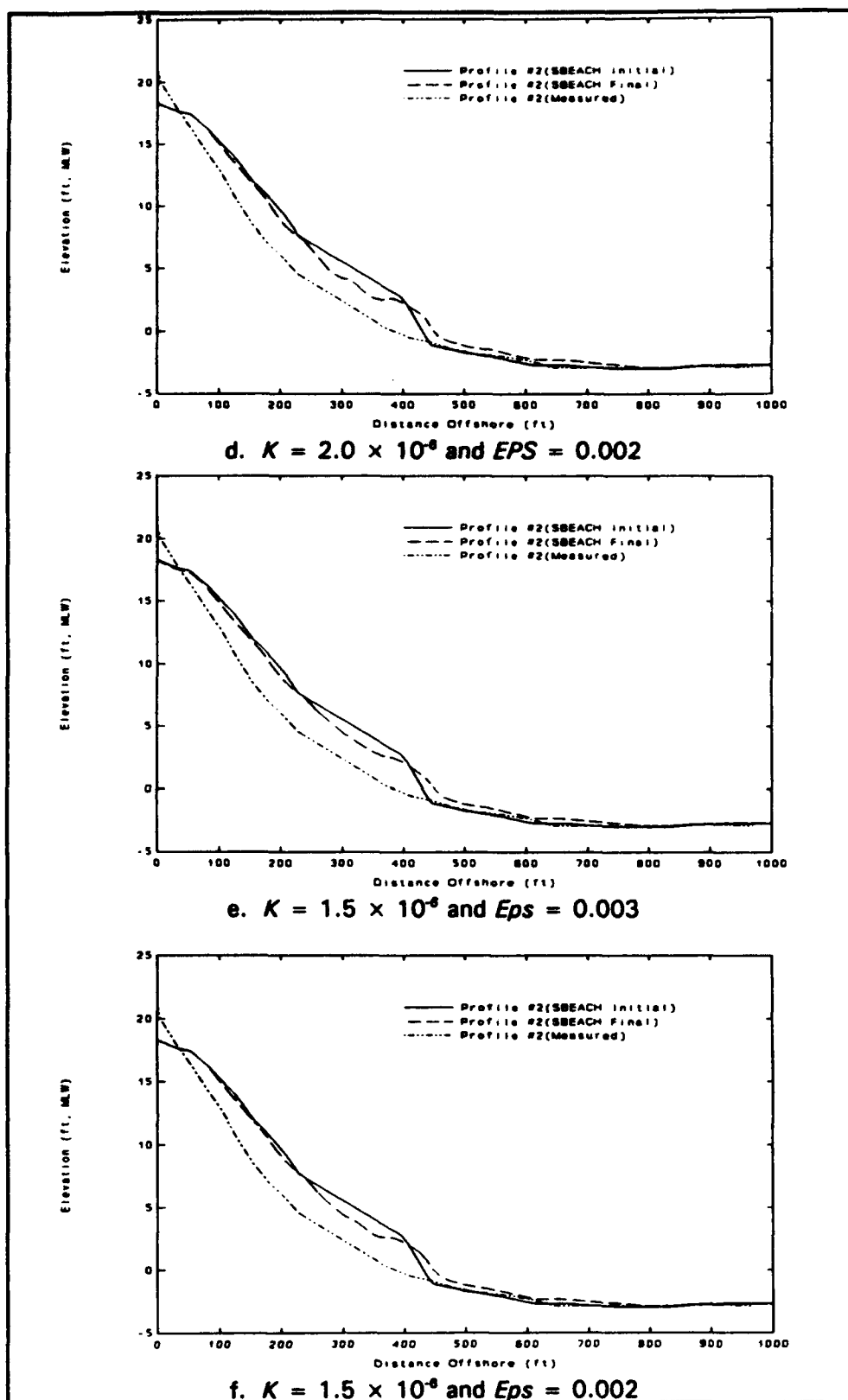


Figure 42. (Concluded)

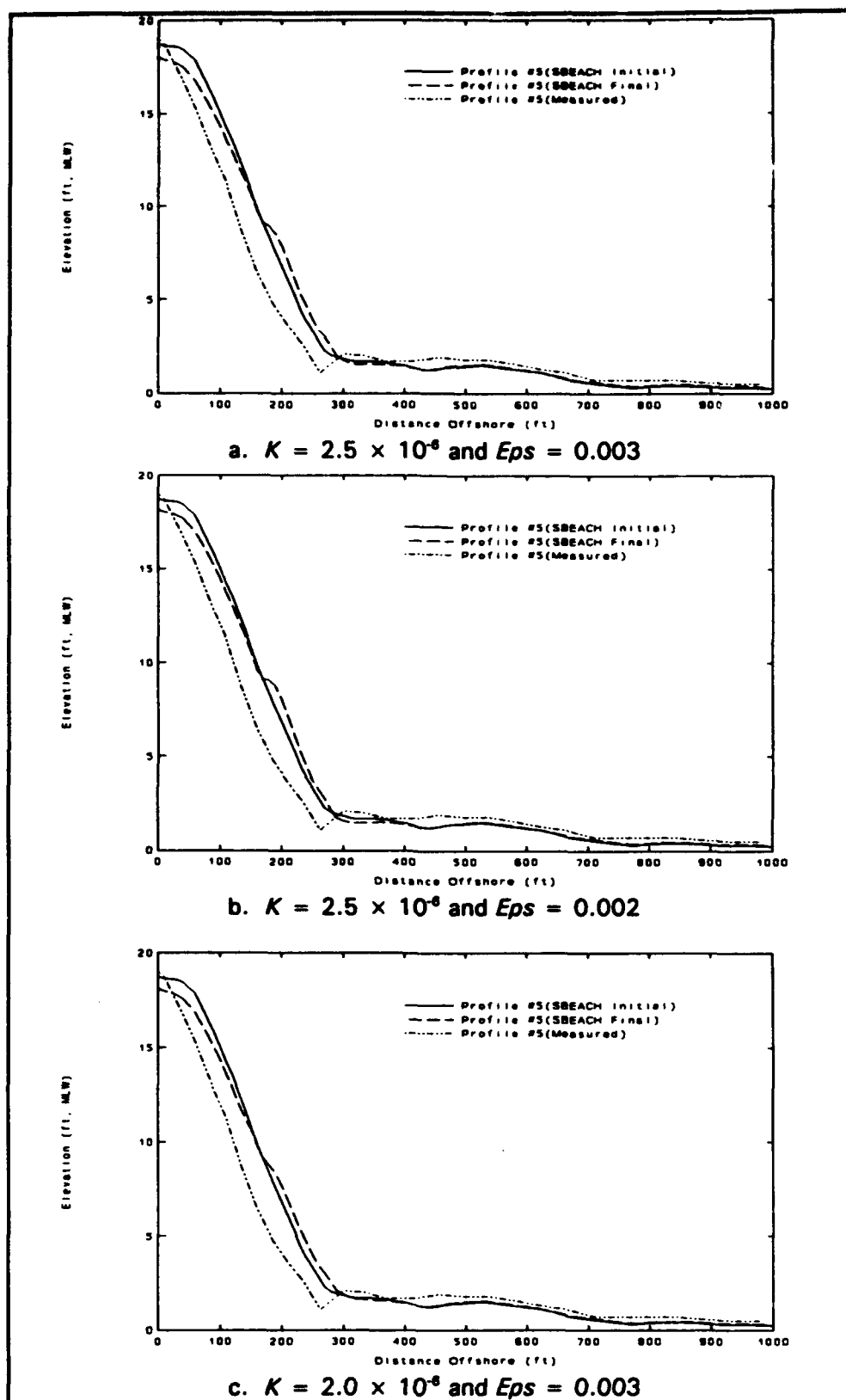


Figure 43. Calibration iterations for Profile 5 (Continued)

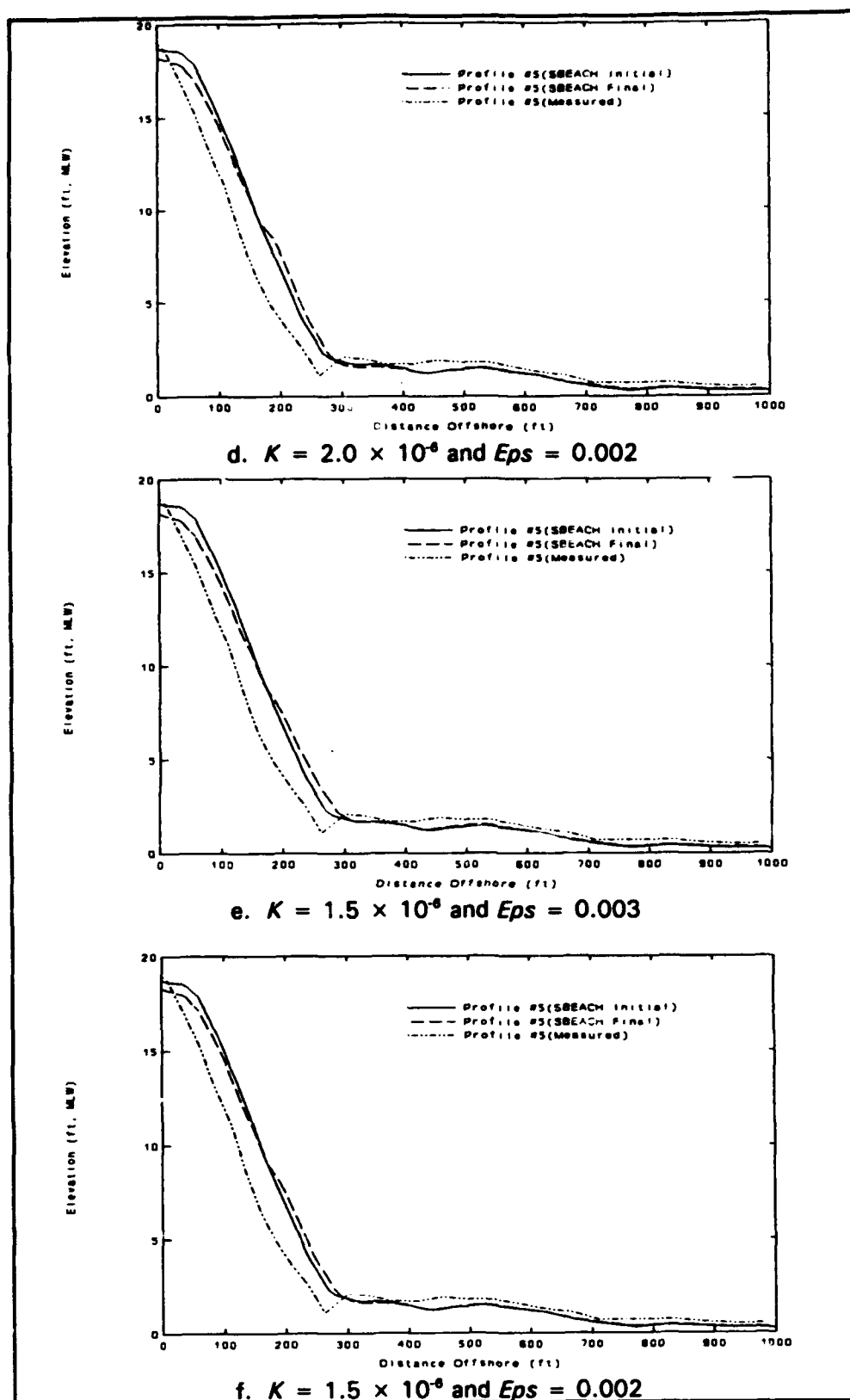


Figure 43. (Concluded)

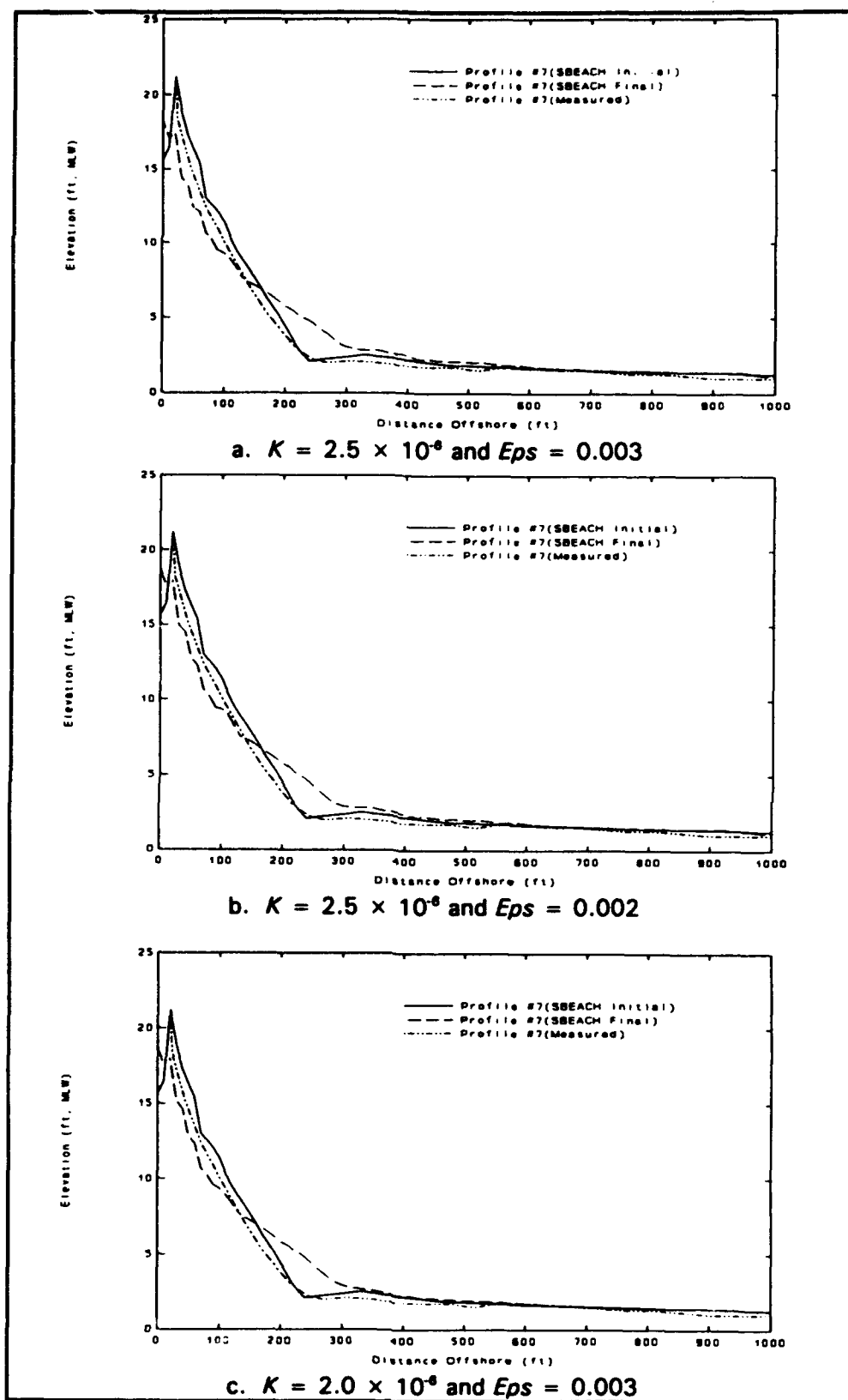


Figure 44. Calibration iterations for Profile 7 (Continued)

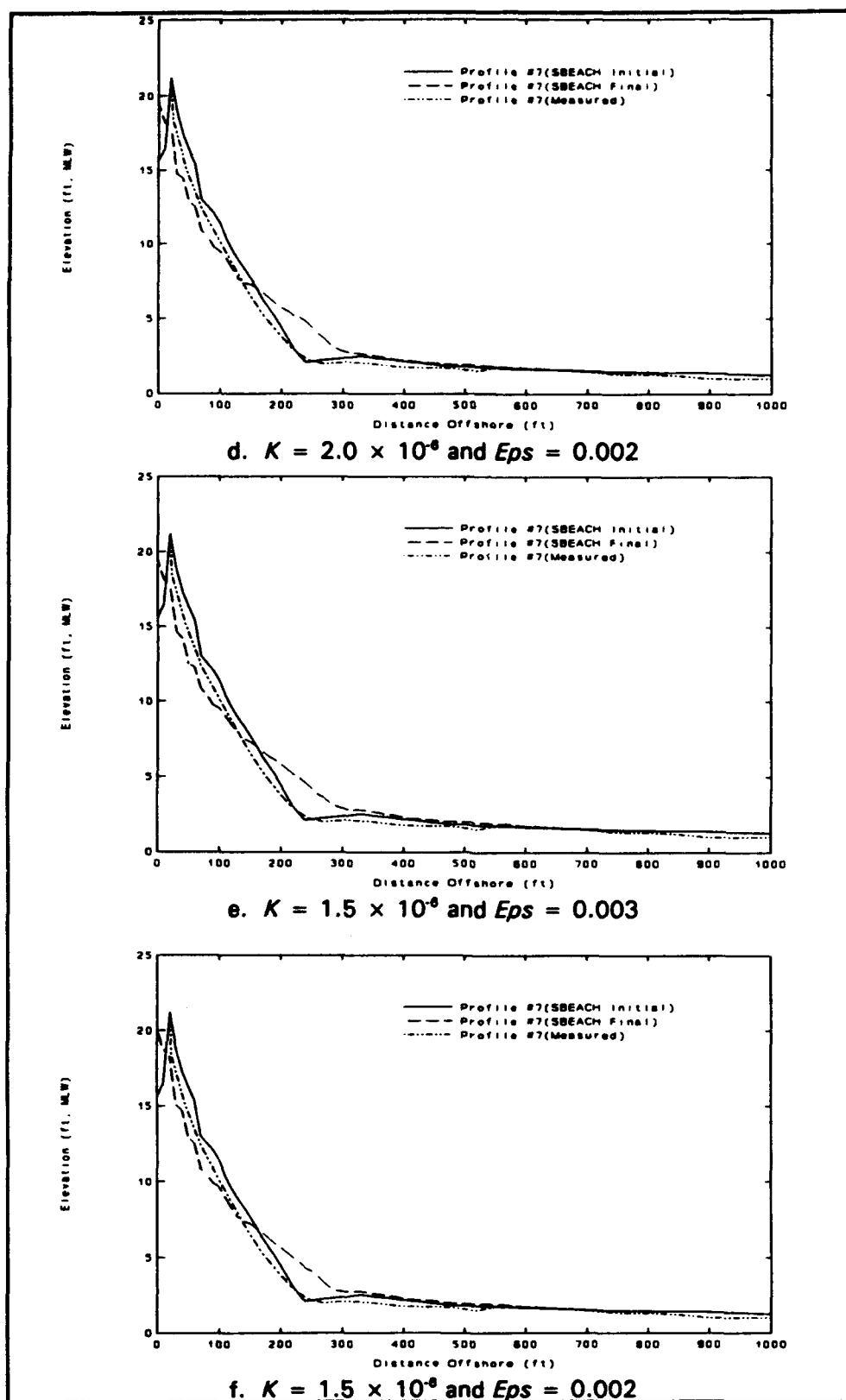


Figure 44. (Concluded)

Table 6
Error Calculations Associated with
SBEACH Calibration Sequence

Profile Number:		2	5	7
Calibration Parameters		Error of SBEACH Predicted Profile (ft ²)		
K	Eps			
2.5×10^{-6}	0.003	233.1	336.8	105.8
2.5×10^{-6}	0.002	240.4	339.0	94.5
2.0×10^{-6}	0.003	244.3	335.1	99.0
2.0×10^{-6}	0.002	250.9	338.8	89.3
1.5×10^{-6}	0.003	256.5	331.0	87.4
1.5×10^{-6}	0.002	263.8	335.6	74.8

allows more wave energy to attack the foreshore and swash portions of the profile. Profile 7 experiences the greatest predicted alteration of the three profiles examined despite decreased wave energy. A smaller grain size results in degradation of the dune and greater foreshore recession.

Calibration of Profiles 2, 5, and 7 as a group was unsuccessful; however, the effort illuminated some characteristics of the project site, augmenting observed profile response traits. In general, SBEACH predicts the formation of a profile approaching equilibrium, with the steeper profiles (Profiles 5 and 7) becoming more gentle, and the model filling the transition from the flat gentle slope to the steep beach slope at approximately 5 ft mlw. Response at Profile 2 shows an increase in beach slope with the offshore movement of material due to the large volume of material contained within the pre-storm nearshore profile. The absence of a predicted bar form out to the apparent point of closure (approximately 350 to 500 ft offshore for the Halloween Storm) is consistent with the lack of an observed bar, also confirming that the observed stripping of material from the profile was, most likely, due to material transport alongshore during the storm. The effort also supported the need to consider Profile 7 separately from Profiles 2 and 5, because of significantly altered waves and different beach grain size at POP. It was concluded that SBEACH could not be used to quantify profile response at Revere Beach (represented by Profiles 2 and 5), because of strong gradients in longshore sediment transport. However, the wave transformation capabilities of SBEACH at Revere Beach were considered to be superior to any other predictions planned by CENED, and use of the model for sensitivity testing of relative profile response for cross-shore dominated events was considered reasonable, given past SBEACH results. Note that the effects of longshore variations of longshore sediment transport have an uncertain effect on the

validity of sensitivity results at the project site, but past applications have indicated SBEACH as valid in determining relative effects of variable input parameters.

Calibration of SBEACH was conducted separately at Profile 7 due to promising results during the calibration of all profiles. More dominant cross-shore sediment transport mechanisms and greater conservation of material were indicative of a profile more suited for calibration of SBEACH. The longshore variability of longshore transport at POP is unknown, but it should be expected to be less than at Profiles 2 and 5 due to milder gradients in incident wave conditions. Figure 45 depicts the finalized Profile 7 calibration (calibration parameters of $K = 0.5 \times 10^6$ and $Eps = 0.001$). Calibration to a single profile, without further validation, suggests that results should be viewed cautiously. However, given the agreement shown in Figure 45, profile response simulations at POP were conducted to provide an assessment of profile response.

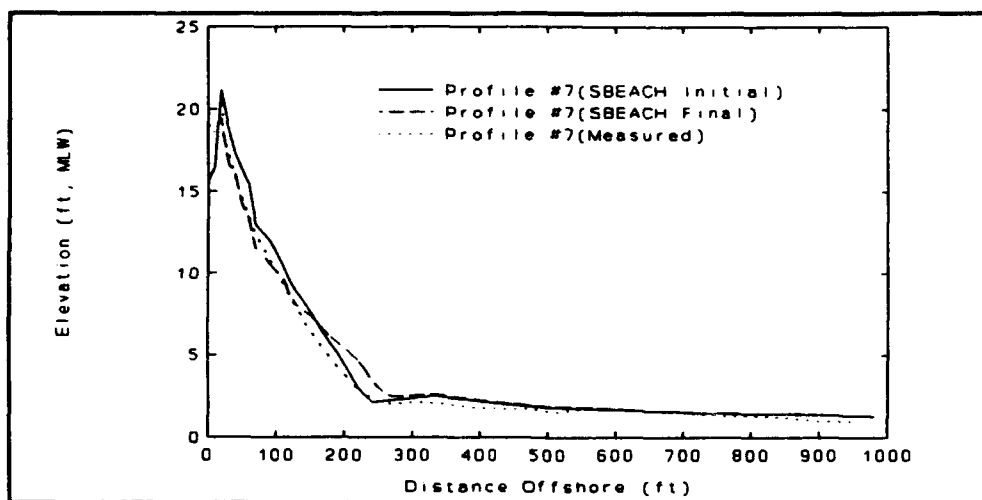


Figure 45. Predicted SBEACH results for the Halloween storm (Profile 7)

SBEACH Sensitivity Analyses

Overview

Sensitivity testing was conducted to evaluate the effects of varying wave direction and height, and beach grain size on relative profile response as predicted by SBEACH. Sensitivity testing was conducted with a standard set of calibration parameters ($K=2.0 \times 10^6$ and $Eps=0.003$). A single calibration parameter set was necessary for all profile sensitivity testing to allow relative comparison of wave angle and height, and grain size effects for the profile set. A relative change in erosion characteristics is presented as the

ratio between the recession of the 12-ft mhw elevation contour resulting from a base set of test conditions and the comparable recession resulting from the varied input (Table 7). The 12-ft mhw contour was deemed a representative contour given the water levels that characterized the Halloween storm. This ratio serves as an indication of sensitivity of the model and aids in determining input parameter effects on model results. Profiles are presented showing the specific adjustment of the profile resulting from the altered input (Figures 46-48) with measured Halloween profiles included for assessment of the relative magnitude of predicted profile response.

Wave height and direction

Halloween storm wave directions were adjusted by altering wave input by ± 15 deg. Using the REF/DIF wave transformation model, these adjusted wave directions were brought inshore to the SBEACH offshore boundary, resulting in different wave heights in addition to the adjusted angles. REF/DIF used altered wave angles to compute new sets of refraction/diffraction coefficients augmenting SBEACH wave transformation methods. Altering the wave angle alone at the SBEACH boundary would lead to an erroneous input data set in that the wave heights and angles, and refraction/diffraction coefficients, are interdependent in REF/DIF. For wave height sensitivity tests, wave heights were adjusted at the SBEACH offshore boundary by ± 25 percent to describe a range of model results dependent solely upon variation in wave height. Collectively, these tests provide for variations in wave output generated from offshore wave analysis and indicate project site coastal processes.

Sensitivity to adjustments of input wave angle appears to be profile dependent (Table 7 and Figure 46). For the alteration of the wave angle, there is no consistent link between the profile responses. Profile 2, because it does not experience significant sheltering from Nahant Peninsula for the wave directions tested, showed only minor dependence. Profile 7 showed minor variations, most likely because it is sheltered by Nahant Peninsula for the wave directions tested. Profile 5 was extremely sensitive to wave angle adjustments, with the foreshore beach response ranging from accretional to strongly erosional. Exposure of Profile 5 to different levels of wave energy, caused by variations of the diffractive effects of Nahant Peninsula, strongly influenced profile response for the evaluated wave angles. It is noted that results for Profile 2 displayed in Table 7 are distorted due to minor predicted recession distances; however, conclusions presented are supported by graphical interpretation of sensitivity tests.

Adjustment of the wave height at the SBEACH offshore boundary yielded results similar to sensitivity tests of input wave angles (Table 7 and Figure 47). Profiles 2 and 7 were insensitive to variations in wave height, whereas Profile 5 experienced a wide range of responses. Major differences

Table 7
Sensitivity Analysis Results

Profile Number	Change in Input Wave Angle (deg)	Grain Size (mm)	Change in Input Wave Height (%)	Relative Profile Response Change ¹
2	0	0.21	0	5.0
2	0	0.30	0	3.0
2	0	0.40	0	1.5
2	-15	0.49	0	0.9
2	+15	0.49	0	0.2
2	0	0.49	+25	1.1
2	0	0.49	-25	0.6
5	0	0.21	0	5.1
5	0	0.30	0	3.8
5	0	0.40	0	2.3
5	-15	0.49	0	2.8
5	+15	0.49	0	. ²
5	0	0.49	+25	2.4
5	0	0.49	-25	. ²
7	0	0.30	0	0.7
7	0	0.40	0	. ²
7	0	0.49	0	. ²
7	-15	0.21	0	1.0
7	+15	0.21	0	0.9
7	0	0.21	+25	1.1
7	0	0.21	-25	1.0

¹ Ratio of recession of adjusted 12-ft mhw contour to recession of actual calibrated 12-ft mhw elevation contour.

² Recession of 12-ft mhw contour did not occur.

in profile response were realized at Profile 5, with the reduction of wave heights resulting in an accretional profile response. Therefore, wave height sensitivity tests suggest a strong dependence at Profile 5, with profile responses at Profiles 2 and 7 appearing independent of the completed adjustments to the input wave data set.

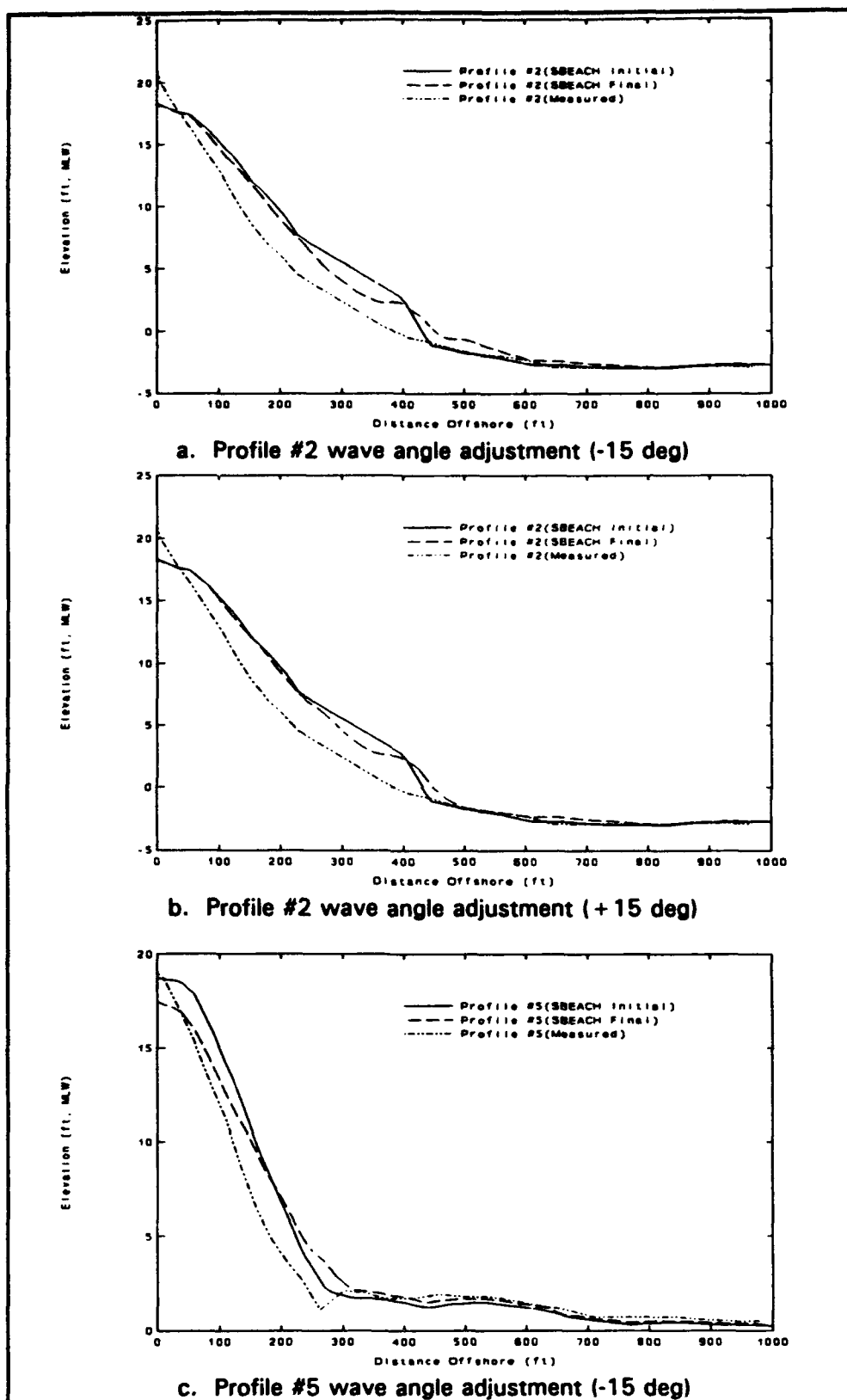


Figure 46. Wave angle sensitivity testing (Continued)

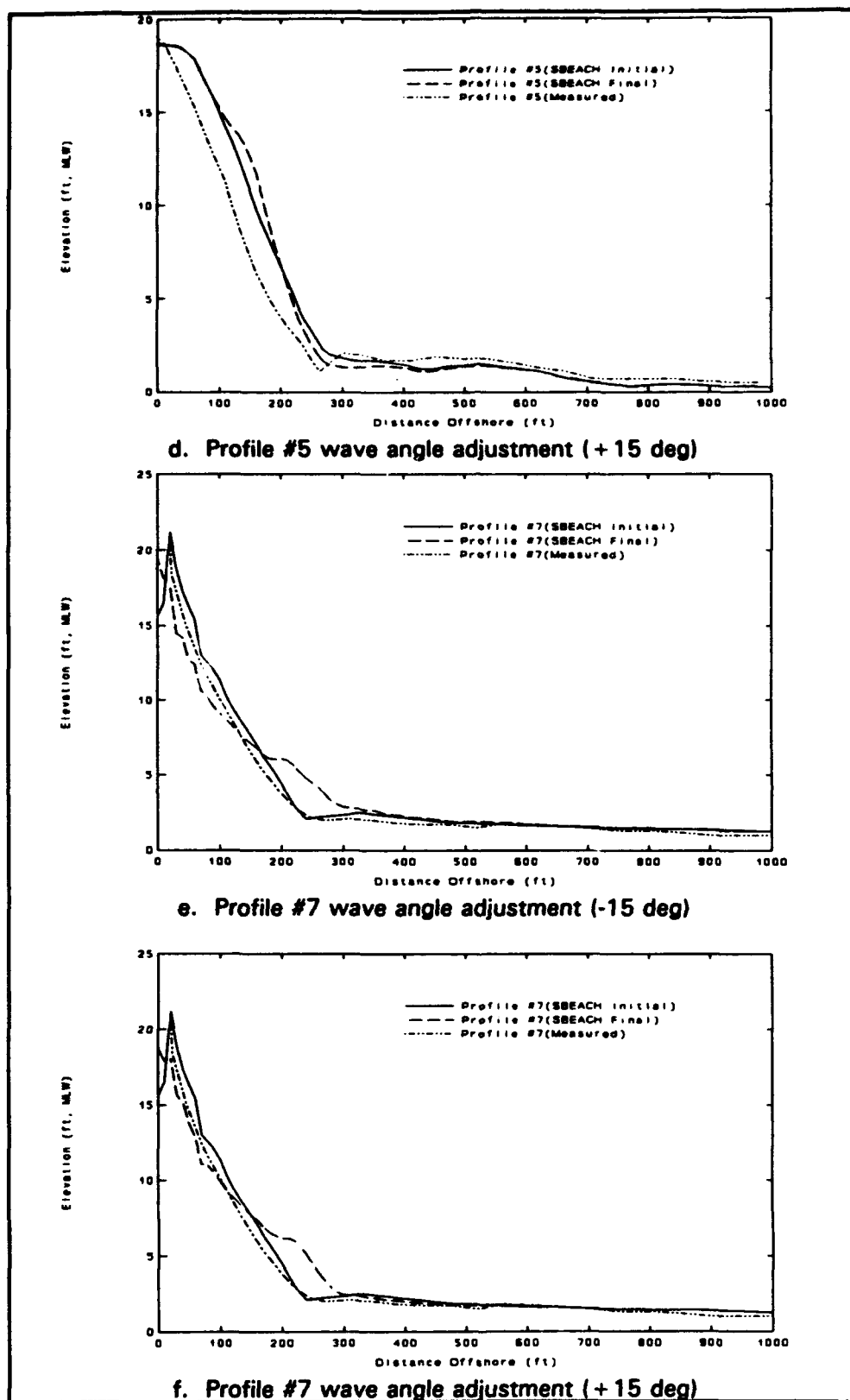


Figure 46. (Concluded)

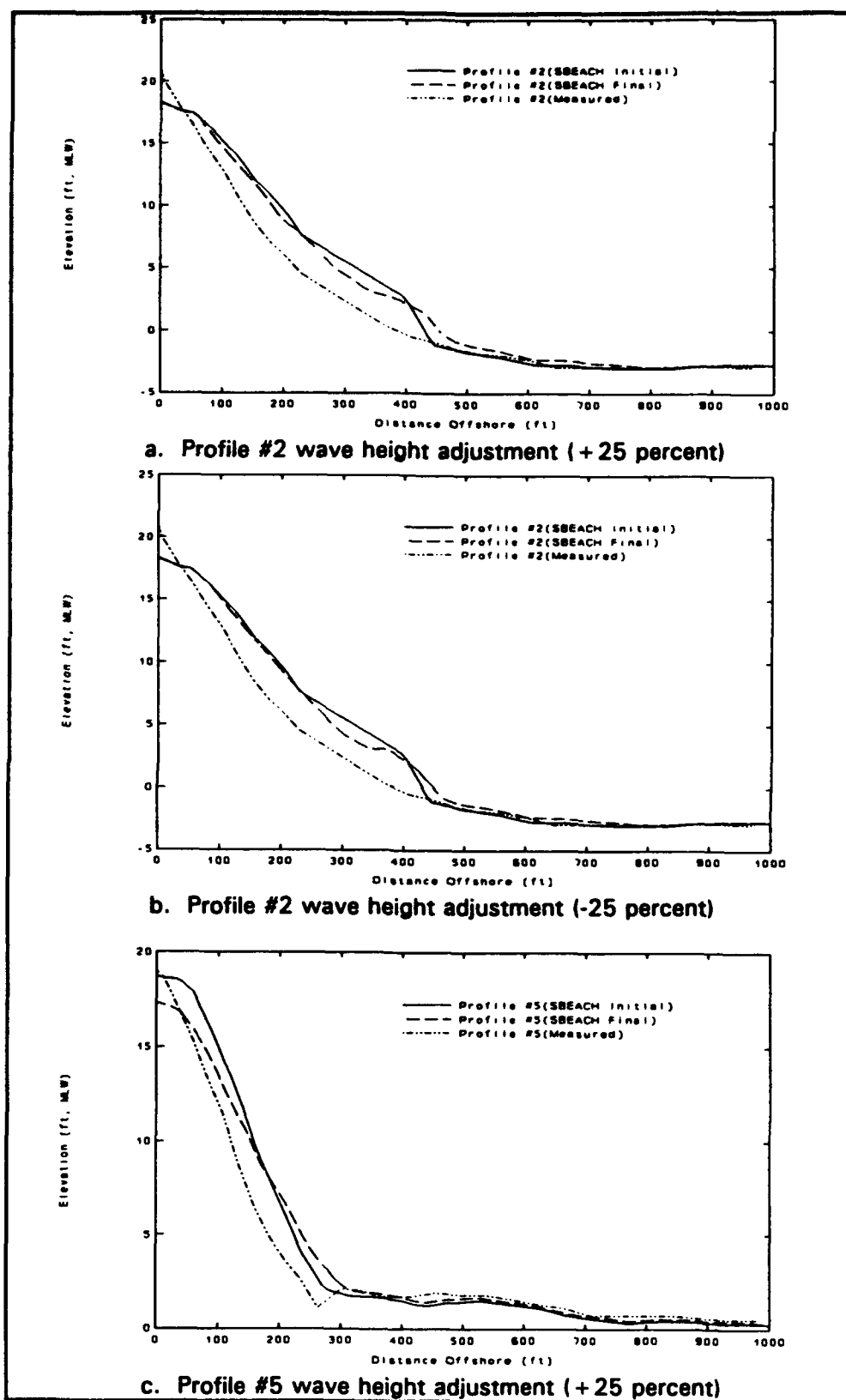


Figure 47. Wave height sensitivity testing (Continued)

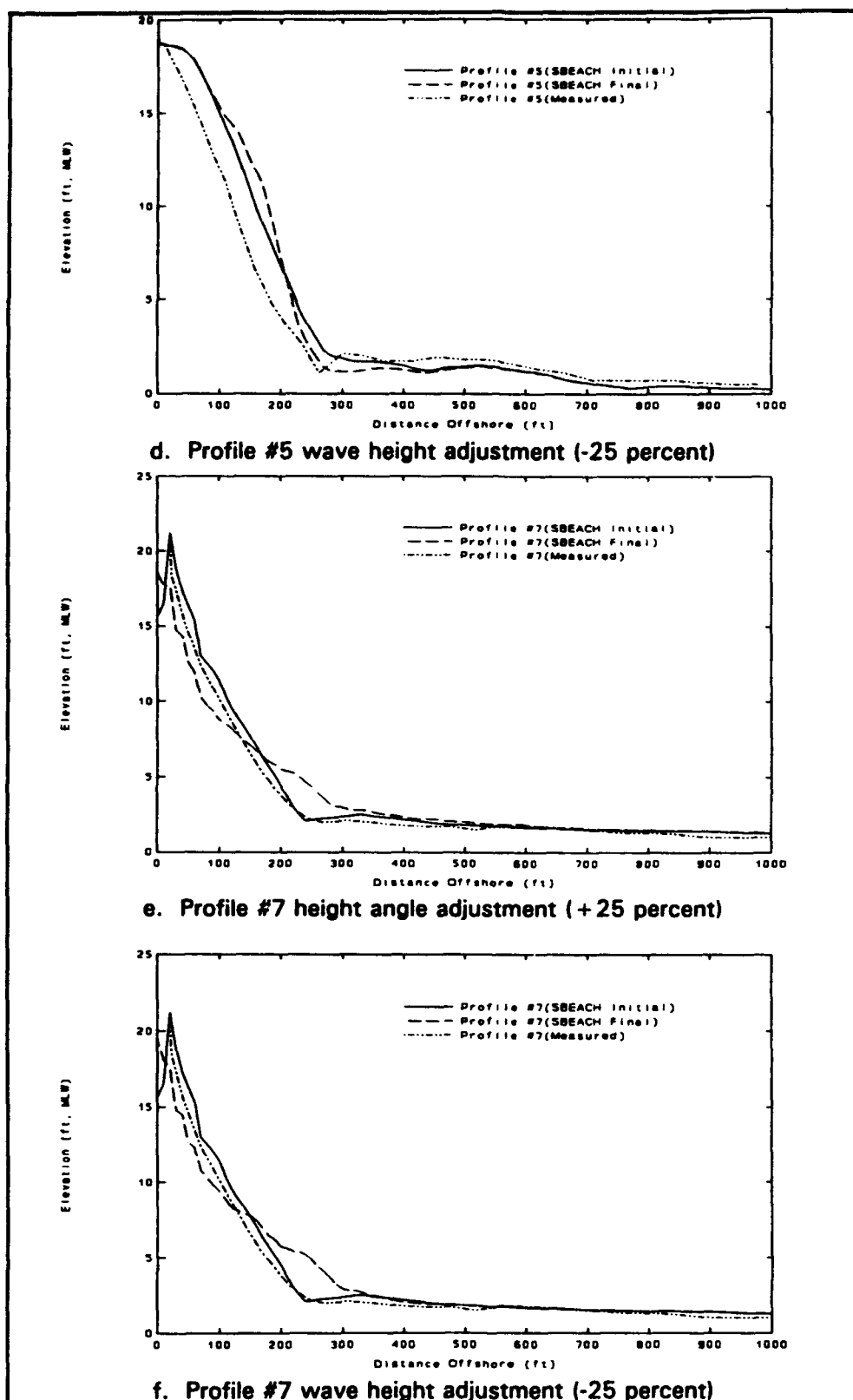


Figure 47. (Concluded)

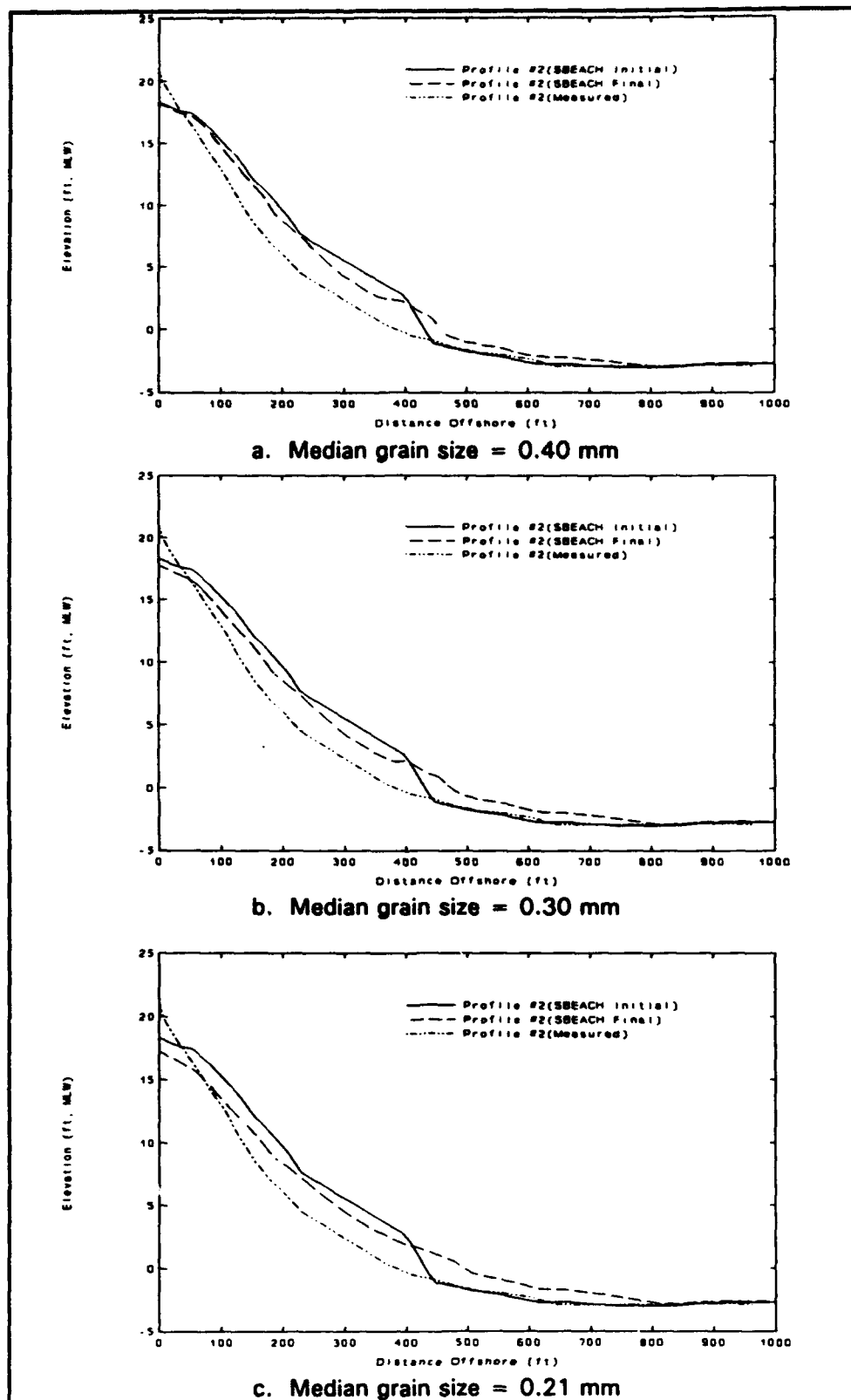


Figure 48. Grain size sensitivity testing (Profile 2) (Page 1 of 3)

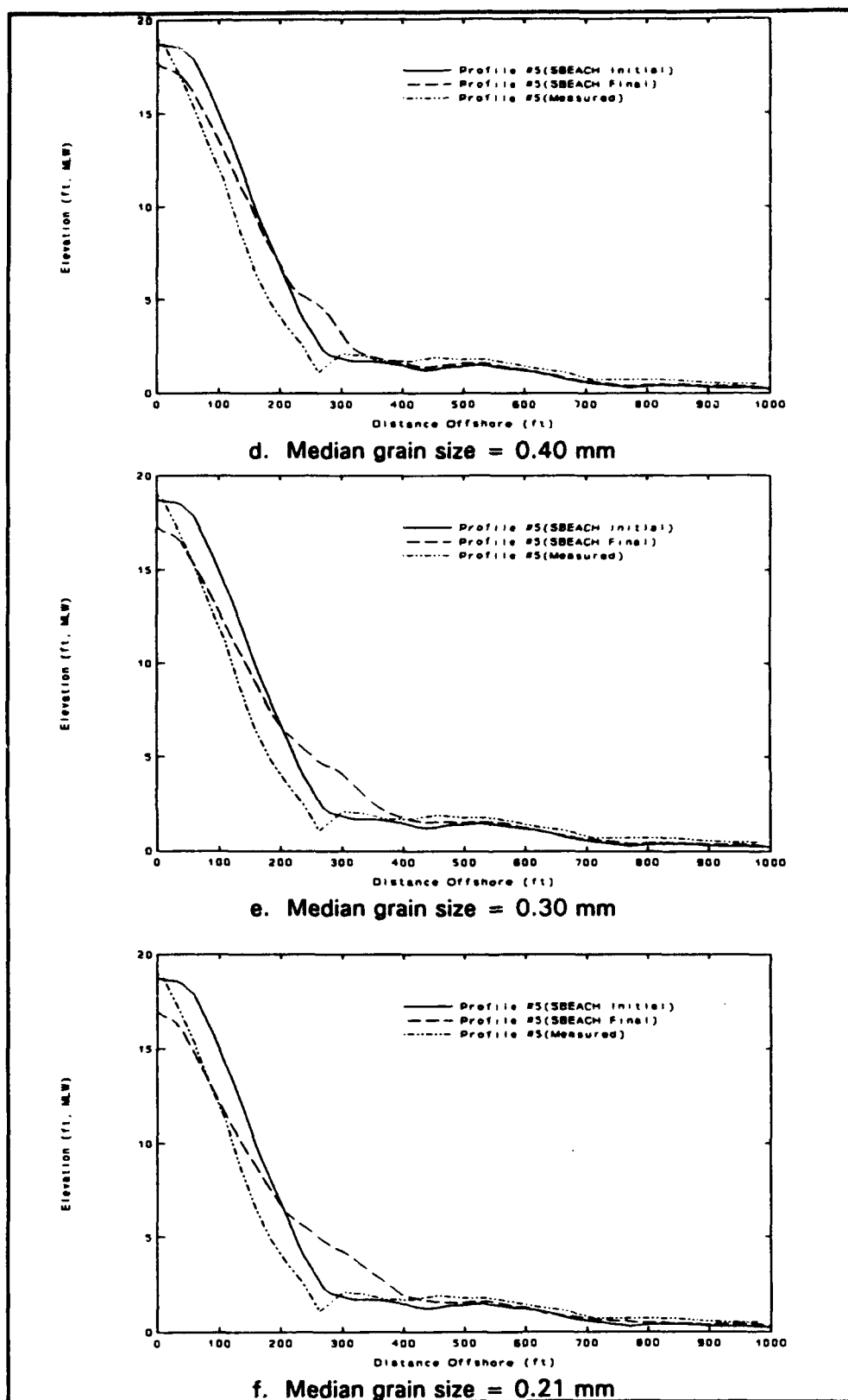


Figure 48. (Profile 5) (Page 2 of 3)

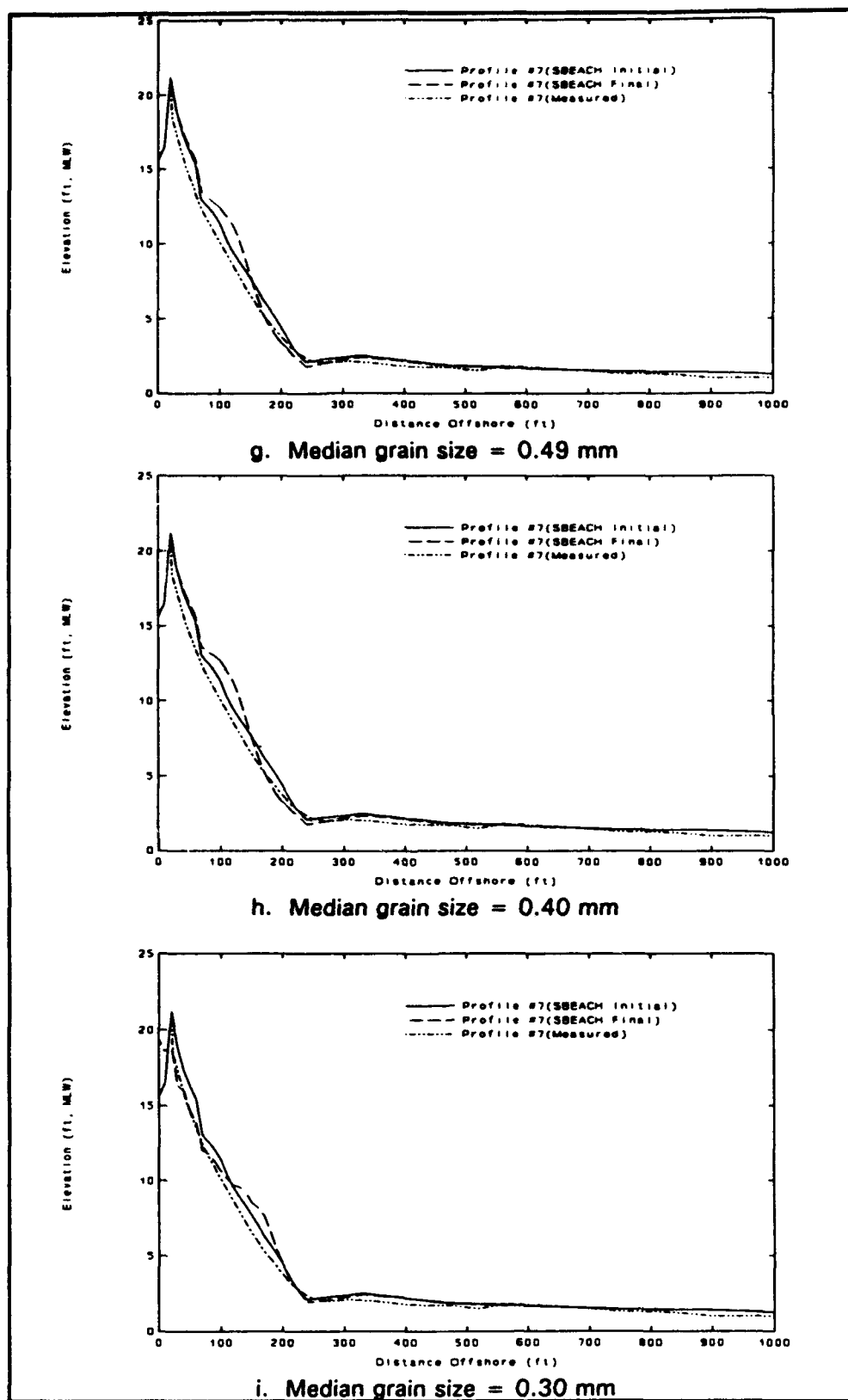


Figure 48. (Profile 7) (Page 3 of 3)

Wave sensitivity tests indicated that Profile 5 is most sensitive to adjustments of wave input with meaningful adjustments in profile response occurring during sensitivity tests. Responses at Profiles 2 and 7 showed no clear dependence on adjusted input, where differences for the wave angle and height tests were minor. The variable response during the wave data tests indicates that profiles were subject to different wave transformation processes, thus responding to testing in different ways. Finally, it is evident that an accurate input wave data set is necessary; however, only at Profile 5 does there appear to be substantial sensitivity to wave input.

Grain size

Sensitivity of SBEACH output to median grain size was conducted to indicate the extent of protection to be expected for a given fill material. Relatedly, project observations (visual and profile data) indicated significant longshore movement and sorting of the fill material; therefore, assumption of a median grain size in SBEACH might be further compromised by longshore processes in addition to inherent limitations due to cross-shore sorting. Grain size testing provided an error estimate for the median grain size assumption, as well as indicating the median grain size required to realize benefits of a coarse-grained beach fill.

Sensitivity testing was conducted using four median grain sizes: 0.21 mm (native), 0.30 mm, 0.40 mm, and 0.49 mm (beach fill). Results indicated that an apparent boundary existed at approximately 0.40 mm, with erosive resistance significantly reduced below this level (Table 7 and Figure 48). Profile 7 (Figure 48) maintained a dune form for the 0.40- and 0.49-mm median grain sizes, but experienced significant dune degradation for smaller grain sizes. Similarly, Figure 48 indicates that Profiles 2 and 5 suffer higher levels of foreshore recession below the 0.40-mm grain size with less noticeable differences between the 0.40- and 0.49-mm results. Table 7 results support the inferred grain size dependency evident in simulated profile responses. Profiles 2 and 5, for the pre-fill 0.21-mm grain size, indicate recession approximately five times that estimated for the 0.49-mm material. At Profile 7, recession of the 12-ft elevation contour fails to occur for larger grain sizes. Similar results were found by Larson and Kraus (1989b) with eroded volumes decreasing significantly through the range of 0.2 to 0.40 mm and decreasing less noticeably above 0.40 mm.

Sensitivity testing indicated that grain size is the major parameter consistently affecting SBEACH results, with benefits realized for median grain-sized material greater than 0.40 mm. Predicted results also suggest that the 0.49-mm material is resistant to erosion. These modeling results are consistent with the degree of unexpected protection provided by the coarse-grained beach fill at Revere Beach during the Halloween storm.

Role of Longshore Processes

The importance of longshore processes during the Halloween storm was discussed in previous sections based upon profile data, visual observations, and engineering judgement. The importance of longshore processes led to the decision not to use SBEACH to predict quantitative profile response at Revere Beach. Longshore variations in longshore transport were then evaluated using wave data and empirical sediment transport equations. Wave output from SBEACH was used to calculate the potential longshore transport at Profiles 2, 5, and 7 using the "CERC" formula described by the *Shore Protection Manual* (SPM 1984), and the formula given by Kamphius (1991). SBEACH was modified to calculate sediment transport rates using breaking wave data obtained from the model. Predicted rates are presented as relative values normalized using the transport rate calculated at Profile 2, similar to relative volumetric changes presented in Table 5. Results are listed in Table 8. Values using the SPM method appear distorted due to the extreme transport rate computed at Profile 2 relative to the rates calculated at Profiles 5 and 7, but a trend is apparent.

Table 8 Predicted Relative Longshore Transport Rates (Halloween storm)			
Profile Number	Magnitude of Relative Volumetric Change (see Table 5)	Relative Transport Rate	
		CERC Formula	Kamphius
2	1.00	1.00	1.00
5	0.41	0.05	0.20
7	0.34	0.03	0.16

Results using the Kamphius formula show that relative change in the predicted transport rate parallels the trend of relative volumetric losses. These parallel trends indicate that the gradient of longshore transport lessens towards POP, with a tendency for movement and deposition of material into the POP area due to the decreasing ability of the longshore current to transport material. Deposition of material along POP agrees with earlier conclusions concerning sediment redistribution, and lends credence to previous analyses. Furthermore, these results, as well as dune profile response simulations to be discussed in a forthcoming section, indicate that material potentially moved into the POP area during storms may help buffer the berm/dune system.

Profile Response Simulations at POP

Calibration and verification of SBEACH was shown to be more successful at POP (Profile 7) due to a reduction in the longshore transport gradient as shown above. Thus, application of the model to simulate profile response at POP could be completed with more confidence. Results of profile response simulations would be indicative of dune capabilities, further defining flood protection provided by the dune system. SBEACH simulations were conducted using the 23-ft mhw dune crest elevation and the set of 50 storms. Results for Profiles 6-8 are located in Appendix F. Calibration parameters were set based upon the improved results at Profile 7 with $K = 0.5 \times 10^6$ and $Eps = 0.001$.

Profiles 7 and 8 appear to be highly resistant to erosion for all storms, with Profile 6 experiencing slightly more profile degradation for the November 1945 events. As will be discussed in conjunction with dune optimization, Profiles 7 and 8 exhibit a buffering of the dune with the transport of material onshore due to the coarse grain size, low wave heights, and long period waves associated with the extreme events. Only at Profile 6 does it appear that any notable erosion occurs due to the storm set. Overall, minor degradation of the dune system is predicted with negligible response predicted for a large number of the simulations. Furthermore, the influence of longshore transport has been observed to offer additional material into the POP littoral system, resulting in potentially higher erosive resistance during the Halloween storm, and thus indicating that similar buffering is possible for other events.

Model results indicate that a beach/dune system at POP constructed of the 0.49-mm sand would be very resistant to erosion and provide considerable overtopping protection, even considering model limitations and the limited data available for SBEACH validation. A lack of flooding at Revere Beach and observed beach responses during recent storms appear to verify the modeling results and discussed conclusions.

4 Development of Runup and Overtopping Module

Overview

CENED required evaluation of a number of flood protection design options by predicting levels of potential overtopping in response to the storm database. A runup and overtopping module (ROTM) was developed that uses wave, water level, and profile response output from SBEACH, as well as profile structural characteristics determined by CENED. Despite limitations in the ability of SBEACH to accurately simulate beach change at Revere Beach, it was decided that the model output constituted the best available information. Overtopping rates are determined for selected profiles and structural conditions along Revere Beach and POP, and integrated along respective sections throughout the design storm to determine potential overtopping volumes.

Development of the ROTM progressed iteratively until a partially verified module was employed to quantify overtopping volumes in response to the wave and water level database described in Chapter 2. The initial ROTM consisted of existing methodologies found in the technical literature base that were selected based upon suitability to the project site and intent of study. Field data were utilized in an attempt to calibrate and verify the initial ROTM. Following the calibration stage, a physical model study of overtopping was initiated to better define overtopping processes at the site. Finally, a partially site-specific ROTM was developed using regression analyses for a subset of overtopping conditions present during simulation of the storm database. This chapter focuses on the development of the ROTM and describes physical model issues only pertaining to the rationale behind the ROTM. Details of the physical model setup, regression analyses, and input data set are given in Appendix A.

Initial ROTM development

An extensive literature review of potential runup and overtopping methods was conducted to determine which methods were most applicable to the study. Numerous references describing various runup and overtopping methods were reviewed. The literature emphasized the fact that the phenomena of runup and overtopping remain poorly understood. Until better data are available, existing methods used to estimate overtopping should be considered to be within, at best, a factor of three, and conservatively, an order of magnitude of the actual overtopping rate.

Available methods were evaluated for potential use with three main considerations: (a) type of structure the method was developed for and how closely the conditions tested resemble expected project conditions; (b) data requirements of the method versus data available from SBEACH; and (c) ability to code the method into a computer program. The literature review and evaluation led to the selection and development of viable methods to be used in the ROTM. The methods were expected to provide reasonable results; however, if expected overtopping rates were to be used for design purposes, a physical model study was initially recommended to verify and calibrate the proposed methods for site-specific conditions.

Algorithms for selected methods were developed, coded, and assembled into the ROTM. The ROTM was applied to three general types of structures present along Revere Beach and POP: (a) a berm/dune system at POP designed to prevent overtopping during the SPN, (b) a proposed revetment at POP, and (c) existing vertical seawalls of various crest elevations fronted by post-fill beach of various shapes. Wave conditions determined for individual profiles along Revere Beach and POP (Figure 2) were applied to appropriate seawall sections of varying crest elevation and length (Table 9). Resulting overtopping rates per unit width of seawall or dune were integrated along respective sections and combined for each tidal flood zone (Figure 2 and Table 9) to determine storage requirements.

Runup/overtopping configurations for vertical seawall

A vertical seawall fronted by an approximately 1:15 sloped natural beach extends from Elliot Circle to Carey Circle. The seawall varies in crest elevation for different sections, ranging from 19.8 to 24.9 ft mhw. The beach/seawall intersection will also vary with each section, averaging approximately 19 ft mhw according to the latest profile data. The resulting erosion or accretion due to the wave and water level database will vary the beach/seawall intersection point. The relationship of the still-water level (swl) to the beach/seawall intersection and the crest elevation of the seawall will determine the type of overtopping that can occur. The three expected overtopping

Table 9
Site Configurations for Overtopping Calculations

Overtopping Reach	Tidal Flood Zone	CERC Profile Number	Seawall Crest Elevation (ft. mhw)	Wall Length (ft)
Crescent Beach	1	1	23.8	525
Crescent Beach	1	1	20.7	1430
Crescent Beach	1	1	19.8	400
Park Dike	2A	1	20.9	865
Park Dike	2A	2	20.9	610
Park Dike	2A	2	22.9	570
Park Dike	2A	2	21.3	280
Park Dike	2A	2	21.3	1205
Park Dike	2A	2	21.3	30
Park Dike	2A	2	22.5	330
Oak Island	4A	2	22.5	115
Oak Island	4A	2	21.4	935
Oak Island	4A	3	21.4	420
Oak Island	4A	3	24.9	285
Oak Island	4A	3	24.9	280
Oak Island	4C	3	20.6	1360
Oak Island	5B	3	20.4	870
North Beach	5B	3	20.4	1090
North Beach	5B	5	20.4	1480
North Beach	5B	5	20.3	900
North Beach	5B	5	21.3	230
POP	PP	6	NA*	870**
POP	PP	7	NA*	900**
POP	PP	8	NA*	1270**

* Revetment or dune exists at this location.

** Distance represented by profile indicated.

mechanisms shown (Figure 49) are: (a) weir flow when unbroken waves impact the wall during extreme water levels, (b) broken waves overtopping the seawall when the swl is at or above the beach/seawall intersection, and (c) bore waves with sufficient energy to run up the beach slope and impact and overtop the seawall when the swl is below the beach/seawall intersection.

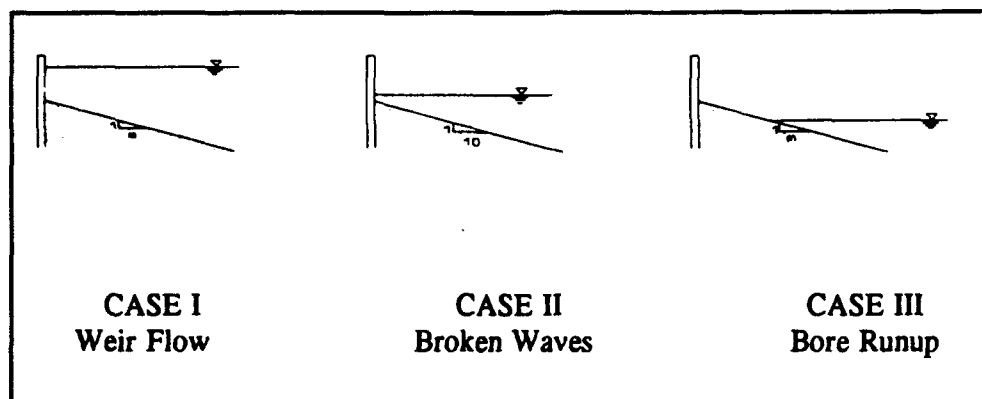


Figure 49. Overtopping conditions expected at vertical seawall

Selected methods

There exists no single method to calculate expected overtopping rates for all conditions described above (Cases I, II, III, dune overtopping, and revetment overtopping). Each of the above five conditions involves different overtopping mechanisms, requiring the use of different methodologies to estimate expected overtopping rates. Three of the conditions, CASE I, CASE II, and revetment overtopping were able to use available methods derived from laboratory experiments with conditions similar to expected conditions. The lack of data and existing methods for conditions similar to those found in CASE III and dune overtopping required development of new methods to estimate overtopping. Without proper calibration and verification, the proposed methods can be assumed to be accurate only within an order of magnitude. Methods selected, conditions under which the method is to be applied, and required input are described in the following sections.

Dune overtopping. A method was first developed to determine if runup values for incident wave conditions exceeded the dune crest (Resio 1987a). Next, the resulting overtopping when such conditions occur was determined (Battjes 1974). Resio estimates extreme runup statistics on natural beaches. The method is capable of predicting a frequency distribution for runup values, including maximum runup. Given a fixed dune crest elevation and incident wave conditions, Resio's model can be used to determine the number of runups exceeding the crest height. The result of Battjes and Roos (1975) relating runup to volume of water on a slope is then used to estimate the overtopping rate per unit of longshore length.

Resio reanalyzes Holman's field data (Holman 1986) obtained at Duck, North Carolina, to apply an extreme value model to runup on natural beaches.

A strength of this method is the use of actual field data; however, it is assumed that runup conditions at the study site are expected to be similar to those observed at Duck, North Carolina. Resio's model for large values of runup can be written as:

$$R' = 1.25 - 1.05 (T_r - 0.5)^{-0.19} \quad (5)$$

or

$$R' = 1.25 - 1.05 [(1/P_e) - 0.5]^{-0.19} \quad (6)$$

where T_r = the return period of interest in number of runups, $P_e = 1/T_r$ = the probability of exceedence, and R' = the coefficient of a form of Hunt's equation

$$(R_p^* - \eta)/H_{mo} = R' \xi \quad (7)$$

with

$$\xi = \alpha / (H_{mo}/L_p)^{0.5} \quad (8)$$

so

$$R' = \frac{(R_p^* - \eta)/H_{mo}}{\xi} = (R_p^* - \eta) \alpha^{-1} (H_{mo} L_p)^{-0.5} \quad (9)$$

where

R_p^* = the runup statistic of interest as defined by the local peak method

H_{mo} = incident spectral significant wave height in water depth of 8 m

L_p = wavelength corresponding to peak period

α = beach face slope

η = average vertical distance from the swl to the intersection of the water surface at the beach

Battjes and Roos (1975) determined a relationship between estimated runup and the volume of water on a slope. The estimated volume is primarily a function of the runup height and the slope of the beach. The maximum quantity of water stored above a certain location on the slope per wave (B_{max}), as measured in runup experiments with no overtopping (Figure 50), will overtop per wave if the crest of the dune would be situated at that location (Figure 50). Combined with the number of runups exceeding the crest of the dune, estimates of overtopping volumes are determined. The overtopping discharge averaged over the wave period is expressed by the formula:

$$\bar{q}(x_c)T = B_{max} |_{x=x_c} \quad (10)$$

in which \bar{q} is the discharge of overtopping averaged over the wave period, and x_c is the x-coordinate of the crest. B_{max} and \bar{q} are taken per unit width.

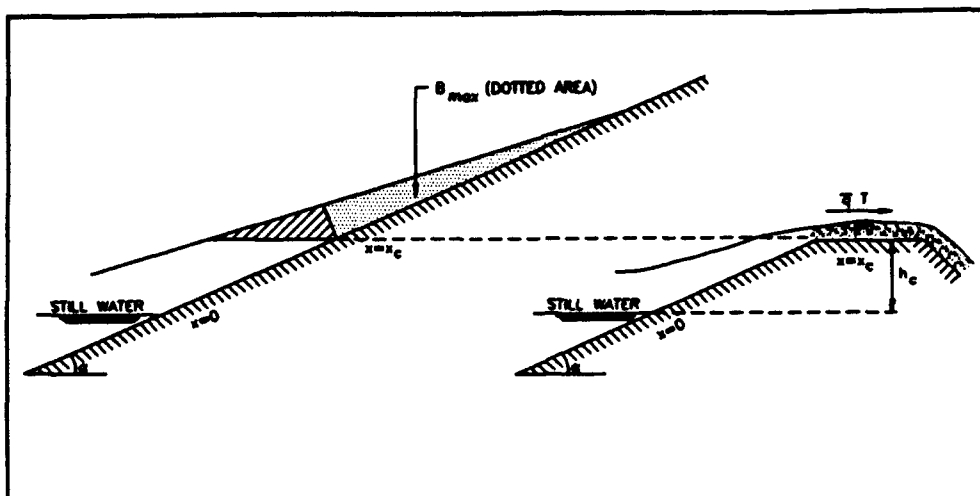


Figure 50. Definition sketch for the hypothesis $B_{max} = qT$ (Battjes and Roos 1975)

REQUIRED INPUT:

- H_{mo} - incident spectral significant wave height at 8 m depth
- T_p - peak wave period
- L_p - wavelength corresponding to peak period
- α - beach face slope
- η - average vertical distance from the swl to the intersection of the water surface at the beach

RESULTING OUTPUT:

- R_{max} - Maximum runup for incident wave conditions (ft)
- N_R - Number of runups exceeding crest of dune
- \bar{q} - overtopping rate averaged over the wave period per unit width (ft³/sec/ft)

Revetment overtopping. A series of physical model tests was previously conducted at CERC to measure overtopping rates for a range of incident irregular wave conditions on model revetments (Ward 1992). The results of the study provided a means for predicting overtopping rates on riprap revetments under irregular wave conditions as a function of dimensionless overtopping rate and relative freeboard. Relative freeboard is defined as

$$F' = \frac{F}{(H_{mo}^2 L_o)^{1/6}} \quad (11)$$

where F' is the relative freeboard, F is freeboard (height of structure crest above swl), and L_o is the deepwater wavelength. This parameter is particularly effective, as it accounts for different water levels, wave heights, and wavelengths.

The overtopping rate is nondimensionalized as

$$q' = \frac{q}{(gH_{m0}^3)^{1/4}} \quad (12)$$

where q' is the dimensionless overtopping rate per unit length of structure, q is the overtopping rate per unit length of structure, and g is gravitational acceleration.

Regression analysis of relative freeboard versus dimensionless overtopping rates for the conditions tested yielded a relationship

$$q' = C_0 [\exp(C_1 * F')] [\exp(C_2 * m)] \quad (13)$$

where m is the cotangent of the structure slope and C_0 , C_1 , and C_2 are dimensionless regression coefficients with best fit values of $C_0=0.457847$, $C_1=-29.4467$, and $C_2=0.846428$.

The use of irregular wave conditions at the toe of the structure should provide more reasonable overtopping rates than other methods which often use deepwater monochromatic wave conditions. The conditions tested in the study, structure slope, beach slope, and armor characteristics, are also similar to conditions expected for the proposed revetment.

REQUIRED INPUT:

- H_{m0} - zero moment wave height at the toe of the structure
- L_0 - deepwater wavelength
- F - freeboard
- m - cotangent of structure slope (3.0 for structure tested)

RESULTING OUTPUT:

- q - volume of overtopping per unit time per unit width of structure (ft³/sec/ft)

Vertical seawalls. Three methods were developed for the module that address potential overtopping conditions at vertical seawalls: weir flow, broken waves, and bore runup.

CASE I: Weir Flow. Extreme water levels allow unbroken waves to impact the seawall or broken waves of sufficient height to flow over the top of the wall ($F/H_i < 0.5$) (Figure 51).

A Japanese method proposed by Kikkawa, Shi-igai, and Kono (1968) is based on an extension of the steady-state weir flow equation of the form:

$$q = 0.667 m F (2gF)^{1/4} \quad (14)$$

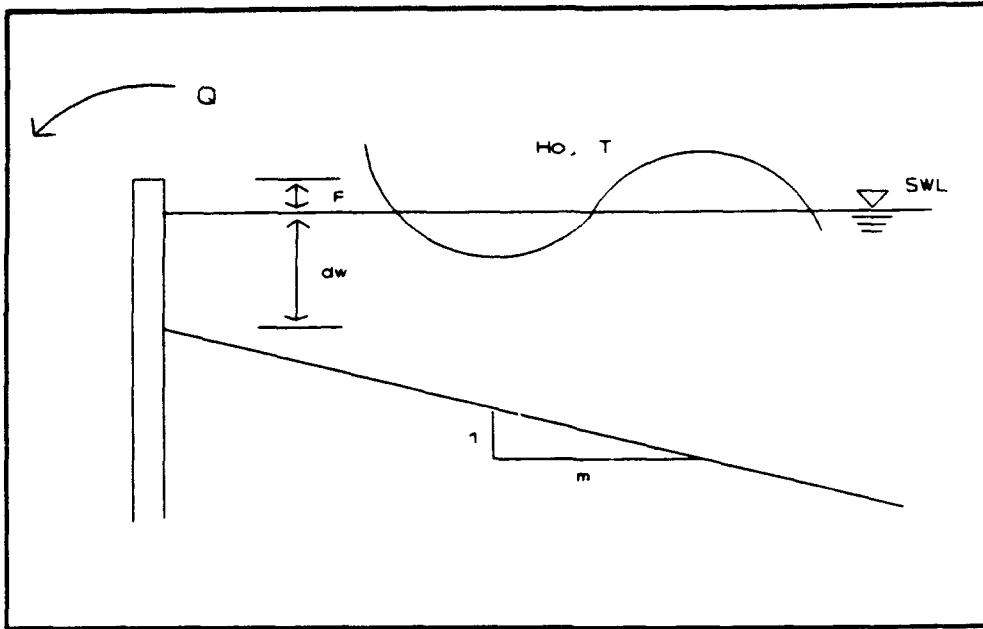


Figure 51. Weir flow overtopping condition

where

q = volume of overtopping per unit time per unit width (ft³/sec/ft)

m = discharge coefficient (assumed = 0.5)

F = freeboard

By extending the method to the dynamic (unsteady) case and assuming a triangular wave form, a solution was proposed of the form:

$$q = H_o (2gH_o)^{1/2} \left[\frac{2}{15} \right] m k^{3/2} \left[1 - \frac{F}{kH_o} \right]^{3/2} \quad (15)$$

where k is a dimensionless empirically determined coefficient influenced mainly by wave steepness and beach slope. To obtain the coefficient k , a very limited set of data is used consisting of a few Japanese monochromatic tests on vertical walls and some of the Beach Erosion Board (BEB)/WES (BEB 1956) monochromatic overtopping data. The physical approach of weir flow appears to be solid, although input wave conditions are in deep water and involve wave transformation uncertainty. Analysis of expected water levels and potential wave conditions indicates that weir flow conditions may not occur during modeled storms with the exception of the SPN. Results of the method are expected to be reasonable since unbroken waves able to impact the seawall undergo little transformation, removing part of the uncertainty involving deepwater input.

REQUIRED INPUT:

- H_o - deepwater wave height
- T - wave period
- L_o - deepwater wavelength
- F - freeboard

RESULTING OUTPUT:

- q - volume of overtopping per unit time per unit width ($\text{ft}^3/\text{sec}/\text{ft}$)

CASE II: Broken Waves. The swl must be at or above the beach/seawall intersection and the waves must be broken prior to interaction with the seawall (Figure 52).

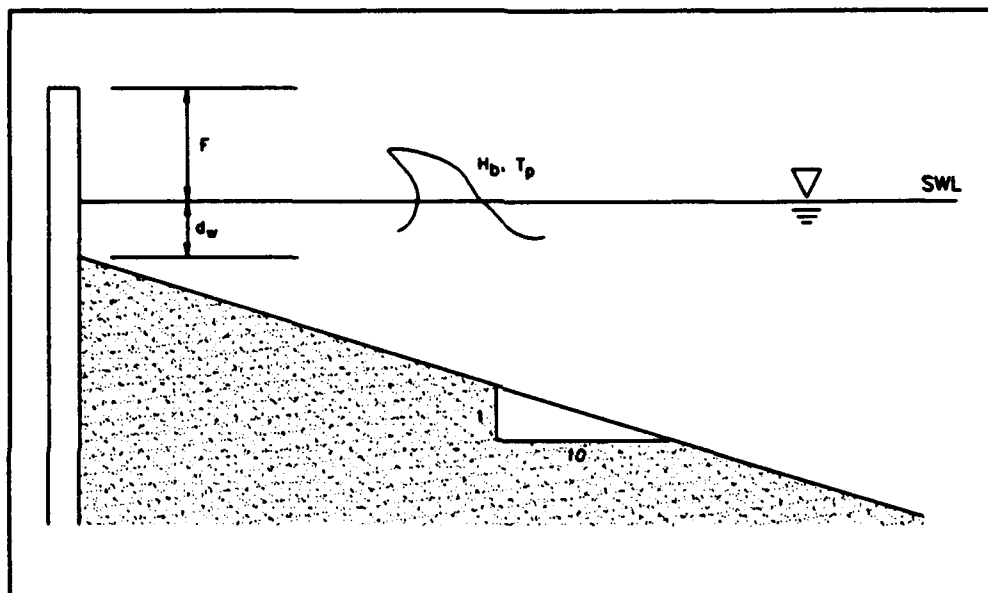


Figure 52. Broken waves overtopping condition

Saville and Caldwell's (1953) original BEB overtopping studies on vertical seawalls fronted by a 1V:10H slope closely simulate expected conditions. The original data were reviewed to determine which tests were applicable to expected conditions. Saville's original data consisted of three different wave conditions measured at or near the structure; breaking, surging, or reflecting. Of the original data set, a special subset of only breaking wave conditions is used for this method. The data set consists of three design water levels, $d_w = 0, 4.5$, and 9.0 ft, with incident breaking wave conditions of 3- to 14-ft wave heights, 22- to 129-ft wavelengths, and a resulting wave steepness range of 0.0465 to 0.1800 measured at or near the structure. Freeboard values ranged from 3 to 12 ft. Given breaking wave and water level conditions from SBEACH and available freeboard for each profile, resulting overtopping rates were determined by interpolating between original data points. A series of dimensionless graphs were developed from the original Saville data in the form of dimensionless overtopping, Q' , versus relative freeboard, F' . An example of a dimensionless graph (Figure 53) for the swl at the toe of the structure ($d_w = 0$) and the resulting equation are presented.

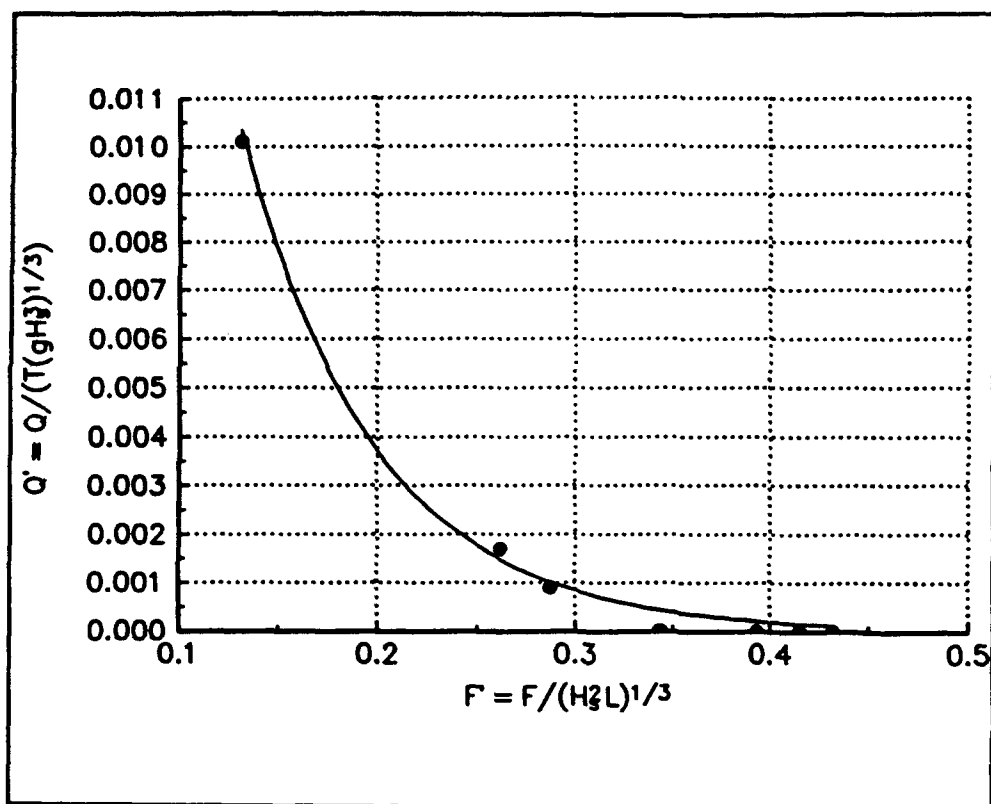


Figure 53. Dimensionless overtopping versus dimensionless freeboard graph

A conservative exponential fit is represented by the equation

$$Q' = \exp(-12.6995 \cdot F') + 0.0370 \quad (16)$$

where

$$Q' = \frac{Q}{T(gH_s^3)^{1/3}} \quad (17)$$

and

$$F' = \frac{F}{(H_s^2 L_p)^{1/3}} \quad (18)$$

REQUIRED INPUT:

- H_b - incident breaking wave height from SBEACH
- T_p - peak wave period
- L_p - wavelength corresponding to peak period
- d_w - water depth at toe of seawall
- F - freeboard

RESULTING OUTPUT:

Q - volume of overtopping per unit width of structure (ft³/ft)

CASE III: Bore Runup. Runup must first reach the seawall and secondly have enough energy remaining to overtop the seawall (Figure 54).

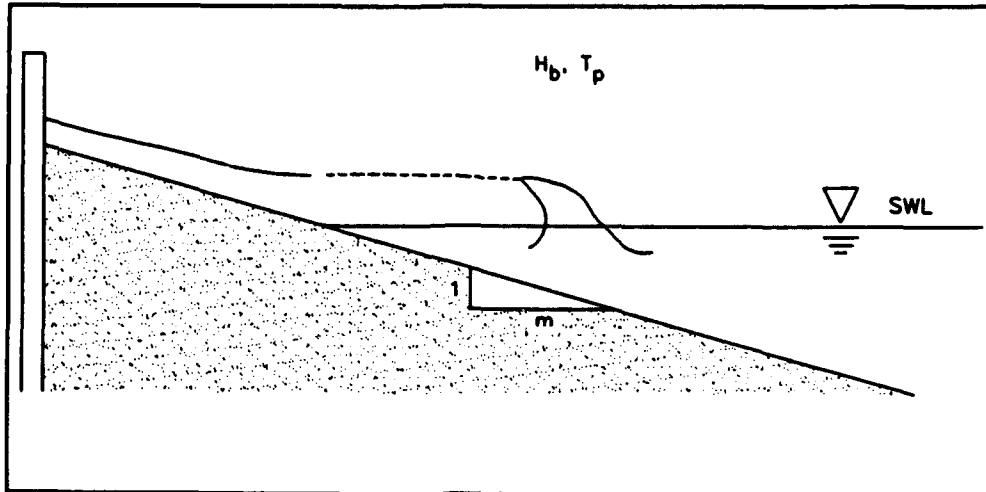


Figure 54. Bore runup overtopping conditions

Existing methods or data simulating this overtopping condition were unavailable. Therefore, it was proposed to develop a hybrid method which separates the above condition into two separate processes, overtopping of a sloping beach (A) and overtopping of a vertical seawall (B). The resulting overtopping due to each was weighted according to the vertical exposure of each condition. Because of the unverified nature of this approach, it can only be assumed to be accurate within an order of magnitude.

Initially, Resio's (1987a) method for extremal runup on natural beaches was used to determine if actual runup (R_{max}) reached the seawall. If the estimated maximum runup failed to reach the seawall, then zero overtopping occurs. When runup impacts the seawall, the proposed hybrid method was used as described in Figure 55.

The total overtopping is the sum of the weighted overtopping rates.

$$Q = Q_A \left[\frac{h_b}{h_b + h_c} \right] + Q_B \left[\frac{h_c}{h_b + h_c} \right] \quad (19)$$

Overtopping of the natural beach slope Q_A is determined using the same method implemented for dune overtopping (Resio 1987a, Battjes and Roos 1975). Overtopping of the vertical seawall Q_B is determined using a special subset of Saville and Caldwell (1953) data with $d_w = 0$.

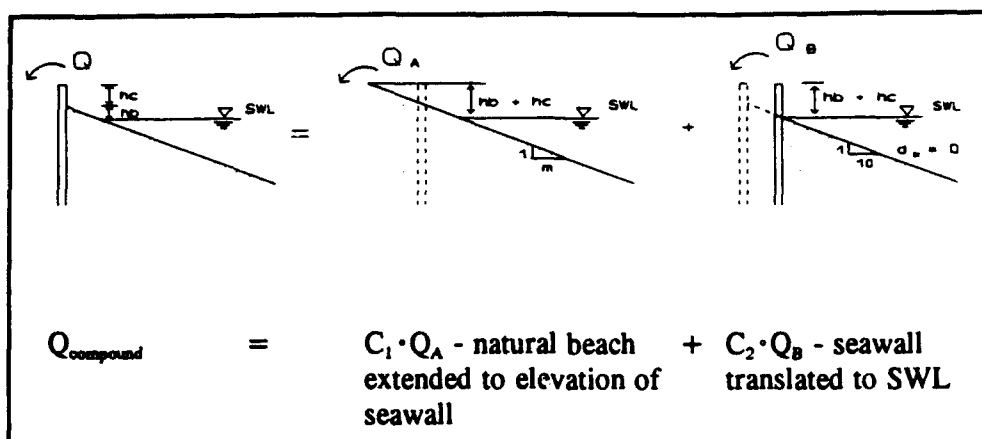


Figure 55. Graphical presentation of hybrid method proposed for bore runup overtopping condition

REQUIRED INPUT:

- H_b - incident breaking wave height from SBEACH
- T_p - peak wave period
- L_p - wavelength corresponding to peak wave period
- d_w - water depth at toe of seawall
- F - freeboard

- H_{mo} - incident spectral significant wave height at 8-m depth
- T_p - peak wave period
- L_p - wavelength corresponding to peak wave period
- h_b - height of beach/seawall intersection above swl
- h_s - height of seawall crest above beach/seawall intersection
- α - beach face slope
- η - average vertical distance from the swl to the intersection of the water surface at the beach

RESULTING OUTPUT:

- R_{max} - maximum runup for incident wave conditions (ft)
- N_R - number of runups exceeding crest of dune
- Q - volume of overtopping per unit width of structure (ft³/ft)

Selection of ROTM methods

Each method is to be applied under specific conditions. The dune overtopping would obviously be applied only at POP. The revetment overtopping would only be applied at POP for revetment analysis. When vertical seawalls are present, the selected method will depend on the still-water level (swl) position relative to the beach/seawall intersection and the wave conditions relative to existing freeboard. Weir flow is applied during extreme water levels when either unbroken waves impact the seawall or the available freeboard is less than one half the incident wave height ($F/H_i < 0.5$). The broken waves method will be used when the swl is at or above the

beach/seawall intersection and waves break at or near the seawall. The bore runup method will be applied when the swl is below the beach/seawall intersection and maximum runup is able to impact the seawall. A schematic of the ROTM is presented in Figure 56.

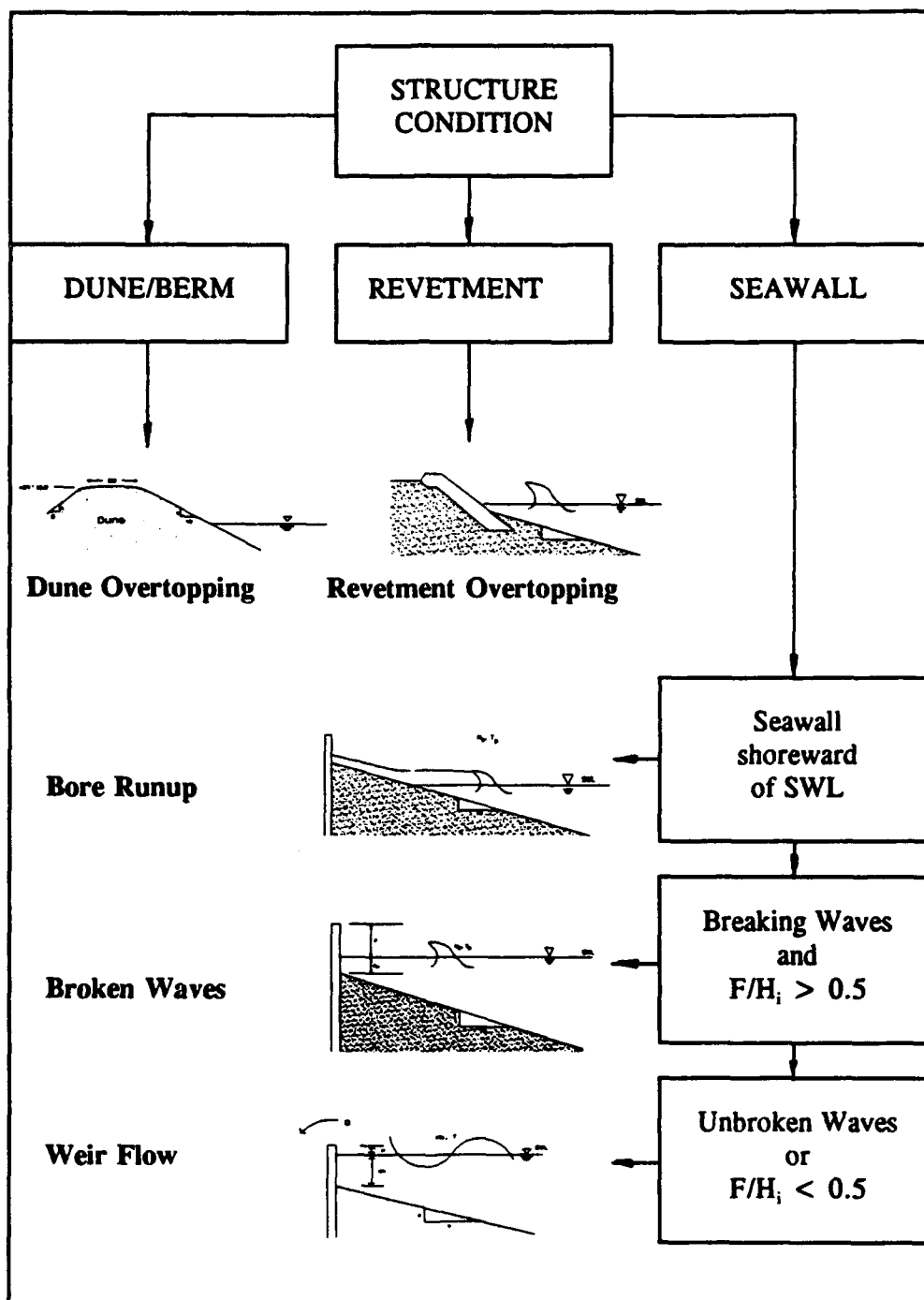


Figure 56. Schematic of the ROTM

Calibration of initial ROTM

CENED requested overtopping predictions for a few given data sets prior to simulation using the wave and water level database. Predicted overtopping volumes and rates were submitted for the following cases: (a) November 1991 profiles and November 1945 SPN storm to describe a worst-case existing condition, (b) November 1991 profiles and October 1991 storm to indicate the vulnerability of a post-Halloween storm beach condition in response to a storm of characteristics similar to the Halloween storm, (c) October 1991 profiles and October 1991 storm to allow qualitative verification of the ROTM given observed levels of overtopping during the Halloween storm, and (d) February 1978 profiles and February 1978 100-year storm (Great Blizzard) to reproduce observed and measured overtopping volumes in order to calibrate and verify application of the ROTM to Revere Beach and POP.

Overtopping volumes obtained from the ROTM simulations of the Great Blizzard were deemed excessive by CENED. Results given in Table 10 list the total overtopping volumes predicted for each tidal flood zone (defined in Table 9) for the data sets described. Qualitative comparison of the predicted and actual Halloween overtopping volumes indicates realistic results. Also, POP predicted overtopping volumes appear to be reasonable for each of the simulations. Relatedly, quantitative comparison of overtopping volumes predicted for the Great Blizzard against measured overtopping volumes was conducted. Overtopping volumes for each tidal flood zone were inferred from stage-volume curves for the Great Blizzard, and were obtained from the CENED. The original ROTM overpredicted rates, as shown in Table 11 for the Great Blizzard.

Due to the outcome of the simulations using the original ROTM, an attempt was made to calibrate the ROTM given overtopping volumes from the Great Blizzard. Due to the conditional nature of the ROTM, it was not possible to merely adjust the module with a simple scaling of the output. Calibration of the ROTM required an investigation into the percentage of time each method (or submodule) within the ROTM was active, and in turn what magnitude of the total volume resulted for each given submodule. Table 11 indicates that the prediction for flood zone 5B was accurate, but predicted volumes for the remaining flood zones exhibit significant differences relative to the CENED data. It was found that the broken waves submodule and condition dominated the overtopping prediction for the Great Blizzard, indicating that the broken waves method had difficulties accurately modeling the Great Blizzard. Further investigation of the data set upon which the broken waves method is founded produced no explanation for the nature of the predictions. In the absence of a pattern upon which to base a calibration methodology, the broken waves method was deemed invalid for this application. Since the ROTM could not be calibrated or further refined with this limited data set, a physical model study of various overtopping conditions was suggested to generate an ROTM better suited to the project site.

Table 10
Overtopping Predictions for Original ROTM

Storm	Total Overtopping Volume/Tidal Flood Zone (acre-ft)					
	TFZ 1	TFZ 2A	TFZ 4A	TFZ 4C	TFZ 5B	TFZ PP
November 1991 profiles & SPN	2465	3655	1060	555	1665	80
November 1991 profiles & Halloween storm	5	5	5	15	25	15
October 1991 profiles & Halloween storm	.. ¹	15	.. ¹	.. ¹	15	0
1978 profiles & Great Blizzard	400	2000	670	65	215	.. ¹

¹ Insufficient data to complete overtopping prediction.

Table 11
Predicted and Measured Overtopping Volumes for Great Blizzard (Original ROTM)

Tidal Flood Zone	Approximate Measured Volume (acre-ft)	Predicted Volume (acre-ft)	Approximate Module Error(%)
1	80-100	400	400
2A	600	2000	333
4A/4C	70-115	670(4A),65(4C)	640
5B	215	215	0

Physical Model Tests

As originally proposed, a physical model study was to concentrate on overtopping of the park dike located landward of the seawall at Revere Beach. Due to the inability to calibrate the ROTM, it was proposed to augment the originally proposed physical model study with a segment that would produce information to improve the ROTM. Justification for the work arose from a number of questions surrounding the proposed physical model tests and the possibility to overcome the limitations of the original ROTM. First, a numerical ROTM was capable of simulating numerous overtopping conditions, including various seawall elevations and different profile shapes, that the physical model study would not address due to time and funding constraints. Also, a numerical study would produce predictions for a large set of storms, whereas a physical study was limited to a few cases. Conversely, a physical model was capable of producing site-specific data that could be used to calibrate and verify a numerical simulation without relying on applicability of

results from other tests to the site conditions at Revere Beach. The physical/numerical approach could be used to support one another's results, and produce a reliable ROTM due to the ability of a site-specific physical model to produce good results for limited conditions and the ability of a numerical method to extrapolate to more general site and storm conditions.

A revised scope was developed and implemented, and reflected the need to conduct tests that allowed the development of the ROTM. Physical modeling work focused on verification of the physical model setup using the Great Blizzard data, then generating site-specific relationships to predict overtopping dependent upon the bore runup and broken waves overtopping conditions. Development of the bore runup condition was necessary due to preliminary analyses that indicated existing condition simulations at Revere Beach would be strongly dependent upon bore runup. Concisely, physical model work had three major tasks (as related to the development of the ROTM): (a) verification of the physical model study to the project site using the Great Blizzard data set; (b) generation of data necessary to develop the bore runup submodule; and (c) acquisition of data to develop the broken waves submodule.

Verification of physical model overtopping

Verification of the physical model setup utilized data from the Great Blizzard and 1978 profile information. Tidal flood zone 2A was selected for the verification, and Profile 2 was chosen as the dominant contributor to overtopping volumes along this reach. Model tests focused on reproducing response to changes in water level, wave characteristics, and duration of existence for a given set of conditions. Output of SBEACH was used as input to the physical model tests, and included the transformed significant wave height at a location corresponding to the position of the wave paddle in relationship to the seawall (approximately 2,000 ft offshore, see Appendix A for physical model dimensions). The output covered the anticipated interval when overtopping occurred during the actual storm, so a discretized storm simulation was modeled in the wave flume. Discrete storm parameters were input to the physical model and were interpolated in order to model the storm duration when overtopping occurred. Data input to the physical model study for the verification stage as output by SBEACH are summarized in Table 12. The actual data selected for use in the model are a subset of this data and are described in Appendix A.

Total overtopping volume for tidal flood zone 2A was estimated as 600 acre/ft for the Great Blizzard. Surveys of high water marks in a ponding area provided this estimate of total overtopping for flood zone 2A. The total overtopping volume obtained from the physical model study was approximately 780 acre/ft (see Appendix A). The increased overtopping in the physical model is likely the result of a number of factors, including modeling tidal flood zone 2A with only Profile 2 and a seawall elevation of 21.0 ft mhw which is possibly a conservative figure. The model setup ignores the contributions of Profile 1 and higher seawall elevations which would likely reduce

Table 12
Physical Model Verification Input Data (Profile 2)

Hour of Storm	Time Step of SBEACH Simulation	SWL (ft. MLW)	Total Water Level (ft. MLW)	H_s (ft)	T_p (sec)
13	156	10.1	10.5	6.0	8.1
14	168	13.2	13.5	7.2	8.6
15	180	14.3	14.2	10.8	9.0
16	192	13.0	13.0	10.1	9.7
17	204	12.1	13.0	6.8	10.3
18	216	10.2	11.2	6.1	11.0
24	288	7.5	9.0	5.3	12.0
25	300	10.0	10.8	6.0	12.3
26	312	12.9	13.6	7.0	12.7
27	324	14.8	15.4	7.7	13.0
28	336	14.7	15.5	7.7	13.0
29	348	13.4	14.2	7.2	13.0
30	360	11.0	11.5	6.3	13.0
31	372	8.1	8.8	5.3	12.7

overtopping. The 30-percent overprediction was considered acceptable given the necessary approximations inherent in the physical model development and application, and in the inferred actual overtopping volumes, plus the improvement in comparison with the initial ROTM estimates. Completion of the verification stage allowed physical model tests dedicated to the development of the ROTM to proceed.

Worst case/bore runup simulations

Following verification of the physical model methodologies, it was necessary to meet CENED requirements to define overtopping volumes for a worst-case existing condition. Total overtopping volumes for a worst-case event will be used to determine the required flood mitigation and retention structures. Furthermore, all simulations conducted with the November 1991 profiles and any of the storm database result in the bore runup condition due to the still-water levels associated with the water level data and the elevation of the beach/seawall intersections. It was possible, therefore, to obtain the data needed by CENED and at the same time develop the bore runup submodule of the ROTM with a single series of model runs. This series of tests made use of November 1991 profile data and the SPN event. Profiles 1-5 were incorporated in the tests because Profiles 6-8 were designed with either a

dune or revetment, thus the bore runup relationships were necessary only at Profiles 1-5.

As stated in a previous section, bore runup is the overtopping condition resulting from swl intersection with the beach face below the beach/seawall intersection elevation. Making use of the higher water levels within the SPN and site-specific profile data generated a relationship representative of Revere Beach. Output from SBEACH for Profiles 1-5 and the SPN, and data input for the physical model, are summarized in Table 13. Specific data implemented in the model are outlined in Appendix A. The data indicate a wide range of tested parameters dependent upon profile location and depict the ranges when overtopping occurred for the specific model setup. Despite the modeling of only one wave period, it is anticipated that the long wave period resulted in conservative regressions when applied to storms of lesser period due to the increase of runup potential with increases in wave period. Output from the physical model tests included overtopping rates per linear foot of prototype seawall for Profiles 1-5 and each hour of the storm that had measurable overtopping. Regression analyses were conducted to generate predictive relationships for overtopping rates given variable wave, water level, profile, and structural conditions. Regression analyses and the bore runup data set are detailed in Appendix A.

Table 13 Worst-Case/Bore Runup Physical Model Input				
Profile Number	SWL (ft, mlw)	Total Water Level (ft, mlw)	Hs	Tp
1	9.7-16.6	10.7-17.4	2.8-9.8	15.9
2	9.7-16.6	11.4-18.6	9.8-14.2	15.9
3	9.7-16.6	11.6-19.0	4.1-4.4	15.9
4	9.7-16.6	10.6-18.0	7.1-7.9	15.9
5	9.7-16.6	10.7-17.4	2.8-9.8	15.9

The regression relationship developed for bore runup is given by

$$Q' = \frac{Q_{BR}}{(g * f^3)^{1/2}} \quad (20)$$

where

Q_{BR} = overtopping rate (cfs/ft) due to bore runup

g = gravitational acceleration

$$Q' = - 0.036533 + 0.099865 \cdot PI1 - 0.003554 \cdot PI5 - 0.062324 \cdot PI1^2 + 0.001114 \cdot PI5^2 \quad (21)$$

where

$PI1 = b/f$ (Buckingham PI dimensional analysis term)

$PI5 = d/f$ (Buckingham PI dimensional analysis term)

$b =$ beach freeboard, height of the beach at the base of the seawall above the swl

$d =$ water depth in the wave flume at wave paddle location

$f =$ structure freeboard, height of the seawall crest above the swl

Broken waves simulations

The broken waves overtopping condition occurs when the swl is located at an elevation above the beach/seawall elevation. The 1978 profile data set, which was implemented in a number of overtopping simulations, causes the broken waves condition to occur for some of the storms contained in the wave and water level database. Attempted calibration of the initial ROTM indicated difficulties for the broken waves method originally used at Revere Beach. Thus, it was necessary to include a series of physical model tests to improve the ability of the ROTM to predict overtopping for broken waves type water levels, and wave conditions below the level where weir flow occurs.

Profile 2 data from 1978 were used in the physical model to satisfy the broken waves condition. This setup provided conservative data since Profile 2 historically experiences the greatest overtopping rates along Revere Beach and POP. Storms were selected based upon results from original ROTM simulations with the 1978 profile data that identified the storms for which broken waves overtopping predominated. It was deemed necessary that a very high percentage of overtopping obtained in the physical study must be due to broken waves so that the regression equation was applicable. Due to difficulties related to monitoring overtopping conditions, as defined at Revere Beach, in the wave flume, the ROTM was used to track wave heights and water levels following procedures initially used in calibration of the ROTM.

Table 14 shows the storms tested for possible use in the physical model tests. The percent occurrence of overtopping in terms of time and magnitude due to the broken waves submodule (original version) is listed, as are total overtopping volumes (Profile 2 only) computed using the initial overtopping module. Storms selected for inclusion in the physical study are indicated by asterisks. It is evident that the six selected storms are nearly totally dependent upon the broken waves condition, with the lowest percentage magnitude occurring for the February 1972 20-year event at 92 percent due to broken

Table 14
Storms Used in Development of Broken Wave Submodule

Storm	Percent Occurrence of Overtopping Due to Broken Wave Conditions		Predicted Overtopping Volumes (acre-ft) Profile 2 only
	Time	Magnitude	
November 1945 20-yr	86	22	15405
February 1958 50-yr	92	95	15
March 1958 50-yr*	100	100	1885
January 1961 100-yr*	100	100	1215
April 1961 100-yr	100	100	270
December 1962 20-yr*	100	100	1820
December 1962 50-yr	95	86	1780
February 1972 20-yr*	99	92	1045
February 1972 50-yr	98	84	1315
November 1972 50-yr*	100	100	375
February 1978 50-yr*	97	98	840
February 1978 100-yr	89	80	2515
*Storms selected for inclusion in the physical model study of broken waves overtopping condition.			

waves. Lastly, Table 14 indicates that the range of predicted overtopping resulting from the initial ROTM for the selected storms was 375-1,885 acre/ft. It was anticipated that these values were representative of the storm set and would create a reasonably well-sorted data set upon which to perform the regression analyses.

Output from SBEACH for Profile 2 and the selected storm subset, and data input for the physical model are given in Table 15. Specific input utilized in the physical model is detailed in Appendix A. Output from the physical model tests included overtopping rates per linear foot of prototype seawall for Profile 2 and each hour of the selected storms that had measurable overtopping. Regression analyses were conducted to generate predictive relationships for overtopping rates given variable wave, water level, profile, and structural conditions. Appendix A details the regression analysis.

The regression equation developed for the broken waves submodule is given as

$$Q' = \frac{Q_{BW}}{(g \cdot f^3)^{1/2}} \quad (22)$$

Table 15 Broken Waves Physical Model Input (Profile 2)				
Storm	swl (ft, mlw)	Total Water Level (ft, mlw)	H_s	T_p
March 1958 50-yr	12.6-14.6	12.9-14.4	7.6-10.6	10.7-12.0
January 1961 100-yr	10.5-14.9	10.6-14.4	6.7-10.5	8.6-9.0
December 1962 20-yr	9.5-14.2	10.3-14.4	6.5-11.7	12.0-14.1
February 1972 20-yr	10.9-14.2	12.4-15.2	7.3-8.5	12.0-13.0
November 1972 20-yr	10.7-14.6	10.8-14.6	5.5-8.1	8.3-9.0
February 1978 50-yr	11.5-14.6	12.4-15.1	3.1-7.6	11.0-12.0

where

Q_{BW} = overtopping rate (cfs/ft) due to broken waves

$$Q' = 0.004162 - 0.007285 \cdot PI1 - 0.000025997 \cdot PI3 + 0.003252 \cdot PI1^2 + 0.001559 \cdot PI2^2 + 0.000000217 \cdot PI3^2 \quad (23)$$

where

$PI1 = swl/f$

$PI2 = H/f$

$PI3 = L_o/f$

H_s = Incident significant wave height corresponding to the approximate position of the wave paddle

L_o = Deepwater wave length $\left(\frac{gT^2}{2\pi} \right)$

T_p = Peak wave period

Worst-case overtopping

Additional physical model tests were added to address an extreme worst-case overtopping condition. CENED required information to envelope possible overtopping conditions. The developed worst-case ROTM submodule made use of specific worst-case data (1978 profile and SPN storm),

verification data (1978 profile and Great Blizzard storm), and broken waves data (1978 profile and storm data shown in Table 15) to generate a comprehensive database upon which to base a regression equation capable of handling a wide range of broken waves conditions, as well as weir conditions resulting due to the SPN. For the physical model study of the worst-case condition, Profile 2, which was previously used in the verification stage, was used along with the SPN event. Time and monetary constraints limited worst-case tests to a single profile condition. Portions of the worst-case storm were not modeled due to physical scale limitations imposed by the testing facility; thus, information concerning extreme overtopping conditions is limited. Information on input and physical-model-generated worst-case data is contained in Appendix A, as are details of the regression analysis. The developed regression incorporated into the ROTM for the worst-case application is given by

$$Q' = \frac{Q_{wc}}{(g \cdot f_b)^{1/2}} \quad (24)$$

where

Q_{wc} = overtopping rate (cfs/ft) due to worst-case

$$\begin{aligned} Q' = & -0.000338 + 0.001912 \cdot PI2 + 0.000000212 \cdot PI3 \\ & - 0.004788 \cdot PI5 + 0.002530 \cdot PI1^2 - 0.000322 \cdot PI2^2 \\ & - 6.92E-12 \cdot PI3^2 \end{aligned} \quad (25)$$

where

$$PI1 = (f_b/f)^2$$

$$PI2 = (H/f)^3$$

$$PI3 = (L_w/f)^2$$

$$PI5 = (SWL/f)^2$$

$$f_b = \begin{array}{l} \text{beach/structure freeboard, seawall crest height above beach} \\ \text{crest} \end{array}$$

This regression was applied only to the worst-case condition and was not used for other simulations. The broken waves/weir flow condition, as defined by Equation 25, was assumed dominant with overtopping due to bore runup neglected due to the setup of the "worst-case" ROTM. Limits as defined by the data set were used to create a lower bound on overtopping predictions; however, due to an inability to conduct extreme portions of the physical model tests, caused by physical scale constraints, no upper limit was enforced. This resulted in allowing the regression to be applied to extreme conditions beyond the limits of the regression database where results are uncertain.

Reliability of ROTM

Generation of improved broken waves and bore runup submodules covered a substantial portion of overtopping conditions that were considered during the course of the study. In summary the conditions addressed by the physical model study and regression development were: (a) existing condition overtopping at Revere Beach with the bore runup work (Profiles 1-5, November 1991 profile data, and wave and water level data set); (b) broken waves condition using profile/structural conditions similar to Profile 2/1978 data set (swl level above base of seawall and roughly 10-12 ft of seawall/beach freeboard); and (c) worst-case condition using Profile 2/1978 data set and the SPN. However, several conditions were not represented by the physical model work and will be discussed as relevant in Chapter 5. The data set used in the development of the regression equations is limited; therefore, overtopping predictions that require extrapolating beyond the limit of the input data set will provide results of questionable reliability.

Conditions represented well by the physical model tests are those with profile and structural conditions similar to those implemented in the physical model. Dominant storm parameters most influential on overtopping predictions were well represented by conducting physical tests over a wide range of water levels and wave heights. For the bore runup simulations, model tests covered all conditions resulting in measurable overtopping for the SPN and present profile. However, constant wave periods during the peak of the SPN resulted in the exclusion of this anticipated important parameter, which, given the large wave period used in the physical tests, should create a conservative relationship with respect to wave period. Broken waves physical tests included a wide range of water levels, and wave heights and periods; however, were conducted using only one profile. It is anticipated that the broken waves condition was well-represented by Profile 2 and tested storm conditions, but the exclusion of different profile shapes leads to questions when the module is applied to different profiles. Overall, the ROTM's reliability decreases with applications utilizing significantly different profile geometries than tested with less noticeable effects when applied to untested waves and water levels.

Data points used to complete the regression analyses were associated with times of greatest overtopping representing approximately 15 hr of each selected storm. The final ROTM is a site-specific calculation method based upon profile, structural, and storm information obtained for the study site. Regression equations were derived using all data points from the physical model study; thus there exists no data with which to independently verify the ROTM module with other situations. The ROTM was verified to the physical model study with the numerical simulation of the events studied in the wave tank. This verification provided confidence in the physical model and ROTM setup, and proof of the ROTM concept. The algorithms describing runup and overtopping on a dune/berm and revetment remain unverified due to a lack of data. Finally, it is suggested that the ROTM results be used with caution despite an apparent improvement of the module through the physical model work.

5 Assessment of Storm-Induced Overtopping

Overview

Design of the Revere Beach park dike and ponding and estuary storage areas requires overtopping volumes and rates as a function of storm intensity. For POP, comparison of dune/beach fill and revetment response is necessary to determine which flood protection structure(s) will provide the required level of protection while minimizing costs. Estimates of overtopping rates were generated using the developed ROTM which uses wave, water level, and profile response information output from SBEACH, as well as profile structural characteristics considered in design. The ROTM, described in the previous chapter, was applied to address design and performance of flood mitigation structures. Applicability of the ROTM to each condition considered herein is discussed as relevant.

Application of Runup and Overtopping Methods

The ROTM was utilized at Revere Beach and POP to determine required flood protection and to predict the performance of the coarse-grained beach fill. The goals of this work were: (a) optimize dune design at POP, (b) evaluate revetment design at POP, (c) estimate flood protection provided by coarse-grained beach fill and seawalls subject to the wave and water level database, (d) predict overtopping associated with the Halloween storm, using both pre- and post-storm profile information, and Great Blizzard, and (e) evaluate worst-case overtopping conditions possibly present at the project site due to the loss of sand from the beach profiles. This chapter describes this work and addresses proposed flood protection designs, pre-fill flood vulnerability, envelope of expected coarse-grained fill response to severe events, and provides other needed information to generate an effective design, both physically and economically.

Dune optimization

Dune optimization refers to the iterative evaluation of overtopping potential as a function of dune crest elevation and corresponding fill volume at POP (Profiles 6, 7, and 8). Dune design is characterized by placement of a 1:5 shoreward slope up to a given crest elevation, a 50-ft-wide dune crest, and a seaward slope of 1:15 down to existing grade. Profile data from 27 November 1991 were used as existing grade, and more shoreward data were obtained using photogrammetric maps from July 1991. Shoreward dune origins were located approximately at the edge of the beach road fronting POP, and the grain size used was 0.49 mm. Dune crest elevations were increased in 2-ft increments from an initial elevation of 21 ft mlw until no overtopping occurred as predicted within SBEACH and requested by CENED due to the most extreme event, the SPN. The design proposed was selected due to limited construction space caused by navigation channels offshore of the project site, which prohibited the construction of a dune/berm combination. The 1:15 seaward slope for the coarse-grained beach fill matched the nearshore beach slope present at Revere Beach, and it is anticipated that the seaward slope would equilibrate in a shape similar to present conditions at Revere Beach with minimal effect on the integrity of the dune feature.

SBEACH runup estimates were initially used to infer overtopping of the dune crest. The dune elevation was considered insufficient if runup exceeded the crest during a significant portion of the simulation, thus initiating the overwash algorithm contained within SBEACH (Wise and Kraus 1993). Final overtopping results were obtained using the dune overtopping portion of the ROTM. Conclusions concerning dune effectiveness were made using altered beach profiles (Chapter 3), which indicate runup exceedance and dune degradation as predicted by SBEACH in response to the storm database, and computed overtopping volumes as calculated by the ROTM. Iteration of dune crests was continued until a maximum elevation of 25 ft mlw, which was above the elevation recommended by CENED to ensure project aesthetics, 23 ft mlw.

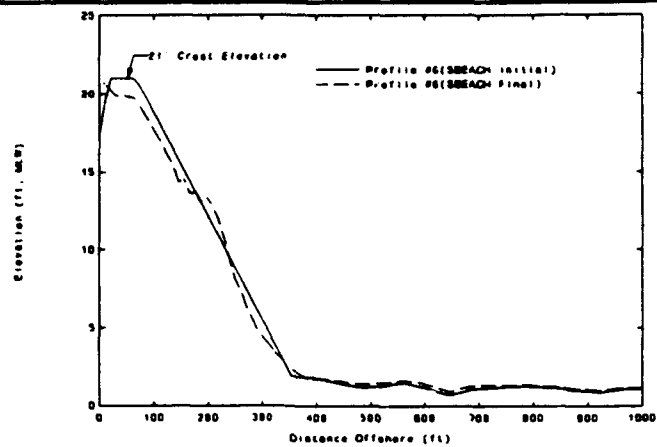
Dune optimization was conducted using combinations of SBEACH calibration parameters in order to generate a range of anticipated results. Because the optimal POP calibration parameters were developed for a beach with 0.21-mm grain size and dune optimization was conducted with 0.49-mm material, different beach grain size could play a role in determining optimal calibration parameters. Additionally, complete verification of SBEACH is not possible with only one profile; thus, multiple runs with different calibration sets attempt to account for a range of predicted results. Profile simulations (Chapter 3) were conducted with $K = 0.005 \times 10^{-6}$ and $Eps = 0.001$ due to improved profile prediction as partially verified by the Halloween storm data. For dune optimization, more erosive calibration parameters were also tested in order to maintain a level of conservatism. As stated in Chapter 3, profile

response simulations yield only qualitative results, but optimization requires the specification of a single dune design; therefore, the range of erosive calibration parameters was implemented.

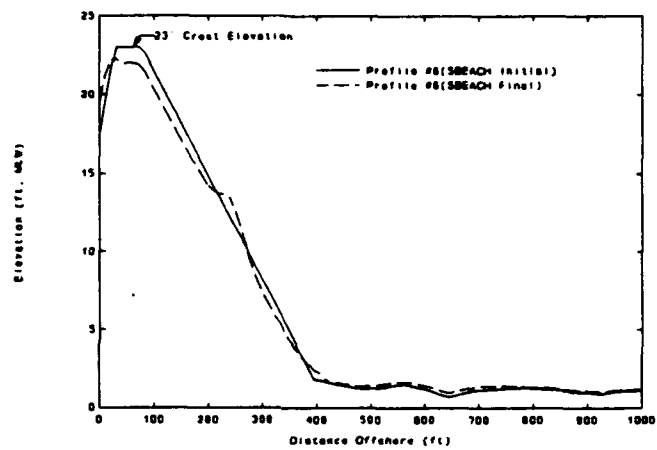
Figures 57-65 present the results of the dune optimization simulations using more erosive calibration parameters and the calibration set used for the profile simulations in Chapter 3. Larger values of the calibration parameter K produce greater sand transport and more prominent bar features, and larger values of Eps produce a more subdued bar. These runs were conducted using the SPN as a worst-case event.

Based upon profile response only, it is evident in Figures 60-65 that Profiles 7 and 8 are resistant to dune degradation for either 21- or 23-ft mlw dune crest elevations. Note that accretive effects of this long wave period event, the SPN, in conjunction with the coarse beach fill and low wave heights caused a buffering of the dune/berm system at Profiles 7 and 8. At Profile 6, dune erosion was more evident except for simulations conducted with the lower calibration parameters (Figure 59). Using more erosive calibration parameters, Profile 6 experiences notable dune degradation due to overwashing mechanisms. The 23- and 25-ft mlw dune crest elevations, however, appear to maintain high dune crests (above approximately 22 ft mlw) and intuitively still provide a high level of flood protection. Figures 57a and 58a depict significantly eroded dune features for the 21-ft mlw dune crest elevation, thus precluding the selection of this design. Analysis of the dune optimization profile response results indicates that the dune designs tested with a coarse-grained beach fill are extremely resistant to erosion in response to the SPN. Only at Profile 6 for the 21-ft mlw dune crest elevation is a high degree of dune degradation predicted.

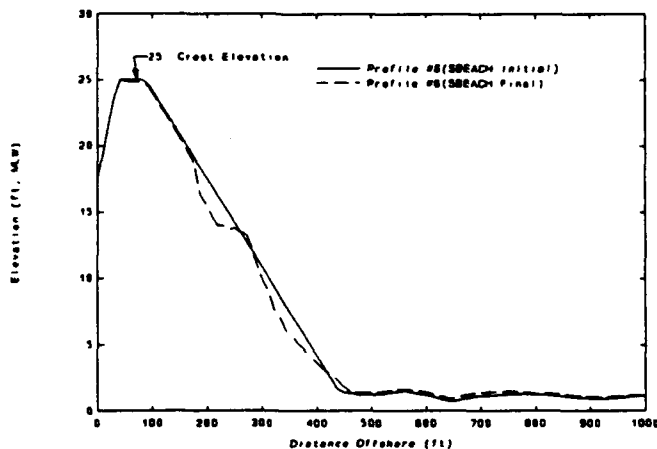
The ROTM was utilized to quantify the performance of the different dune designs in order to augment conclusions drawn from profile response simulations. Table 16 lists results of the ROTM for some of the calibration parameters considered for the analyzed dune designs. Only at Profile 6 with a 21-ft mlw dune crest is there notable overtopping predicted in response to the SPN. Results in Table 16 show overtopping volumes at Profile 6 to be approximately 55-80 acre-ft, which intuitively would agree with the profile response simulations. It was tentatively concluded based upon profile response results that a 23-ft dune would suffice at Profile 6, and ROTM predictions agree. Similarly, profile response simulations indicated negligible overtopping at Profiles 7 and 8, and results of the ROTM support this observation. Finally, it is anticipated that a dune crest of 23 ft mlw would provide substantial flood protection against the SPN event. The fully optimized dune elevation of 21 ft is not suggested at Profiles 7 and 8, so that a continuous dune system is implemented to eliminate possible three-dimensional effects not accounted for in the analysis. One additional consideration not evaluated during dune optimization using the ROTM is the width of the dune crest that would serve to augment protective characteristics of the



a. 21-ft mlw crest elevation



b. 23-ft mlw crest elevation



c. 25-ft mlw crest elevation

Figure 57. $K = 2.5 \times 10^{-6}$ and $Eps = 0.003$ (Profile 6)

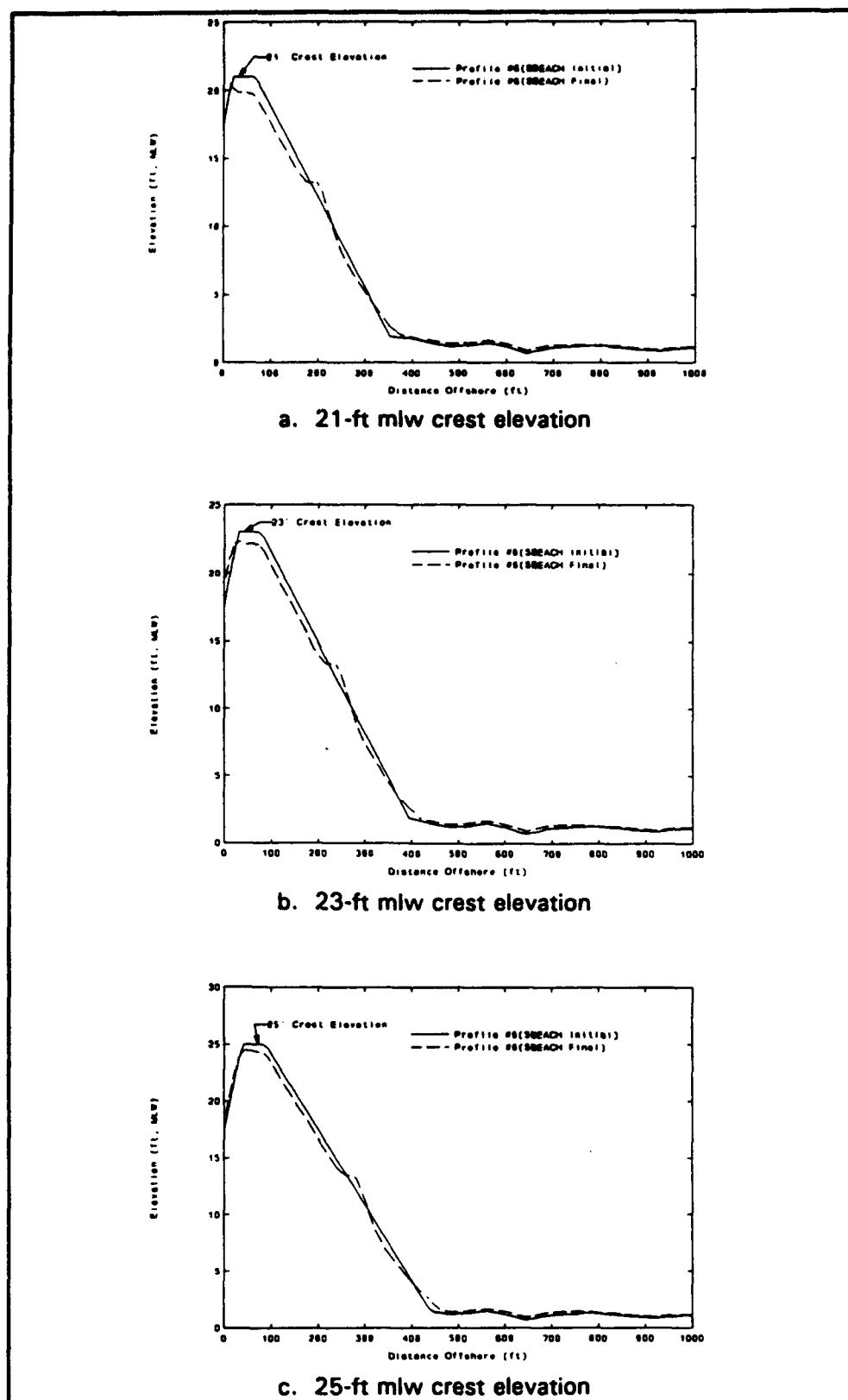


Figure 58. $K = 2.0 \times 10^{-6}$ and $Eps = 0.003$ (Profile 6)

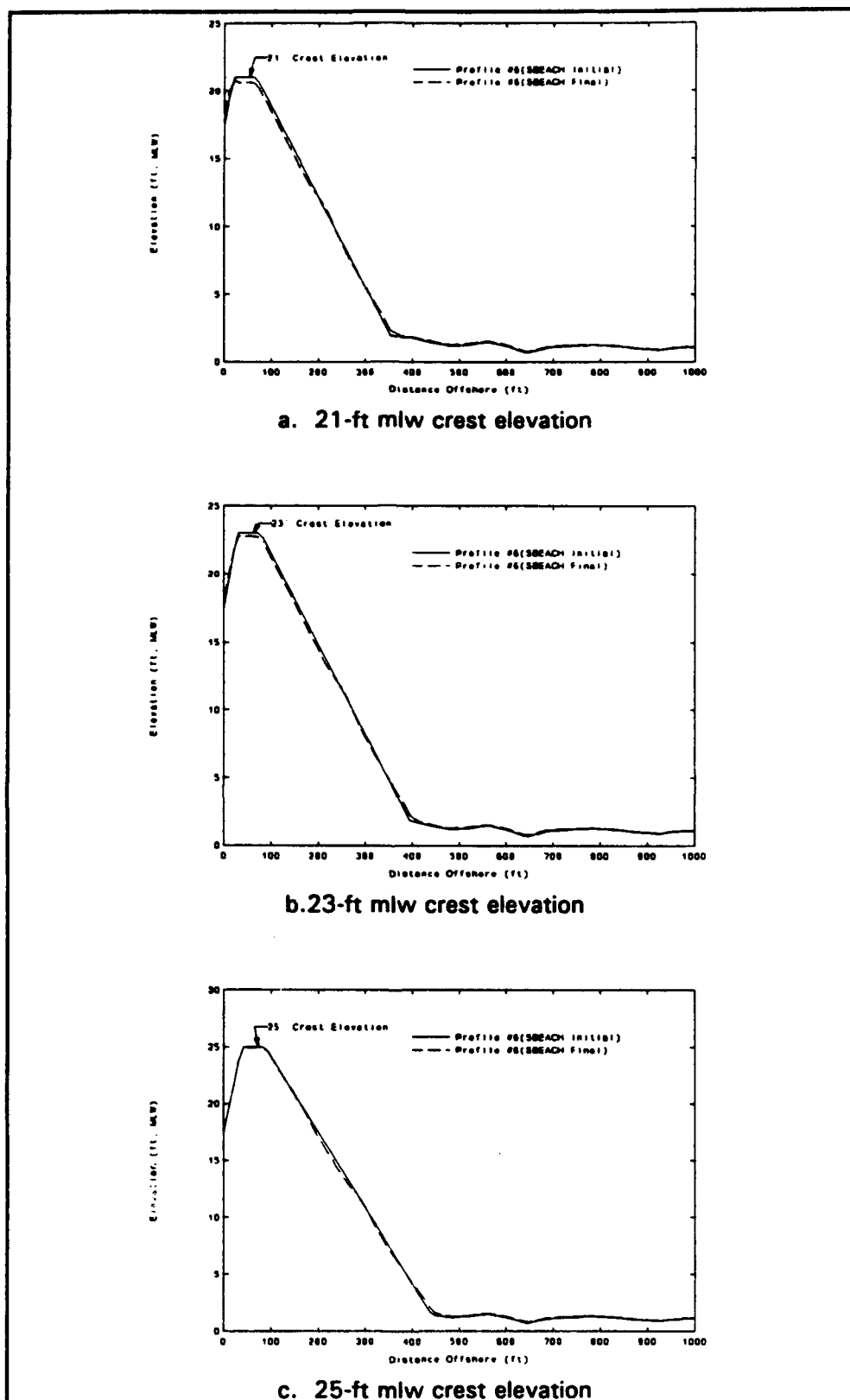


Figure 59. $K = 0.5 \times 10^{-6}$ and $Eps = 0.001$ (Profile 6)

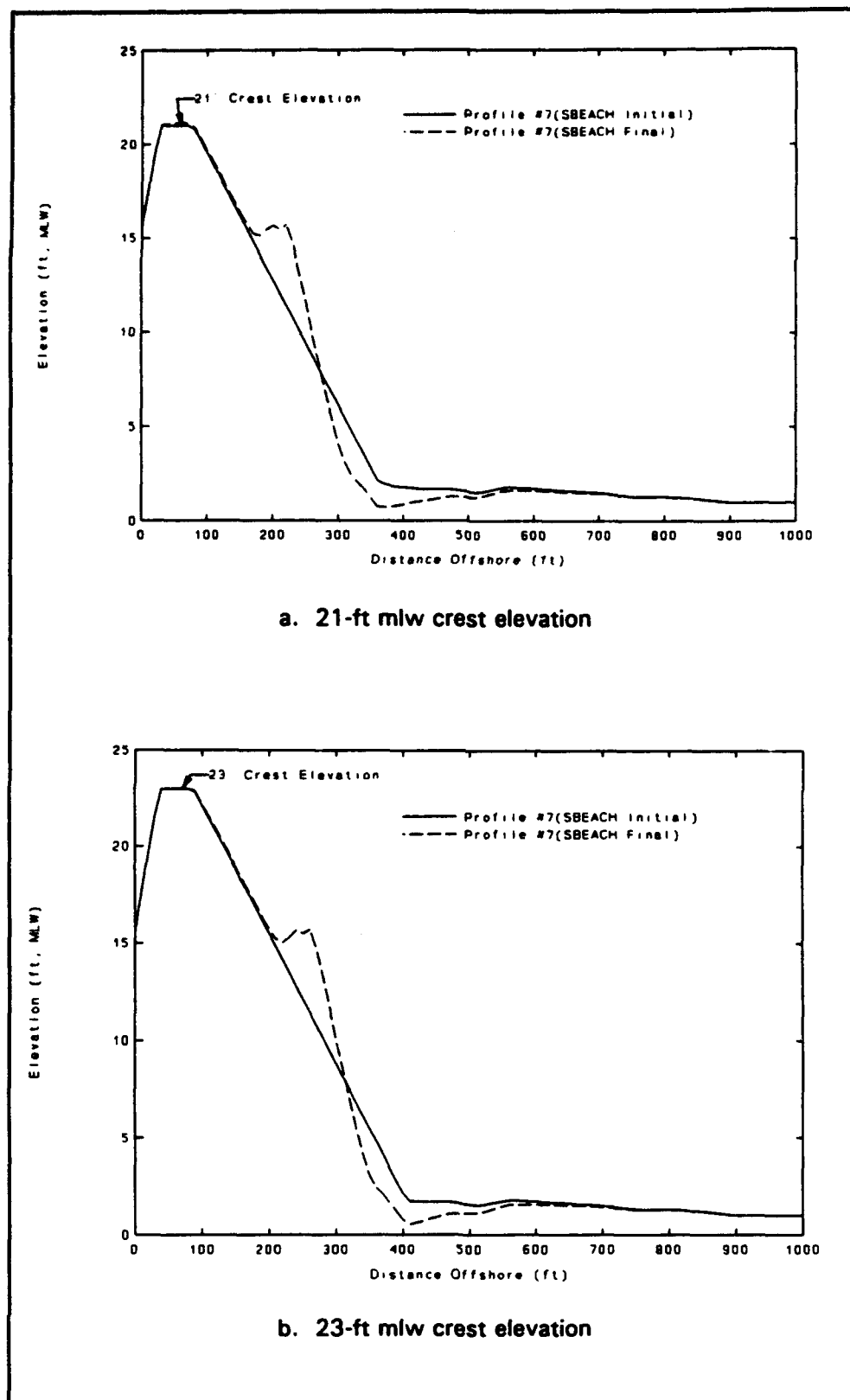


Figure 60. $K = 2.5 \times 10^{-6}$ and $Eps = 0.003$ (Profile 7)

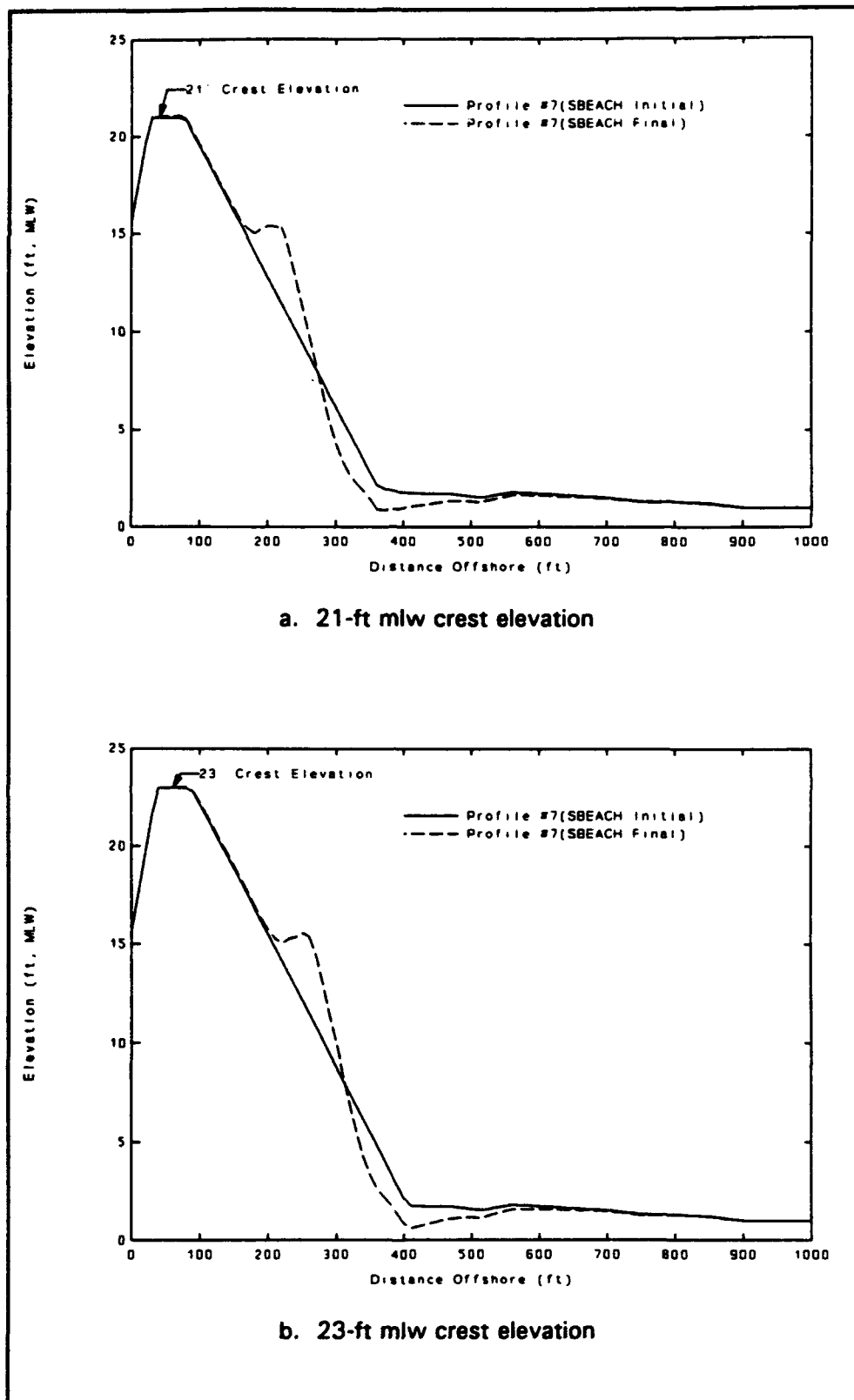
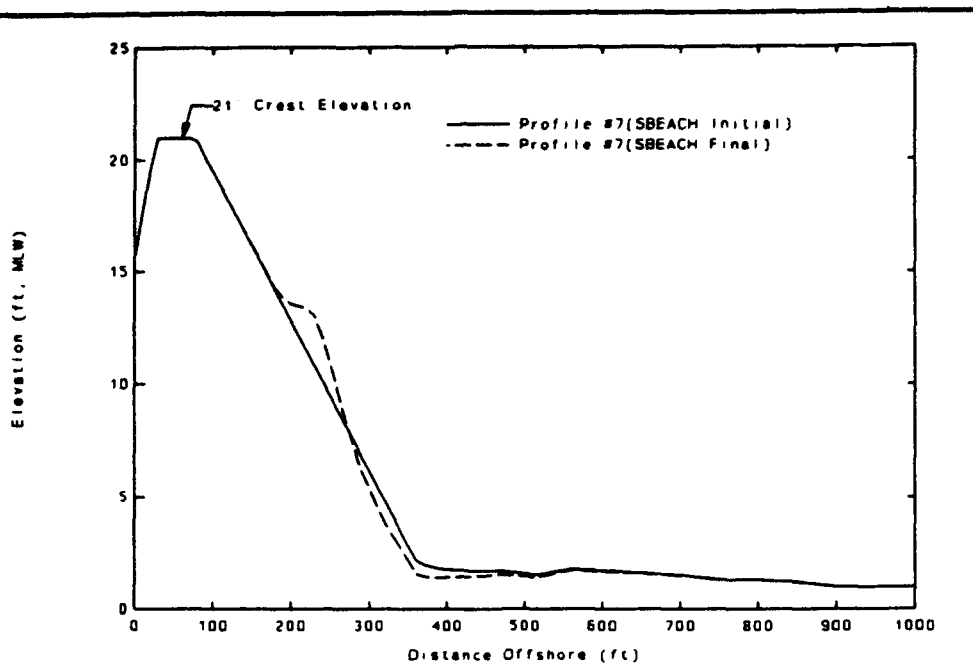
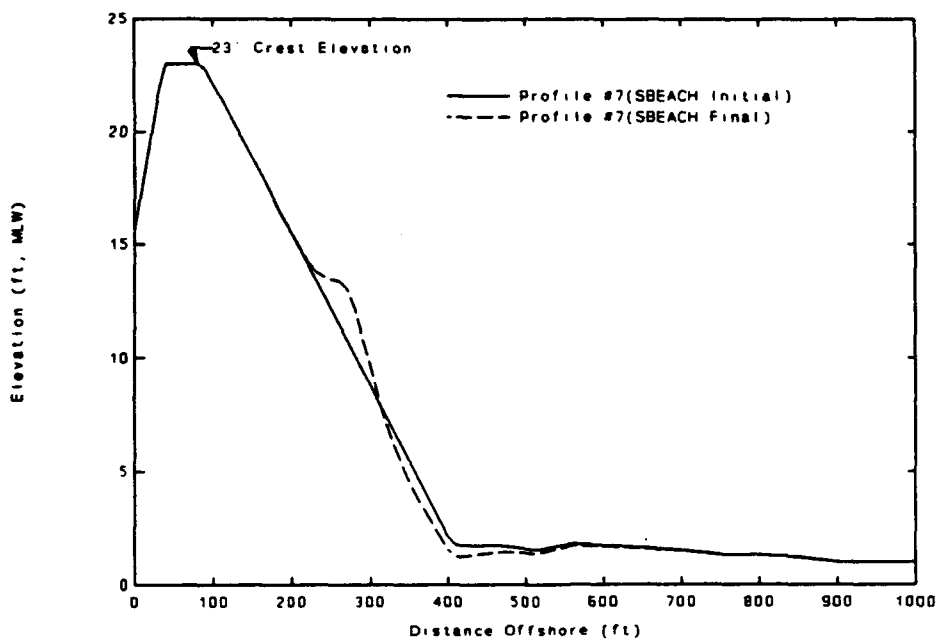


Figure 61. $K = 2.0 \times 10^{-8}$ and $Eps = 0.003$ (Profile 7)



a. 21-ft mlw crest elevation



b. 23-ft mlw crest elevation

Figure 62. $K = 0.5 \times 10^{-6}$ and $Eps = 0.001$ (Profile 7)

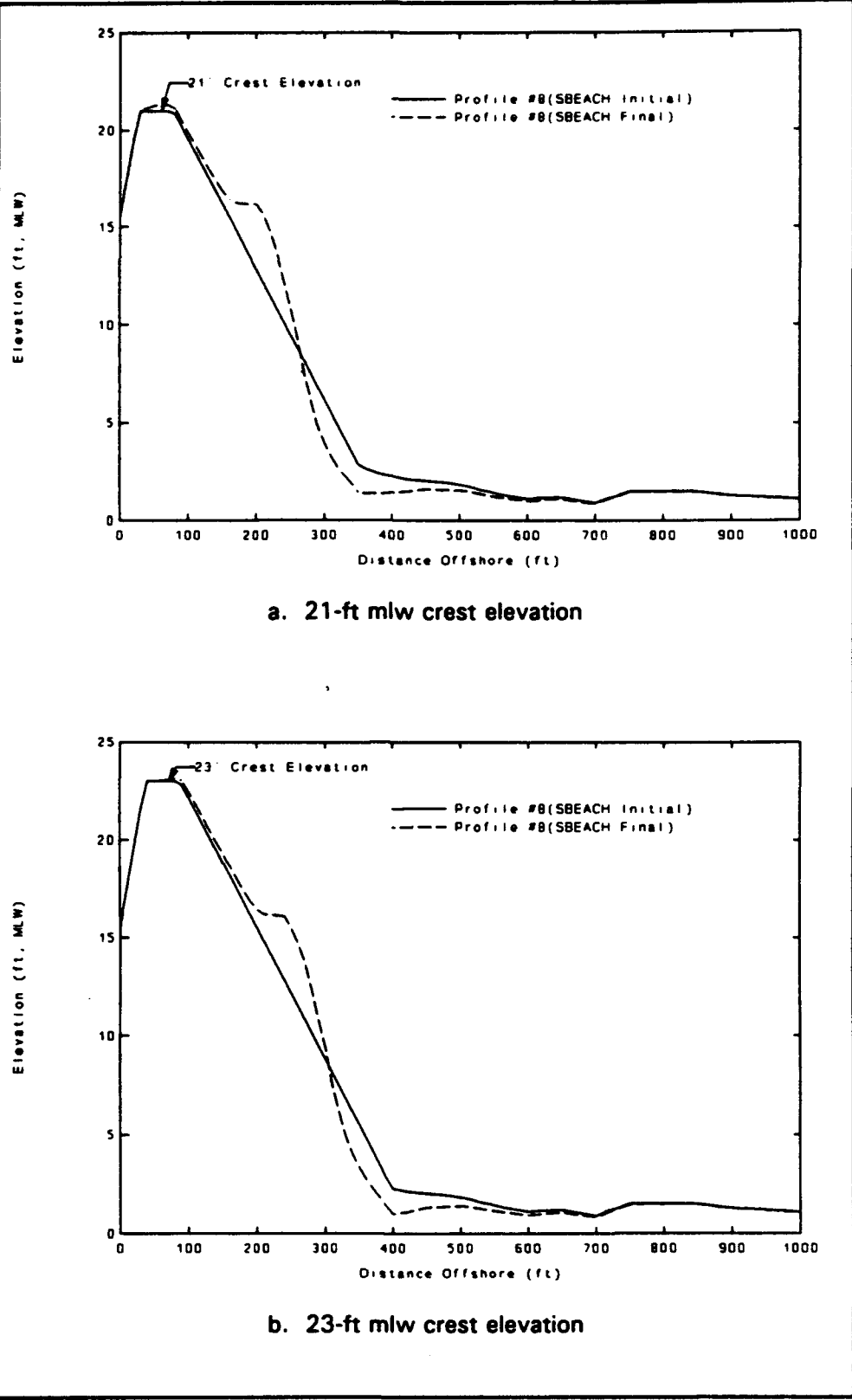
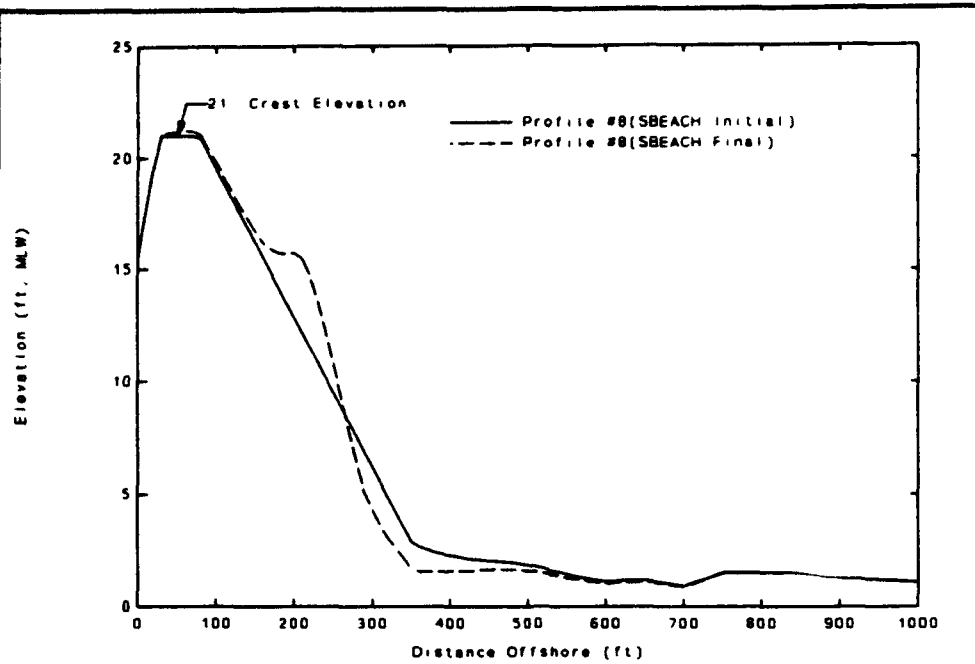
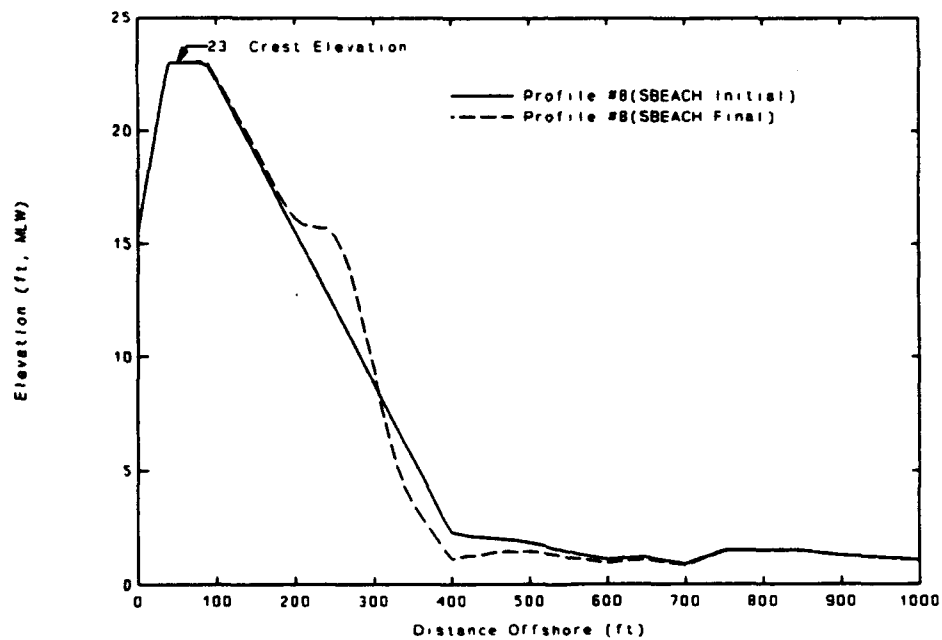


Figure 63. $K = 2.5 \times 10^{-6}$ and $Eps = 0.003$ (Profile 8)



a. 21-ft mhw crest elevation



b. 23-ft mhw crest elevation

Figure 64. $K = 2.0 \times 10^{-6}$ and $Eps = 0.003$ (Profile 8)

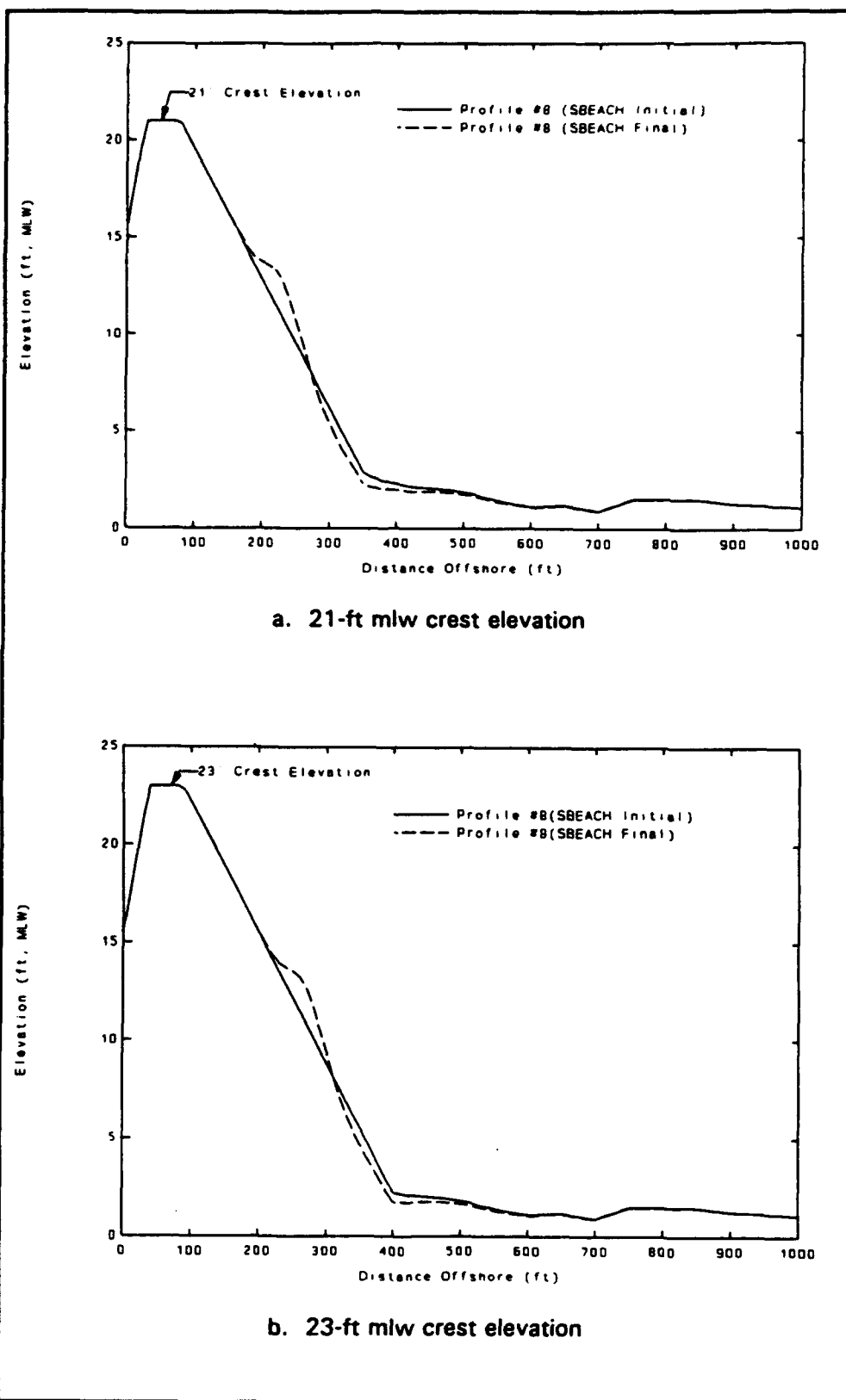


Figure 65. $K = 0.5 \times 10^{-6}$ and $Eps = 0.001$ (Profile 8)

Table 16 Dune Optimization Results					
Profile Number	Crest Elevation (ft, mhw)	Calibration Parameters		Overtopping Volume Q(acre-ft)	Maximum Overtopping Rate q(ft³/sec)
		K	Eps		
6	21	2.5 x 10 ⁻⁶	0.003	79	2.6
6	21	2.0 x 10 ⁻⁶	0.003	76	2.4
6	21	0.5 x 10 ⁻⁶	0.001	57	1.7
6	23	2.5 x 10 ⁻⁶	0.003	0	0.0
6	23	2.0 x 10 ⁻⁶	0.003	0	0.0
6	23	0.5 x 10 ⁻⁶	0.001	0	0.0
6	25	2.5 x 10 ⁻⁶	0.003	0	0.0
6	25	2.0 x 10 ⁻⁶	0.003	0	0.0
6	25	0.5 x 10 ⁻⁶	0.001	0	0.0
7	21	2.5 x 10 ⁻⁶	0.003	1	0.1
7	21	2.0 x 10 ⁻⁶	0.003	0	0.0
7	21	0.5 x 10 ⁻⁶	0.001	0	0.0
7	23	2.5 x 10 ⁻⁶	0.003	0	0.0
7	23	2.0 x 10 ⁻⁶	0.003	0	0.0
7	23	0.5 x 10 ⁻⁶	0.001	0	0.0
8	21	2.5 x 10 ⁻⁶	0.003	1	0.0
8	21	2.0 x 10 ⁻⁶	0.003	1	0.0
8	21	0.5 x 10 ⁻⁶	0.001	1	0.1
8	23	2.5 x 10 ⁻⁶	0.003	0	0.0
8	23	2.0 x 10 ⁻⁶	0.003	0	0.0
8	23	0.5 x 10 ⁻⁶	0.001	0	0.0

dune. The ROTM does not consider the crest width, calculating overtopping over a single crest point. It is expected that the dune crest would reduce overtopping of the entire dune feature, which logically will differ from overtopping of a single point.

Because the SPN tended to move the coarse-grained material onshore at Profiles 7 and 8, and Profile 6 was predicted to perform well in mitigating overtopping, further dune optimization was conducted to test different dune designs requiring less beach fill material. Two analyses were completed: (a) testing of a smaller dune with a 30-ft crest width, and (b) creating and

testing of a more "erosive" SPN event in response to the onshore movement of material predicted for the "original" SPN. Additionally, the CENED proposed to optimize dune seaward slopes. However, the match between the 1:15 dune slope and natural beach slopes, and relatively minor predicted profile responses, suggesting a profile essentially at equilibrium, eliminated this work. As stated, the ROTM does not account for dune crest widths and profile response was used as indicative of the capabilities of the narrower dune crest. The "erosive" SPN was created from the "original" SPN by decreasing wave periods, which influences the direction of transport as predicted by SBEACH, with steeper waves causing a more erosive storm. Also tested with the "erosive" SPN was the effect of the narrower crest width on beach response, and ultimately overtopping. Again, results indicated that the dune feature was very stable, with no increase in overtopping given the 30-ft crest width and/or the "erosive" SPN. Finally, dune optimization indicated that a 30-ft crest width at either 21 ft (Profiles 7 and 8) or 23 ft mhw is sufficient to mitigate flooding at POP, assuming proper maintenance.

Revetment evaluation

Performance comparisons between dune and revetment designs were completed with the prediction of overtopping of the proposed revetment. A revetment submodule was incorporated into the ROTM using the method developed by Ward (1992) (see Chapter 4). The ROTM was used in conjunction with SBEACH to evaluate the revetment at POP (Profiles 6, 7, and 8), for cases with and without protective beach fill fronting the structure. Figure 66 depicts the revetment design at Profile 6 both with and without beach fill. Revetment design at Profile 6 consists of a revetment with a 10-ft-wide crest at 20.5 ft mhw starting at the existing seawall, with a 1:3 seaward slope down to a 20-ft-wide beach fill at 10.5 ft mhw. The revetment design at Profiles 7 and 8 is shown in Figures 67 and 68 both with and without protective beach fill fronting the structure. Revetment design at Profiles 7 and 8 is characterized by a crest elevation of 18.5 ft mhw, and proposed burial of the entire structure beneath a dune feature with a 1:12 seaward slope down to existing grade. The SPN was used to simulate profile response and yield ROTM input. With- and without-beach fill conditions were simulated to give a range of conditions encompassing the potential pre-storm profile shape. It is important to note that Profiles 7 and 8 with-beach fill conditions were treated as a dune, because it was found that the revetment never became exposed during SPN simulations.

Results of the revetment evaluation are presented in Table 17. Note that overtopping volumes are significantly reduced when beach fill is used in conjunction with the revetment, due to the dissipative characteristics of the fronting beach. Comparison of overtopping volumes for the dune systems and

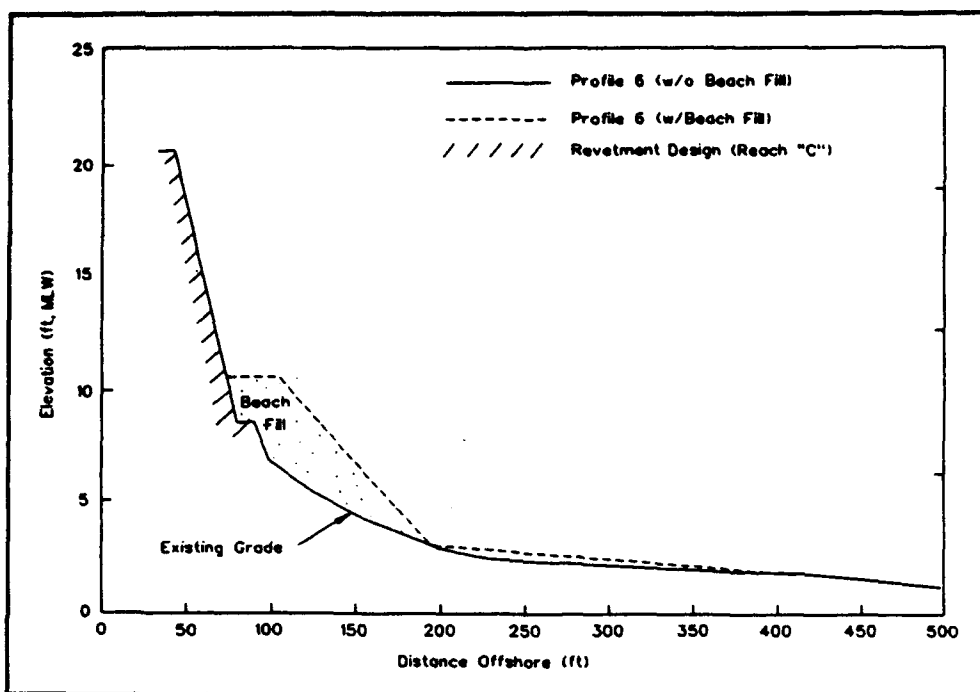


Figure 66. Revetment design at Profile 6

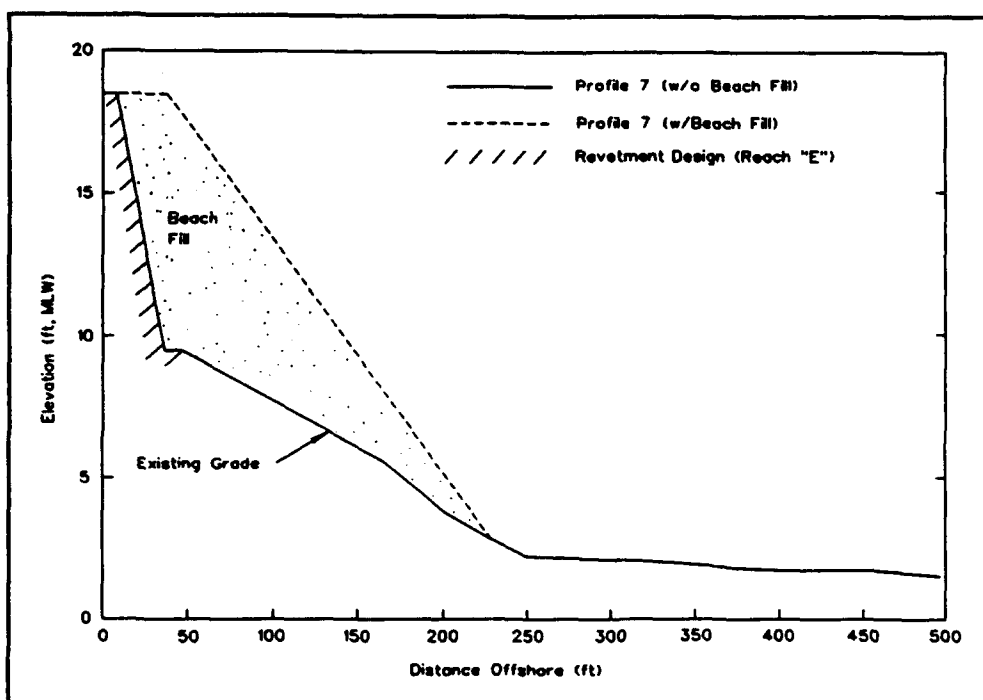


Figure 67. Revetment design at Profile 7

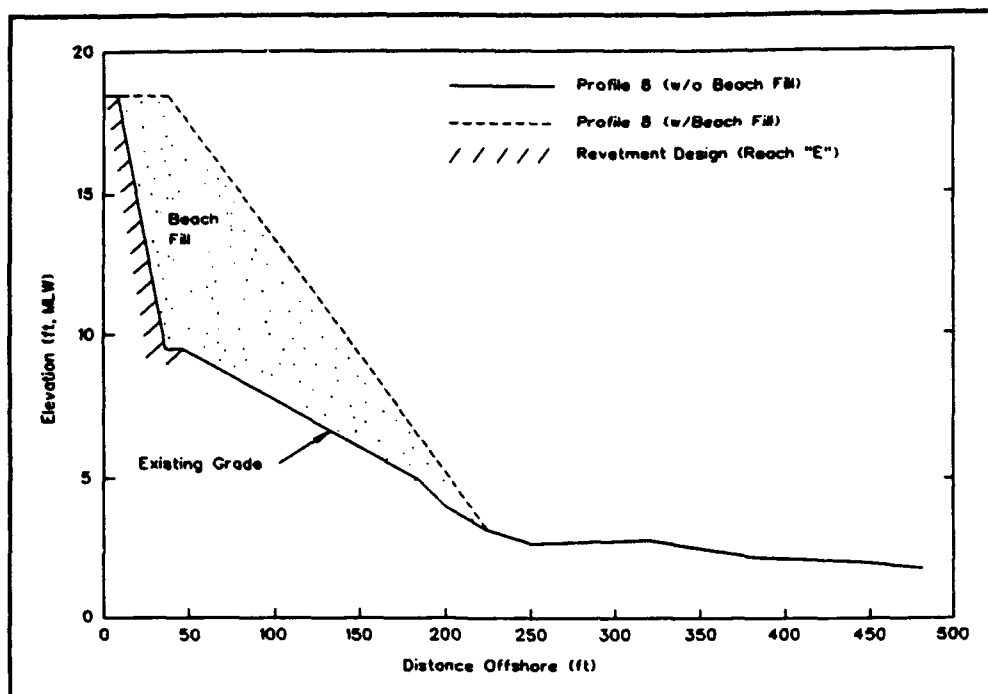


Figure 68. Revetment design at Profile 8

Table 17 Revetment Optimization Results			
Profile Number	Fill Status	Crest Elevation (ft. mhw)	Overtopping Volume, Q (acre-ft)
6	Without Fill	20.5	7341
6	With Fill	20.5	2671
7	Without Fill	18.5	7350
7	With Fill	18.5	271
8	Without Fill	18.5	13664
8	With Fill	18.5	642

revetment designs indicates that the dunes in the design configurations are significantly more effective in mitigating overtopping. This evaluation points to the resistance of the coarse fill to erosion and overtopping, and advantages associated with increased dune elevations. Lastly, relative to revetment results for the SPN, it appears that implementation of a dune system at POP most likely would provide the required level of flood protection.

Overtopping simulations

Based upon results of dune optimization and revetment evaluation, design options at POP were selected and extensive evaluation of the Revere Beach and POP reach was completed. Dune optimization, revetment evaluation, and profile response simulations indicated the effectiveness of a dune system at POP. CENED directed to test revetment options only at Profile 6 where dune capabilities appear less certain, eliminating the revetment option at Profiles 7 and 8. A dune elevation of 23 ft mlw was selected for further testing at POP. In order to maintain consistency along the dune section and eliminate potential three-dimensional effects, a single dune was selected in lieu of the fully optimized dune elevations as discussed in a previous section. Concisely, Revere Beach was evaluated with the structural/profile conditions present on 27 November 1991, which were considered existing conditions, and POP was tested with revetment (with and without beach fill) and dune designs at Profile 6, and dune designs at Profiles 7 and 8.

The range of application of the regression equations is discussed here to augment Chapter 4 and Appendix A with evaluation of specific applications and assessment of ROTM performance.

Bore runup was tested in the physical model for a wide range of overtopping conditions for each individual profile. It is assumed that data points outside the tested range at each profile result in zero overtopping, because all storm conditions that caused notable overtopping as a result of the SPN and given profile were modeled in the laboratory. Ranges of data are presented in Appendix A for storm and profile combinations. Application of the bore runup regression was conducted using only the data within the tested ranges (in terms of Buckingham PI terms given for bore runup) for each profile, and all data outside of these limits were assigned a value of zero.

Similarly, simulations utilizing the broken waves submodule were for the range of data tested in the physical model. The verification portion of the physical model tests was completed with Profile 2; therefore, Profile 2 was the 1978 profile tested in the physical model. This resulted in a single application range (range of Buckingham PI terms) for this submodule, as opposed to the bore runup situation where five separate ranges resulted due to the construction of five different profiles. Appendix A contains the range of tested data and application of the broken waves regression was limited to data within the tested range with the remainder of the simulation assumed to result in minimal overtopping.

Overtopping results for the entire project in response to the set of 50 storms are located in Appendix B with revetment and fronting beach fill at Profile 6. Appendix C presents overtopping results for Profile 6 only, for two design options, revetment without fronting beach fill and a dune with a 23-ft crest elevation. Profiles dated 27 November 1991 were used to represent existing

conditions, along with the dune cross sections at POP. Application of the ROTM followed methods previously discussed with results of SBEACH used as input to the revised ROTM. All simulations (Profiles 1-5) contained in Tables B2-B51 utilized the physical model generated regression equation for bore runup. Examination of overtopping rates as a function of storm parameters indicated reasonable predictions. ROTM output for the SPN event was verified using overtopping volumes measured in the physical model study, thus providing for validation of the ROTM setup. Table B1, which summarizes Tables B2-B51, contains only total overtopping volumes for the entire site, which may be used to evaluate the total flood mitigation scheme. Tables B2-B51 contain information that may be used to further design or optimize individual flood protection structures.

It is obvious from Appendix B results that the November 1945 event is the most severe in terms of overtopping; however, the coarse-grained beach fill at Revere Beach appears effective in mitigating flooding even in response to the SPN. Overtopping for the November 1945 event at various return frequency water levels ranges from approximately 133 to 943 acre-ft (with dune at Profile 6) and 148 to 3,614 acre-ft (with revetment at Profile 6), and 29 to 287 acre-ft (with dune) and 29 to 291 acre-ft (with revetment) for the February 1978 storm (see Appendices B and C). Sustained high water levels and storm duration are responsible for the increase in overtopping for the SPN relative to other storms. From Tables B2-B51, it is evident that for a set of storms with the same return period (maximum water levels) maximum overtopping rates are comparable. However, large differences in overtopping volumes result from storm sub-peaks for sustained storms where overtopping occurs over numerous tidal cycles. Overall, overtopping volumes appear rather well controlled for all but the most extreme storm events with revetment at Profile 6. Attention should be given to the overtopping volumes predicted at POP, where essentially no overtopping occurs for any of the storms in the set for the continuous dune. This again points to the effectiveness of the dune system. Also, the revetment with beach fill appears capable of reducing potential flooding in response to storms between the 50- and 100-year return period level. It is not possible to analyze a deteriorated beach/dune system, which might result in an increase in damage susceptibility and should be considered in the interpretation of the results presented and in development of a fill maintenance plan. A lack of maintenance to sustain the beach and dune in a near-design state would negate the work conducted herein, thus creating an uncertain level of flood protection.

Table B1 depicts the relationship between storm return periods and predicted overtopping volumes. The November 1945 SPN, 500-, and 100-year storms result in substantial overtopping volumes, primarily at Profile 6 (with revetment). Overtopping at Profile 6 for these events resulted due to the presence of input conditions that well exceeded the range of applicability of the revetment equation, thus leading to apparently extreme results. It is obvious from Tables B2-B4 that overtopping rates at Profile 6 are excessive,

but should be considered indicative of anticipated high levels of flooding. It is noted that the revetment portion of the ROTM includes dependency on wave length and wave height at the structure. This causes the November 1945 event to far exceed other storms in overtopping volumes at the revetment due to associated long wave periods and large wave heights.

The four 100-year storm events range in predicted overtopping from 151-663 acre-ft. Profile 6 contributes 300 acre-ft to the November 1945 100-year event, but portions of this event exceed the range of applicability of the revetment relationship. The range of overtopping is 151-363 acre-ft for the 100-year events if a dune is implemented at Profile 6. Overtopping for the nine 50-year storms varies from 111-548 acre-ft (with revetment) and from 111-457 acre-ft (with dune). These results indicate an increase in revetment effectiveness at approximately the 50-year return period level with revetment capabilities more closely modeling predicted overtopping with a dune at Profile 6. Ranges of total overtopping volumes decrease for the higher frequency events with the ten 20-year events predicted to yield 71-184 acre-ft and the ten 10-year storms from 42-148 acre-ft. The wide variance of overtopping for the low frequency events relative to high frequency storms is a result of the definition of return period based only upon maximum total water level. It is evident that hydrograph shape (duration of storm peak and significance of storm sub-peaks) plays a major role in determining total overtopping volumes. Only the November 1945 event has numerous storm peaks that cause notable overtopping to occur over several consecutive high tide cycles. These sub-peaks are only slightly greater than those associated with other storm events, which points to the dependence of overtopping on water level changes.

The sensitivity of the bore runup regression equation to data that extrapolate beyond the tested data set is observed for a limited number of cases. From Tables B2-B7, an inaccurate trend of results is observed for the Oak Island/Profile 2/22.5-ft mlw wall height overtopping condition. As storm return period decreased, it was anticipated that overtopping volumes would also decrease. However, only one wall height was tested at Profile 2, and it is uncertain how representative the 21.0-ft mlw wall height that was tested is for the entire section. It is probable that the 22.5-ft wall height causes an unusual combination of parameters, resulting in a "stretch" of the regression equation. It is suggested that results corresponding to wall heights significantly different from the tested wall height at a given profile be interpreted conservatively.

One additional irregularity that must be addressed in more detail appears in Appendix B, where the total overtopping calculated at Revere Beach (Profiles 1-5) for the November 1945 50-year event is greater than the volume output for the November 1945 100-year event. An explanation of the volumes obtained from the November 1945 50- and 100-year storms can be traced to the differences in the storm hydrographs. Figure 69 depicts the swl (surge +

tide) used in SBEACH simulations of these events. Note that the peak water level for the 100-year storm exceeds the peak of the 50-year storm, and subsequently the 100-year maximum overtopping rate exceeds the 50-year rate (see Tables B4 and B5). Storm return periods were assigned in Part I of this study based solely on this peak water level; however, it is unknown a priori that a higher return period event will result in increased overtopping (or recession if pertinent). Many factors play a role in determining total overtopping volumes for a given storm event, including water level (both peak and significant sub-peaks), wave height, storm duration, wave period, and hydrograph shape (i.e., the duration of the peak of the storm). It is not totally correct, due to the influence of many factors on storm effects, to assume that total water level (specifically peak water level) is the defining storm parameter; however, such assumptions are currently common practice.

Importance of the storm sub-peaks can be seen from comparison of the predicted overtopping rates for the 50- and 100-year November 1945 storms. From Figure 69, it can be seen that it is not solely the major storm peak that determines overtopping, but instead the summation of all storm peaks significant enough to cause overtopping. Despite the correct trend in overtopping rates at the storm peak, it is evident from Figure 69 that other portions of a storm will result in different overtopping trends due to the relative shape differences between the storm hydrographs. These sub-peaks demonstrate the importance of storm duration and hydrograph shape, including the magnitude and phasing of the astronomical tide, for the 50- and 100-year storms. In Figure 69, the 50-year event maintains a higher water level than does the 100-year event during 60 percent of the high tide cycles resulting in greater overtopping for the 50-year storm. Relatedly, Figure 70 depicts similar data for the February 1978 50- and 100-year storm events. Figure 70 shows a different hydrograph shape from Figure 69 with the 50-year sub-peaks below the level where overtopping initiates. Comparison of the two events (November 1945 and February 1978) shows the effect of storm hydrograph shape on the prediction of overtopping. It is noted that all other storms in the data set of equal or lesser return period contained only one significant storm peak that resulted in overtopping. Therefore, trends in overtopping volumes were dependent upon only one storm peak, which, given the method of ranking events, creates what is assumed to be the appropriate trend in overtopping rates (i.e., 100-year volume greater than 50-year volume). The November 1945 storm results in an apparent reversal in overtopping trends; however, it is again important to mention that storm return periods based solely on total peak water level are not totally indicative of storm severity due to the effects of other storm parameters not represented.

Despite the discussed difficulties associated with the analyses conducted within this study, it is anticipated that results provide for significant improvements over any previous results and any other potential types of analyses. This study presents an innovative method in the prediction of overtopping with the incorporation of both numerical and physical models and

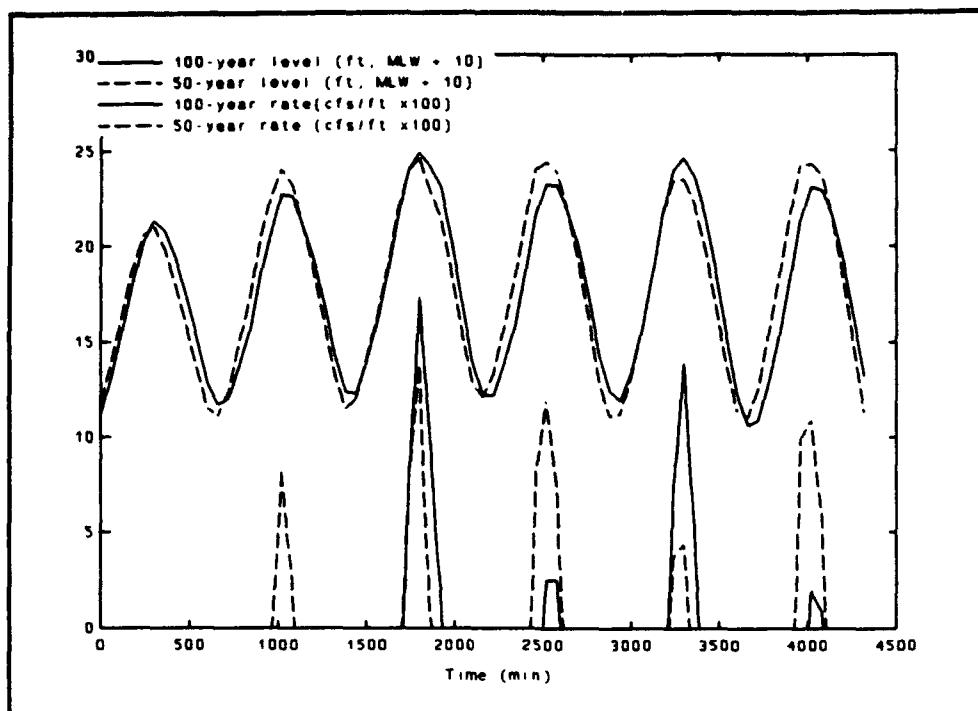


Figure 69. November 1945 (50- and 100-year): Water levels and predicted overtopping rates

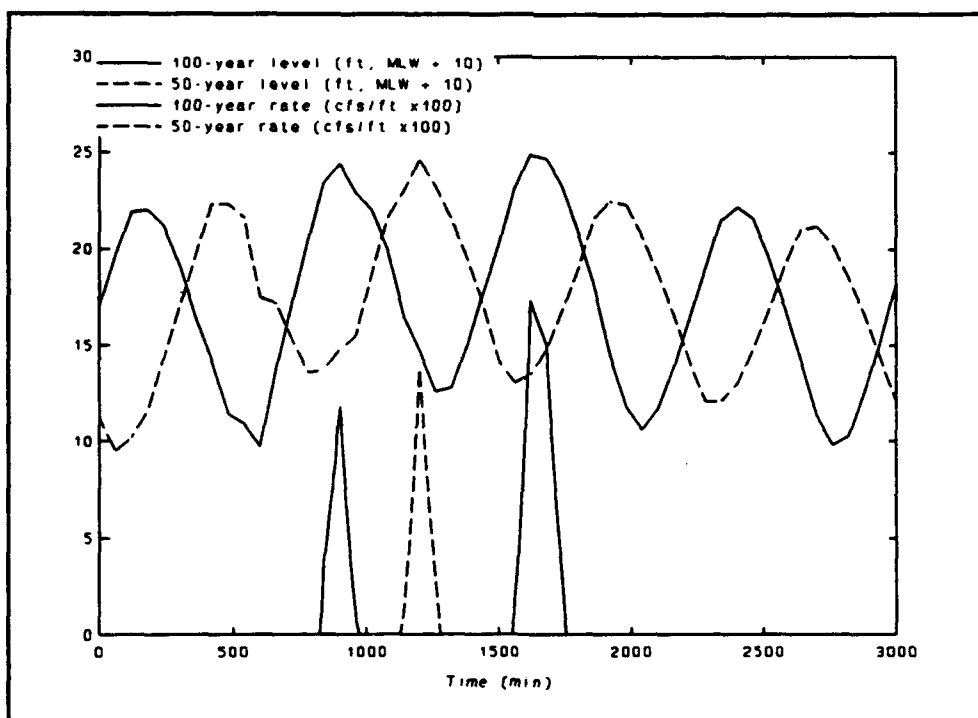


Figure 70. February 1978 (50- and 100-year): Water levels and predicted overtopping rates

actual physical data available to validate the work completed. For instance, SBEACH results were fully evaluated considering the Halloween storm data set and physical model and numerical simulation overtopping volumes were verified with the data available from the Great Blizzard. Site-specific data, no matter the limitations, provide verification for the broad range of analyses conducted, allow for relatively high confidence in study output, identify difficulties, and indicate where caution is necessary.

Indicative of the output contained in Appendix B and the success of the study in producing consistent and accurate overtopping volumes are the plots depicting the expected value and 90-percent confidence limit lines (Figures 71-75). An analysis of confidence intervals provides additional information about the frequency of occurrence of different overtopping volumes in light of the fact that the frequencies are defined solely on maximum total water level and other parameters such as duration and hydrograph shape are important in determining overtopping. Shown are results for each individual tidal flood zone with overtopping volumes plotted against storm return periods. Confidence limits were calculated based upon the entire data set; therefore, it is anticipated that the sole 500-year event may not be the expected overtopping that occurs with this frequency. Additionally, the SPN event is not included due to an undefined return period. Results for tidal flood zone 4C are not shown because no overtopping was predicted. Interpretation of the confidence limits assumes a comprehensive database sufficient enough to fully envelope all expected overtopping conditions. The expected values and the mean confidence level may be used to represent the probable overtopping volume expected to occur for a given storm return period. The upper and lower confidence limits bracket the range over which overtopping volumes may be expected to occur, with 90-percent confidence. Realizing the limits of the conducted analysis, the range between the 90-percent confidence lines may be taken as indicative of the uncertainty associated with a limited storm series and innovative methodology in predicting overtopping. Also, imbedded in the confidence interval are the overtopping conditions falling outside the applicability limits of the ROTM. Results indicate that the 50-year overtopping volumes are well grouped with the exception of one storm, the previously discussed November 1945 50-year storm. This suggests that, given the limits of the storm set, it is possible to infer that this event was erroneously labeled a 50-year event and should instead be considered as a lower frequency storm (if overtopping volume frequency is used to determine storm return period). Furthermore, the spread in output data is evident with increasing storm severity, which points to the difficulties associated with labeling more extreme events due to limited amounts of data and difficulties associated with modeling such events.

Further evaluation of the ROTM and project site was conducted using additional overtopping simulation input. Three cases were tested: (a) Halloween storm data set utilizing Halloween pre-storm profiles and Halloween storm parameters; (b) 1978 profile data simulated using storm data from the Great

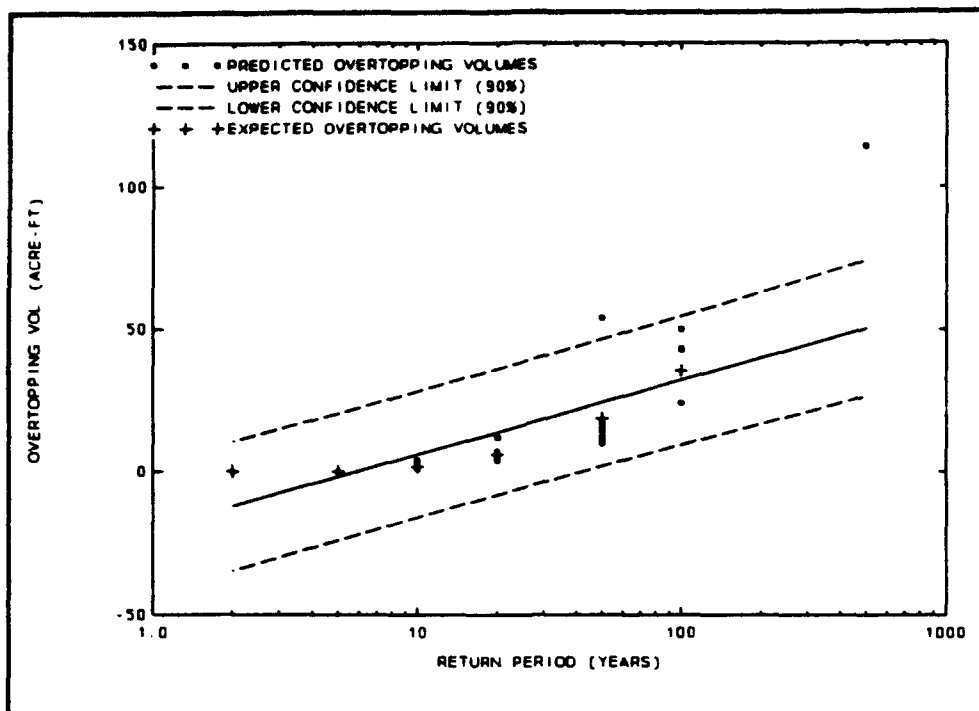


Figure 71. Predicted overtopping confidence intervals (Tidal Flood Zone 1)

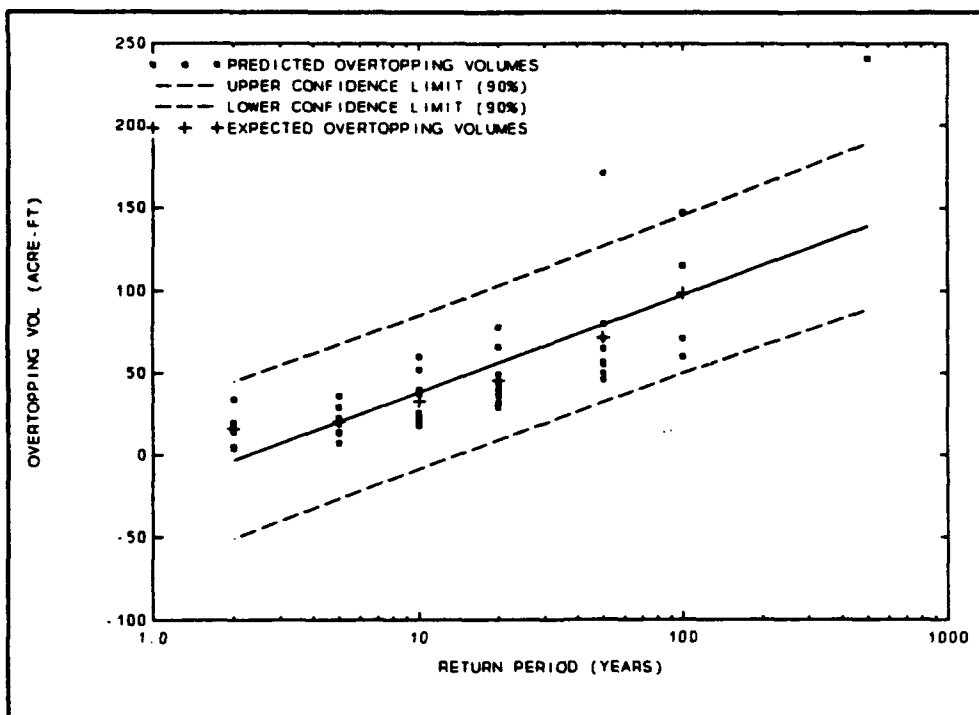


Figure 72. Predicted overtopping confidence intervals (Tidal Flood Zone 2A)

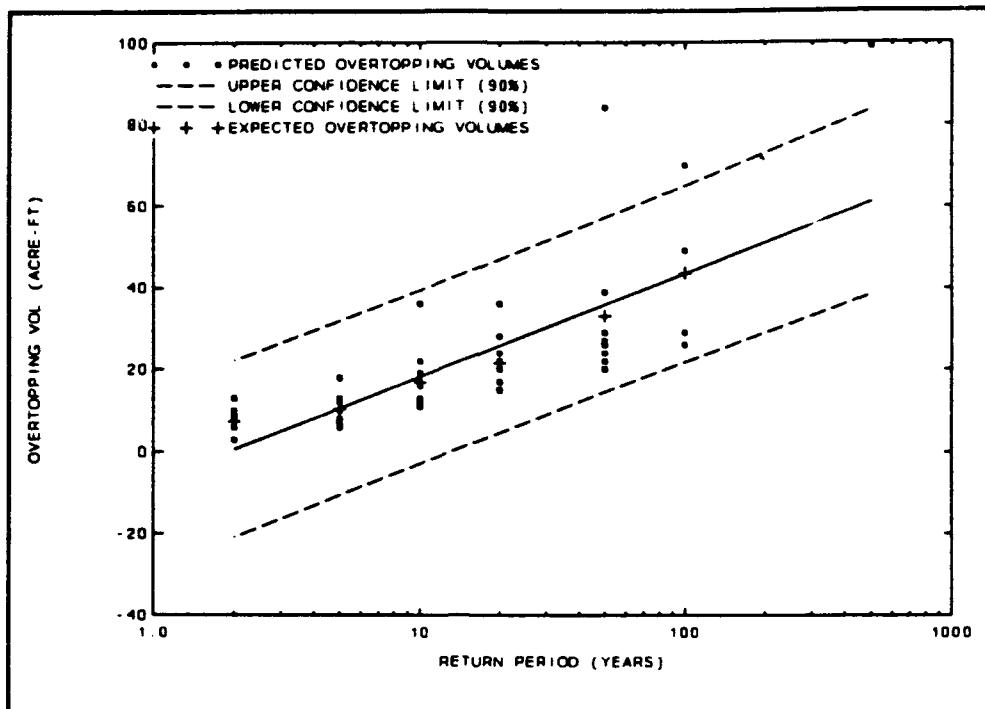


Figure 73. Predicted overtopping confidence intervals (Tidal Flood Zone 4A)

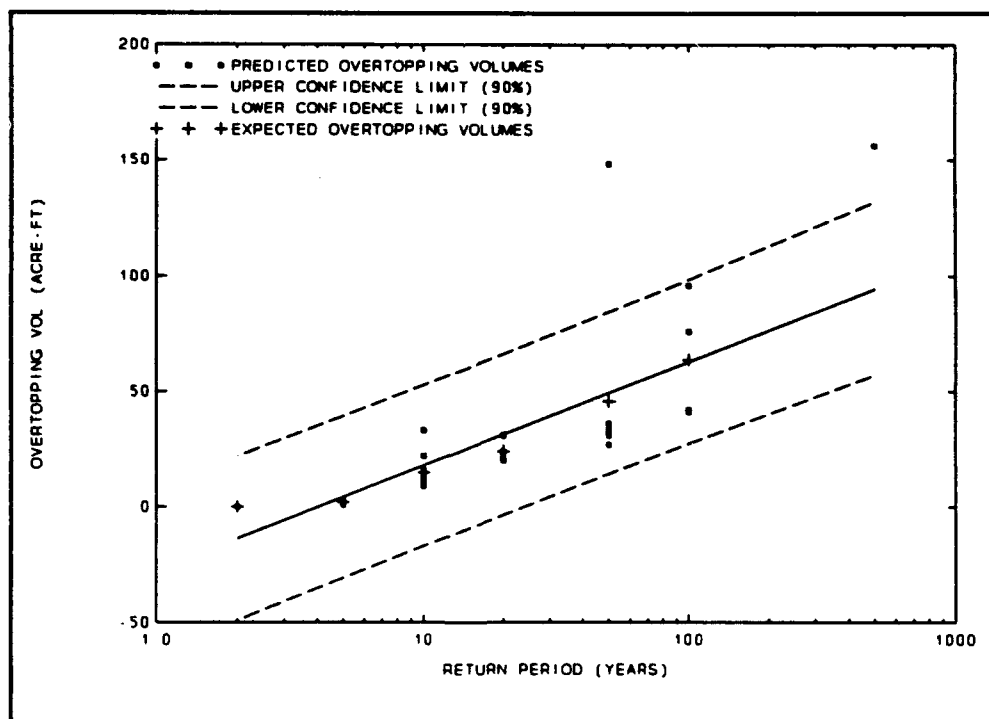


Figure 74. Predicted overtopping confidence intervals (Tidal Flood Zone 5B)

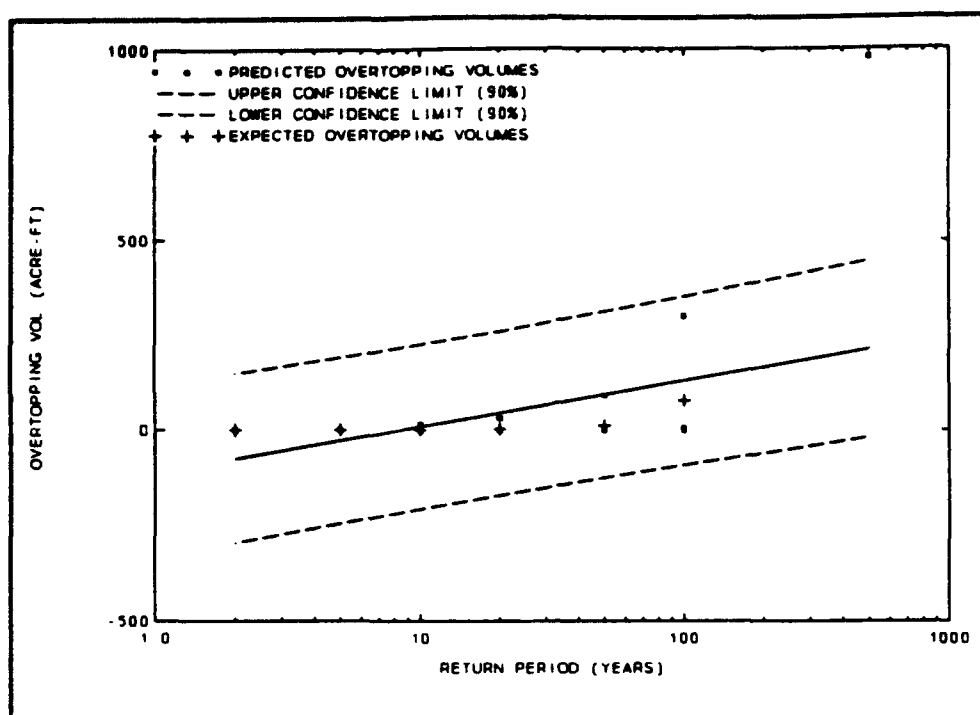


Figure 75. Predicted overtopping confidence intervals (Tidal Flood Zone PP)

Blizzard in order to test the capabilities of the ROTM when run under multiple conditions (i.e., bore runup, broken waves, and weir flow conditions); and (c) Halloween storm parameters simulated using 27 November 1991 profile data to indicate post-storm vulnerability to another storm of magnitude similar to the Halloween event.

Results of the alternative overtopping simulations are contained in Appendix D. Two sets of output were generated for the Halloween and Great Blizzard data sets. The simulations utilizing the 27 November 1991 profiles fit neatly within the range of tested results (physical model results for Profiles 1-5 covering entire range of overtopping). Simulations conducted using other combinations of profile, structural, and storm data tend to "stretch" the capabilities of the regression equations. Appendix D, therefore, contains two module output sets for two cases: (a) output results from a set of tight overtopping ranges (physical model data used to strictly enforce applicable range of regression equations); and (b) output resulting from a "relaxed" application of the ROTM where the input parameters falling outside the physical model tests are implemented in calculating overtopping. Simply, the "relaxed" application computes overtopping for each time step and ignores the range of applicability established for the regression equation based upon the physical model tests.

It can be seen that the Halloween storm output varies significantly utilizing the two different approaches (Tables D1 and D2). Overtopping for both cases

is rather moderate (in comparison with Great Blizzard overtopping volumes) and Table D1 agrees reasonably well with actual overtopping occurring during the storm. Output for the Great Blizzard shows negligible differences for the two approaches (Tables D3 and D4). This result indicates that conditions tested in the physical model closely approximated the conditions of the Great Blizzard (February 1978 50-year event is very similar to the Great Blizzard) for Profile 2. Examining other profiles indicates difficulties due to extrapolating the capabilities of the regression equations. Overall, agreement between predicted and measured Great Blizzard overtopping is questionable at profiles other than Profile 2, for which the physical model was verified, and results due to the failure to model multiple profile conditions in the laboratory. Lastly, the post-Halloween storm vulnerability of the project site was evaluated. The ROTM output shown in Table D5 indicates that a high level of protection was in place following the Halloween storm, and suggests that overtopping utilizing the Halloween data set is likely best represented by the strict ROTM (Table D1), because of an increase in confidence in Table D5 results due to the testing of all five Revere Beach profiles used in the ROTM simulations.

The CENED also requested testing of a worst-case condition. A simulation was conducted with the defined worst-case overtopping condition, 1978 profile data and the November 1945 SPN storm. Results of this procedure are given in Appendix D. Table D6 depicts results obtained from the ROTM, and indicates extremely high overtopping volumes. It is noted that the ROTM was not developed beyond the limits of the broken waves condition, and that the worst-case simulation utilized the weir flow submodule for a high majority of the overtopping volumes shown. It is suggested that these results be neglected, because they represent an extreme "stretch" of the capabilities of the ROTM.

A physical model study of the worst-case overtopping condition was undertaken based upon the inability to apply the existing ROTM with much confidence to these extreme conditions. The worst-case developed ROTM made use of specific worst-case data (1978 profile and SPN storm), calibration data (1978 profile and Great Blizzard storm), and broken waves data (1978 profile and storm data shown in Table 7). These data consist of water levels above the beach/seawall intersection, and overlap the broken waves and weir flow conditions. It was anticipated that an ROTM designed for a broad range of applications (utilizing the 1978 profile), with the capability to extrapolate to extreme conditions, would be produced. Application difficulties arose due to the limited number of different combinations of seawall crest elevation and profile shape that were modeled. The worst-case overtopping data and resulting regression equation proved highly sensitive to profile shapes, crest elevations, and input conditions (waves and water levels) during ROTM simulations. Results are presented in Table D7.

Table D7 depicts intuitively incorrect maximum overtopping rates for some of the overtopping conditions; however, these rates represent a "snapshot" in time which is potentially not representative of actual overtopping conditions due to an anomaly in the regression results. As an example, at Profile 2, the 22.5- and 22.9-ft seawall crest elevations are estimated to yield higher maximum overtopping rates than are the 20.9- and 21.3-ft crest elevations. It might be more useful to consider time-averaged overtopping rates associated with a given time interval (e.g., average rate over the duration of a tidal cycle or rate extrapolated to the duration of the storm). However, it is also important to consider the total overtopping volumes for a given section of wall, in relation to total overtopping for a given profile reach. Even though the maximum overtopping rate for a higher wall section may be greater than the rate for a slightly lower section, the total volume overtopping the higher wall may be much less than that overtopping the lower sections. This is the case for the 24.9-ft section of wall backing the Profile 3 reach.

Results reasonably well represented by the physical model do provide useful information. Considering the same example discussed above, the 20.9- and 21.3-ft crest elevation conditions for Profile 2 were well represented in the physical model. The higher maximum overtopping rate for the 21.3-ft condition is likely a result of the sensitivity of the regression equation to slight variations in input, with the overtopping volumes and average overtopping rates over the duration of the storm appearing reasonable. If these values are considered quality data, then estimates for higher wall elevations can be derived from these results by considering quality results as conservative predictions or extrapolating overtopping volumes or rates using volumes and rates for conditions that were well represented in the physical model tests. At other profiles, results may be interpreted in a similar manner by utilizing what is labeled as reasonably well represented conditions. Asterisks in Table D7 indicate which conditions are believed to be higher quality data. Note that conclusions at profiles other than Profile 2 are based upon seawall crest elevations, profile shape (elevation of seawall/beach intersection), project site overtopping characteristics, and engineering judgement. For instance, confidence in the Profile 3/21.4-ft overtopping condition stems from characteristic similarities to the physically modeled conditions and engineering judgement. Specifically, conclusions concerning the reliability of this estimate result from: (a) the 21.4-ft seawall crest elevation is similar to that tested; (b) the overtopping volume of 109 acre-ft and rate of 0.25 cfs/ft are reasonable considering the overtopping history at Profile 3, which historically experiences little if any overtopping; and (c) the consistency of the overtopping predictions along the Profile 3 reach. It is suggested that these types of considerations be applied when interpreting any regression results, especially for overtopping conditions not well represented by the ROTM.

Lastly, CENED required overtopping volumes occurring during the maximum high water cycle. The simultaneous occurrence of a storm surge and a high tide cycle often determines the severity of the storm, and utilization of

the ROTM and SBEACH allows for the numerical simulation of these events. Assuming the flood retention structures drain during low water time periods when overtopping does not occur, design may be conducted using only overtopping during a single high water cycle. Appendix E presents the peak overtopping volumes predicted at the peak storm condition of each event considered herein. Comparison of the data in Appendix B and Appendix E shows that a large majority of the storms resulted in a significant percentage of total overtopping during a single time span. Only the extreme events and a few other exceptions produced multiple occurrences of overtopping at different high water conditions and few storms had less than 50 percent of the total overtopping occurring at the peak storm condition. The November 1945 50-year event proved a consistent exception to this rule where this is indicative of the influence of the sub-peaks as discussed. Overall, it appears that storm events may be characterized by one extreme water level with caution noted concerning the shape of the hydrograph with regards to storm duration and effectiveness of storm sub-peaks in producing overtopping and possibly beach recession.

ROTM results

Evaluation of proposed flood mitigation and retention structures has been completed through the application of the developed ROTM. Numerous difficulties were encountered during numerical modeling of a wide range of overtopping conditions; because of the highly complex nature of overtopping processes. Seawall height, profile shape, wave period, storm hydrograph shape, and physical model scale were just a few of the items that presented the analyses with difficulties at some point during the study. However, as stated, it is anticipated that results provide for significant improvements over any previous results and any other potential types of analyses.

Dune optimization and profile response simulations were conducted with a partially verified SBEACH, and yielded a broad range of anticipated profile responses. Within the limits of tested ranges, using different calibration parameters, the tested dune system (23-ft mhw dune crest) proved highly resistant to erosion, and, subsequently, overtopping. ROTM simulations supported profile response results with little or no overtopping predicted when subjected to the wave and water level database. The dune overtopping submodule is unproven; however, it is based upon accepted methodologies and is intuitively realistic.

Existing profile condition simulations using the ROTM depended upon the physical model tests of overtopping for the bore runup condition. The full range of overtopping was tested at Profiles 1-5 for the SPN storm. Different storm events were not tested and wave period was excluded from the regression due to a constant value during the peak of the SPN. Results for these simulations proved qualitatively correct with simple explanations for apparent

ROTM difficulties. Modeling of the range of overtopping allowed for strict application of the regression to each profile during every storm event. Results shown in Tables B1-B50 represent the output of these simulations.

Application of the revetment submodule at Profile 6 proved difficult for the November 1945 SPN, 500- and 100-year events. Portions of these three storms, due to combinations of large wave heights and periods, exceeded the applicability range of the revetment regression equation resulting in excessive overtopping rates. It is not possible to estimate the quality of these predictions except that it is suggested these extremes only be used as conservative estimates of expected overtopping. Input parameters met with regression criteria at approximately the 50-year storm.

Alternative overtopping predictions (Appendix D) contained a number of different storm and profile combinations. Halloween storm overtopping predictions appeared to be modeled moderately well with the "strict" ROTM resulting in reasonable overtopping volumes in comparison to actual overtopping. Testing the Halloween storm with present profile conditions indicated that a high level of flood protection remained present along Revere Beach. At Profile 6, there exists a lower amount of flood protection, but likely similar to that of the pre-Halloween storm profile. Physical modeling of the broken waves condition generated a site-specific regression equation that was used to predict overtopping during the Great Blizzard. Application of a "strict" and "relaxed" ROTM suggested that predictions for the Great Blizzard were reasonably accurate when applied to conditions modeled in the laboratory, but questions arose when the ROTM failed to agree with measured Great Blizzard overtopping volumes at profiles other than the tested profile, Profile 2. Overall, results support the previous conclusion that conditions represented by the physical model would produce improved overtopping predictions, whereas conditions resulting from extrapolation of the regression equations would create output of uncertain accuracy.

Modeling of the worst-case condition was limited due to time and physical model scale restraints. Results provide high-end overtopping volumes which are considered conservative due to the physical model setup with a low sea-wall elevation and highly eroded beach.

6 Summary and Conclusions

Investigation of coastal processes at Revere Beach and POP has proven to be a challenging endeavor due to varying wave and beach characteristics along the project site. Longshore variations of longshore sand transport present during the Halloween storm and presumably other storms limit applicability of the cross-shore profile response model SBEACH to this site. Confidence in SBEACH predictions is greater at POP than along Revere Beach. Calibration and verification of the original ROTM was limited by available data sets. However, some model results were substantiated with field observations. Physical model tests provided an opportunity to study site-specific runup and overtopping processes. Results and intuitive analyses have indicated improved capabilities in predicting overtopping for a majority of cases, but some are limited by the inability to test all conditions.

Despite the complexities of coastal processes at the project site, it is anticipated that design of flood protection structures will be greatly augmented by study findings. Results have strongly indicated potential flood protection benefits associated with a coarse-grained beach fill at Revere Beach and POP. Observations of beach stability and minimal seawall overtopping during the Halloween storm substantiate modeling results at Revere Beach. Dune optimization and profile response simulations along POP have indicated potential benefits of a dune system for flood protection, with minor predicted erosion and overtopping levels indicating advantages over the proposed revetment. The revetment design provided significant flood protection at or near the 50-year return period level. Results for low frequency November 1945 storms are less certain due to limitations of the applied revetment equation. Revetment and dune simulation results in response to the wave and water level database show a coarse-grained beach/dune system at POP to be extremely effective.

The developed ROTM, using data from a series of physical model tests, allowed the evaluation of a number of flood protection designs for a large number of storm events. Simulations indicated that few storm events result in potential flooding problems, with storms based on the November 1945 event proving to be most severe. Overall, it appears that a high level of flood protection is currently present at Revere Beach which has been substantiated

in response to two major storm events, and is possible at POP through implementation of either a coarse-grained dune/berm system or through construction of a combination of revetment and beach fill. A number of uncertainties are embedded within the development of the ROTM regression equations, thus results must be analyzed cautiously. However, given the utilization of extreme events (SPN and February 1978 100-year storm) in the physical model study, it is anticipated that a level of conservatism has been built into the ROTM. It is noted that the level of conservatism is limited by the exclusion of wind effects and beach profile response in the physical study, both of which could prove important in determining project flooding under certain conditions.

Consideration should be given to the construction of a full dune system of constant elevation at POP. Assuming a design storm with a 100-year return period and possibly higher, it is evident from the results that dunes of the design suggested with coarse-grain size (0.49 mm) are resistant and would experience minor damages. Additionally, total project site analyses indicate a buffering of the beach at POP with introduction of material from the updrift beaches and a lack of substantial offshore movement associated with the typical severe storm events as indicated by profile response simulations. The dune system at POP has historically proven effective, but it remains totally dependent upon the condition to which it is maintained, and results discussed herein are likely negated by failure to sustain a beach/dune at or near design conditions.

Finally, total study results represent an innovative methodology to predict flood protection capabilities for both hard and soft coastal structures. It is anticipated that the study could have been improved with more physical model studies and improved field data; however, the combination of physical, numerical, and field data provided a unique opportunity to study coastal processes. Results have been described as qualitative and should be taken with caution for some conditions. This information still provides valuable insight into project performance and capabilities. Therefore, it is anticipated that study results have clearly depicted the structural types and other measures necessary to provide the required level of protection along Revere Beach and POP.

Concisely, the conclusions of Part II of the CERC study are:

- a.* The existing Revere Beach coarse-grained beach fill (median grain size of 0.49 mm) appears extremely resistant to cross-shore erosion as observed for the Halloween Storm.
- b.* The Halloween storm data set and SBEACH profile response predictions indicate that minor offshore losses of the coarse-grained material occur in response to even extreme storm events.

- c. Sensitivity testing using SBEACH and the Halloween storm data set indicated that beach fill at Revere Beach and POP with median grain sizes above approximately 0.40 mm exhibits significantly higher erosive resistance compared to natural beach material (median grain size of 0.21 mm).
- d. Longshore movement appeared to be a dominant process distributing sediment along Revere Beach and Point of Pines and aided in the buffering of the POP reach during the Halloween storm because of the predominant northerly transport at the site.
- e. Longshore variations in longshore sediment transport during the Halloween storm limited calibration and verification of SBEACH, and analysis of cross-shore erosion along Revere Beach was hindered due to an assumed longshore gradient for all storms tested. Uniformity of longshore transport seemed to be better satisfied at Point of Pines, allowing profile response simulations to be completed.
- f. Wave transformation in the lee of Nahant Peninsula is quite complex, and variations in wave height and direction have the most influence along the northern reach of Revere Beach in the vicinity of Carey Circle.
- g. The existing Revere Beach coarse-grained beach fill appears highly effective in mitigating overtopping of seawalls relative to pre-fill conditions.
- h. Bore runup overtopping conditions are dominant along Revere Beach for present profile conditions with the water levels associated with the storm data-base below the beach/seawall intersection elevations; bore runup conditions greatly reduce predicted overtopping volumes for the storm set.
- i. Broken waves overtopping conditions are dominant along Revere Beach for pre-fill profile conditions with water levels associated with the storm database above the beach/seawall intersection elevations; broken wave conditions greatly increase predicted overtopping volumes for the storm set relative to bore runup conditions.
- j. Dune optimization indicated that properly maintained dunes with a crest width of 30 ft or greater and a crest elevation of 21 ft mlw (23 ft mlw near Carey Circle, Profile 6) or greater at Point of Pines are extremely resistant to erosion and overtopping associated with severe storms, including the SPN.
- k. The revetment design that was evaluated at Point of Pines with a crest elevation of 20.5 ft mlw appeared effective in mitigating overtopping

for all but the most extreme storms when fronted with a coarse-grained beach fill with a berm elevation of 10.5 ft mlw.

- l.* In the absence of the protective beach fill, the revetment design that was evaluated at Point of Pines with a crest elevation of 20.5 ft mlw appeared effective in mitigating overtopping for only high frequency storms.
- m.* Post-Halloween storm (November 1991) profiles along Revere Beach maintained a high level of flood protection according to simulations using post-storm profile data and the Halloween storm, which is indicative of the erosive resistance of the coarse-grained fill.

References

- Battjes, J. A. (1974). "Computation of set-up, longshore currents, runup, and overtopping due to wind-generated waves," Ph.D. diss., Delft University of Technology, The Netherlands.
- Battjes, J. A., and Roos, A. (1975). "Characteristics of flow in runup of periodic waves," Report No. 75-3, Department of Civil Engineering, Delft University of Technology, The Netherlands.
- Beach Erosion Board. (1956). "Laboratory data on wave runup and overtopping on shore structures," Technical Memorandum No. 64, Washington, DC.
- Berkoff, J. C. W. (1972). "Computation of combined refraction-diffraction." *Proceedings of the 13th International Conference on Coastal Engineering*. American Society of Civil Engineers, 471-90.
- Bohlen, W. F. (1978). "On the response of the Revere Beach shorefront to the storm of February 6-7 1978," Revere Beach storm report: *The blizzard of February 1978*. Carol R. Johnson & Associates Inc., ed., Cambridge, MA, 66-79.
- Camp, Dresser, and McKee, Inc. (1978). "Revere Beach development project," Environmental Impact Report, prepared for the Metropolitan District Commission.
- Corson, W. D., et al. (1981). "Wave information studies of U.S. coastlines; Atlantic Coast hindcast, deepwater, significant wave information," WIS Report 2, U.S. Army Engineer Waterways Experiment Station, Coastal Engineering Research Center, Vicksburg, MS.
- Dally, W. R., Dean, R. G., and Dalrymple, R. A. (1985a). "Wave height variation across beaches of arbitrary profile," *Journal of Geophysical Research* 90(C6), 11917-27.

- Dally, W. R., Dean, R. G., and Dalrymple, R. A. (1985b). "A model for breaker decay on beaches." *Proceedings of the 19th Coastal Engineering Conference*. American Society of Civil Engineers, 82-98.
- Dalrymple, R. A., Kirby, J. T., and Hwang, P. A. (1984). "Wave diffraction due to areas of energy dissipation," *Journal of Waterway, Port, Coastal and Ocean Division*, American Society of Civil Engineers, 67-79.
- Driver, D. B., Bratos, S. M., and Rosati, J. D. "Storm-induced beach erosion and flooding at Revere Beach and Point of Pines, Massachusetts," in preparation, U.S. Army Engineer Waterways Experiment Station, Coastal Engineering Research Center, Vicksburg, MS.
- Gilhousen, D. B., Changery, M. J., Baldwin, R. G., Karl, T. R., and Burgin, M. G. (1986). "Climatic summaries for NDBC data buoys," National Data Buoy Center, NSTL, MS.
- Hasselmann, K., Barnett, T. P., Bouws, E., Carlso, H., Cartwright, D. C., Enke, K., Ewing, J., Gienapp, H., Hasslemann, D. E., Sell, W., and Walden, H. (1973). "Measurements of wind-wave growth and swell decay during the Joint Sea Wave Project (JONSWAP)," Deutsches Hydrographisches Institute, Hamburg, Germany.
- Hardy, T. A., and Crawford, P. L. (1986). "Frequency of coastal flooding at Roughans Point, Broad Sound, Lynn Harbor, and the Saugus-Pines River System," Technical Report CERC-86-8, U.S. Army Engineer Waterways Experiment Station, Coastal Engineering Research Center, Vicksburg, MS.
- Hedges, T. S. (1976). "An empirical modification to linear wave theory." *Proceedings of the Inst. Civil Engineering*. 575-79.
- Hughes, S. A. (1984). "The TMA shallow-water spectrum description and applications," Technical Report CERC-84-7, U.S. Army Engineer Waterways Experiment Station, Coastal Engineering Research Center, Vicksburg, MS.
- Jensen, R. E. (1983). "Atlantic coast hindcast, shallow-water significant wave information," WIS Report 9, U.S. Army Engineer Waterways Experiment Station, Hydraulics Laboratory, Vicksburg, MS.
- Kamphius, J. W. (1991). "Alongshore sediment transport rate," *Journal of Waterway, Port, Coastal, and Ocean Engineering* 117(6), American Society of Civil Engineers, 624-40.
- Kikkawa, H., Shi-igai, H., and Kono, T. (1968). "Fundamental study of wave overtopping on levees," *Coastal Engineering in Japan* 11, 107-15.

- Kirby, J. T., and Dalrymple, R. A. (1983). "A parabolic equation method for the combined refraction-diffraction of stokes waves by mildly varying topography," *Journal of Fluid Mechanics* 136, 543-66.
- Kirby, J. T., and Dalrymple, R. A. (1986). "Modelling waves in surf zones and around islands," *Journal of Waterway, Port, Coastal and Ocean Division*, American Society of Civil Engineers, 78-93.
- Kraus, N. C., and Larson, M. (1988). "Prediction of initial profile adjustment of nourished beaches to waves action." *Proceedings Beach Preservation Technology '88*. Florida Shore and Beach Preservation Association, Inc., 125-37.
- Larson, M., and Kraus, N. C. (1989a). "SBEACH: Numerical model for simulating storm-induced beach change, Report 1: Empirical foundation and model development," Technical Report CERC-89-9, U.S. Army Engineer Waterways Experiment Station, Coastal Engineering Research Center, Vicksburg, MS.
- _____. (1989b). "Prediction of beach fill response to varying waves and water levels." *Proceedings of Coastal Zone '89*. American Society of Civil Engineers, NY, 607-21.
- Larson, M., Kraus, N. C., and Byrnes, M. R. (1990). "SBEACH: Numerical model for simulating storm-induced beach change, Report 2: Numerical formulation and model tests," Technical Report CERC-89-9, U.S. Army Engineer Waterways Experiment Station, Coastal Engineering Research Center, Vicksburg, MS.
- Raytheon Company. (1974). "Massport Marine Deepwater Terminal study," Prepared for the Massachusetts Port Authority BR8032, Interim Report Phase IIA.
- Resio, D. T. (1987a). "Extreme runup statistics on natural beaches," Miscellaneous Paper CERC-87-11, U.S. Army Engineer Waterways Experiment Station, Coastal Engineering Research Center, Vicksburg, MS.
- Rosati, J. D., Wise, R. A., Kraus, N. C., and Larson, M. (1993). "SBEACH: Numerical model for simulating storm-induced beach change; Report 3, User's manual," Instruction Report CERC-93-2, U.S. Army Engineer Waterways Experiment Station, Coastal Engineering Research Center, Vicksburg, MS.
- Saville, T., Jr., and Caldwell, J. M. (1953). "Experimental study of wave overtopping on shore structures." *Proceedings Minnesota International Hydraulics Convention*. Minneapolis, MN.

Shore Protection Manual. (1984). 4th ed., 2 Vol, U.S. Army Engineer Waterways Experiment Station, Coastal Engineering Research Center, U.S. Government Printing Office, Washington, DC.

WAMDI (WAM Development and Implementation Group). (1988). "The WAM model - a third generation ocean wave prediction model," *Journal of Physical Oceanography*, 1775-1810.

Ward, D. L. (1992). "Prediction of overtopping rates for irregular waves on riprap revetments," Miscellaneous Report CERC-92-4, U.S. Army Engineer Waterways Experiment Station, Coastal Engineering Research Center, Vicksburg, MS.

_____. "Physical model study of Revere Beach, Massachusetts," in preparation, U.S. Army Engineer Waterways Experiment Station, Coastal Engineering Research Center, Vicksburg, MS.

Wise, R. A., and Kraus, N. C. "Simulation of beach fill response, Ocean City, MD," *Proceedings Coastal Zone '93*, in preparation, American Society of Civil Engineers, NY.

Wu, J. (1980). "Wind stress coefficients over the sea surface near neutral conditions - a revisit," *Journal of Physical Oceanography* 10, 727-40.

Appendix A

Physical Model Testing of Overtopping

Overview

Physical model tests were initiated midway into the U.S. Army Engineer Waterways Experiment Station's Coastal Engineering Research Center (CERC) Part II study to provide the U.S. Army Engineer Division, New England (CENED) overtopping volumes due to a design storm event (the Standard Project Northeaster (SPN)), as well as to provide data with which to further refine the runup and overtopping module (ROTM). The physical modeling pertinent to the study discussed herein was divided into three tasks.

- a.* Verify numerical model provided input data and physical models using overtopping volumes inferred from high water marks surveyed in a ponding area due to the "Great Blizzard" of 1978, using February 1978 profile data.
- b.* Measure the total overtopping volume using SPN waves and water levels, and post-fill, post-Halloween storm profile data (dated 27 November 1991). This task also provided information with which to refine the bore runup submodule of the ROTM.
- c.* Measure overtopping rates due to the broken waves overtopping condition (still water level (swl) above beach/seawall intersection and waves such that weir flow over the seawall does not occur), using wave and water level data selected from the suite of 50 storms, and February 1978 profile data.

A fourth task was added, as follows:

- d.* Measure overtopping rates due to a worst-case condition with minimum beach, and extreme wave and water level conditions (SPN storm with February 1978 profile data).

Wave and water level data used in the physical model tests were output from the Storm-Induced **BE**ach **CH**ange (SBEACH) profile response model at the physical model offshore boundary. This appendix discusses development of the physical model input data set, describes the facility and testing procedures, and presents regression equations applied in the ROTM. Descriptions of the facility and testing procedures presented in this appendix have been taken from Ward (1993).

Facility

Physical model tests were conducted in CERC's 150-ft-long by 1.5-ft-wide by 3.0-ft-deep wave tank ("18-in. flume") (Figure A1) and 150-ft-long by 3.0-ft-wide by 3.0-ft-deep wave tank ("3-ft flume") (Figure A2). In both flumes, waves were generated by a piston-type wave board powered by an electro-hydraulic pump controlled by a computer-generated signal. The 18-in. flume had an existing 1:30 (V:H) concrete slope starting 60 ft from the wave board; the 3-ft flume had a 1:20 concrete slope starting 36 ft from the wave board and extending for 10 ft, followed by an approximately 1:100 slope.

The models were built to a non-distorted linear scale of 1:20 (model:prototype) for Task A and 1:30 for Tasks B, C, and D. Water that overtopped the seawalls during a physical model test was pumped into a rectangular catch basin at the conclusion of the test run. The change in elevation of the water in the catch basin was then measured with a point gauge and converted to a prototype overtopping rate in cubic feet per second per linear foot of prototype seawall (cfs/ft). For each set of tests, the cross-sectional area of the catch basin, width of the flume, time of model run, and scale factor were all constants.

Testing

Physical model verification (Task A)

Overview. The purpose of Task A was to verify the physical model setup by reproducing overtopping volumes due to the February 1978 Great Blizzard. Surveys of high water marks in ponding areas provided an estimate of the total overtopping in tidal flood zone 2A (Table 9, Chapter 4 for tidal flood zone definitions), represented by Profile 2. Using wave and water level information from SBEACH, Task A attempted to reproduce the 1978 storm in the physical model to determine if overtopping measured in the model matched the estimated prototype overtopping volume.

Selection of test conditions. Wave height and period and swl were determined for each hour during the selected storm at Profile 2 dated February 1978 (Figure A3). Water level at the peak of the second tide cycle (27th hour) was selected to test the worst recorded conditions, a low water level was selected to allow estimation of the period of the storm in which overtopping could be neglected (approximately hours 13, 18, 25, and 30), and an intermediate water level was selected to represent the rest of the storm (approximately hours 14, 16, 26, and 29). Each of the lower water levels selected was tested with wave conditions on the incoming and outgoing tides of both tide cycles. Storm hour, swl, wave height, and wave period are shown in Table A1 after shoaling in SBEACH to the approximate location of the wave generator (approximately 2,000 ft offshore).

Because of the amount of time involved in changing water levels in the wave flume, a constant water level was used for the lower two conditions tested. The swl at hour 25 was chosen for the lowest water level (10.8 ft mean low water (mlw)) and the swl at hour 16 was chosen for the next lowest water level (13.0 ft mlw). Linear interpolation based on water level and two surrounding data points was used to adjust wave conditions to the selected points in the storm profile. For example, the swl at hour 13 was 10.5 ft mlw, and 13.5 ft at hour 14. Linear interpolation determined that the test conditions of 10.8 ft mlw and 13.0 ft mlw occurred at hours 13.27 and 13.83, respectively. Using the same interpolation for wave height and wave period yielded the interpolated results shown in Table A1.

Physical model tests were conducted with irregular waves following the TMA spectrum (Hughes 1984), which is a shallow-water modification of the JONSWAP spectrum (Hassellman et al. 1973). Wave heights and periods were obtained from SBEACH at the approximate location of the wave generator. Wave information input to SBEACH is random, but is transformed using monochromatic wave theory. Wave height and period output from SBEACH were taken to represent the zeroth moment H_{m0} and the peak spectral period T_p for the wave spectra.

Physical model tests were conducted for 30 min for each of the four test conditions at each of the two lower water levels (10.8 and 13.0 ft mlw). Due to the small amount of overtopping at these water levels, the water level in the flume did not decrease appreciably during the tests. During tests at the highest water level (hour 27), test runs were limited to 2 min each to allow the overtopped water to be added back into the flume to maintain the desired water level. Ten independent 2-min runs were conducted at the highest water level.

After completing the test series, a revised estimate of input test conditions was determined to better represent actual overtopping conditions and the storm profile was retested with the new information. Wave conditions and water levels for the second set of tests are shown in Table A2. Note that hours 15 and 28 were added to the second set of tests to more accurately reflect the

storm profile. Results of only the second set of tests were used to calculate overtopping during the storm.

For the second set of tests, the swl at hour 30 was chosen for the lowest water level (11.0 ft mlw), and the swl at hour 14 was chosen for the next lower water level (13.2 ft mlw). Similar to the first set of tests, linear interpolation was used to determine the time at which the swl to be tested occurred and the wave height and period at that time. Test conditions are shown in Table A2.

Because of time restraints imposed by having to rerun the storm profile, the second set of tests was reduced to one 20-min run at each of the four test conditions at the lowest water level (11.0 ft mlw), two 10-min runs at each of the test conditions at the next lower water level (13.2 ft mlw), and five 2-min runs at each of the three highest water levels. As in the earlier set of tests, multiple runs of short duration were used at the highest water levels to allow the overtopped water to be returned to the flume to maintain the swl.

The existing 1:30 concrete slope in the 18-in. flume did not match the beach survey taken after the 1978 storm. Therefore, an entirely new profile was constructed and installed seaward of the existing concrete slope. An idealized profile was determined by matching a series of straight lines to the actual profile as closely as possible, including a horizontal line to use as the flume bottom. The actual profile and the idealized profile are shown in Figure A4.

With the depth at the flume bottom determined, model scale was established by limitations of the wave generator. The wave generator was unable to generate the required signals at scales larger than 1:20; therefore the model was constructed at a 1:20 scale. The idealized profile was constructed of plywood and placed in the wave flume over the concrete slope. When the slope was within 0.75 in. of the flume bottom (thickness of the plywood), 20-gauge sheet metal was used to extend the slope to the bottom of the flume. A vertical seawall was placed at the top of the plywood slope. Water overtopping the seawall accumulated behind the seawall and was pumped into a separate canister for accurate measurement of the overtopping quantity at the end of each test run.

Prototype overtopping rates for the first set of conditions tested are listed in Table A1; overtopping rates for the repeated storm profile are listed in Table A3. To determine total overtopping during the storm, it was assumed that the overtopping rate determined for a given point in the storm profile was constant over the time period extending from halfway between the given point and the preceding point to halfway between the given point and the following point. Because data were available at every 1-hr interval of the storm, overtopping rates at the first and last points tested were assumed to exist for one-half hour before and after the point tested, respectively. Multiplying the

overtopping rate for a tested point in the storm profile by the length of time the storm was assumed constant at those conditions yielded the volume of overtopping for that test per foot of seawall, and multiplying by the length of seawall contributing to the flood zone yielded the total volume of overtopping over the seawall for the time period that was tested. For this series of tests, it was determined that 3,890 ft of seawall would contribute to the flood zone. Overtopping rates and volume for each hour of the storm are shown in Table A3.

Based on surveys of high-water marks, CENED calculated that about 600 acre-ft of water overtopped the seawall during the 1978 storm. The physical model test showed a total overtopping of 773 acre-ft, or roughly 29 percent higher than the surveys had indicated. Due to uncertainties in the surveyed results, physical model tests, and representation of the flood zone with a single seawall height and profile, test results were considered to be very close to the predicted results. Thus, the physical model and methodology used to obtain the input data (i.e., from the numerical model) were considered validated.

Bore Runup (Task B)

The purpose of Task B was to determine total overtopping for the SPN for the beach profiles surveyed in November 1991 (after the beachfill project, and post-Halloween storm), and to generate a database for development of a bore runup submodule. Using wave data and survey data output from SBEACH, Task B reproduced the five beach profiles located along Revere Beach and subjected them to the design storm event. Overtopping was measured for each profile at each hour of the storm tested.

The SPN was based on storm waves and water levels that occurred in November 1945 with 1 ft added to the swl throughout the storm. The SPN storm used as input to SBEACH is shown in Figure A5. Conditions to be tested were selected from the storm profile to include the worst conditions that occurred during the storm (hour 30) plus conditions at two lower water levels during both tide cycles shown in the storm profile (hours 27, 33, 40, and 45 for the lowest water level and hours 28, 32, and 43 for the higher water level). However, the beachfill reduced the overtopping to such an extent that the lowest water level was not producing overtopping; therefore, additional points from the peaks of the tide cycles were selected for testing. As in Task A, linear interpolation was used where possible to adjust wave heights and periods to maintain a constant swl for tests of the incoming and outgoing tides in both tide cycles. Test conditions and the approximate hour of the storm represented are listed in Table A4 after shoaling in SBEACH to the approximate location of the wave generator.

Beach profiles 1, 3, 4, and 5 were reproduced in the 18-in. flume at a nondistorted scale of 1:30. Examination of the beach surveys taken in 1991

indicated portions of the profiles could be represented by the existing 1:30 concrete slope in the wave flume and the flat bottom of the flume. Shoreward of the 1:30 slope, sheet metal was used to reproduce the steeper portion of the beach profile. A vertical seawall was placed at the top of the slope, and water overtopping the seawall was collected and measured to determine the overtopping rates. Surveyed profiles and the model representations of Profiles 1, 3, 4, and 5 are shown in Figures A6 through A9, respectively.

Seawall elevations varied over the reach represented by each profile. A representative seawall height was selected for each profile, with two representative seawall heights selected for Profile 1. Representative seawall elevations were determined by a weighted average, based on wall length associated with each elevation and likelihood of contributing significantly to overtopping along the reach. In certain cases, higher wall elevations were neglected, due to the minor overtopping contribution at that location. Selected seawall elevations are listed in Table A5.

Beach surveys started at the foot of the seawall, and the elevation at the foot of the seawall was reproduced in all model profiles except Profile 1. The beach surveyed at Profile 1 measured an elevation of +21.0 ft mlw at the base of the seawall with a seawall crest elevation reported at +21.4 ft mlw providing a freeboard of 0.4 ft. However, selected representative seawall elevations for that segment of Revere Beach were +20.7 ft mlw and +19.8 ft mlw, both of which are lower than the beach survey. Because the reaches represented by both seawall elevations were significant, it was decided to conduct the Profile 1 test series twice, with one complete set at a seawall elevation of +19.8 ft mlw and one complete set at a seawall elevation of +20.7 ft mlw. The profile was modeled such that the beach slope extended to an elevation of +19.4 ft mlw and then remained at a constant elevation until reaching the seawall, reproducing a freeboard of 0.4 ft. For the second set of tests, the same slope was used to an elevation of +19.4 ft mlw, then an extension was added to continue the slope to an elevation of +20.3 ft mlw, again providing a freeboard of 0.4 ft.

The wave generator in the 18-in. flume was unable to reproduce the wave conditions at Profile 2 at a 1:30 scale. Rather than change to a smaller scale, Profile 2 was reproduced at a 1:30 scale in the 3-ft flume. Similar to the 18-in. flume, the existing 1:20 slope in the 3-ft flume was matched to a portion of the surveyed profile, and the steeper profile shoreward of the 1:20 slope was constructed of sheet metal. Surveyed and idealized profiles for Profile 2 are illustrated in Figure A10.

Overtopping rates per linear foot of prototype seawall for each profile and each hour of the storm that had measurable overtopping are shown in Table A6. Physical model tests were not conducted on Profile 5 at hour 31, or Profiles 3 and 4 at hour 42. Volumes listed in Table A6 for these tests

were obtained by multiple regression analysis using the other results listed in Table A6.

Storm conditions for the SPN are considerably worse than during the 1978 storm, with greater water depths and wave heights and longer wave periods. Overtopping rates, however, were considerably less, attesting to the incidental effectiveness of the beach fill. Overtopping rates measured in the wave flume for Profile 3 were surprisingly low, but incident wave heights for Profile 3 were lower than for the other profiles. NED confirmed that in the prototype, overtopping rates at Profile 3 were lower than at the other profiles, and the general trends observed in the wave flume agreed with observations made in the prototype.

Broken waves (Task C)

The purpose of Task C was to reproduce a selected set of conditions present in the suite of 50 storms to obtain data to calibrate the ROTM for the broken waves subroutine. Overtopping due to broken waves was defined to occur when the swl was above the beach/seawall intersection, and waves were below the level initiating weir flow. Storm conditions that were expected to produce overtopping from broken waves runup were selected from the suite of 50 storms as described in Chapter 4. All tests were conducted on the model of the 1978 survey of Profile 2 in the 18-in. flume.

Conditions selected for testing are listed in Table A7 as Tests 1 through 30, and correspond to the storms listed in Table 15, Chapter 4. The selected tests were separated into groups with similar water depths to allow multiple tests to be conducted without changing water level in the wave flume. Table A7 also lists the actual test conditions used. The wave generator in the 18-in. flume was unable to produce the wave conditions for tests 1 and 6; therefore, these tests were eliminated from the test series. Tests 25 and 26 were identical after adjusting the water level; therefore, test 26 was deleted. The remaining tests were completed.

It was desired to perform a multiple regression analysis on the results of the tests to obtain a relationship among overtopping rate, wave height, wave period, and swl. Eight additional tests were therefore conducted to provide a better range of test conditions on which to base the analysis. The additional test conditions are shown in Table A7 as tests 31-38, and were obtained from the selected storms described in Table 15, Chapter 4.

Worst case (Task D)

At the conclusion of Task C, storm conditions selected from the SPN were tested with the 1978 profile to provide data with which to develop an upward limit of overtopping for extreme conditions. Six conditions representing peak

hours of the storm were selected for testing. The wave generator in the 18-in. flume was unable to produce the wave heights at these conditions; therefore, the tests were conducted at the highest obtainable H_{∞} for the given swl and T_p . These conditions resulted in a combination of bore runup, broken waves, and weir flow conditions in the physical model, and represented the worst-case overtopping condition. Input to the worst-case overtopping condition study is given in Table A8.

Development of Regression Equations

Regression analyses were performed on combinations of results to determine the required relationships between overtopping rates, swl, profile, structural, and wave conditions. Dimensionless parameters were selected that were suitable for the numerical models for which the regression models were designed. The overtopping rate was presented as

$$Q [=] \text{ cfs/ft} = L^2 T^{-1}$$

where Q is overtopping rate, [=] indicates the appropriate dimensional units, L is length, and T is time. Dimensional parameters affecting overtopping rate include the following:

$$\begin{aligned} f [=] \text{ ft} &= L \\ b [=] \text{ ft} &= L \\ d [=] \text{ ft} &= L \\ H [=] \text{ ft} &= L \\ T [=] \text{ sec} &= T \\ g [=] \text{ ft/sec}^2 &= LT^{-2} \end{aligned}$$

where f is structure freeboard defined as height of the seawall crest above swl, b is beach freeboard defined as height of the beach at the base of the seawall above the swl, d is water depth at the flat bottom of the wave flume, H is wave height defined as the wave height at the approximate location of the wave generator in model flume tests and the wave height on which the physical model tests were based, T is wave period, and g is gravitational acceleration. For the regression analysis, these dimensional parameters were combined to represent physically representative dimensionless variables, referred to as Buckingham PI terms.

Dimensionless parameters that may also affect overtopping rates include:

$$\begin{aligned} \cot \theta & \\ d/d_{2000} & \end{aligned}$$

where $\cot \theta$ is the cotangent of the beach slope (from the base of the seawall to the swl), and d_{2000} is the depth at a distance of 2,000 ft offshore. The ratio d/d_{2000} is therefore the ratio of the actual depth used in the flume to the depth where the wave heights were determined from the numerical model. Because input wave height and period were obtained from SBEACH at the approximate location of the wave generator (2,000 ft offshore from the seawall), it was thought that the difference in depths, d/d_{2000} , could play a role in defining the overtopping rates. Because depths at 2,000 ft offshore varied somewhat throughout the storm due to sediment movement, variations in depth at 2,000 ft offshore were included in the analysis while the profile in the flume remained constant.

Data collected in the physical model tests were converted to prototype scale for the regression analysis. Input data are shown in Tables A9 and A10 for bore runup, broken waves and worst case, respectively. Note that the last three lines in Table A9 give the input data for the three points in Table A6 determined by regression analysis.

Regression analysis was conducted on the dimensionless variable Q' , where $Q' = Q/(g \cdot f)^{1/2}$. Any negative overtopping rates predicted were set to zero, and results were converted to predicted dimensional overtopping rates. Model selection was then based on the sum of squares of the observed and predicted overtopping rates.

Bore runup (Task B)

Data input to the development of a regression equation for bore runup is given in Table A9. These data represent actual data implemented into the physical model and regression analysis, and measured overtopping rates used in the regression analysis. The regression relationship developed for bore runup is given by Equations 20 and 21 (see Chapter 4). This simple model provided a reasonable fit to the data and used only two dimensionless variables, PI_1 and PI_5 (related to beach elevation and water depth). The exclusion of beach slope in this simplified model was probably due to the small range of the variable (14.0 to 19.5) and the relatively short distance that the slope was used in the wave flume. Wave period does not appear in the relationship due to the constant value of this variable at the peak of the SPN. It seemed unreasonable to omit wave height (PI_2) from the model, especially when a correlation analysis revealed that Q' was more highly correlated with dimensionless wave height than any other single variable. However, there was a very high correlation between dimensionless wave height and dimensionless water depth (PI_2 and PI_5 , 76 percent correlation), which was expected for depth-limited breaking waves, and effects of wave height were therefore reflected in PI_5 .

This equation fit the dimensionless overtopping rates with a correlation coefficient of 0.969 ($R^2 = 0.939$), and the sum of squares of differences

between the overtopping rates (dimensional) and measured overtopping was only 0.0796. There were 36 data points in the analysis; therefore, the average difference between calculated and measured overtopping was ± 0.0470 cfs/ft. It should be emphasized that regression models presented herein are only valid within the range of conditions tested. The range of variables used, both dimensional and nondimensional, is given in Table A11.

Broken waves (Task C)

Data used in the regression analysis for the broken waves overtopping condition are listed in Table A10. Data labelled as "Task C" were used solely for the regression relationship describing broken waves. The regression equation developed for the broken waves submodule is given by Equations 22 and 23 (see Chapter 4). This model had a correlation coefficient for the dimensionless overtopping rates of 0.987 ($R^2 = 973$). Sum squares of the residuals of dimensional overtopping was 0.0511 for the 35 tests, therefore the average error was ± 0.382 cfs/ft. This model is only valid for the range of conditions tested. The range of variables, both dimensional and nondimensional, used in this analysis is given in Table A12.

Worst-case (Task D)

Table A10, data for Tasks A, C, and D, contains the database for the generation of the regression relationship used for the worst-case overtopping condition. The regression relationship representing the worst-case overtopping condition is as given by Equations 24 and 25 (see Chapter 4). This model had a correlation coefficient of 0.992 ($R^2 = 0.984$). The sum of squares of differences between predicted and measured dimensional overtopping rates was 0.3106 which, for 40 data points, yielded an average difference of ± 0.072 cfs/ft. The range of variables, both dimensional and nondimensional, used in this analysis is given in Table A13.

Discussion

A major uncertainty in the physical model tests was the wave spectrum being tested. Wave information furnished for the storms consisted of wave height and period, obtained by shoaling representative random wave parameters using monochromatic wave transformation relationships. This representative wave, after shoaling to the approximate distance offshore, was used to represent the peak period and height of the zeroth moment to reproduce a new spectrum. This would be accurate if the entire spectrum was shoaled to the same extent as the representative wave. In reality, each frequency in the incident spectrum will shoal differently, and an entirely new spectrum will exist after shoaling. Although we have the capability of dividing the incident

spectrum into a number of bandwidths, shoaling each bandwidth individually through numerical model SBEACH, and then reassembling the shoaled spectrum from the individual bandwidths, the procedure is time-consuming, not economically feasible, and other uncertainties in the prototype and physical model do not justify attempting such a level of precision. However, spectral shape has been described as less important for storm conditions inside of Broad Sound (Chapter 2); thus, the waves produced by SBEACH were deemed representative. This uncertainty applied to Tasks A, B, C, and D, and the net effect on overtopping rate caused by this approximation of the wave spectrum is unknown.

With the 1978 profiles used in Tasks A, C, and D, there was considerable freeboard between the beach and seawall crest. Waves striking the seawall were forced into a vertical sheet of water and spray, frequently exceeding the height of the seawall. Because the motion was nearly vertical, much of this water fell back on the seaward side of the seawall in the flume, but wind effects may cause more of the water to overtop the seawall in the prototype.

Wind effects on overtopping rates in Task B are expected to be minimal. Wind has two effects on seawall overtopping rates: modification of the wave runup on the beach, and blowing spray over the seawall. Modification of the wave runup has been calculated to have little effect on overtopping (Resio¹). Due to the low freeboard between the 1991 beach profiles and seawall crest elevations, waves overtopping the seawall tended to flow over the wall in a bore rather than be deflected vertically as in Task A. Because the water movement was horizontal rather than vertical, wind effects are not expected to be significant.

Due to high reflection coefficients from the high seawall freeboard in models of the 1978 profile, wave energy reflected from the seawall remained in the wave flume and increased the total energy in the flume. Avoiding this effect would require that each test run be terminated before energy reflected from the structure could reach the wave generator and return to the structure. Each test would then be on the order of 2 min, after which the testing would be halted until the energy in the flume had dissipated. A series of short tests would then be used to ensure that the entire wave spectrum was represented.

Because of the low seawall freeboards and extended beach profiles compared to Task A, reflection coefficients for Tasks B, C, and D were small and reflected wave energy was not a significant factor in the tests.

¹ Resio, D. T. (1987b). "Assessment of wind effects on wave overtopping of proposed Virginia beach seawall," memorandum to Joan Pope, Coastal Engineering Research Center, Vicksburg, MS, from OCTI, Vicksburg, MS.

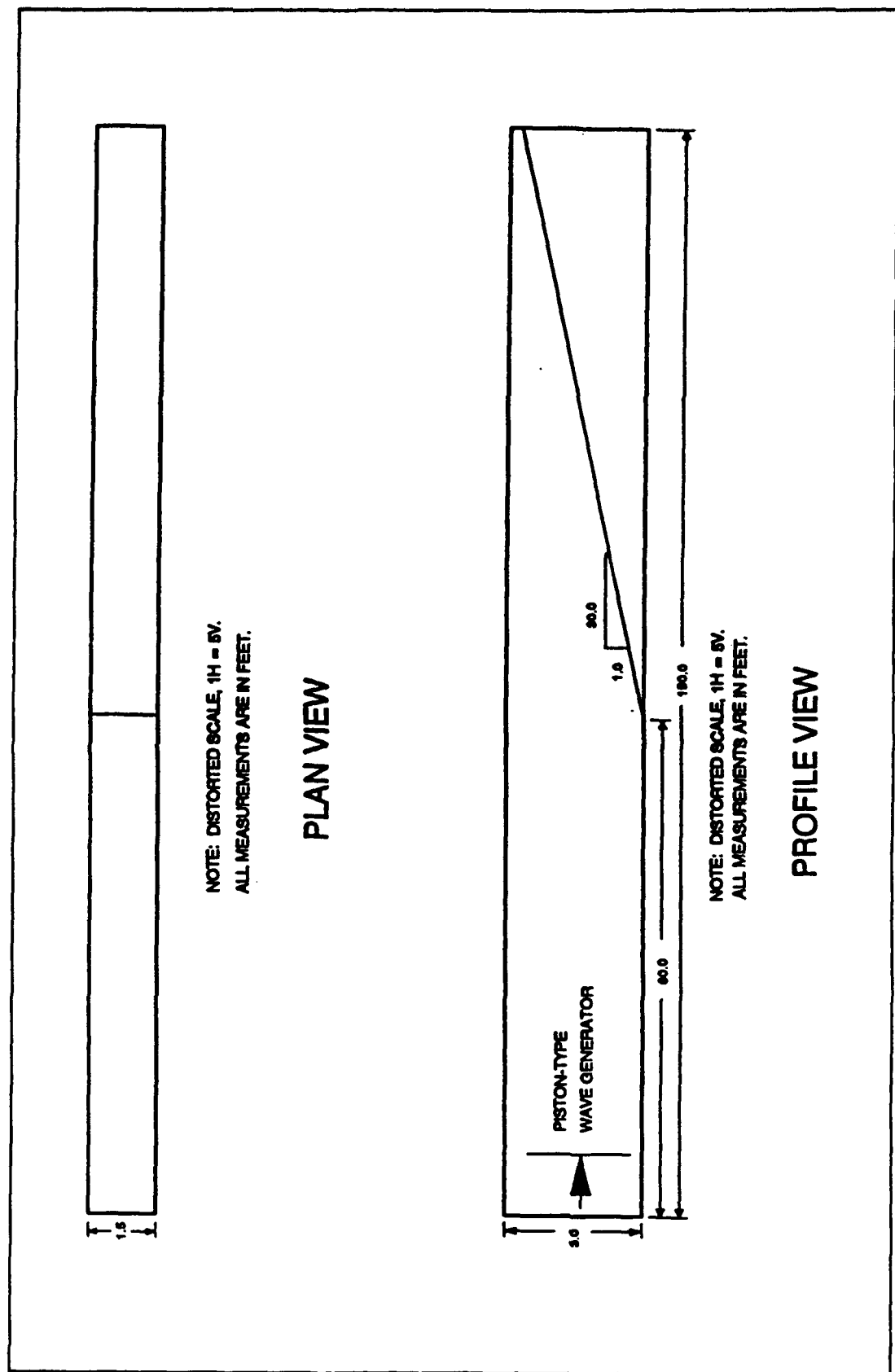


Figure A1. Plan and profile views of 18-in. wave flume

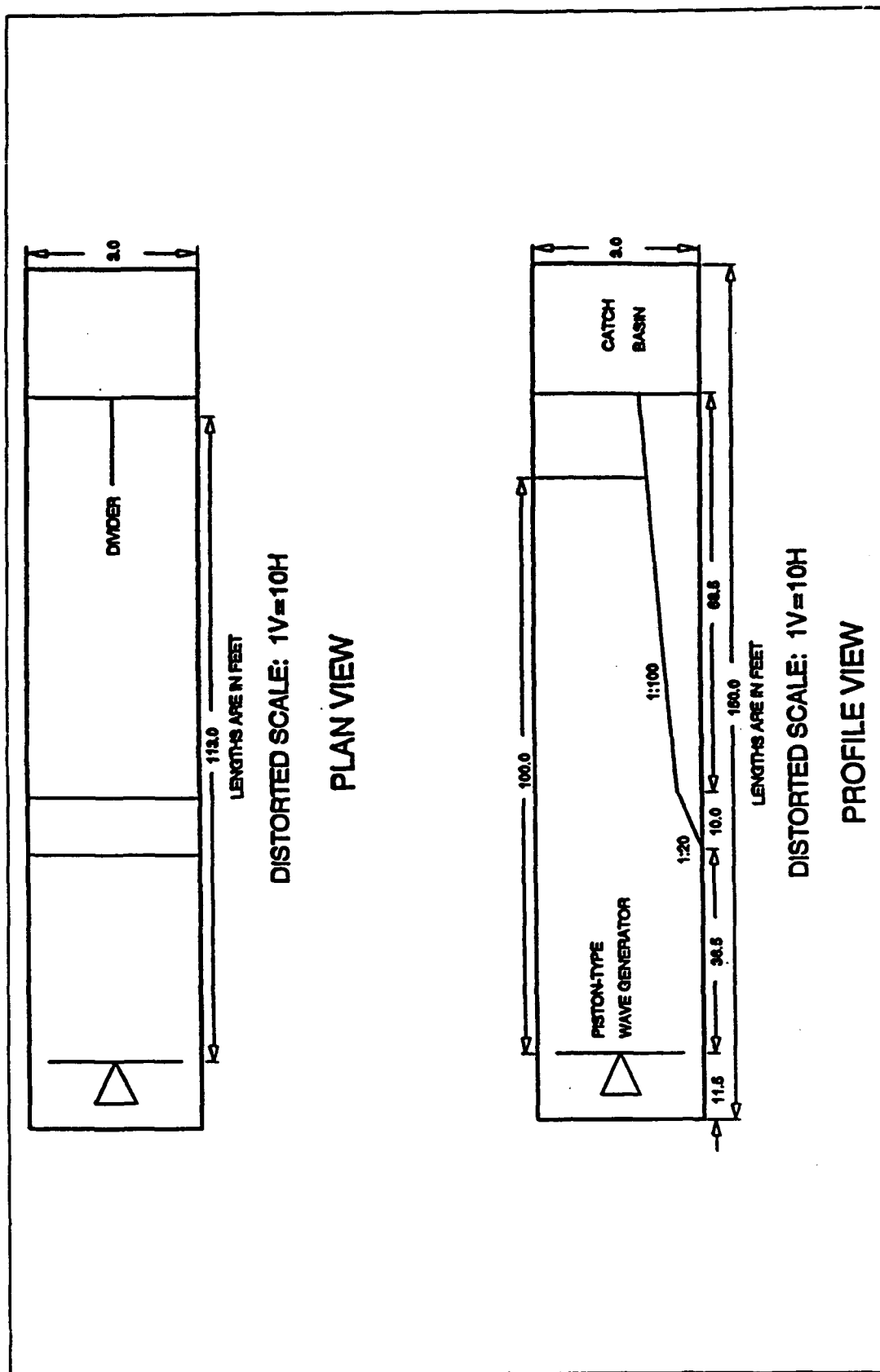


Figure A2. Plan and profile views of 3-ft wave flume

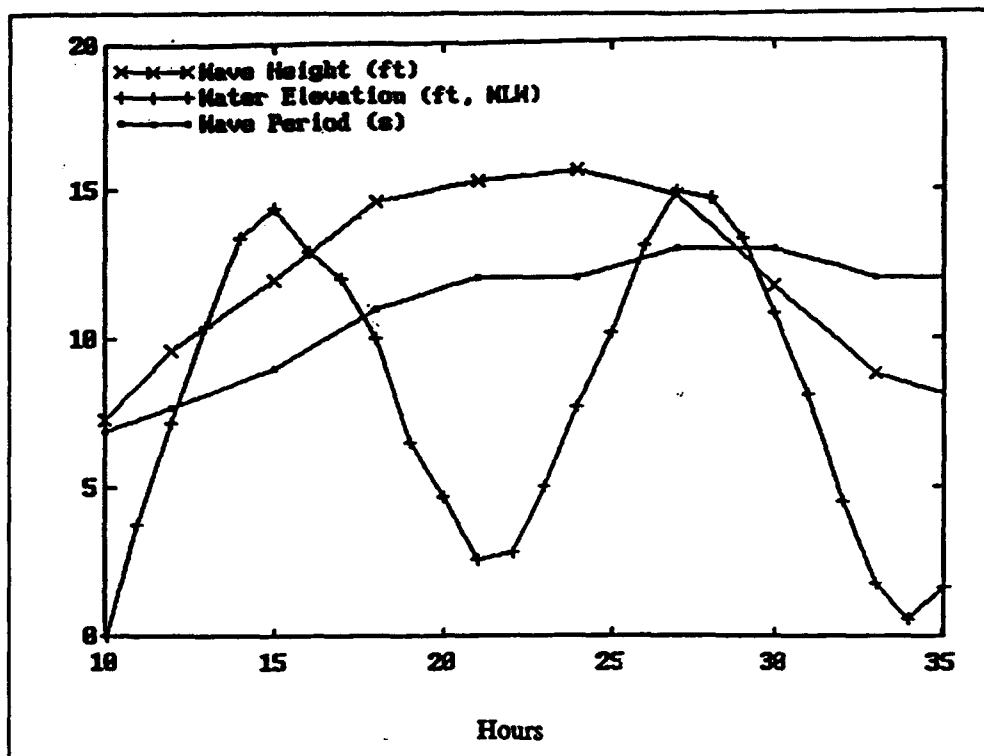


Figure A3. Great Blizzard storm profile

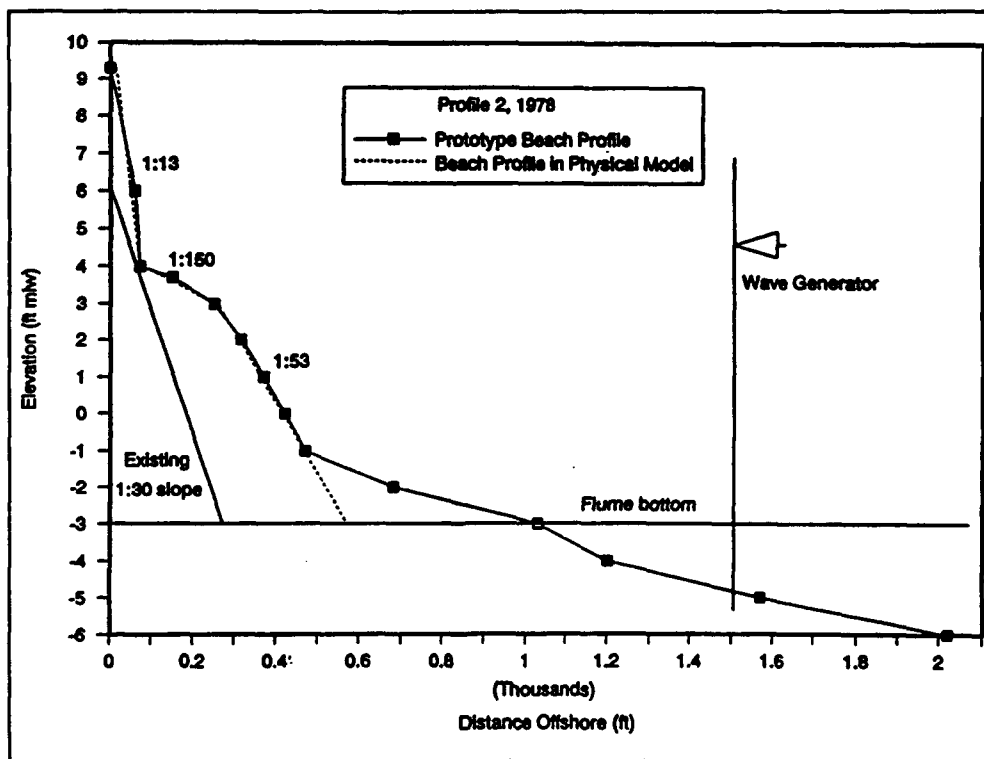


Figure A4. Profile 2 (1978) as reproduced in physical model

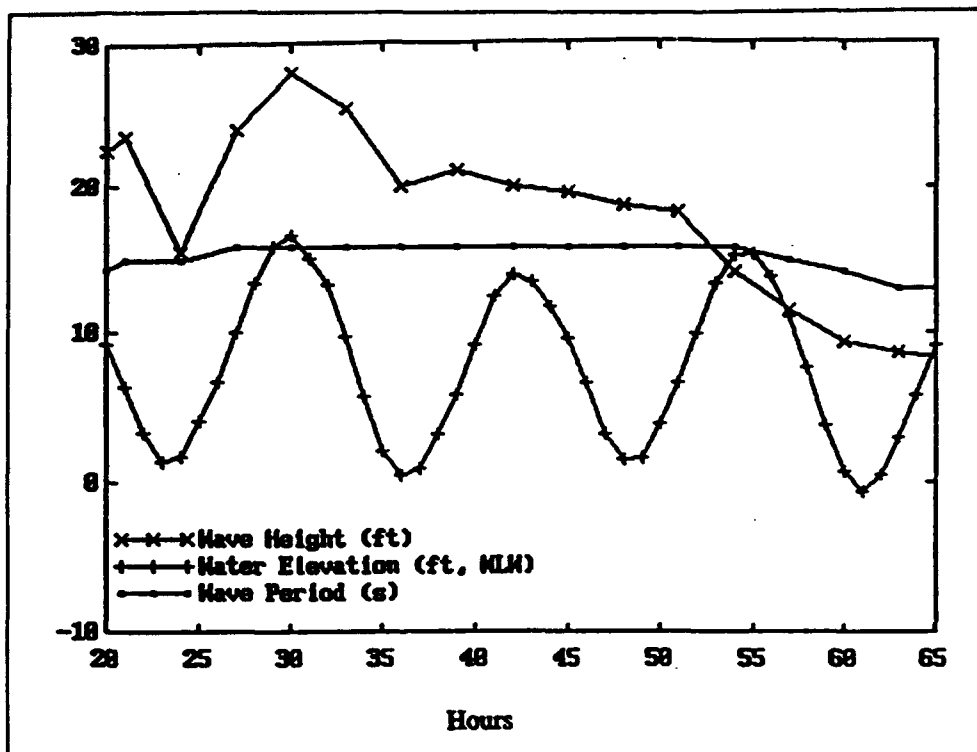


Figure A5. Standard Project Northeaster (SPN) storm profile

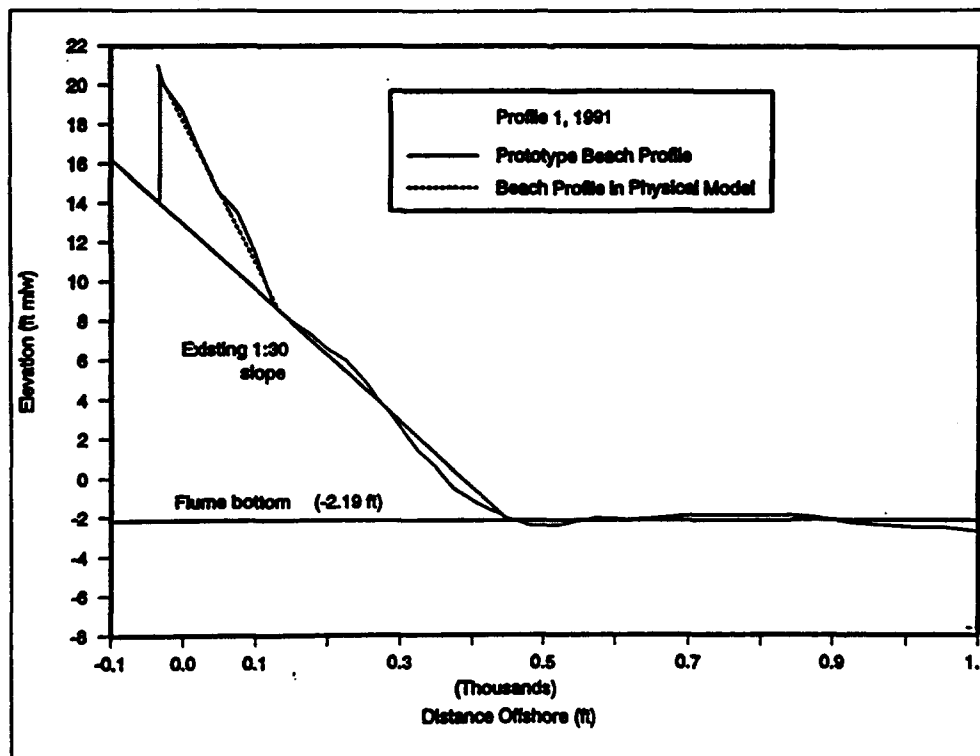


Figure A6. Profile 1 (November 1991) as reproduced in physical model

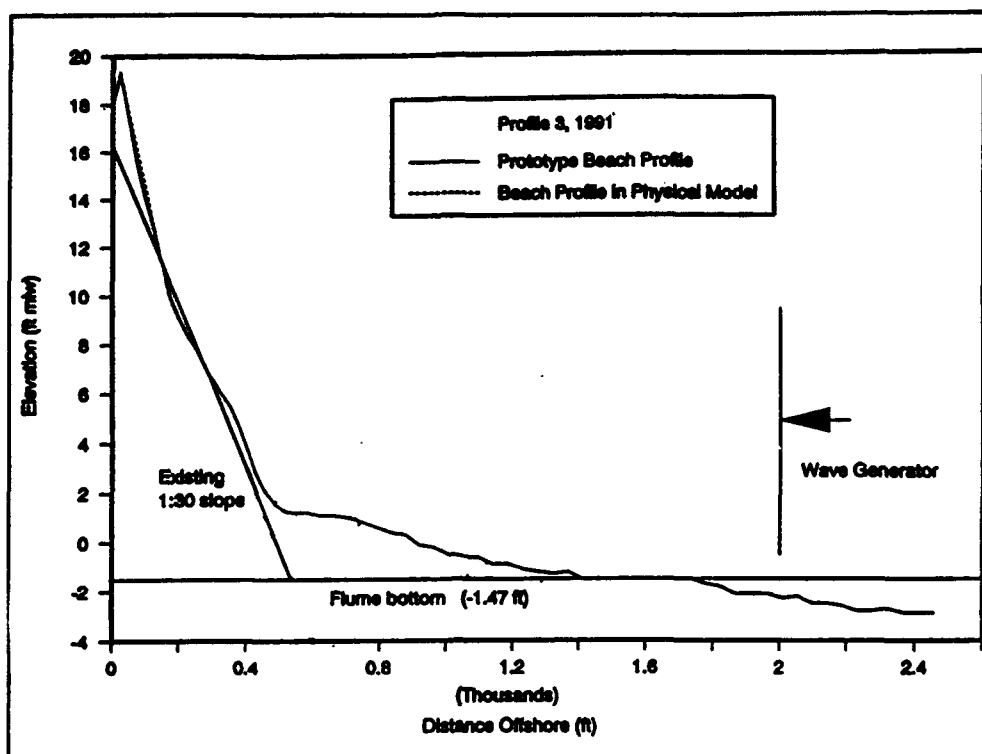


Figure A7. Profile 3 (November 1991) as reproduced in physical model

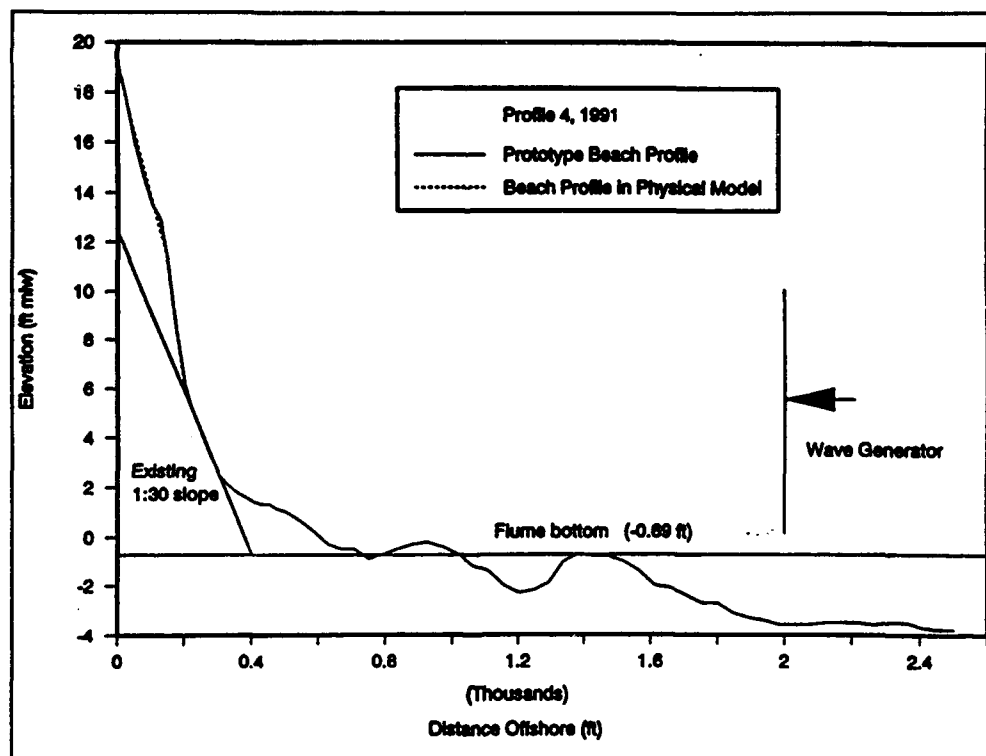


Figure A8. Profile 4 (November 1991) as reproduced in physical model

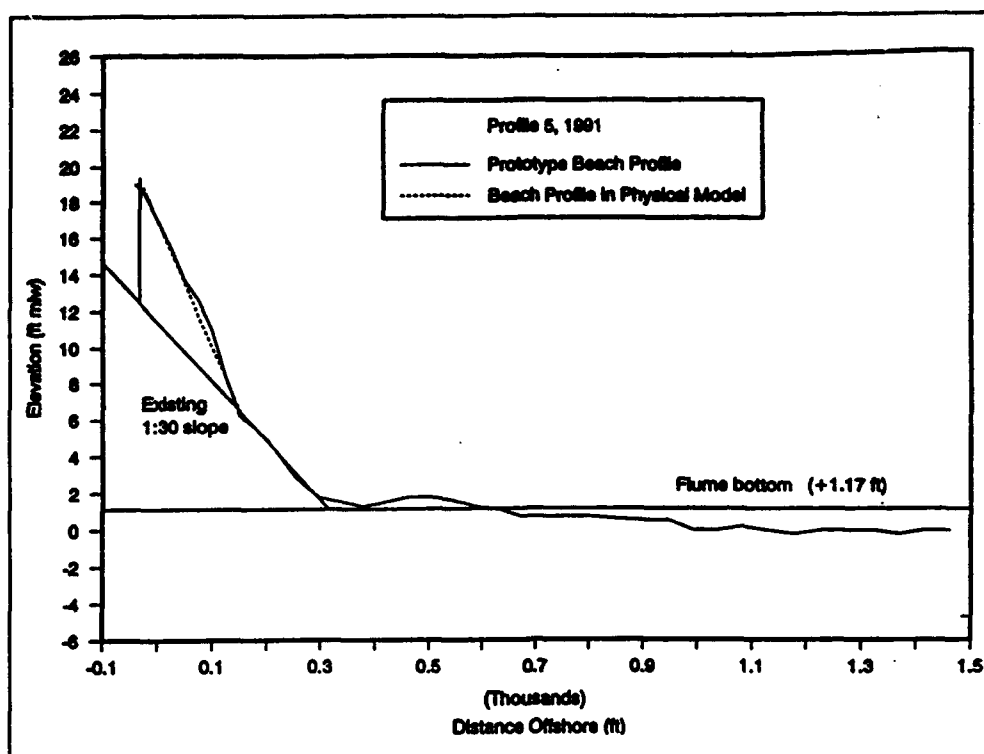


Figure A9. Profile 5 (November 1991) as reproduced in physical model

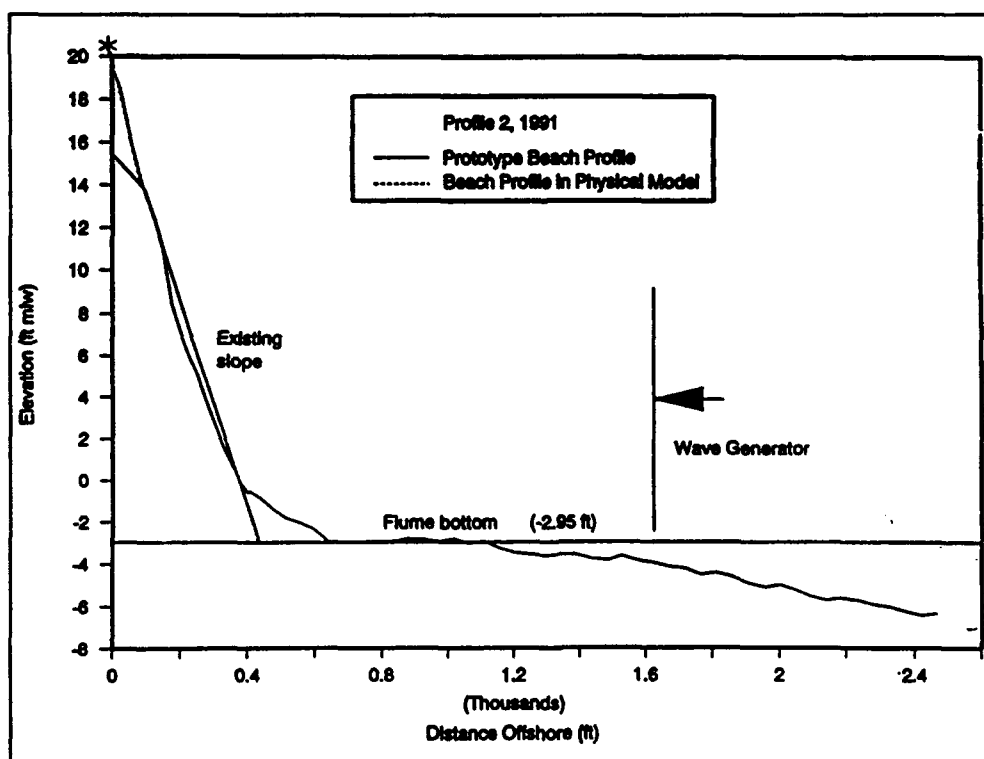


Figure A10. Profile 2 (November 1991) as reproduced in physical model

Table A1
Wave Data from SBEACH and Interpolated Wave Conditions
Physical Model Verification (First Test Series)

Hour	SWL (ft,mlw)	Wave Height (ft)	Wave Period (sec)	SWL Tested (ft,mlw)	Interp Wave Ht (ft)	Interp Wave Period (sec)	Measured Overtop- ping Rate (cfs/ft)
13	10.5	6.0	8.1	10.8	6.1	8.1	0.0066
14	13.5	7.2	8.6	13.0	7.0	8.6	0.0643
15	14.2	10.8	9.0	***	***	***	***
16	13.0	10.1	9.7	13.0	10.1	9.7	0.1004
17	13.0	6.8	10.3	***	***	***	***
18	11.2	6.1	11.0	10.8	6.0	11.0	0.008
19	8.0	5.0	11.3	***	***	***	***
24	9.0	5.3	12.0	***	***	***	***
25	10.8	6.0	12.3	10.8	6.0	12.3	0.0077
26	13.6	7.0	12.7	13.0	6.8	12.6	0.0843
27	15.4	7.7	13.0	15.4	7.7	13.0	1.3553
28	15.5	7.7	13.0	***	***	***	***
29	14.2	7.2	13.0	13.0	6.8	13.0	0.959
30	11.5	6.3	13.0	10.8	6.0	12.9	0.0063
31	8.8	5.3	12.7	***	***	***	***

Table A2
Wave Data from SBEACH and Interpolated Wave Conditions:
Physical Model Verification (Second Test Series)

Hour	SWL (ft.mlw)	Wave Height (ft)	Wave Period (sec)	SWL Tested (ft.mlw)	Interp Wave Ht (ft)	Interp Wave Per (sec)
13	10.1	6.0	8.1	11.0	6.3	8.2
14	13.2	7.2	8.6	13.2	7.2	8.6
15	14.3	10.8	9.0	14.3	10.8	9.0
16	13.0	10.1	9.7	13.2	10.2	9.6
17	12.1	6.8	10.3	***	***	***
18	10.2	6.1	11.0	11.0	6.4	10.5
19	8.0	5.0	11.3	***	***	***
24	7.5	5.3	12.0	***	***	***
25	10.0	6.0	12.3	11.0	6.3	12.4
26	12.9	7.0	12.7	13.2	7.1	12.7
27	14.8	7.7	13.0	14.8	7.7	13.0
28	14.7	7.7	13.0	14.8	7.7	13.0
29	13.4	7.2	13.0	13.2	7.1	13.0
30	11.0	6.3	13.0	11.0	6.3	13.0
31	8.1	5.3	12.7	***	***	***

Table A3
Verification of Physical Model Results (Second Test Series)

Hour	Interp Hour	Begin Hour	End Hour	Total Sec-onds (sec)	Overtopping Rate (cfs/ft)	Calculated Overtopping Volumes (acre-ft)
13	13.29	12.50	13.64	4094	0.0097	3.56
14	13.98	13.64	14.49	3077	0.0994	27.32
15	15.00	14.49	15.44	3421	0.5200	158.88
16	15.88	15.44	16.73	4642	0.1659	68.76
17
18	17.58	16.73	18.50	6366	0.0103	5.86
19
24
25	25.34	24.50	25.74	4458	0.0100	3.97
26	26.13	25.74	26.82	3879	0.1674	57.99
27	27.50	26.82	27.50	2463	0.8141	179.08
28	27.50	27.50	28.30	2888	0.8141	209.93
29	29.10	28.30	29.55	4500	0.1359	54.60
30	30.00	29.55	30.50	3412	0.0116	3.54
STORM TOTAL						773.48

Table A4
Wave Data from SBEACH and Interpolated Wave Conditions
Bore Runup Study

Hour	SWL (ft,mlw)	Wave Height (ft)	Wave Period (sec)	SWL Tested (ft,mlw)	Interp Hour	Interp Wave Ht (ft)	Interp Wave Per (sec)
Profile 5							
27	10.0	8.8	15.9	10.00	27.00	8.80	15.90
28	13.4	9.1	15.9	13.40	28.00	9.10	15.90
29	15.9	8.9	15.9	15.90	29.00	8.90	15.90
30	16.6	8.7	15.9	16.60	30.00	8.70	15.90
31	15.0	8.3	15.9	15.00	31.00	8.30	15.90
32	13.2	9.0	15.9	13.40	31.89	8.92	15.90
33	9.7	8.5	15.9	10.00	32.91	8.54	15.90
43	13.5	7.0	15.9	13.40	43.06	6.89	15.90
44	11.8	5.1	15.9	***	***	***	***
45	9.6	4.6	15.9	10.00	44.82	4.69	15.90
Hour	SWL (ft,mlw)	Wave Height (ft)	Wave Period (sec)	SWL Tested (ft,mlw)	Interp Hour	Interp Wave Ht (ft)	Interp Wave Per (sec)
Profile 4							
27	10.0	7.4	15.9	10.00	27.00	7.40	15.90
28	13.4	7.9	15.9	13.40	28.00	7.90	15.90
29	15.9	10.4	15.9	15.90	29.00	10.40	15.90
30	16.6	7.1	15.9	16.60	30.00	7.10	15.90
31	15.0	9.6	15.9	15.00	31.00	9.60	15.90
32	13.2	7.7	15.9	13.40	31.89	7.91	15.90
33	9.7	7.1	15.9	10.00	32.91	7.15	15.90
42	13.9	9.9	15.9	13.90	42.00	9.90	15.90
43	13.5	7.0	15.9	13.40	43.06	6.96	15.90
44	11.8	6.3	15.9	***	***	***	***
45	9.6	7.5	15.9	10.00	44.82	7.28	15.90
(Sheet 1 of 3)							

Hour	SWL (ft,mlw)	Wave Height (ft)	Wave Period (sec)	SWL Tested (ft,mlw)	Interp Hour	Interp Wave Ht (ft)	Interp Wave Per (sec)
Profile 3							
27	10.0	4.2	15.9	10.00	27.00	4.20	15.90
28	13.4	4.4	15.9	13.40	28.00	4.40	15.90
29	15.9	4.5	15.9	15.90	29.00	4.50	15.90
30	16.6	4.4	15.9	16.60	30.00	4.40	15.90
31	15.0	4.4	15.9	***	***	***	***
32	13.2	4.4	15.9	13.40	31.89	4.40	15.90
33	9.7	4.1	15.9	10.00	32.91	4.13	15.90
42	13.9	7.3	15.9	13.90	42.00	7.30	15.90
43	13.5	7.1	15.9	13.40	43.06	7.04	15.90
44	11.8	6.1	15.9	***	***	***	***
45	9.6	5.9	15.9	10.00	44.82	5.94	15.90
Hour	SWL (ft, mlw)	Wave Height (ft)	Wave Period (sec)	SWL Tested (ft,mlw)	Interp Hour	Interp Wave Ht (ft)	Interp Wave Per (sec)
Profile 2							
27	10.0	9.7	15.9	10.00	27.00	9.66	15.90
28	13.4	11.0	15.9	13.20	27.94	10.89	15.90
29	15.9	12.0	15.9	15.90	29.00	11.97	15.90
30	16.6	12.7	15.9	16.60	30.00	12.65	15.90
31	15.0	11.7	15.9	15.00	31.00	11.70	15.90
32	13.2	11.0	15.9	13.20	32.00	10.95	15.90
33	9.7	9.7	15.9	10.00	32.91	9.78	15.90
42	13.9	8.3	15.9	13.90	42.00	8.30	15.90
43	13.5	7.4	15.9	13.20	43.18	7.29	15.90
44	11.8	6.6	15.9	***	***	***	***
45	9.6	***	15.9	10.00	44.82	***	15.90
(Sheet 2 of 3)							

Hour	SWL (ft,mlw)	Wave Height (ft)	Wave Period (sec)	SWL Tested (ft,mlw)	Interp Hour	Interp Wave Ht (ft)	Interp Wave Per (sec)
Profile 1							
27	10.0	8.8	15.9	10.00	27.00	8.80	15.90
28	13.4	9.1	15.9	13.40	28.00	9.10	15.90
29	15.9	9.3	15.9	15.90	29.00	9.30	15.90
30	16.6	8.7	15.9	16.60	30.00	8.70	15.90
31	15.0	9.1	15.9	15.00	31.00	9.10	15.90
32	13.2	9.0	15.9	13.40	31.89	9.01	15.90
33	9.7	8.5	15.9	10.00	32.91	8.54	15.90
42	13.9	8.9	15.9	13.90	42.00	8.90	15.90
43	13.5	8.2	15.9	13.40	43.06	8.15	15.90
44	11.8	7.3	15.9
45	9.6	9.4	15.9	10.00	44.82	9.02	15.90
(Sheet 3 of 3)							

Table A5 Representative Seawall Crest Elevations	
Profile No.	Crest Elevation (ft,mlw)
1a	19.8
1b	20.7
2	21.3
3	20.6
4	20.3
5	20.4

Table A6
Physical Model Results for Bore Runup Study

Hour	Interp Hour	Begin Hour	End Hour	Total Seconds (sec)	Overtopping Rate (cfs/ft)	Overtopping Volume (cf/ft)
Profile 5						
29	29.00	28.50	29.50	3600	0.1947	701
30	30.00	29.50	30.50	3600	0.3928	1414
*31	31.00	30.50	31.44	3384	0.1729	585
Profile 4						
28	28.00	27.50	28.50	3600	0.0073	26
29	29.00	28.50	29.50	3600	0.3301	1189
30	30.00	29.50	30.50	3600	0.4070	1465
31	31.00	30.50	31.44	3400	0.1986	675
32	31.89	31.44	32.40	3446	0.0075	26
*42	42.00	41.50	42.53	3706	0.0553	205
43	43.06	42.50	43.50	3600	0.0078	28
Profile 3						
29	29.00	28.50	29.50	3600	0.0168	60
30	30.00	29.50	30.50	3600	0.0215	78
*42	42.00	41.50	42.53	3706	0.0000	0
43	43.06	42.53	43.50	3492	0.0022	8
Profile 2						
28	27.94	27.47	28.47	3600	0.0079	28
29	29.00	28.47	29.50	3706	0.2445	906
30	30.00	29.50	30.50	3600	0.4156	1496
31	31.00	30.50	31.50	3600	0.0955	344
32	32.00	31.50	32.46	3446	0.0109	38
42	42.00	41.50	42.59	3918	0.0150	59
43	43.18	42.59	43.50	3282	0.0043	14
(Continued)						
* Determined by regression analysis						

Table A6 (Concluded)						
Hour	Interp Hour	Begin Hour	End Hour	Total Seconds (sec)	Ove: -topping Rate (cfs/ft)	Over-topping Volume (cf/ft)
Profile 1a						
28	28.00	27.50	28.50	3600	0.0336	121
29	29.00	28.50	29.50	3600	0.4211	1552
30	30.00	29.50	30.50	3600	0.8304	2989
31	31.00	30.50	31.44	3400	0.2337	794
32	31.89	31.44	32.40	3446	0.0571	197
42	42.00	41.50	42.53	3706	0.0904	335
43	43.06	42.53	43.50	3494	0.0364	127
Profile 1b						
28	28.00	27.50	28.50	3600	0.0215	78
29	29.00	28.50	29.50	3600	0.3105	1118
30	30.00	29.50	30.50	3600	0.5093	1834
31	31.00	30.50	31.44	3400	0.1329	452
32	31.89	31.44	32.40	3446	0.0258	89
42	42.00	41.50	42.53	3706	0.0396	147
43	43.06	42.53	43.50	3494	0.0155	54
* Determined by regression analysis						

Table A7
Input Conditions for Broken Waves Study

Test No.	SWL (ft.mlw)	SWL Tested (ft.mlw)	Wave Height (ft)	Wave Period (sec)
1	14.9	14.9	10.5	9.0
2	14.6	14.6	7.1	11.7
3	14.6	14.6	8.1	9.0
4	14.6	14.6	10.6	11.3
5	14.2	14.1	8.5	12.7
6	14.2	14.1	11.7	13.4
7	14.1	14.1	6.1	8.7
8	14.1	14.1	8.1	9.0
9	14.0	14.1	9.0	10.7
10	13.5	13.4	8.5	12.7
11	13.3	13.4	7.6	12.0
12	13.3	13.4	7.8	9.0
13	13.3	13.4	7.9	12.3
14	13.2	13.1	7.7	11.3
15	13.1	13.1	7.8	12.0
16	13.0	13.1	4.7	11.3
17	13.0	13.1	8.1	13.0
18	12.9	13.1	6.6	9.0
19	12.6	12.6	7.6	11.7
20	12.1	12.0	7.5	14.1
21	12.0	12.0	6.5	8.3
22	11.9	12.0	8.1	12.0
23	11.6	11.6	3.1	11.0
24	11.6	11.6	7.1	9.0
25	11.6	11.6	7.3	12.0
(Continued)				

Table A7 (Concluded)				
Test No.	SWL (ft.mlw)	SWL Tested (ft.mlw)	Wave Height (ft)	Wave Period (sec)
26	11.5	11.6	7.3	12.0
27	10.9	10.7	7.4	13.0
28	10.7	10.7	5.5	9.0
29	10.5	10.7	6.7	8.6
30	9.5	9.5	6.5	14.1
31	***	14.2	6.0	12.7
32	***	14.2	6.0	9.0
33	***	14.2	6.0	10.7
34	***	13.2	5.1	13.0
35	***	13.2	5.4	9.0
36	***	13.2	6.2	11.3
37	***	12.1	6.0	14.1
38	***	12.1	7.8	8.3

Table A8 Input Conditions for Worst-Case Study				
Test No.	SWL (ft.mlw)	SWL Tested (ft.mlw)	Wave Height (ft)	Wave Period (sec)
39	15.9	15.9	8.4	15.9
40	16.6	16.6	8.9	15.9
41	15.0	15.0	9.4	15.9
42	13.2	13.2	8.8	15.9
43	10.0	10.0	7.8	15.9
44	13.2	13.2	7.3	15.9

Table A9
Bore Runup Regression Input

Prof No.	Storm Hour	SWL (ft, mllw)	Depth in Flume (ft)	Wave Ht (ft)	Wave Per (sec)	Seawall Crest Elev (ft, mllw)	Base of Seawall (ft, mllw)	Overtopping Rate (cfs/ft)	Coten Beach Slope	Elev at 2000 ft Offshore (ft)
5	28	13.4	12.23	9.1	15.9	20.4	19.1	0.0000	14.5	-1.40
5	29	15.9	14.73	8.9	15.9	20.4	19.1	0.1947	14.5	-1.40
5	30	16.6	15.43	8.7	15.9	20.4	19.1	0.3928	14.5	-1.40
4	27	10.0	10.69	7.4	15.9	20.3	19.1	0.0000	19.5	-3.57
4	28	13.4	14.09	7.9	15.9	20.3	19.1	0.0073	19.5	-3.57
4	29	15.9	16.59	10.4	15.9	20.3	19.1	0.3301	19.5	-3.57
4	30	16.6	17.29	7.1	15.9	20.3	19.1	0.4070	19.5	-3.57
4	31	15.0	15.69	9.6	15.9	20.3	19.1	0.1986	19.5	-3.57
4	32	13.4	14.09	7.9	15.9	20.3	19.1	0.0075	19.5	-3.57
4	43	13.4	14.09	7.0	15.9	20.3	19.1	0.0078	19.5	-3.56
3	29	15.9	17.37	4.5	15.9	20.5	18.2	0.0168	15.5	-2.25
3	30	16.6	18.07	4.4	15.9	20.5	18.2	0.0215	15.5	-2.25
3	32	13.4	14.87	4.4	15.9	20.5	18.2	0.0000	15.5	-2.25
3	43	13.4	14.87	7.0	15.9	20.5	18.2	0.0022	15.5	-2.23
2	28	13.2	16.15	10.9	15.9	21.3	20.5	0.0079	16.0	-5.03
2	29	15.9	18.85	12.0	15.9	21.3	20.5	0.2445	16.0	-5.02
2	30	16.6	19.55	12.7	15.9	21.3	20.5	0.4156	16.0	-5.02

(Sheet 1 of 3)

Table A9
Bore Runup Regression Input

Prof No.	Storm Hour	SWL (ft, mllw)	Depth in Flume (ft)	Wave Ht (ft)	Wave Per (sec)	Seawall Crest Elev (ft, mllw)	Base of Seawall (ft, mllw)	Overtopping Rate (cfs/ft)	Coten Beach Slope	Elev at 2000 ft Offshore (ft)
2	31	15.0	17.95	11.70	15.9	20.7	20.5	0.0955	16.0	-5.02
2	32	13.2	16.15	10.95	15.9	20.7	20.5	0.0109	16.0	-5.02
2	33	10.0	12.95	9.78	15.9	20.7	20.5	0.0000	16.0	-5.02
2	42	13.9	16.85	8.30	15.9	20.7	20.5	0.0150	16.0	-5.04
2	43	13.2	16.15	7.29	15.9	20.7	20.5	0.0043	16.0	-5.04
1	28	13.4	15.59	9.10	15.9	19.8	19.4	0.0336	14.0	-5.42
1	29	15.9	18.09	9.30	15.9	19.8	19.4	0.4311	14.0	-5.41
1	30	16.6	18.79	8.70	15.9	19.8	19.4	0.8304	14.0	-5.41
1	31	15.0	17.19	9.10	15.9	19.8	19.4	0.2337	14.0	-5.41
1	32	13.4	15.59	9.01	15.9	19.8	19.4	0.0571	14.0	-5.41
1	42	13.9	16.09	8.90	15.9	19.8	19.4	0.0904	14.0	-5.45
1	43	13.4	15.59	8.15	15.9	19.8	19.4	0.0364	14.0	-5.45
1	45	10.0	12.19	9.02	15.9	19.8	19.4	0.0000	14.0	-5.45
1	28	13.4	15.59	9.10	15.9	20.7	20.3	0.0215	14.0	-5.42
1	29	15.9	18.09	9.30	15.9	20.7	20.3	0.3105	14.0	-5.41
1	30	16.6	18.79	8.70	15.9	20.7	20.3	0.5093	14.0	-5.41
1	31	15.0	17.19	9.10	15.9	20.7	20.3	0.1329	14.0	-5.41

(Sheet 2 of 3)

Table A9
Bore Runup Regression Input

Prof No.	Storm Hour	SWL (ft.mlw)	Depth in Flume (ft)	Wave Ht (ft)	Wave Per (sec)	Seawall Crest Elev (ft.mlw)	Base of Seawall (ft.mlw)	Overtopping Rate (cfs/ft)	Coten Beach Slope	Elev at 2000 ft Offshore (ft)
1	32	13.4	15.59	9.01	15.9	20.7	20.3	0.0258	14.0	-5.41
1	42	13.9	16.09	8.90	15.9	20.7	20.3	0.0396	14.0	-5.45
1	43	13.4	15.59	8.15	15.9	20.7	20.3	0.0155	14.0	-5.45
1	45	10.0	12.19	9.02	15.9	20.7	20.3	0.0000	14.0	-5.45
5	31	15.0	13.83	8.30	15.9	20.4	19.1	***	14.5	-1.40
4	42	13.9	14.59	9.90	15.9	20.3	19.1	***	19.5	-3.57
3	42	13.9	15.37	7.30	15.9	20.5	18.2	***	15.5	-2.23

(Sheet 3 of 3)

Table A10
Broken Waves and Worst-Case Regression Input

Task	Prof No.	Survey Year	SWL (ft.mlw)	Wave Ht (ft)	Wave Per (sec)	Seawall Crest Elev (ft.mlw)	Base of Seawall (ft.mlw)	Cotan Beach Slope	Elev at Flume Bottom (ft.mlw)	Overtopping Rate (cfs/ft)
A	2	1978	10.82	6.14	8.10	21.0	9.2	10.7	-3.00	0.0066
A	2	1978	12.96	6.99	8.60	21.0	9.2	10.7	-3.00	0.0643
A	2	1978	12.96	10.05	9.70	21.0	9.2	10.7	-3.00	0.1004
A	2	1978	10.82	5.99	11.00	21.0	9.2	10.7	-3.00	0.0080
A	2	1978	10.82	6.00	12.30	21.0	9.2	10.7	-3.00	0.0077
A	2	1978	12.96	6.76	12.60	21.0	9.2	10.7	-3.00	0.0843
A	2	1978	15.40	7.65	13.00	21.0	9.2	10.7	-3.00	1.3553
A	2	1978	12.96	6.79	13.00	21.0	9.2	10.7	-3.00	0.0959
A	2	1978	10.82	6.01	12.90	21.0	9.2	10.7	-3.00	0.0063
A	2	1978	11.00	6.35	8.25	21.0	9.2	10.7	-3.00	0.0097
A	2	1978	13.15	7.18	8.59	21.0	9.2	10.7	-3.00	0.0994
A	2	1978	14.30	10.80	9.00	21.0	9.2	10.7	-3.00	0.5200
A	2	1978	13.15	10.18	9.62	21.0	9.2	10.7	-3.00	0.1659
A	2	1978	11.00	6.39	10.45	21.0	9.2	10.7	-3.00	0.0103
A	2	1978	11.00	6.34	12.44	21.0	9.2	10.7	-3.00	0.0100
A	2	1978	13.15	7.09	12.74	21.0	9.2	10.7	-3.00	0.1674
A	2	1978	14.75	7.70	13.00	21.0	9.2	10.7	-3.00	0.8141

(Sheet 1 of 4)

Table A10
Broken Waves and Worst-Case Regression Input

Task	Prof No.	Survey Year	SWL	Wave Ht.	Wave Per.	Seawall Crest Elev	Base of Sea-wall	Coten Beach Slope	Elev at Flume Bottom	Overtopping Rate
A	2	1978	14.75	7.70	13.00	21.0	9.2	10.7	-3.00	0.8141
A	2	1978	13.15	7.11	13.00	21.0	9.2	10.7	-3.00	0.1359
A	2	1978	11.00	6.30	13.00	21.0	9.2	10.7	-3.00	0.0116
C	2	1978	14.90	10.50	9.00	21.0	9.2	10.7	-3.00	...
C	2	1978	14.60	7.10	11.70	21.0	9.2	10.7	-3.00	0.6431
C	2	1978	14.60	8.10	9.00	21.0	9.2	10.7	-3.00	0.5498
C	2	1978	14.60	10.60	11.30	21.0	9.2	10.7	-3.00	0.7475
C	2	1978	14.10	8.50	12.70	21.0	9.2	10.7	-3.00	0.5472
C	2	1978	14.10	11.70	13.40	21.0	9.2	10.7	-3.00	...
C	2	1978	14.10	6.10	8.70	21.0	9.2	10.7	-3.00	0.2550
C	2	1978	14.10	8.10	9.00	21.0	9.2	10.7	-3.00	0.4331
C	2	1978	14.10	9.00	10.70	21.0	9.2	10.7	-3.00	0.6230
C	2	1978	13.40	8.50	12.70	21.0	9.2	10.7	-3.00	0.3711
C	2	1978	13.40	7.60	12.00	21.0	9.2	10.7	-3.00	0.3002
C	2	1978	13.40	7.80	9.00	21.0	9.2	10.7	-3.00	0.2530
C	2	1978	13.40	7.90	12.30	21.0	9.2	10.7	-3.00	0.2970
C	2	1978	13.10	7.70	11.30	21.0	9.2	10.7	-3.00	0.2397
C	2	1978	13.10	7.80	12.00	21.0	9.2	10.7	-3.00	0.2589

(Sheet 2 of 4)

Table A10
Broken Waves and Worst-Case Regression Input

Task	Prof No.	Survey Year	SWL	Wave Ht.	Wave Per.	Seawall Crest Elev	Base of Seawall	Coten Beach Slope	Elev at Flume Bottom	Over-topping Rate
C	2	1978	13.10	4.70	11.30	21.0	9.2	10.7	-3.00	0.1380
C	2	1978	13.10	8.10	13.00	21.0	9.2	10.7	-3.00	0.2679
C	2	1978	13.10	6.60	8.60	21.0	9.2	10.7	-3.00	0.2001
C	2	1978	12.60	7.60	11.70	21.0	9.2	10.7	-3.00	0.1658
C	2	1978	12.00	7.50	14.10	21.0	9.2	10.7	-3.00	0.1109
C	2	1978	12.00	6.50	8.30	21.0	9.2	10.7	-3.00	0.0889
C	2	1978	12.00	8.10	12.00	21.0	9.2	10.7	-3.00	0.1098
C	2	1978	11.60	3.10	11.00	21.0	9.2	10.7	-3.00	0.0278
C	2	1978	11.60	7.10	9.00	21.0	9.2	10.7	-3.00	0.0691
C	2	1978	11.60	7.30	12.00	21.0	9.2	10.7	-3.00	0.0812
C	2	1978	10.70	7.40	13.00	21.0	9.2	10.7	-3.00	0.0334
C	2	1978	10.70	5.50	9.00	21.0	9.2	10.7	-3.00	0.0274
C	2	1978	10.70	6.70	8.60	21.0	9.2	10.7	-3.00	0.0314
C	2	1978	9.50	6.50	14.10	21.0	9.2	10.7	-3.00	0.0052
C	2	1978	14.10	6.00	12.70	21.0	9.2	10.7	-3.00	0.4309
C	2	1978	14.10	6.00	9.00	21.0	9.2	10.7	-3.00	0.2795
C	2	1978	14.10	6.00	10.70	21.0	9.2	10.7	-3.00	0.3192
C	2	1978	13.10	5.10	13.00	21.0	9.2	10.7	-3.00	0.2018

(Sheet 3 of 4)

Table A10
Broken Waves and Worst-Case Regression Input

Task	Prof No.	Survey Year	SWL	Wave Ht.	Wave Per.	Seawall Crest Elev	Base of Seawall	Cotan Beach Slope	Elev at Flume Bottom	Over-topping Rate
C	2	1978	13.10	5.40	9.00	21.0	9.2	10.7	-3.00	0.1396
C	2	1978	13.10	6.21	11.30	21.0	9.2	10.7	-3.00	0.2061
C	2	1978	12.00	6.00	14.10	21.0	9.2	10.7	-3.00	0.1049
C	2	1978	12.00	7.80	8.30	21.0	9.2	10.7	-3.00	0.0963
D	2	1978	15.90	8.38	15.90	21.0	9.2	10.7	-3.00	0.8489
D	2	1978	16.60	8.86	15.90	21.0	9.2	10.7	-3.00	1.1980
D	2	1978	15.00	9.36	15.90	21.0	9.2	10.7	-3.00	1.0337
D	2	1978	13.20	8.76	15.90	21.0	9.2	10.7	-3.00	0.4049
D	2	1978	10.00	7.82	15.90	21.0	9.2	10.7	-3.00	0.3915
D	2	1978	13.20	7.29	15.90	21.0	9.2	10.7	-3.00	0.0181

(Sheet 4 of 4)

Table A11
Bore Runup Parameter Ranges

Parameter	Minimum	Maximum
SWL (ft,mlw)	10.0000	16.6000
Wave Height (ft)	4.2000	12.6500
Wave Period (sec)	15.9000	15.9000
Seawall Freeboard (ft)	3.2000	11.3000
Beach Freeboard (ft)	1.6000	10.5000
Cotan Beach Slope	14.0000	19.5000
Overtopping Rate (cfs/ft)	0.0000	0.8304
PI1	0.4103	0.9626
PI2	0.6197	2.6915
PI3	0.7878	0.9586
PI4	14.0000	19.5000
PI5	1.0379	4.6730

Table A12
Broken Wave Parameter Ranges

Parameter	Minimum	Maximum
SWL (ft,mlw)	9.5	14.9
Wave Height (ft)	3.1	11.7
Wave Period (sec)	8.3	14.1
Seawall Freeboard (ft)	6.1	11.5
Beach Freeboard (ft)	-5.7	-0.3
Overtopping Rate (cfs/ft)	0.0052	1.3553
PI1	0.8261	2.4426
PI2	0.3298	1.7213
PI3	36.8	133.3

Table A13
Worst-Case Parameter Ranges

Parameter	Minimum	Maximum
SWL (ft,mlw)	9.5	16.6
Wave Height (ft)	3.1	11.7
Wave Period (sec)	8.1	15.9
Seawall Freeboard (ft)	4.4	11.5
Freeboard between beach & seawall(ft)	-7.4	-0.3
Cotan Beach Slope	10.7	19.5
Overtopping Rate (cfs/ft)	0.0000	1.3553
P11	0.0374	2.6818
P12	0.3298	2.7188
P13	33.0292	404.8744
P14	10.7000	19.5000
P15	0.8261	5.1875
Q'	0.0000	0.0256

Appendix B

Overtopping Calculations

The following tables contain overtopping volumes as calculated with the revised runup and overtopping module. The module has been updated to include regression equations as derived from a physical model study of predominant overtopping conditions along Revere Beach. The output obtained utilized the set of 50 storms previously described, and the 27 November 1991 profile data. Note that calculations at Profiles 7 and 8 use a dune with a 23-ft mean low water crest elevation, and the revetment design (with beach fill fronting the structure) at Profile 6. Overtopping calculations for a 23-ft dune at Profile 6 and the revetment design without a protective beach fill are located in Appendix C. Total overtopping volumes both for the project site (Table B1) and by tidal flood zone utilize the revetment design at Profile 6 as depicted in Tables B2-B51.

Each table contains information describing a given overtopping configuration, and the corresponding calculated overtopping volume and maximum overtopping rate. The data listed are as follows:

Storm identifier (i.e., NV45SPN => November 1945 SPN event)

Overtopping Reach: CB => Crescent Beach
PD => Park Dike area
OI => Oak Island area
PA => Ponding area/North Beach
PP => Point of Pines

Profile: Profile used in the storm simulation

Wall Height: Seawall elevation used in storm simulation

Wall Length: Length of reach represented by overtopping condition

Overtopping Volume (acre-ft)

Maximum Overtopping Rate (cfs/wall length)

Included in Table B2 are markers (*) to indicate which of the site conditions were closely (or approximately) modeled in the physical study. Site conditions that were closely modeled should be expected to yield relatively reliable estimates of overtopping. Other situations not modeled

(i.e., significantly different seawall elevations) should be considered cautiously as described previously. Each of these conditions can be used for the remainder of the tables (B3-B51), which contain the same structural and profile conditions, but for different storm events.

Table B1
Total Overtopping Calculations

Storm	Total Overtopping (acre-ft)	Storm	Total Overtopping (acre-ft)
NV45SPN	3614	AP6110	58
NV45500	1588	DC6250	127
NV45100	663	DC6220	101
NV4550	548	DC6210	68
NV4520	184	DC625	32
NV4510	148	DC622	28
FB5850	111	FB645	21
FB5820	71	FB642	20
FB5810	42	FB6920	80
FB585	15	FB6910	48
FB582	8	FB695	32
MR5850	133	FB7250	151
MR5820	90	FB7220	83
MR5810	53	FB7210	53
MR585	38	NV7250	172
MR582	26	NV7220	124
JN61100	151	NV7210	86
JN6150	119	NV725	56
JN6120	105	NV722	47
JN6110	51	FB78100	291
JN615	24	FB7850	112
JN612	7	FB7820	90
AP61100	167	FB7810	67
AP6150	141	FB785	44
AP6120	76	FB782	29

Table B2
Storm: NV45SPN

Overtopping Reach	Profile	Wall Height (ft)	Wall Length (ft)	Overtopping Volume (acre-ft)	Overtopping Rate (cfs/ft)
CB	1	23.8	525	0	0.00
CB*	1	20.7	1430	140	0.47
CB*	1	19.8	400	45	0.46
PD*	1	20.9	865	94	0.46
PD*	2	20.9	610	54	0.43
PD	2	22.9	570	0	0.00
PD*	2	21.3	1515	206	0.46
PD	2	22.5	330	21	0.20
OI	2	22.5	115	7	0.20
OI*	2	21.4	935	126	0.40
OI	3	21.4	420	0	0.00
OI	3	24.9	565	0	0.00
OI*	3	20.6	1360	0	0.01
OI*	3	20.4	870	18	0.11
PA*	3	20.4	1090	23	0.11
PA*	5	20.4	1480	137	0.26
PA*	5	20.3	900	72	0.28
PA	5	21.3	230	0	0.01
PP	6	20.5	870	2671	20.06
PP	7	23.0	900	0	0.00
PP	8	23.0	1270	0	0.00

Total Overtopping Volumes		
Tidal Flood Zone	Flood Zone Length (ft)	Overtopping Volumes (acre-ft)
1	2355	185
2A	3890	375
4A	2035	133
4C	1360	0
5B	4570	250
PP	3040	2671

Table B3
Storm: NV45500

Overtopping Reach	Profile	Wall Height (ft)	Wall Length (ft)	Overtopping Volume (acre-ft)	Overtopping Rate (cfs/ft)
CB	1	23.8	525	0	0.00
CB	1	20.7	1430	73	0.28
CB	1	19.8	400	41	0.43
PD	1	20.9	865	54	0.29
PD	2	20.9	610	34	0.30
PD	2	22.9	570	0	0.00
PD	2	21.3	1515	129	0.30
PD	2	22.5	330	24	0.20
OI	2	22.5	115	8	0.20
OI	2	21.4	935	91	0.30
OI	3	21.4	420	0	0.00
OI	3	24.9	565	0	0.00
OI	3	20.6	1360	0	0.00
OI	3	20.4	870	9	0.05
PA	3	20.4	1090	11	0.05
PA	5	20.4	1480	90	0.17
PA	5	20.3	900	46	0.18
PA	5	21.3	230	0	0.01
PP	6	20.5	870	978	7.12
PP	7	23.0	900	0	0.00
PP	8	23.0	1270	0	0.00

Total Overtopping Volumes		
Tidal Flood Zone	Flood Zone Length (ft)	Overtopping Volumes (acre-ft)
1	2355	114
2A	3890	241
4A	2035	99
4C	1360	0
5B	4570	156
PP	3040	978

Table B4
Storm: NV45100

Overtopping Reach	Profile	Wall Height (ft)	Wall Length (ft)	Overtopping Volume (acre-ft)	Overtopping Rate (cfs/ft)
CB	1	23.8	525	0	0.00
CB	1	20.7	1430	28	0.13
CB	1	19.8	400	22	0.23
PD	1	20.9	865	27	0.15
PD	2	20.9	610	14	0.14
PD	2	22.9	570	0	0.00
PD	2	21.3	1515	76	0.17
PD	2	22.5	330	30	0.20
OI	2	22.5	115	11	0.20
OI	2	21.4	935	59	0.18
OI	3	21.4	420	0	0.00
OI	3	24.9	565	0	0.00
OI	3	20.6	1360	0	0.00
OI	3	20.4	870	4	0.02
PA	3	20.4	1090	5	0.02
PA	5	20.4	1480	56	0.11
PA	5	20.3	900	31	0.11
PA	5	21.3	230	0	0.01
PP	6	20.5	870	300	3.08
PP	7	23.0	900	0	0.00
PP	8	23.0	1270	0	0.00

Total Overtopping Volumes		
Tidal Flood Zone	Flood Zone Length (ft)	Overtopping Volumes (acre-ft)
1	2355	50
2A	3890	147
4A	2035	70
4C	1360	0
5B	4570	96
PP	3040	300

Table B5
Storm: NV4550

Overtopping Reach	Profile	Wall Height (ft)	Wall Length (ft)	Overtopping Volume (acre-ft)	Overtopping Rate (cfs/ft)
CB	1	23.8	525	0	0.00
CB	1	20.7	1430	26	0.09
CB	1	19.8	400	28	0.18
PD	1	20.9	865	32	0.11
PD	2	20.9	610	13	0.10
PD	2	22.9	570	0	0.00
PD	2	21.3	1515	100	0.14
PD	2	22.5	330	26	0.20
OI	2	22.5	115	9	0.20
OI	2	21.4	935	75	0.15
OI	3	21.4	420	0	0.00
OI	3	24.9	565	0	0.00
OI	3	20.6	1360	0	0.00
OI	3	20.4	870	6	0.01
PA	3	20.4	1090	8	0.01
PA	5	20.4	1480	92	0.09
PA	5	20.3	900	42	0.10
PA	5	21.3	230	0	0.01
PP	6	20.5	870	91	0.71
PP	7	23.0	900	0	0.00
PP	8	23.0	1270	0	0.00

Total Overtopping Volumes		
Tidal Flood Zone	Flood Zone Length (ft)	Overtopping Volumes (acre-ft)
1	2355	54
2A	3890	171
4A	2035	84
4C	1360	0
5B	4570	148
PP	3040	91

Table B6
Storm: NV4520

Overtopping Reach	Profile	Wall Height (ft)	Wall Length (ft)	Overtopping Volume (acre-ft)	Overtopping Rate (cfs/ft)
CB	1	23.8	525	0	0.00
CB	1	20.7	1430	2	0.04
CB	1	19.8	400	5	0.12
PD	1	20.9	865	5	0.07
PD	2	20.9	610	1	0.05
PD	2	22.9	570	0	0.00
PD	2	21.3	1515	20	0.10
PD	2	22.5	330	52	0.20
OI	2	22.5	115	18	0.20
OI	2	21.4	935	18	0.11
OI	3	21.4	420	0	0.00
OI	3	24.9	565	0	0.00
OI	3	20.6	1360	0	0.00
OI	3	20.4	870	1	0.01
PA	3	20.4	1090	2	0.01
PA	5	20.4	1480	20	0.08
PA	5	20.3	900	8	0.08
PA	5	21.3	230	0	0.01
PP	6	20.5	870	32	0.42
PP	7	23.0	900	0	0.00
PP	8	23.0	1270	0	0.00

Total Overtopping Volumes		
Tidal Flood Zone	Flood Zone Length (ft)	Overtopping Volumes (acre-ft)
1	2355	7
2A	3890	78
4A	2035	36
4C	1360	0
5B	4570	31
PP	3040	32

Table 37
Storm: NV4510

Overtopping Reach	Profile	Wall Height (ft)	Wall Length (ft)	Overtopping Volume (acre-ft)	Overtopping Rate (cfs/ft)
CB	1	23.8	525	0	0.00
CB	1	20.7	1430	0	0.00
CB	1	19.8	400	4	0.07
PD	1	20.9	865	3	0.03
PD	2	20.9	610	0	0.00
PD	2	22.9	570	0	0.00
PD	2	21.3	1515	24	0.07
PD	2	22.5	330	33	0.20
OI	2	22.5	115	12	0.20
OI	2	21.4	935	24	0.08
OI	3	21.4	420	0	0.00
OI	3	24.9	565	0	0.00
OI	3	20.6	1360	0	0.00
OI	3	20.4	870	2	0.01
PA	3	20.4	1090	2	0.01
PA	5	20.4	1480	26	0.07
PA	5	20.3	900	3	0.07
PA	5	21.3	230	0	0.00
PP	6	20.5	870	15	0.16
PP	7	23.0	900	0	0.00
PP	8	23.0	1270	0	0.00

Total Overtopping Volumes		
Tidal Flood Zone	Flood Zone Length (ft)	Overtopping Volumes (acre-ft)
1	2355	4
2A	3890	60
4A	2035	36
4C	1360	0
5B	4570	33
PP	3040	15

Table B8
Storm: FB5850

Overtopping Reach	Profile	Wall Height (ft)	Wall Length (ft)	Overtopping Volume (acre-ft)	Overtopping Rate (cfs/ft)
CB	1	23.8	525	0	0.00
CB	1	20.7	1430	7	0.09
CB	1	19.8	400	7	0.18
PD	1	20.9	865	8	0.11
PD	2	20.9	610	4	0.10
PD	2	22.9	570	0	0.00
PD	2	21.3	1515	23	0.14
PD	2	22.5	330	11	0.20
OI	2	22.5	115	4	0.20
OI	2	21.4	935	16	0.15
OI	3	21.4	420	0	0.00
OI	3	24.9	565	0	0.00
OI	3	20.6	1360	0	0.00
OI	3	20.4	870	1	0.01
PA	3	20.4	1090	2	0.01
PA	5	20.4	1480	18	0.09
PA	5	20.3	900	10	0.10
PA	5	21.3	230	0	0.01
PP	6	20.5	870	0	0.00
PP	7	23.0	900	0	0.00
PP	8	23.0	1270	0	0.00

Total Overtopping Volumes		
Tidal Flood Zone	Flood Zone Length (ft)	Overtopping Volumes (acre-ft)
1	2355	14
2A	3890	46
4A	2035	20
4C	1360	0
5B	4570	31
PP	3040	0

Table B9
Storm: FB5820

Overtopping Reach	Profile	Wall Height (ft)	Wall Length (ft)	Overtopping Volume (acre-ft)	Overtopping Rate (cfs/ft)
CB	1	23.8	525	0	0.00
CB	1	20.7	1430	2	0.04
CB	1	19.8	400	3	0.12
PD	1	20.9	865	3	0.07
PD	2	20.9	610	1	0.05
PD	2	22.9	570	0	0.00
PD	2	21.3	1515	13	0.10
PD	2	22.5	330	12	0.20
OI	2	22.5	115	4	0.20
OI	2	21.4	935	11	0.11
OI	3	21.4	420	0	0.00
OI	3	24.9	565	0	0.00
OI	3	20.6	1360	0	0.00
OI	3	20.4	870	1	0.01
PA	3	20.4	1090	1	0.01
PA	5	20.4	1480	14	0.08
PA	5	20.3	900	6	0.08
PA	5	21.3	230	0	0.01
PP	6	20.5	870	0	0.00
PP	7	23.0	900	0	0.00
PP	8	23.0	1270	0	0.00

Total Overtopping Volumes		
Tidal Flood Zone	Flood Zone Length (ft)	Overtopping Volumes (acre-ft)
1	2355	5
2A	3890	29
4A	2035	15
4C	1360	0
5B	4570	22
PP	3040	0

Table B10
Storm: FB5810

Overtopping Reach	Profile	Wall Height (ft)	Wall Length (ft)	Overtopping Volume (acre-ft)	Overtopping Rate (cfs/ft)
CB	1	23.8	525	0	0.00
CB	1	20.7	1430	0	0.00
CB	1	19.8	400	1	0.07
PD	1	20.9	865	1	0.03
PD	2	20.9	610	0	0.00
PD	2	22.9	570	0	0.00
PD	2	21.3	1515	7	0.07
PD	2	22.5	330	10	0.20
OI	2	22.5	115	4	0.20
OI	2	21.4	935	7	0.08
OI	3	21.4	420	0	0.00
OI	3	24.9	565	0	0.00
OI	3	20.6	1360	0	0.00
OI	3	20.4	870	1	0.01
PA	3	20.4	1090	1	0.01
PA	5	20.4	1480	8	0.07
PA	5	20.3	900	2	0.07
PA	5	21.3	230	0	0.00
PP	6	20.5	870	0	0.00
PP	7	23.0	900	0	0.00
PP	8	23.0	1270	0.00	0.00

Total Overtopping Volumes		
Tidal Flood Zone	Flood Zone Length (ft)	Overtopping Volumes (acre-ft)
1	2355	1
2A	3890	18
4A	2035	11
4C	1360	0
5B	4570	12
PP	3040	0

Table B11
Storm: FB585

Overtopping Reach	Profile	Wall Height (ft)	Wall Length (ft)	Overtopping Volume (acre-ft)	Overtopping Rate (cfs/ft)
CB	1	23.8	525	0	0.00
CB	1	20.7	1430	0	0.00
CB	1	19.8	400	0	0.02
PD	1	20.9	865	0	0.00
PD	2	20.9	610	0	0.00
PD	2	22.9	570	0	0.00
PD	2	21.3	1515	3	0.04
PD	2	22.5	330	4	0.20
OI	2	22.5	115	2	0.20
OI	2	21.4	935	4	0.05
OI	3	21.4	420	0	0.00
OI	3	24.9	565	0	0.00
OI	3	20.6	1360	0	0.00
OI	3	20.4	870	0	0.01
PA	3	20.4	1090	0	0.01
PA	5	20.4	1480	2	0.07
PA	5	20.3	900	0	0.00
PA	5	21.3	230	0	0.00
PP	6	20.5	870	0	0.00
PP	7	23.0	900	0	0.00
PP	8	23.0	1270	0	0.00

Total Overtopping Volumes		
Tidal Flood Zone	Flood Zone Length (ft)	Overtopping Volumes (acre-ft)
1	2355	0
2A	3890	7
4A	2035	6
4C	1360	0
5B	4570	2
PP	3040	0

Table B12
Storm: FB582

Overtopping Reach	Profile	Wall Height (ft)	Wall Length (ft)	Overtopping Volume (acre-ft)	Overtopping Rate (cfs/ft)
CB	1	23.8	525	0	0.00
CB	1	20.7	1430	0	0.00
CB	1	19.8	400	0	0.00
PD	1	20.9	865	0	0.00
PD	2	20.9	610	0	0.00
PD	2	22.9	570	0	0.00
PD	2	21.3	1515	0	0.00
PD	2	22.5	330	5	0.20
OI	2	22.5	115	2	0.20
OI	2	21.4	935	1	0.02
OI	3	21.4	420	0	0.00
OI	3	24.9	565	0	0.00
OI	3	20.6	1360	0	0.00
OI	3	20.4	870	0	0.00
PA	3	20.4	1090	0	0.00
PA	5	20.4	1480	0	0.00
PA	5	20.3	900	0	0.00
PA	5	21.3	230	0	0.00
PP	6	20.5	870	0	0.00
PP	7	23.0	900	0	0.00
PP	8	23.0	1270	0	0.00

Total Overtopping Volumes		
Tidal Flood Zone	Flood Zone Length (ft)	Overtopping Volumes (acre-ft)
1	2355	0
2A	3890	5
4A	2035	3
4C	1360	0
5B	4570	0
PP	3040	0

Table B13
Storm: MR5850

Overtopping Reach	Profile	Wall Height (ft)	Wall Length (ft)	Overtopping Volume (acre-ft)	Overtopping Rate (cfs/ft)
CB	1	23.8	525	0	0.00
CB	1	20.7	1430	9	0.09
CB	1	19.8	400	8	0.18
PD	1	20.9	865	9	0.11
PD	2	20.9	610	4	0.10
PD	2	22.9	570	0	0.00
PD	2	21.3	1515	27	0.14
PD	2	22.5	330	15	0.20
OI	2	22.5	115	5	0.20
OI	2	21.4	935	21	0.15
OI	3	21.4	420	0	0.00
OI	3	24.9	565	0	0.00
OI	3	20.6	1360	0	0.00
OI	3	20.4	870	1	0.01
PA	3	20.4	1090	2	0.01
PA	5	20.4	1480	21	0.09
PA	5	20.3	900	11	0.10
PA	5	21.3	230	0	0.01
PP	6	20.5	870	0	0.00
PP	7	23.0	900	0	0.00
PP	8	23.0	1270	0	0.00

Total Overtopping Volumes		
Tidal Flood Zone	Flood Zone Length (ft)	Overtopping Volumes (acre-ft)
1	2355	17
2A	3890	55
4A	2035	26
4C	1360	0
5B	4570	35
PP	3040	0

Table B14
Storm: MR5820

Overtopping Reach	Profile	Wall Height (ft)	Wall Length (ft)	Overtopping Volume (acre-ft)	Overtopping Rate (cfs/ft)
CB	1	23.8	525	0	0.00
CB	1	20.7	1430	2	0.04
CB	1	19.8	400	4	0.12
PD	1	20.9	865	4	0.07
PD	2	20.9	610	1	0.05
PD	2	22.9	570	0	0.00
PD	2	21.3	1515	18	0.10
PD	2	22.5	330	16	0.20
OI	2	22.5	115	6	0.20
OI	2	21.4	935	16	0.11
OI	3	21.4	420	0	0.00
OI	3	24.9	565	0	0.00
OI	3	20.6	1360	0	0.00
OI	3	20.4	870	1	0.01
PA	3	20.4	1090	1	0.01
PA	5	20.4	1480	15	0.08
PA	5	20.3	900	6	0.08
PA	5	21.3	230	0	0.01
PP	6	20.5	870	0	0.00
PP	7	23.0	900	0	0.00
PP	8	23.0	1270	0	0.00

Total Overtopping Volumes		
Tidal Flood Zone	Flood Zone Length (ft)	Overtopping Volumes (acre-ft)
1	2355	6
2A	3890	39
4A	2035	22
4C	1360	0
5B	4570	23
PP	3040	0

Table B15
Storm: MR5810

Overtopping Reach	Profile	Wall Height (ft)	Wall Length (ft)	Overtopping Volume (acre-ft)	Overtopping Rate (cfs/ft)
CB	1	23.8	525	0	0.00
CB	1	20.7	1430	0	0.00
CB	1	19.8	400	1	0.07
PD	1	20.9	865	1	0.03
PD	2	20.9	610	0	0.00
PD	2	22.9	570	0	0.00
PD	2	21.3	1515	9	0.07
PD	2	22.5	330	15	0.20
OI	2	22.5	115	5	0.20
OI	2	21.4	935	11	0.08
OI	3	21.4	420	0	0.00
OI	3	24.9	565	0	0.00
OI	3	20.6	1360	0	0.00
OI	3	20.4	870	1	0.01
PA	3	20.4	1090	1	0.01
PA	5	20.4	1480	8	0.07
PA	5	20.3	900	1	0.07
PA	5	21.3	230	0	0.00
PP	6	20.5	870	0	0.00
PP	7	23.0	900	0	0.00
PP	8	23.0	1270	0	0.00

Total Overtopping Volumes		
Tidal Flood Zone	Flood Zone Length (ft)	Overtopping Volumes (acre-ft)
1	2355	1
2A	3890	25
4A	2035	16
4C	1360	0
5B	4570	11
PP	3040	0

Table B16
Storm: MR585

Overtopping Reach	Profile	Wall Height (ft)	Wall Length (ft)	Overtopping Volume (acre-ft)	Overtopping Rate (cfs/ft)
CB	1	23.8	525	0	0.00
CB	1	20.7	1430	0	0.00
CB	1	19.8	400	0	0.02
PD	1	20.9	865	0	0.00
PD	2	20.9	610	0	0.00
PD	2	22.9	570	0	0.00
PD	2	21.3	1515	4	0.04
PD	2	22.5	330	19	0.20
OI	2	22.5	115	7	0.20
OI	2	21.4	935	5	0.05
OI	3	21.4	420	0	0.00
OI	3	24.9	565	0	0.00
OI	3	20.6	1360	0	0.00
OI	3	20.4	870	0	0.01
PA	3	20.4	1090	0	0.01
PA	5	20.4	1480	3	0.07
PA	5	20.3	900	0	0.00
PA	5	21.3	230	0	0.00
PP	6	20.5	870	0	0.00
PP	7	23.0	900	0	0.00
PP	8	23.0	1270	0	0.00

Total Overtopping Volumes		
Tidal Flood Zone	Flood Zone Length (ft)	Overtopping Volumes (acre-ft)
1	2355	0
2A	3890	23
4A	2035	12
4C	1360	0
5B	4570	3
PP	3040	0

Table B17
Storm: MR582

Overtopping Reach	Profile	Wall Height (ft)	Wall Length (ft)	Overtopping Volume (acre-ft)	Overtopping Rate (cfs/ft)
CB	1	23.8	525	0	0.00
CB	1	20.7	1430	0	0.00
CB	1	19.8	400	0	0.00
PD	1	20.9	865	0	0.00
PD	2	20.9	610	0	0.00
PD	2	22.9	570	0	0.00
PD	2	21.3	1515	0	0.00
PD	2	22.5	330	17	0.20
OI	2	22.5	115	6	0.20
OI	2	21.4	935	3	0.02
OI	3	21.4	420	0	0.00
OI	3	24.9	565	0	0.00
OI	3	20.6	1360	0	0.00
OI	3	20.4	870	0	0.00
PA	3	20.4	1090	0	0.00
PA	5	20.4	1480	0	0.00
PA	5	20.3	900	0	0.00
PA	5	21.3	230	0	0.00
PP	6	20.5	870	0	0.00
PP	7	23.0	900	0	0.00
PP	8	23.0	1270	0	0.00

Total Overtopping Volumes		
Tidal Flood Zone	Flood Zone Length (ft)	Overtopping Volumes (acre-ft)
1	2355	0
2A	3890	17
4A	2035	9
4C	1360	0
5B	4570	0
PP	3040	0

Table B18
Storm: JN61100

Overtopping Reach	Profile	Wall Height (ft)	Wall Length (ft)	Overtopping Volume (acre-ft)	Overtopping Rate (cfs/ft)
CB	1	23.8	525	0	0.00
CB	1	20.7	1430	14	0.13
CB	1	19.8	400	10	0.23
PD	1	20.9	865	12	0.15
PD	2	20.9	610	7	0.14
PD	2	22.9	570	0	0.00
PD	2	21.3	1515	31	0.17
PD	2	22.5	330	10	0.20
OI	2	22.5	115	4	0.20
OI	2	21.4	935	22	0.18
OI	3	21.4	420	0	0.00
OI	3	24.9	565	0	0.00
OI	3	20.6	1360	0	0.00
OI	3	20.4	870	2	0.02
PA	3	20.4	1090	2	0.02
PA	5	20.4	1480	24	0.11
PA	5	20.3	900	13	0.11
PA	5	21.3	230	0	0.01
PP	6	20.5	870	0	0.00
PP	7	23.0	900	0	0.00
PP	8	23.0	1270	0	0.00

Total Overtopping Volumes		
Tidal Flood Zone	Flood Zone Length (ft)	Overtopping Volumes (acre-ft)
1	2355	24
2A	3890	60
4A	2035	26
4C	1360	0
5B	4570	41
PP	3040	0

Table B19
Storm: JN6150

Overtopping Reach	Profile	Wall Height (ft)	Wall Length (ft)	Overtopping Volume (acre-ft)	Overtopping Rate (cfs/ft)
CB	1	23.8	525	0	0.00
CB	1	20.7	1430	7	0.09
CB	1	19.8	400	7	0.18
PD	1	20.9	865	8	0.11
PD	2	20.9	610	3	0.10
PD	2	22.9	570	0	0.00
PD	2	21.3	1515	23	0.14
PD	2	22.5	330	16	0.20
OI	2	22.5	115	6	0.20
OI	2	21.4	935	16	0.15
OI	3	21.4	420	0	0.00
OI	3	24.9	565	0	0.00
OI	3	20.6	1360	0	0.00
OI	3	20.4	870	1	0.01
PA	3	20.4	1090	2	0.01
PA	5	20.4	1480	20	0.09
PA	5	20.3	900	10	0.10
PA	5	21.3	230	0	0.01
PP	6	20.5	870	0	0.00
PP	7	23.0	900	0	0.00
PP	8	23.0	1270	0	0.00

Total Overtopping Volumes		
Tidal Flood Zone	Flood Zone Length (ft)	Overtopping Volumes (acre-ft)
1	2355	14
2A	3890	50
4A	2035	22
4C	1360	0
5B	4570	33
PP	3040	0

Table B20
Storm: JN6120

Overtopping Reach	Profile	Wall Height (ft)	Wall Length (ft)	Overtopping Volume (acre-ft)	Overtopping Rate (cfs/ft)
CB	1	23.8	525	0	0.00
CB	1	20.7	1430	6	0.04
CB	1	19.8	400	6	0.12
PD	1	20.9	865	7	0.07
PD	2	20.9	610	3	0.05
PD	2	22.9	570	0	0.00
PD	2	21.3	1515	21	0.10
PD	2	22.5	330	11	0.19
OI	2	22.5	115	4	0.19
OI	2	21.4	935	16	0.11
OI	3	21.4	420	0	0.00
OI	3	24.9	565	0	0.00
OI	3	20.6	1360	0	0.00
OI	3	20.4	870	1	0.01
PA	3	20.4	1090	2	0.01
PA	5	20.4	1480	19	0.08
PA	5	20.3	900	9	0.08
PA	5	21.3	230	0	0.01
PP	6	20.5	870	0	0.00
PP	7	23.0	900	0	0.00
PP	8	23.0	1270	0	0.00

Total Overtopping Volumes		
Tidal Flood Zone	Flood Zone Length (ft)	Overtopping Volumes (acre-ft)
1	2355	12
2A	3890	42
4A	2035	20
4C	1360	0
5B	4570	31
PP	3040	0

Table B21
Storm: JN6110

Overtopping Reach	Profile	Wall Height (ft)	Wall Length (ft)	Overtopping Volume (acre-ft)	Overtopping Rate (cfs/ft)
CB	1	23.8	525	0	0.00
CB	1	20.7	1430	0	0.00
CB	1	19.8	400	2	0.07
PD	1	20.9	865	2	0.03
PD	2	20.9	610	0	0.00
PD	2	22.9	570	0	0.00
PD	2	21.3	1515	10	0.07
PD	2	22.5	330	10	0.20
OI	2	22.5	115	3	0.20
OI	2	21.4	935	8	0.08
OI	3	21.4	420	0	0.00
OI	3	24.9	565	0	0.00
OI	3	20.6	1360	0	0.00
OI	3	20.4	870	1	0.01
PA	3	20.4	1090	1	0.01
PA	5	20.4	1480	11	0.07
PA	5	20.3	900	3	0.07
PA	5	21.3	230	0	0.00
PP	6	20.5	870	0	0.00
PP	7	23.0	900	0	0.00
PP	8	23.0	1270	0	0.00

Total Overtopping Volumes		
Tidal Flood Zone	Flood Zone Length (ft)	Overtopping Volumes (acre-ft)
1	2355	2
2A	3890	22
4A	2035	11
4C	1360	0
5B	4570	16
PP	3040	0

Table B22
Storm: JN615

Overtopping Reach	Profile	Wall Height (ft)	Wall Length (ft)	Overtopping Volume (acre-ft)	Overtopping Rate (cfs/ft)
CB	1	23.8	525	0	0.00
CB	1	20.7	1430	0	0.00
CB	1	19.8	400	0	0.02
PD	1	20.9	865	0	0.00
PD	2	20.9	610	0	0.00
PD	2	22.9	570	0	0.00
PD	2	21.3	1515	3	0.04
PD	2	22.5	330	11	0.20
OI	2	22.5	115	4	0.20
OI	2	21.4	935	4	0.05
OI	3	21.4	420	0	0.00
OI	3	24.9	565	0	0.00
OI	3	20.6	1360	0	0.00
OI	3	20.4	870	0	0.01
PA	3	20.4	1090	0	0.01
PA	5	20.4	1480	2	0.07
PA	5	20.3	900	0	0.00
PA	5	21.3	230	0	0.00
PP	6	20.5	870	0	0.00
PP	7	23.0	900	0	0.00
PP	8	23.0	1270	0	0.00

Total Overtopping Volumes		
Tidal Flood Zone	Flood Zone Length (ft)	Overtopping Volumes (acre-ft)
1	2355	0
2A	3890	14
4A	2035	8
4C	1360	0
5B	4570	2
PP	3040	0

Table B23
Storm: JN612

Overtopping Reach	Profile	Wall Height (ft)	Wall Length (ft)	Overtopping Volume (acre-ft)	Overtopping Rate (cfs/ft)
CB	1	23.8	525	0	0.00
CB	1	20.7	1430	0	0.00
CB	1	19.8	400	0	0.00
PD	1	20.9	865	0	0.00
PD	2	20.9	610	0	0.00
PD	2	22.9	570	0	0.00
PD	2	21.3	1515	0	0.00
PD	2	22.5	330	4	0.20
OI	2	22.5	115	2	0.20
OI	2	21.4	935	1	0.02
OI	3	21.4	420	0	0.00
OI	3	24.9	565	0	0.00
OI	3	20.6	1360	0	0.00
OI	3	20.4	870	0	0.00
PA	3	20.4	1090	0	0.00
PA	5	20.4	1480	0	0.00
PA	5	20.3	900	0	0.00
PA	5	21.3	230	0	0.00
PP	6	20.5	870	0	0.00
PP	7	23.0	900	0	0.00
PP	8	23.0	1270	0	0.00

Total Overtopping Volumes		
Tidal Flood Zone	Flood Zone Length (ft)	Overtopping Volumes (acre-ft)
1	2355	0
2A	3890	4
4A	2035	3
4C	1360	0
5B	4570	0
PP	3040	0

Table B24
Storm: AP61100

Overtopping Reach	Profile	Wall Height (ft)	Wall Length (ft)	Overtopping Volume (acre-ft)	Overtopping Rate (cfs/ft)
CB	1	23.8	525	0	0.00
CB	1	20.7	1430	14	0.13
CB	1	19.8	400	10	0.23
PD	1	20.9	865	12	0.15
PD	2	20.9	610	7	0.14
PD	2	22.9	570	0	0.00
PD	2	21.3	1515	32	0.17
PD	2	22.5	330	21	0.20
OI	2	22.5	115	7	0.20
OI	2	21.4	935	22	0.18
OI	3	21.4	420	0	0.00
OI	3	24.9	565	0	0.00
OI	3	20.6	1360	0	0.00
OI	3	20.4	870	2	0.02
PA	3	20.4	1090	2	0.02
PA	5	20.4	1480	25	0.11
PA	5	20.3	900	13	0.11
PA	5	21.3	230	0	0.00
PP	6	20.5	870	0	0.00
PP	7	23.0	900	0	0.00
PP	8	23.0	1270	0	0.00

Total Overtopping Volumes		
Tidal Flood Zone	Flood Zone Length (ft)	Overtopping Volumes (acre-ft)
1	2355	24
2A	3890	72
4A	2035	29
4C	1360	0
5B	4570	42
PP	3040	0

Table B25
Storm: AP6150

Overtopping Reach	Profile	Wall Height (ft)	Wall Length (ft)	Overtopping Volume (acre-ft)	Overtopping Rate (cfs/ft)
CB	1	23.8	525	0	0.00
CB	1	20.7	1430	8	0.09
CB	1	19.8	400	7	0.18
PD	1	20.9	865	9	0.11
PD	2	20.9	610	4	0.10
PD	2	22.9	570	0	0.00
PD	2	21.3	1515	24	0.14
PD	2	22.5	330	28	0.20
OI	2	22.5	115	10	0.20
OI	2	21.4	935	17	0.15
OI	3	21.4	420	0	0.00
OI	3	24.9	565	0	0.00
OI	3	20.6	1360	0	0.00
OI	3	20.4	870	1	0.01
PA	3	20.4	1090	2	0.01
PA	5	20.4	1480	20	0.09
PA	5	20.3	900	11	0.10
PA	5	21.3	230	0	0.01
PP	6	20.5	870	0	0.00
PP	7	23.0	900	0	0.00
PP	8	23.0	1270	0	0.00

Total Overtopping Volumes		
Tidal Flood Zone	Flood Zone Length (ft)	Overtopping Volumes (acre-ft)
1	2355	15
2A	3890	65
4A	2035	27
4C	1360	0
5B	4570	34
PP	3040	0

Table B26
Storm: AP6120

Overtopping Reach	Profile	Wall Height (ft)	Wall Length (ft)	Overtopping Volume (acre-ft)	Overtopping Rate (cft)
CB	1	23.8	525	0	0.00
CB	1	20.7	1430	2	0.04
CB	1	19.8	400	4	0.12
PD	1	20.9	865	4	0.07
PD	2	20.9	610	1	0.05
PD	2	22.9	570	0	0.00
PD	2	21.3	1515	15	0.10
PD	2	22.5	330	13	0.20
OI	2	22.5	115	4	0.20
OI	2	21.4	935	11	0.11
OI	3	21.4	420	0	0.00
OI	3	24.9	565	0	0.00
OI	3	20.6	1360	0	0.00
OI	3	20.4	870	1	0.01
PA	3	20.4	1090	1	0.01
PA	5	20.4	1480	14	0.08
PA	5	20.3	900	6	0.08
PA	5	21.3	230	0	0.01
PP	6	20.5	870	0	0.00
PP	7	23.0	900	0	0.00
PP	8	23.0	1270	0	0.00

Total Overtopping Volumes		
Tidal Flood Zone	Flood Zone Length (ft)	Overtopping Volumes (acre-ft)
1	2355	6
2A	3890	33
4A	2035	15
4C	1360	0
5B	4570	22
PP	3040	0

Table B27
Storm: AP6110

Overtopping Reach	Profile	Wall Height (ft)	Wall Length (ft)	Overtopping Volume (acre-ft)	Overtopping Rate (cfs/ft)
CB	1	23.8	525	0	0.00
CB	1	20.7	1430	0	0.00
CB	1	19.8	400	3	0.07
PD	1	20.9	865	2	0.03
PD	2	20.9	610	0	0.00
PD	2	22.9	570	0	0.00
PD	2	21.3	1515	12	0.07
PD	2	22.5	330	7	0.20
OI	2	22.5	115	2	0.20
OI	2	21.4	935	10	0.08
OI	3	21.4	420	0	0.00
OI	3	24.9	565	0	0.00
OI	3	20.6	1360	0	0.00
OI	3	20.4	870	1	0.01
PA	3	20.4	1090	1	0.07
PA	5	20.4	1480	14	0.07
PA	5	20.3	900	6	0.07
PA	5	21.3	230	0	0.00
PP	6	20.5	870	0	0.00
PP	7	23.0	900	0	0.00
PP	8	23.0	1270	0	0.00

Total Overtopping Volumes		
Tidal Flood Zone	Flood Zone Length (ft)	Overtopping Volumes (acre-ft)
1	2355	3
2A	3890	21
4A	2035	12
4C	1360	0
5B	4570	22
PP	3040	0

Table B28
Storm: DC6250

Overtopping Reach	Profile	Wall Height (ft)	Wall Length (ft)	Overtopping Volume (acre-ft)	Overtopping Rate (cfs/ft)
CB	1	23.8	525	0	0.00
CB	1	20.7	1430	6	0.09
CB	1	19.8	400	6	0.18
PD	1	20.9	865	7	0.11
PD	2	20.9	610	3	0.10
PD	2	22.9	570	0	0.00
PD	2	21.3	1515	23	0.14
PD	2	22.5	330	24	0.20
OI	2	22.5	115	8	0.20
OI	2	21.4	935	18	0.15
OI	3	21.4	420	0	0.00
OI	3	24.9	565	0	0.00
OI	3	20.6	1360	0	0.00
OI	3	20.4	870	1	0.01
PA	3	20.4	1090	2	0.01
PA	5	20.4	1480	19	0.09
PA	5	20.3	900	9	0.10
PA	5	21.3	230	0	0.01
PP	6	20.5	870	0	0.00
PP	7	23.0	900	1	0.00
PP	8	23.0	1270	0	0.00

Total Overtopping Volumes		
Tidal Flood Zone	Flood Zone Length (ft)	Overtopping Volumes (acre-ft)
1	2355	12
2A	3890	57
4A	2035	26
4C	1360	0
5B	4570	31
PP	3040	1

Table B29
Storm: DC6220

Overtopping Reach	Profile	Wall Height (ft)	Wall Length (ft)	Overtopping Volume (acre-ft)	Overtopping Rate (cfs/ft)
CB	1	23.8	525	0	0.00
CB	1	20.7	1430	2	0.04
CB	1	19.8	400	4	0.12
PD	1	20.9	865	4	0.07
PD	2	20.9	610	1	0.05
PD	2	22.9	570	0	0.00
PD	2	21.3	1515	16	0.10
PD	2	22.5	330	28	0.20
OI	2	22.5	115	10	0.20
OI	2	21.4	935	14	0.11
OI	3	21.4	420	0	0.00
OI	3	24.9	565	0	0.00
OI	3	20.6	1360	0	0.00
OI	3	20.4	870	1	0.01
PA	3	20.4	1090	1	0.01
PA	5	20.4	1480	14	0.08
PA	5	20.3	900	6	0.08
PA	5	21.3	230	0	0.01
PP	6	20.5	870	0	0.00
PP	7	23.0	900	0	0.00
PP	8	23.0	1270	0	0.00

Total Overtopping Volumes		
Tidal Flood Zone	Flood Zone Length (ft)	Overtopping Volumes (acre-ft)
1	2355	6
2A	3890	49
4A	2035	24
4C	1360	0
5B	4570	22
PP	3040	0

Table B30
Storm: DC6210

Overtopping Reach	Profile	Wall Height (ft)	Wall Length (ft)	Overtopping Volume (acre-ft)	Overtopping Rate (cfs/ft)
CB	1	23.8	525	0	0.00
CB	1	20.7	1430	0	0.00
CB	1	19.8	400	1	0.07
PD	1	20.9	865	1	0.03
PD	2	20.9	610	0	0.00
PD	2	22.9	570	0	0.00
PD	2	21.3	1515	8	0.07
PD	2	22.5	330	28	0.20
OI	2	22.5	115	10	0.20
OI	2	21.4	935	9	0.08
OI	3	21.4	420	0	0.00
OI	3	24.9	565	0	0.00
OI	3	20.6	1360	0	0.00
OI	3	20.4	870	1	0.01
PA	3	20.4	1090	1	0.01
PA	5	20.4	1480	7	0.07
PA	5	20.3	900	2	0.07
PA	5	21.3	230	0	0.00
PP	6	20.5	870	0	0.00
PP	7	23.0	900	0	0.00
PP	8	23.0	1270	0	0.00

Total Overtopping Volumes		
Tidal Flood Zone	Flood Zone Length (ft)	Overtopping Volumes (acre-ft)
1	2355	1
2A	3890	37
4A	2035	19
4C	1360	0
5B	4570	11
PP	3040	0

Table B31
Storm: DC625

Overtopping Reach	Profile	Wall Height (ft)	Wall Length (ft)	Overtopping Volume (acre-ft)	Overtopping Rate (cfs/ft)
CB	1	23.8	525	0	0.00
CB	1	20.7	1430	0	0.00
CB	1	19.8	400	0	0.02
PD	1	20.9	865	0	0.00
PD	2	20.9	610	0	0.00
PD	2	22.9	570	0	0.00
PD	2	21.3	1515	3	0.04
PD	2	22.5	330	18	0.20
OI	2	22.5	115	6	0.20
OI	2	21.4	935	4	0.05
OI	3	21.4	420	0	0.00
OI	3	24.9	565	0	0.00
OI	3	20.6	1360	0	0.00
OI	3	20.4	870	0	0.01
PA	3	20.4	1090	0	0.01
PA	5	20.4	1480	1	0.07
PA	5	20.3	900	0	0.00
PA	5	21.3	230	0	0.00
PP	6	20.5	870	0	0.00
PP	7	23.0	900	0	0.00
PP	8	23.0	1270	0	0.00

Total Overtopping Volumes		
Tidal Flood Zone	Flood Zone Length (ft)	Overtopping Volumes (acre-ft)
1	2355	0
2A	3890	21
4A	2035	10
4C	1360	0
5B	4570	1
PP	3040	0

Table B32
Storm: DC622

Overtopping Reach	Profile	Wall Height (ft)	Wall Length (ft)	Overtopping Volume (acre-ft)	Overtopping Rate (cfs/ft)
CB	1	23.8	525	0	0.00
CB	1	20.7	1430	0	0.00
CB	1	19.8	400	0	0.00
PD	1	20.9	865	0	0.00
PD	2	20.9	610	0	0.00
PD	2	22.9	570	0	0.00
PD	2	21.3	1515	0	0.00
PD	2	22.5	330	20	0.20
OI	2	22.5	115	7	0.20
OI	2	21.4	935	1	0.02
OI	3	21.4	420	0	0.00
OI	3	24.9	565	0	0.00
OI	3	20.6	1360	0	0.00
OI	3	20.4	870	0	0.00
PA	3	20.4	1090	0	0.00
PA	5	20.4	1480	0	0.00
PA	5	20.3	900	0	0.00
PA	5	21.3	230	0	0.00
PP	6	20.5	870	0	0.00
PP	7	23.0	900	0	0.00
PP	8	23.0	1270	0.00	0.00

Total Overtopping Volumes		
Tidal Flood Zone	Flood Zone Length (ft)	Overtopping Volumes (acre-ft)
1	2355	0
2A	3890	20
4A	2035	8
4C	1360	0
5B	4570	0
PP	3040	0

Table B33
Storm: FB645

Overtopping Reach	Profile	Wall Height (ft)	Wall Length (ft)	Overtopping Volume (acre-ft)	Overtopping Rate (cfs/ft)
CB	1	23.8	525	0	0.00
CB	1	20.7	1430	0	0.00
CB	1	19.8	400	0	0.02
PD	1	20.9	865	0	0.00
PD	2	20.9	610	0	0.00
PD	2	22.9	570	0	0.00
PD	2	21.3	1515	2	0.04
PD	2	22.5	330	11	0.20
OI	2	22.5	115	4	0.20
OI	2	21.4	935	3	0.05
OI	3	21.4	420	0	0.00
OI	3	24.9	565	0	0.00
OI	3	20.6	1360	0	0.00
OI	3	20.4	870	0	0.01
PA	3	20.4	1090	0	0.01
PA	5	20.4	1480	1	0.07
PA	5	20.3	900	0	0.00
PA	5	21.3	230	0	0.00
PP	6	20.5	870	0	0.00
PP	7	23.0	900	0	0.00
PP	8	23.0	1270	0	0.00

Total Overtopping Volumes		
Tidal Flood Zone	Flood Zone Length (ft)	Overtopping Volumes (acre-ft)
1	2355	0
2A	3890	13
4A	2035	7
4C	1360	0
5B	4570	1
PP	3040	0

Table B34
Storm: FB642

Overtopping Reach	Profile	Wall Height (ft)	Wall Length (ft)	Overtopping Volume (acre-ft)	Overtopping Rate (cfs/ft)
CB	1	23.8	525	0	0.00
CE	1	20.7	1430	0	0.00
CB	1	19.8	400	0	0.00
PD	1	20.9	865	0	0.00
PD	2	20.9	610	0	0.00
PD	2	22.9	570	0	0.00
PD	2	21.3	1515	0	0.00
PD	2	22.5	330	14	0.20
OI	2	22.5	115	5	0.20
OI	2	21.4	935	1	0.02
OI	3	21.4	420	0	0.00
OI	3	24.9	565	0	0.00
OI	3	20.6	1360	0	0.00
OI	3	20.4	870	0	0.00
PA	3	20.4	1090	0	0.00
PA	5	20.4	1480	0	0.00
PA	5	20.3	900	0	0.00
PA	5	21.3	230	0	0.00
PP	6	20.5	870	0	0.00
PP	7	23.0	900	0	0.00
PP	8	23.0	1270	0	0.00

Total Overtopping Volumes		
Tidal Flood Zone	Flood Zone Length (ft)	Overtopping Volumes (acre-ft)
1	2355	0
2A	3890	14
4A	2035	6
4C	1360	0
5B	4570	0
PP	3040	0

Table B35
Storm: FB6920

Overtopping Reach	Profile	Wall Height (ft)	Wall Length (ft)	Overtopping Volume (acre-ft)	Overtopping Rate (cfs/ft)
CB	1	23.8	525	0	0.00
CB	1	20.7	1430	2	0.04
CB	1	19.8	400	3	0.12
PD	1	20.9	865	3	0.07
PD	2	20.9	610	1	0.05
PD	2	22.9	570	0	0.00
PD	2	21.3	1515	14	0.10
PD	2	22.5	330	19	0.20
OI	2	22.5	115	6	0.20
OI	2	21.4	935	11	0.11
OI	3	21.4	420	0	0.00
OI	3	24.9	565	0	0.00
OI	3	20.6	1360	0	0.00
OI	3	20.4	870	1	0.01
PA	3	20.4	1090	1	0.01
PA	5	20.4	1480	14	0.08
PA	5	20.3	900	5	0.08
PA	5	21.3	230	0	0.01
PP	6	20.5	870	0	0.00
PP	7	23.0	900	0	0.00
PP	8	23.0	1270	0	0.00

Total Overtopping Volumes

Tidal Flood Zone	Flood Zone Length (ft)	Overtopping Volumes (acre-ft)
1	2355	5
2A	3890	37
4A	2035	17
4C	1360	0
5B	4570	21
PP	3040	0

Table B36
Storm: FB6910

Overtopping Reach	Profile	Wall Height (ft)	Wall Length (ft)	Overtopping Volume (acre-ft)	Overtopping Rate (cfs/ft)
CB	1	23.8	525	0	0.00
CB	1	20.7	1430	0	0.00
CB	1	19.8	400	1	0.07
PD	1	20.9	865	1	0.03
PD	2	20.9	610	0	0.00
PD	2	22.9	570	0	0.00
PD	2	21.3	1515	7	0.07
PD	2	22.5	330	18	0.20
OI	2	22.5	115	6	0.20
OI	2	21.4	935	6	0.08
OI	3	21.4	420	0	0.00
OI	3	24.9	565	0	0.00
OI	3	20.6	1360	0	0.00
OI	3	20.4	870	0	0.01
PA	3	20.4	1090	1	0.01
PA	5	20.4	1480	7	0.07
PA	5	20.3	900	1	0.07
PA	5	21.3	230	0	0.00
PP	6	20.5	870	0	0.00
PP	7	23.0	900	0	0.00
PP	8	23.0	1270	0	0.00

Total Overtopping Volumes		
Tidal Flood Zone	Flood Zone Length (ft)	Overtopping Volumes (acre-ft)
1	2355	1
2A	3890	26
4A	2035	12
4C	1360	0
5B	4570	9
PP	3040	0

Table B37
Storm: FB695

Overtopping Reach	Profile	Wall Height (ft)	Wall Length (ft)	Overtopping Volume (acre-ft)	Overtopping Rate (cfs/ft)
CB	1	23.8	525	0	0.00
CB	1	20.7	1430	0	0.00
CB	1	19.8	400	0	0.02
PD	1	20.9	865	0	0.00
PD	2	20.9	610	0	0.00
PD	2	22.9	570	0	0.00
PD	2	21.3	1515	4	0.04
PD	2	22.5	330	15	0.20
OI	2	22.5	115	5	0.20
OI	2	21.4	935	5	0.05
OI	3	21.4	420	0	0.00
OI	3	24.9	565	0	0.00
OI	3	20.6	1360	0	0.00
OI	3	20.4	870	0	0.01
PA	3	20.4	1090	0	0.01
PA	5	20.4	1480	3	0.07
PA	5	20.3	900	0	0.00
PA	5	21.3	230	0	0.00
PP	6	20.5	870	0	0.00
PP	7	23.0	900	0	0.00
PP	8	23.0	1270	0	0.00

Total Overtopping Volumes		
Tidal Flood Zone	Flood Zone Length (ft)	Overtopping Volumes (acre-ft)
1	2355	0
2A	3890	19
4A	2035	10
4C	1360	0
5B	4570	3
PP	3040	0

Table B38
Storm: FB7250

Overtopping Reach	Profile	Wall Height (ft)	Wall Length (ft)	Overtopping Volume (acre-ft)	Overtopping Rate (cfs/ft)
CB	1	23.8	525	0	0.00
CB	1	20.7	1430	7	0.09
CB	1	19.8	400	7	0.18
PD	1	20.9	865	9	0.11
PD	2	20.9	610	4	0.10
PD	2	22.9	570	0	0.00
PD	2	21.3	1515	25	0.14
PD	2	22.5	330	33	0.20
OI	2	22.5	115	12	0.20
OI	2	21.4	935	18	0.15
OI	3	21.4	420	0	0.00
OI	3	24.9	565	0	0.00
OI	3	20.6	1360	0	0.00
OI	3	20.4	870	1	0.01
PA	3	20.4	1090	2	0.01
PA	5	20.4	1480	21	0.09
PA	5	20.3	900	11	0.10
PA	5	21.3	230	0	0.01
PP	6	20.5	870	1	0.00
PP	7	23.0	900	0	0.00
PP	8	23.0	1270	0	0.00

Total Overtopping Volumes		
Tidal Flood Zone	Flood Zone Length (ft)	Overtopping Volumes (acre-ft)
1	2355	14
2A	3890	71
4A	2035	30
4C	1360	0
5B	4570	35
PP	3040	1

Table B39
Storm: FB7220

Overtopping Reach	Profile	Wall Height (ft)	Wall Length (ft)	Overtopping Volume (acre-ft)	Overtopping Rate (cfs/ft)
CB	1	23.8	525	0	0.00
CB	1	20.7	1430	2	0.04
CB	1	19.8	400	4	0.12
PD	1	20.9	865	4	0.07
PD	2	20.9	610	1	0.05
PD	2	22.9	570	0	0.00
PD	2	21.3	1515	15	0.10
PD	2	22.5	330	16	0.20
OI	2	22.5	115	5	0.20
OI	2	21.4	935	12	0.11
OI	3	21.4	420	0	0.00
OI	3	24.9	565	0	0.00
OI	3	20.6	1360	0	0.00
OI	3	20.4	870	1	0.01
PA	3	20.4	1090	1	0.01
PA	5	20.4	1480	16	0.08
PA	5	20.3	900	6	0.08
PA	5	21.3	230	0	0.01
PP	6	20.5	870	0	0.00
PP	7	23.0	900	0	0.00
PP	8	23.0	1270	0	0.00

Total Overtopping Volumes		
Tidal Flood Zone	Flood Zone Length (ft)	Overtopping Volumes (acre-ft)
1	2355	6
2A	3890	36
4A	2035	17
4C	1360	0
5B	4570	24
PP	3040	0

Table B40
Storm: FB7210

Overtopping Reach	Profile	Wall Height (ft)	Wall Length (ft)	Overtopping Volume (acre-ft)	Overtopping Rate (cfs/ft)
CB	1	23.8	525	0	0.00
CB	1	20.7	1430	0	0.00
CB	1	19.8	400	2	0.07
PD	1	20.9	865	1	0.03
PD	2	20.9	610	0	0.00
PD	2	22.9	570	0	0.00
PD	2	21.3	1515	9	0.07
PD	2	22.5	330	14	0.20
OI	2	22.5	115	5	0.20
OI	2	21.4	935	8	0.08
OI	3	21.4	420	0	0.00
OI	3	24.9	565	0	0.00
OI	3	20.6	1360	0	0.00
OI	3	20.4	870	1	0.01
PA	3	20.4	1090	1	0.01
PA	5	20.4	1480	10	0.07
PA	5	20.3	900	2	0.07
PA	5	21.3	230	0	0.00
PP	6	20.5	870	0	0.00
PP	7	23.0	900	0	0.00
PP	8	23.0	1270	0	0.00

Total Overtopping Volumes		
Tidal Flood Zone	Flood Zone Length (ft)	Overtopping Volumes (acre-ft)
1	2355	2
2A	3890	24
4A	2035	13
4C	1360	0
5B	4570	14
PP	3040	0

Table B41
Storm: NV7250

Overtopping Reach	Profile	Wall Height (ft)	Wall Length (ft)	Overtopping Volume (acre-ft)	Overtopping Rate (cfs/ft)
CB	1	23.8	525	0	0.00
CB	1	20.7	1430	9	0.09
CB	1	19.8	400	8	0.18
PD	1	20.9	865	9	0.11
PD	2	20.9	610	5	0.10
PD	2	22.9	570	0	0.00
PD	2	21.3	1515	32	0.14
PD	2	22.5	330	34	0.20
OI	2	22.5	115	12	0.20
OI	2	21.4	935	27	0.15
OI	3	21.4	420	0	0.00
OI	3	24.9	565	0	0.00
OI	3	20.6	1360	0	0.00
OI	3	20.4	870	1	0.01
PA	3	20.4	1090	2	0.01
PA	5	20.4	1480	22	0.09
PA	5	20.3	900	11	0.10
PA	5	21.3	230	0	0.01
PP	6	20.5	870	0	0.00
PP	7	23.0	900	0	0.00
PP	8	23.0	1270	0	0.00

Total Overtopping Volumes		
Tidal Flood Zone	Flood Zone Length (ft)	Overtopping Volumes (acre-ft)
1	2355	17
2A	3890	80
4A	2035	39
4C	1360	0
5B	4570	36
PP	3040	0

Table B42
Storm: NV7220

Overtopping Reach	Profile	Wall Height (ft)	Wall Length (ft)	Overtopping Volume (acre-ft)	Overtopping Rate (cfs/ft)
CB	1	23.8	525	0	0.00
CB	1	20.7	1430	2	0.04
CB	1	19.8	400	4	0.12
PD	1	20.9	865	4	0.07
PD	2	20.9	610	1	0.05
PD	2	22.9	570	0	0.00
PD	2	21.3	1515	15	0.10
PD	2	22.5	330	46	0.20
OI	2	22.5	115	16	0.20
OI	2	21.4	935	12	0.11
OI	3	21.4	420	0	0.00
OI	3	24.9	565	0	0.00
OI	3	20.6	1360	0	0.00
OI	3	20.4	870	1	0.01
PA	3	20.4	1090	1	0.01
PA	5	20.4	1480	16	0.08
PA	5	20.3	900	6	0.08
PA	5	21.3	230	0	0.01
PP	6	20.5	870	0	0.00
PP	7	23.0	900	0	0.00
PP	8	23.0	1270	0	0.00

Total Overtopping Volumes		
Tidal Flood Zone	Flood Zone Length (ft)	Overtopping Volumes (acre-ft)
1	2355	6
2A	3890	66
4A	2035	28
4C	1360	0
5B	4570	24
PP	3040	0

Table B43
Storm: NV7210

Overtopping Reach	Profile	Wall Height (ft)	Wall Length (ft)	Overtopping Volume (acre-ft)	Overtopping Rate (cfs/ft)
CB	1	23.8	525	0	0.00
CB	1	20.7	1430	0	0.00
CB	1	19.8	400	1	0.07
PD	1	20.9	865	1	0.03
PD	2	20.9	610	0	0.00
PD	2	22.9	570	0	0.00
PD	2	21.3	1515	7	0.07
PD	2	22.5	330	44	0.20
OI	2	22.5	115	15	0.20
OI	2	21.4	935	7	0.08
OI	3	21.4	420	0	0.00
OI	3	24.9	565	0	0.00
OI	3	20.6	1360	0	0.00
OI	3	20.4	870	1	0.01
PA	3	20.4	1090	1	0.01
PA	5	20.4	1480	8	0.07
PA	5	20.3	900	1	0.07
PA	5	21.3	230	0	0.00
PP	6	20.5	870	0	0.00
PP	7	23.0	900	0	0.00
PP	8	23.0	1270	0	0.00

Total Overtopping Volumes		
Tidal Flood Zone	Flood Zone Length (ft)	Overtopping Volumes (acre-ft)
1	2355	1
2A	3890	52
4A	2035	22
4C	1360	0
5B	4570	11
PP	3040	0

Table B44
Storm: NV725

Overtopping Reach	Profile	Wall Height (ft)	Wall Length (ft)	Overtopping Volume (acre-ft)	Overtopping Rate (cfs/ft)
CB	1	23.8	525	0	0.00
CB	1	20.7	1430	0	0.00
CB	1	19.8	400	0	0.02
PD	1	20.9	865	0	0.00
PD	2	20.9	610	0	0.00
PD	2	22.9	570	0	0.00
PD	2	21.3	1515	4	0.04
PD	2	22.5	330	32	0.20
OI	2	22.5	115	11	0.20
OI	2	21.4	935	7	0.05
OI	3	21.4	420	0	0.00
OI	3	24.9	565	0	0.00
OI	3	20.6	1360	0	0.00
OI	3	20.4	870	0	0.01
PA	3	20.4	1090	0	0.01
PA	5	20.4	1480	2	0.07
PA	5	20.3	900	0	0.00
PA	5	21.3	230	0	0.00
PP	6	20.5	870	0	0.00
PP	7	23.0	900	0	0.00
PP	8	23.0	1270	0	0.00

Total Overtopping Volumes		
Tidal Flood Zone	Flood Zone Length (ft)	Overtopping Volumes (acre-ft)
1	2355	0
2A	3890	36
4A	2035	18
4C	1360	0
5B	4570	2
PP	3040	0

Table B45
Storm: NV722

Overtopping Reach	Profile	Wall Height (ft)	Wall Length (ft)	Overtopping Volume (acre-ft)	Overtopping Rate (cfs/ft)
CB	1	23.8	525	0	0.00
CB	1	20.7	1430	0	0.00
CB	1	19.8	400	0	0.00
PD	1	20.9	865	0	0.00
PD	2	20.9	610	0	0.00
PD	2	22.9	570	0	0.00
PD	2	21.3	1515	0	0.00
PD	2	22.5	330	34	0.20
OI	2	22.5	115	12	0.20
OI	2	21.4	935	1	0.02
OI	3	21.4	420	0	0.00
OI	3	24.9	565	0	0.00
OI	3	20.6	1360	0	0.00
OI	3	20.4	870	0	0.00
PA	3	20.4	1090	0	0.00
PA	5	20.4	1480	0	0.00
PA	5	20.3	900	0	0.00
PA	5	21.3	230	0	0.00
PP	6	20.5	870	0	0.00
PP	7	23.0	900	0	0.00
PP	8	23.0	1270	0	0.00

Total Overtopping Volumes		
Tidal Flood Zone	Flood Zone Length (ft)	Overtopping Volumes (acre-ft)
1	2355	0
2A	3890	34
4A	2035	13
4C	1360	0
5B	4570	0
PP	3040	0

Table B46
Storm: FB78100

Overtopping Reach	Profile	Wall Height (ft)	Wall Length (ft)	Overtopping Volume (acre-ft)	Overtopping Rate (cfs/ft)
CB	1	23.8	525	0	0.00
CB	1	20.7	1430	25	0.13
CB	1	19.8	400	18	0.23
PD	1	20.9	865	23	0.15
PD	2	20.9	610	12	0.14
PD	2	22.9	570	0	0.00
PD	2	21.3	1515	59	0.17
PD	2	22.5	330	21	0.20
OI	2	22.5	115	7	0.20
OI	2	21.4	935	42	0.18
OI	3	21.4	420	0	0.00
OI	3	24.9	565	0	0.00
OI	3	20.6	1360	0	0.00
OI	3	20.4	870	4	0.02
PA	3	20.4	1090	4	0.02
PA	5	20.4	1480	47	0.11
PA	5	20.3	900	25	0.11
PA	5	21.3	230	0	0.01
PP	6	20.5	870	4	0.07
PP	7	23.0	900	0	0.00
PP	8	23.0	1270	0	0.00

Total Overtopping Volumes		
Tidal Flood Zone	Flood Zone Length (ft)	Overtopping Volumes (acre-ft)
1	2355	43
2A	3890	115
4A	2035	49
4C	1360	0
5B	4570	80
PP	3040	4

Table B47
Storm: FB7850

Overtopping Reach	Profile	Wall Height (ft)	Wall Length (ft)	Overtopping Volume (acre-ft)	Overtopping Rate (cfs/ft)
CB	1	23.8	525	0	0.00
CB	1	20.7	1430	5	0.09
CB	1	19.8	400	5	0.18
PD	1	20.9	865	6	0.11
PD	2	20.9	610	3	0.10
PD	2	22.9	570	0	0.00
PD	2	21.3	1515	19	0.14
PD	2	22.5	330	22	0.20
OI	2	22.5	115	8	0.20
OI	2	21.4	935	16	0.15
OI	3	21.4	420	0	0.00
OI	3	24.9	565	0	0.00
OI	3	20.6	1360	0	0.00
OI	3	20.4	870	1	0.01
PA	3	20.4	1090	1	0.01
PA	5	20.4	1480	17	0.09
PA	5	20.3	900	8	0.10
PA	5	21.3	230	0	0.00
PP	6	20.5	870	1	0.05
PP	7	23.0	900	0	0.00
PP	8	23.0	1270	0	0.00

Total Overtopping Volumes		
Tidal Flood Zone	Flood Zone Length (ft)	Overtopping Volumes (acre-ft)
1	2355	10
2A	3890	50
4A	2035	24
4C	1360	0
5B	4570	27
PP	3040	1

Table B48
Storm: FB7820

Overtopping Reach	Profile	Wall Height (ft)	Wall Length (ft)	Overtopping Volume (acre-ft)	Overtopping Rate (cfs/ft)
CB	1	23.8	525	0	0.00
CB	1	20.7	1430	1	0.04
CB	1	19.8	400	3	0.12
PD	1	20.9	865	3	0.07
PD	2	20.9	610	1	0.05
PD	2	22.9	570	0	0.00
PD	2	21.3	1515	13	0.10
PD	2	22.5	330	28	0.20
OI	2	22.5	115	10	0.20
OI	2	21.4	935	11	0.11
OI	3	21.4	420	0	0.00
OI	3	24.9	565	0	0.00
OI	3	20.6	1360	0	0.00
OI	3	20.4	870	1	0.01
PA	3	20.4	1090	1	0.01
PA	5	20.4	1480	13	0.08
PA	5	20.3	900	5	0.08
PA	5	21.3	230	0	0.01
PP	6	20.5	870	0	0.01
PP	7	23.0	900	0	0.00
PP	8	23.0	1270	0	0.00

Total Overtopping Volumes		
Tidal Flood Zone	Flood Zone Length (ft)	Overtopping Volumes (acre-ft)
1	2355	4
2A	3890	45
4A	2035	21
4C	1360	0
5B	4570	20
PP	3040	0

Table B49
Storm: FB7810

Overtopping Reach	Profile	Wall Height (ft)	Wall Length (ft)	Overtopping Volume (acre-ft)	Overtopping Rate (cfs/ft)
CB	1	23.8	525	0	0.00
CB	1	20.7	1430	0	0.00
CB	1	19.8	400	1	0.07
PD	1	20.9	865	1	0.03
PD	2	20.9	610	0	0.00
PD	2	22.9	570	0	0.00
PD	2	21.3	1515	6	0.07
PD	2	22.5	330	33	0.20
OI	2	22.5	115	11	0.20
OI	2	21.4	935	6	0.08
OI	3	21.4	420	0	0.00
OI	3	24.9	565	0	0.00
OI	3	20.6	1360	0	0.00
OI	3	20.4	870	1	0.01
PA	3	20.4	1090	1	0.01
PA	5	20.4	1480	6	0.07
PA	5	20.3	900	1	0.07
PA	5	21.3	230	0	0.00
PP	6	20.5	870	0	0.00
PP	7	23.0	900	0	0.00
PP	8	23.0	1270	0	0.00

Total Overtopping Volumes		
Tidal Flood Zone	Flood Zone Length (ft)	Overtopping Volumes (acre-ft)
1	2355	1
2A	3890	40
4A	2035	17
4C	1360	0
5B	4570	9
PP	3040	0

Table B50
Storm: FB785

Overtopping Reach	Profile	Wall Height (ft)	Wall Length (ft)	Overtopping Volume (acre-ft)	Overtopping Rate (cfs/ft)
CB	1	23.8	525	0	0.00
CB	1	20.7	1430	0	0.00
CB	1	19.8	400	0	0.02
PD	1	20.9	865	0	0.00
PD	2	20.9	610	0	0.00
PD	2	22.9	570	0	0.00
PD	2	21.3	1515	3	0.04
PD	2	22.5	330	26	0.20
OI	2	22.5	115	9	0.20
OI	2	21.4	935	4	0.05
OI	3	21.4	420	0	0.00
OI	3	24.9	565	0	0.00
OI	3	20.6	1360	0	0.00
OI	3	20.4	870	0	0.01
PA	3	20.4	1090	0	0.01
PA	5	20.4	1480	2	0.07
PA	5	20.3	900	0	0.00
PA	5	21.3	230	0	0.00
PP	6	20.5	870	0	0.00
PP	7	23.0	900	0	0.00
PP	8	23.0	1270	0	0.00

Total Overtopping Volumes		
Tidal Flood Zone	Flood Zone Length (ft)	Overtopping Volumes (acre-ft)
1	2355	0
2A	3890	29
4A	2035	13
4C	1360	0
5B	4570	2
PP	3040	0

Table B51
Storm: FB782

Overtopping Reach	Profile	Wall Height (ft)	Wall Length (ft)	Overtopping Volume (acre-ft)	Overtopping Rate (cfs/ft)
CB	1	23.8	525	0	0.00
CB	1	20.7	1430	0	0.00
CB	1	19.8	400	0	0.00
PD	1	20.9	865	0	0.00
PD	2	20.9	610	0	0.00
PD	2	22.9	570	0	0.00
PD	2	21.3	1515	0	0.00
PD	2	22.5	330	19	0.20
OI	2	22.5	115	7	0.20
OI	2	21.4	935	3	0.02
OI	3	21.4	420	0	0.00
OI	3	24.9	565	0	0.00
OI	3	20.6	1360	0	0.00
OI	3	20.4	870	0	0.00
PA	3	20.4	1090	0	0.00
PA	5	20.4	1480	0	0.00
PA	5	20.3	900	0	0.00
PA	5	21.3	230	0	0.00
PP	6	20.5	870	0	0.00
PP	7	23.0	900	0	0.00
PP	8	23.0	1270	0	0.00

Total Overtopping Volumes		
Tidal Flood Zone	Flood Zone Length (ft)	Overtopping Volumes (acre-ft)
1	2355	0
2A	3890	19
4A	2035	10
4C	1360	0
5B	4570	0
PP	3040	0

Appendix C

Revetment/Dune Overtopping Options

Appendix C contains overtopping calculations obtained for the set of 50 storms as applied to Profile 6 alternative design options. Information contained herein pertains only to Profile 6, and can be compared with overtopping volumes contained in Appendix B for Profile 6 to assess effectiveness of different design options. Results for two cases are presented herein: (a) Profile 6 dune design (23-ft dune crest) as optimized in the dune optimization section of this report, and (b) Profile 6 revetment design as proposed without beach fill. Tables C1 and C2 contain overtopping volumes for only Profile 6, and these quantities can replace the values given for Profile 6 in Appendix B to obtain total project site overtopping volumes for different design options. These extremes allow the evaluation of Profile 6 with the revetment design without beach fill representing a "worst-case" condition for the revetment, and the dune results allowing for comparative study of design options.

Table C1
Dune Overtopping (23-ft Dune Crest)

Storm	Total Overtopping (acre-ft)	Storm	Total Overtopping (acre-ft)
NV45SPN	0	AP6110	0
NV45500	0	DC6250	0
NV45100	0	DC6220	0
NV4550	0	DC6210	0
NV4520	0	DC625	0
NV4510	0	DC622	0
FB5850	0	FB645	0
FB5820	0	FB642	0
FB5810	0	FB6920	0
FB585	0	FB6910	0
FB582	0	FB695	0
MR5850	0	FB7250	0
MR5820	0	FB7220	0
MR5810	0	FB7210	0
MR585	0	NV7250	0
MR582	0	NV7220	0
JN61100	0	NV7210	0
JN6150	0	NV725	0
JN6120	0	NV722	0
JN6110	0	FB78100	0
JN615	0	FB7850	0
JN612	0	FB7820	0
AP61100	0	FB7810	0
AP6150	0	FB785	0
AP6120	0	FB782	0

Table C2
Revetment Overtopping (without beach fill)

Storm	Total Overtopping (acre-ft)	Storm	Total Overtopping (acre-ft)
NV45SPN	7341	AP6110	0
NV45500	3301	DC6250	197
NV45100	1613	DC6220	99
NV4550	1251	DC6210	53
NV4520	379	DC625	20
NV4510	343	DC622	3
FB5850	36	FB645	0
FB5820	16	FB642	0
FB5810	3	FB6920	26
FB585	1	FB6910	4
FB582	0	FB695	7
MR5850	3	FB7250	141
MR5820	29	FB7220	73
MR5810	5	FB7210	45
MR585	5	NV7250	0
MR582	2	NV7220	0
JN61100	0	NV7210	0
JN6150	0	NV725	0
JN6120	0	NV722	0
JN6110	0	FB78100	187
JN615	0	FB7850	92
JN612	0	FB7820	42
AP61100	0	FB7810	15
AP6150	0	FB785	8
AP6120	0	FB782	7

Appendix D

Alternative Overtopping Simulations

Overtopping quantities contained in this appendix refer to alternative overtopping simulations discussed previously. Combinations of storm and profile data sets have been implemented along with the runup and overtopping model to acquire further information about Revere Beach and Point of Pines flood mitigation capabilities. The following data sets are summarized herein: (a) Halloween profile and storm data, (b) Great Blizzard and 1978 profile information, and (c) Halloween storm data and 27 November 1991 profile data.

Table D1
Storm: Halloween
Profile Data: 30 October 1991

Overtopping Reach	Profile	Wall Height (ft)	Wall Length (ft)	Overtopping Volume (acre-ft)	Overtopping Rate (cfs/ft)
PD	2	20.9	610	0	0.00
PD	2	22.9	570	0	0.00
PD	2	21.3	1515	0	0.00
PD	2	22.5	330	0	0.00
OI	2	22.5	115	0	0.00
OI	2	21.4	935	0	0.00
PA	5	20.4	1480	7	0.06
PA	5	20.3	900	6	0.07
PA	5	21.3	230	0	0.00
PP	7	21.2	900	0	0.00

Total Overtopping Volumes		
Tidal Flood Zone	Flood Zone Length (ft)	Overtopping Volumes (acre-ft)
2A	3890	0
4A	2035	0
5B	4570	13
PP	3040	0

Table D2				"Relaxed" ROTM	
Storm: Halloween					
Profile Data: 30 October 1991					
Overtopping Reach	Profile	Wall Height (ft)	Wall Length (ft)	Overtopping Volume (acre-ft)	Overtopping Rate (cfs/ft)
PD	2	20.9	610	99	0.23
PD	2	22.9	570	0	0.00
PD	2	21.3	1515	185	0.21
PD	2	22.5	330	0	0.00
OI	2	22.5	115	0	0.00
OI	2	21.4	935	104	0.20
PA	5	20.4	1480	54	0.16
PA	5	20.3	900	33	0.16
PA	5	21.3	230	4	0.15
PP	7	21.2	900	0	0.00

Total Overtopping Volumes		
Tidal Flood Zone	Flood Zone Length (ft)	Overtopping Volumes (acre-ft)
2A	3890	284
4A	2035	104
5B	4570	91
PP	3040	0

Table D3
Storm: Great Blizzard
Profile Data: 1978

Overtopping Reach	Profile	Wall Height (ft)	Wall Length (ft)	Overtopping Volume (acre-ft)	Overtopping Rate (cfs/ft)
CB	1	23.8	525	0	0.00
CB	1	20.7	1430	0	0.00
CB	1	19.8	400	0	0.00
PD	1	20.9	865	0	0.00
PD	2	20.9	610	251	3.03
PD	2	22.9	570	77	0.93
PD	2	21.3	1515	516	2.49
PD	2	22.5	330	57	1.23
OI	2	22.5	115	20	1.23
OI	2	21.4	935	300	2.36
OI	3	21.4	420	53	0.66
OI	3	24.9	565	7	0.15
OI	3	20.6	1360	234	0.85
OI	3	20.4	870	161	0.91
PA	3	20.4	1090	202	0.91
PA	5	20.4	1480	78	0.73
PA	5	20.3	900	49	0.76
PA	5	21.3	230	9	0.52
PP	6	20.7	870	114	0.69

Total Overtopping Volumes		
Tidal Flood Zone	Flood Zone Length (ft)	Overtopping Volumes (acre-ft)
1	2355	0
2A	3890	901
4A	2035	380
4C	1360	234
5B	4570	499
PP	3040	114

Table D4 Storm: Great Blizzard Profile Data: 1978				"Relaxed" ROTM	
Overtopping Reach	Profile	Wall Height (ft)	Wall Length (ft)	Overtopping Volume (acre-ft)	Overtopping Rate (cfs/ft)
CB	1	23.8	525	0	0.00
CB	1	20.7	1430	0	0.00
CB	1	19.8	400	0	0.00
PD	1	20.9	865	0	0.00
PD	2	20.9	610	253	3.03
PD	2	22.9	570	77	0.93
PD	2	21.3	1515	516	2.49
PD	2	22.5	330	57	1.23
OI	2	22.5	115	20	1.23
OI	2	21.4	935	302	2.36
OI	3	21.4	420	53	0.66
OI	3	24.9	565	7	0.15
OI	3	20.6	1360	234	0.85
OI	3	20.4	870	161	0.91
PA	3	20.4	1090	202	0.91
PA	5	20.4	1480	78	0.73
PA	5	20.3	900	49	0.76
PA	5	21.3	230	9	0.52
PP	6	20.7	870	114	0.69

Total Overtopping Volumes		
Tidal Flood Zone	Flood Zone Length (ft)	Overtopping Volumes (acre-ft)
1	2355	0
2A	3890	903
4A	2035	382
4C	1360	234
5B	4570	499
PP	3040	114

Table D5
Storm: Halloween
Profile Data: 27 November 1991

Overtopping Reach	Profile	Wall Height (ft)	Wall Length (ft)	Overtopping Volume (acre-ft)	Overtopping Rate (cfs/ft)
CB	1	23.8	525	0	0.04
CB	1	20.7	1430	0	0.00
CB	1	19.8	400	0	0.03
PD	1	20.9	865	0	0.00
PD	2	20.9	610	0	0.00
PD	2	22.9	570	0	0.00
PD	2	21.3	1515	9	0.08
PD	2	22.5	330	10	0.20
OI	2	22.5	115	4	0.20
OI	2	21.4	935	8	0.09
OI	3	21.4	420	0	0.00
OI	3	24.9	565	0	0.00
OI	3	20.6	1360	0	0.00
OI	3	20.4	870	1	0.01
PA	3	20.4	1090	1	0.01
PA	5	20.4	1480	9	0.07
PA	5	20.3	900	0	0.00
PA	5	21.3	230	0	0.00
PP	6	20.7	870	191	1.76
PP	7	20.8	900	0	0.00
PP	8	20.0	1270	0	0.00

Total Overtopping Volumes		
Tidal Flood Zone	Flood Zone Length (ft)	Overtopping Volumes (acre-ft)
1	2355	0
2A	3890	19
4A	2035	12
4C	1360	0
5B	4570	11
PP	3040	191

Table D6
Worst-Case Simulation (Pre-Physical Model Study of Worst-Case)
(1978 Profile and November 1945 SPN)

Overtopping Reach	Profile	Wall Height (ft)	Wall Length (ft)	Overtopping Volume (acre-ft)	Overtopping Rate (cfs/ft)
CB	1	23.8	525	68	1.04
CB	1	20.7	1430	415	2.31
CB	1	19.8	400	148	2.97
PD	1	20.9	865	238	2.19
PD	2	20.9	610	4025	107.85
PD	2	22.9	570	2548	94.97
PD	2	21.3	1515	9254	105.19
PD	2	22.5	330	1595	97.47
OI	2	22.5	115	556	97.47
OI	2	21.4	935	5602	104.54
OI	3	21.4	420	237	1.67
OI	3	24.9	565	87	0.58
OI	3	20.6	1360	977	2.09
OI	3	20.4	870	664	2.22
PA	3	20.4	1090	831	2.22
PA	5	20.4	1480	1672	8.781
PA	5	20.3	900	1056	8.97
PA	5	21.3	230	180	6.54
PP	6	20.7	870	172796	517.57

Note: These numbers are questionable due to failure to meet ranges established by the physical model study.

Total Overtopping Volumes		
Tidal Flood Zone	Flood Zone Length (ft)	Overtopping Volumes (acre-ft)
1	2355	628
2A	3890	17660
4A	2035	6482
4C	1360	977
5B	4570	4403
PP	3040	172796

Table D7
Worst-Case Simulation (Post-Physical Model Study of Worst-Case)
(1978 Profile and November 1945 SPN)

Overtopping Reach	Profile	Wall Height (ft)	Wall Length (ft)	Overtopping Volume (acre-ft)	Overtopping Rate (cfs/ft)
CB	1	23.8	525	132	0.23
CB*	1	20.7	1430	416	0.27
CB	1	19.8	400	123	0.28
PD*	1	20.9	865	249	0.26
PD*	2	20.9	610	771	0.56
PD	2	22.9	570	1424	1.86
PD*	2	21.3	1515	2382	0.94
PD	2	22.5	330	756	1.75
OI	2	22.5	115	263	1.75
OI*	2	21.4	935	1536	1.06
OI*	3	21.4	420	109	0.24
OI	3	24.9	565	88	0.25
OI*	3	20.6	1360	352	0.25
OI*	3	20.4	870	225	0.25
PA*	3	20.4	1090	282	0.25
PA*	5	20.4	1480	342	0.23
PA*	5	20.3	900	209	0.23
PA*	5	21.3	230	52	0.22
PP*	6	20.7	870	288	0.27

* Overtopping condition reasonably well modeled in physical study of worst-case overtopping conditions.

Total Overtopping Volumes		
Tidal Flood Zone	Flood Zone Length (ft)	Overtopping Volumes (acre-ft)
1	2355	671
2A	3890	5582
4A	2035	1996
4C	1360	352
5B	4570	1110
PP	3040	288

Appendix E

Overtopping Volumes at Peak Storm Conditions

This appendix contains detailed information about overtopping volumes predicted to occur over a single peak water condition. Specifically the tidal flood zones as given in Table 9 are presented for each storm and total overtopping volumes are listed that occur continuously over the maximum tidal/surge time span. Volumes are cumulative over the time period and include all reaches contributing to the given flood zone.

Table E1
Overtopping Volumes Over Peak Storm Condition (Peak Tidal Cycle)
Tidal Flood Zone 1

Storm	Peak Tidal Cycle Overtopping Volume (acre-ft)	Storm	Peak Tidal Cycle Overtopping Volume (acre-ft)
NV45SPN	120	AP6110	3
NV45500	73	DC6250	12
NV45100	32	DC6220	6
NV4550	18	DC6210	1
NV4520	7	DC625	0
NV4510	2	DC622	0
FB5850	14	FB645	0
FB5820	5	FB642	0
FB5810	1	FB6920	5
FB585	0	FB6910	1
FB582	0	FB695	0
MR5850	17	FB7250	14
MR5820	6	FB7220	6
MR5810	1	FB7210	2
MR585	0	NV7250	17
MR582	0	NV7220	6
JN61100	24	NV7210	1
JN6150	14	NV725	0
JN6120	12	NV722	0
JN6110	2	FB78100	35
JN615	0	FB7850	10
JN612	0	FB7820	4
AP61100	24	FB7810	1
AP6150	15	FB785	0
AP6120	6	FB782	0

Table E2
Overtopping Volumes Over Peak Storm Condition (Peak Tidal Cycle)
Tidal Flood Zone 2A

Storm	Peak Tidal Cycle Overtopping Volume (acre-ft)	Storm	Peak Tidal Cycle Overtopping Volume (acre-ft)
NV45SPN	202	AP6110	18
NV45500	130	DC6250	35
NV45100	78	DC6220	27
NV4550	51	DC6210	15
NV4520	38	DC625	10
NV4510	19	DC622	8
FB5850	43	FB645	8
FB5820	21	FB642	8
FB5810	11	FB6920	27
FB585	5	FB6910	16
FB582	3	FB695	8
MR5850	42	FB7250	45
MR5820	25	FB7220	26
MR5810	11	FB7210	20
MR585	11	NV7250	49
MR582	4	NV7220	31
JN61100	53	NV7210	16
JN6150	42	NV725	13
JN6120	35	NV722	11
JN6110	18	FB78100	73
JN615	10	FB7850	38
JN612	2	FB7820	28
AP61100	57	FB7810	18
AP6150	47	FB785	11
AP6120	29	FB782	4

Table E3
Overtopping Volumes Over Peak Storm Condition (Peak Tidal Cycle)
Tidal Flood Zone 4A

Storm	Total Overtopping (acre-ft)	Storm	Total Overtopping (acre-ft)
NV45SPN	42	AP6110	11
NV45500	47	DC6250	17
NV45100	33	DC6220	14
NV4550	24	DC6210	9
NV4520	20	DC625	7
NV4510	12	DC622	4
FB5850	19	FB645	5
FB5820	12	FB642	4
FB5810	8	FB6920	14
FB585	5	FB6910	9
FB582	2	FB695	6
MR5850	19	FB7250	21
MR5820	14	FB7220	14
MR5810	8	FB7210	11
MR585	7	NV7250	22
MR582	3	NV7220	16
JN61100	23	NV7210	10
JN6150	19	NV725	7
JN6120	18	NV722	5
JN6110	10	FB78100	30
JN615	6	FB7850	19
JN612	2	FB7820	15
AP61100	24	FB7810	10
AP6150	20	FB785	7
AP6120	14	FB782	4

Table E4
Overtopping Volumes Over Peak Storm Condition (Peak Tidal Cycle)
Tidal Flood Zone 4C

Storm	Total Overtopping (acre-ft)	Storm	Total Overtopping (acre-ft)
NV45SPN	0	AP6110	0
NV45500	0	DC6250	0
NV45100	0	DC6220	0
NV4550	0	DC6210	0
NV4520	0	DC625	0
NV4510	0	DC622	0
FB5850	0	FB645	0
FB5820	0	FB642	0
FB5810	0	FB6920	0
FB585	0	FB6910	0
FB582	0	FB695	0
MR5850	0	FB7250	0
MR5820	0	FB7220	0
MR5810	0	FB7210	0
MR585	0	NV7250	0
MR582	0	NV7220	0
JN61100	0	NV7210	0
JN6150	0	NV725	0
JN6120	0	NV722	0
JN6110	0	FB78100	0
JN615	0	FB7850	0
JN612	0	FB7820	0
AP61100	0	FB7810	0
AP6150	0	FB785	0
AP6120	0	FB782	0

Table E5
Overtopping Volumes Over Peak Storm Condition (Peak Tidal Cycle)
Tidal Flood Zone 5B

Storm	Total Overtopping (acre-ft)	Storm	Total Overtopping (acre-ft)
NV45SPN	111	AP6110	22
NV45500	86	DC6250	30
NV45100	55	DC6220	22
NV4550	42	DC6210	10
NV4520	31	DC625	1
NV4510	16	DC622	0
FB5850	31	FB645	1
FB5820	22	FB642	0
FB5810	11	FB6920	21
FB585	2	FB6910	9
FB582	0	FB695	3
MR5850	35	FB7250	35
MR5820	23	FB7220	24
MR5810	10	FB7210	10
MR585	3	NV7250	35
MR582	0	NV7220	24
JN61100	41	NV7210	10
JN6150	33	NV725	2
JN6120	31	NV722	0
JN6110	16	FB78100	80
JN615	2	FB7850	27
JN612	0	FB7820	20
AP61100	42	FB7810	8
AP6150	34	FB785	2
AP6120	22	FB782	0

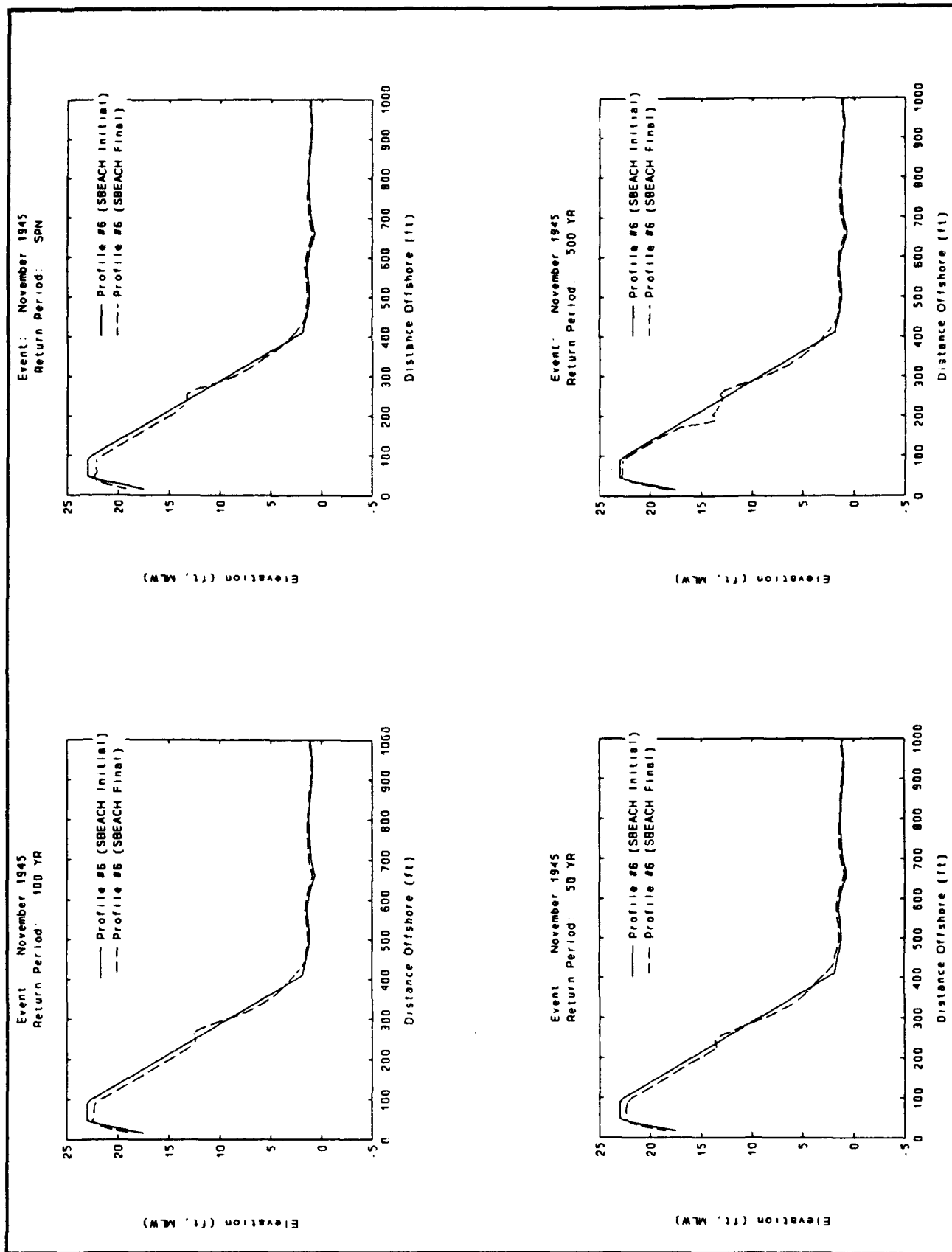
Table E6
Overtopping Volumes Over Peak Storm Condition (Peak Tidal Cycle)
Tidal Flood Zone PP

Storm	Total Overtopping (acre-ft)	Storm	Total Overtopping (acre-ft)
NV45SPN	1685	AP6110	0
NV45500	502	DC6250	0
NV45100	158	DC6220	0
NV4550	47	DC6210	0
NV4520	30	DC625	0
NV4510	10	DC622	0
FB5850	0	FB645	0
FB5820	0	FB642	0
FB5810	0	FB6920	0
FB585	0	FB6910	0
FB582	0	FB695	0
MR5850	0	FB7250	1
MR5820	0	FB7220	0
MR5810	0	FB7210	0
MR585	0	NV7250	0
MR582	0	NV7220	0
JN61100	0	NV7210	0
JN6150	0	NV725	0
JN6120	0	NV722	0
JN6110	0	FB78100	4
JN615	0	FB7850	1
JN612	0	FB7820	0
AP61100	0	FB7810	0
AP6150	0	FB785	0
AP6120	0	FB782	0

Appendix F

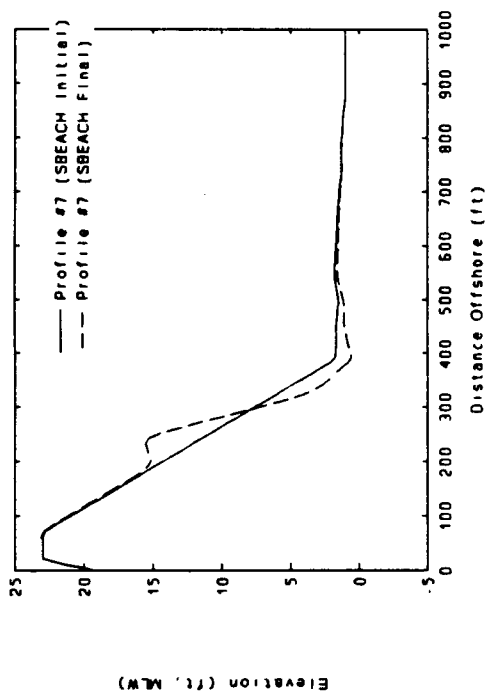
Profile Response Simulations

Appendix F contains profile response as predicted by SBEACH. Calibration parameters correspond to the calibration conducted, with Profile 7 considered separately. Profiles 6-8 were used in the simulations with the set of 50 storms to obtain further information about dune system capabilities. Calibration to Profile 7 was completed successfully; however, due to an inability to verify SBEACH to more than one profile it is suggested that results herein be considered qualitative.

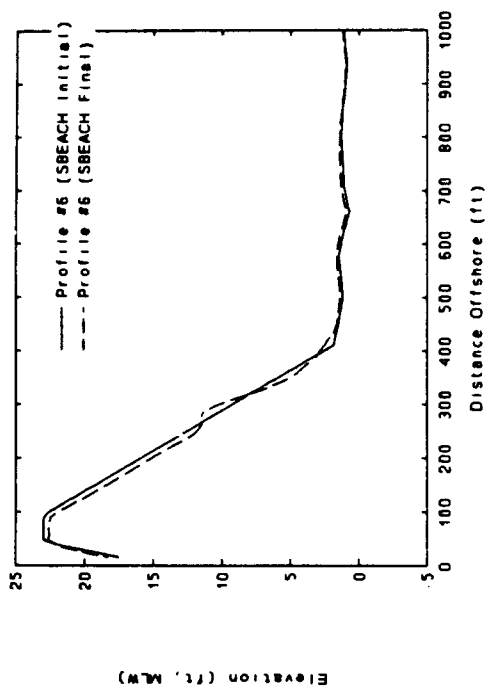


Appendix F Profile Response Simulations

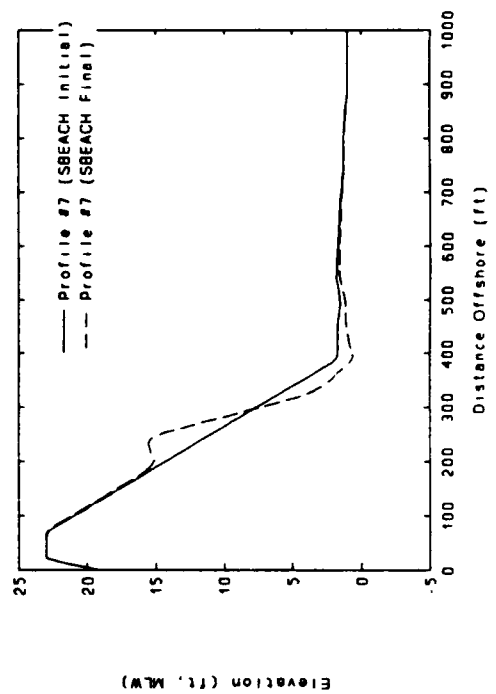
Event: November 1945
Return Period: SPN



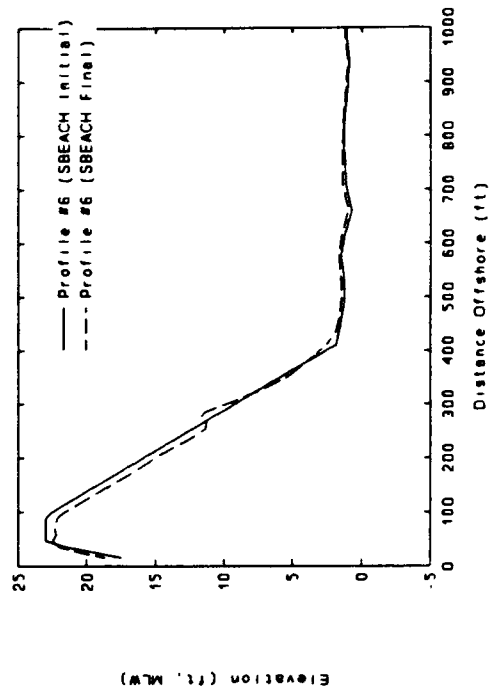
Event: November 1945
Return Period: 20 YR

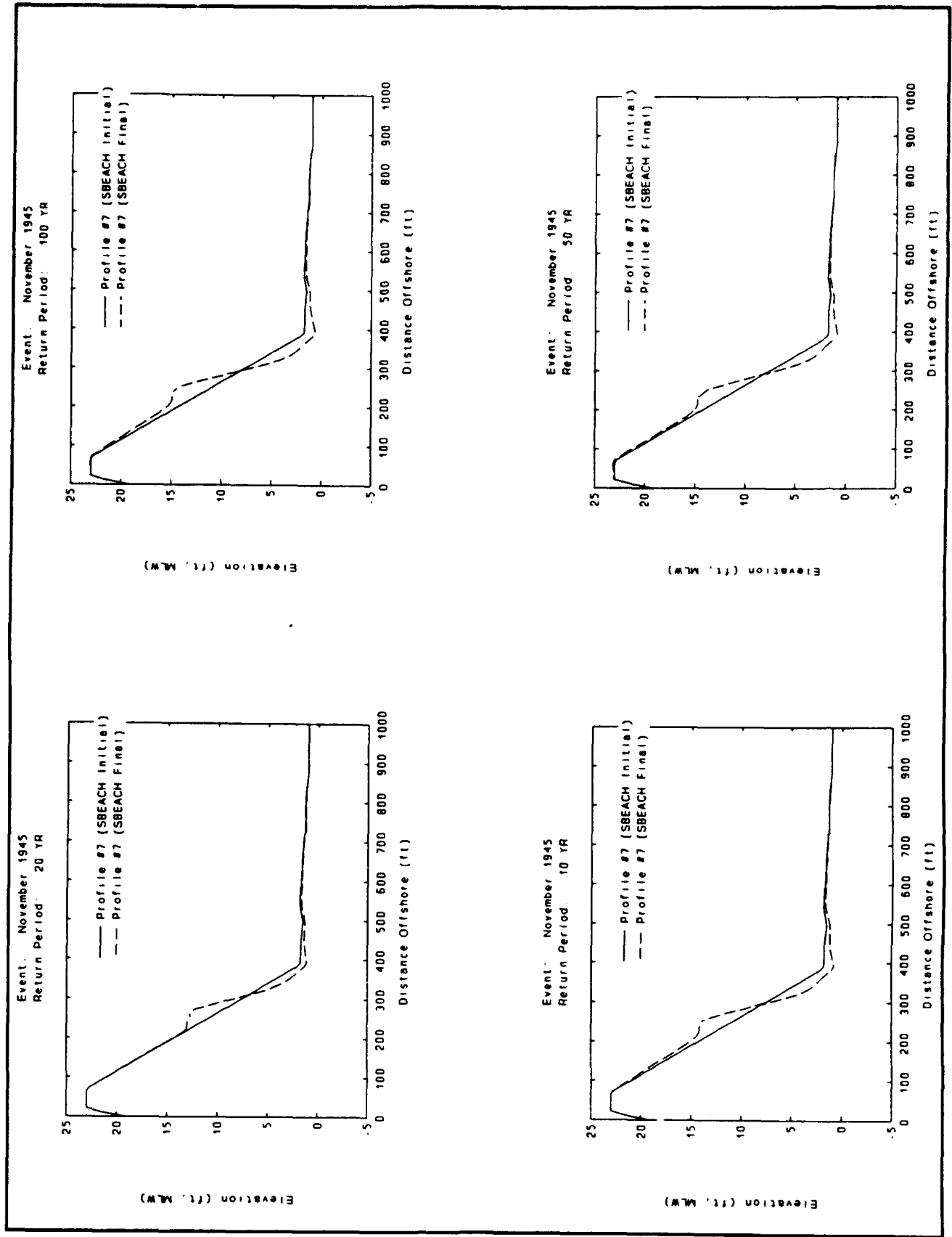


Event: November 1945
Return Period: 500 YR

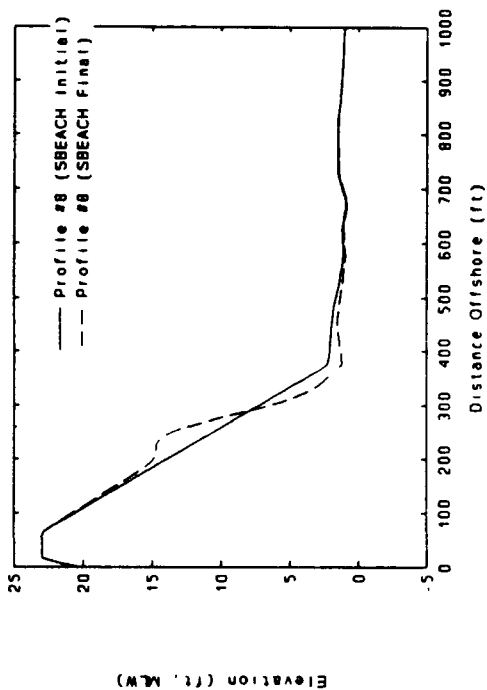


Event: November 1945
Return Period: 10 YR

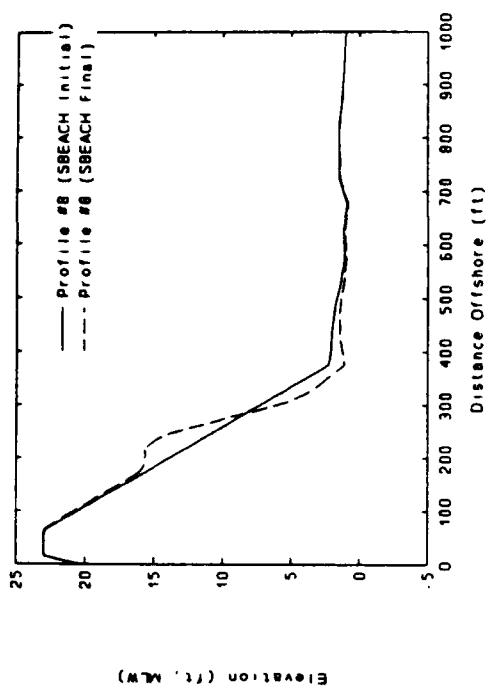




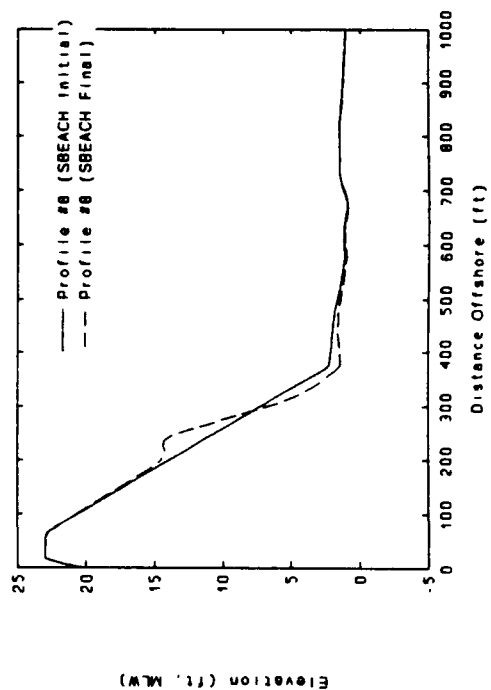
Event: November 1945
Return Period: 100 YR



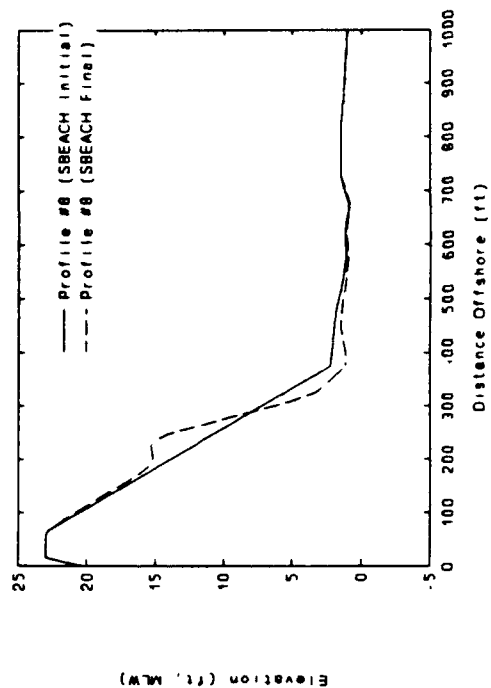
Event: November 1945
Return Period: SPN

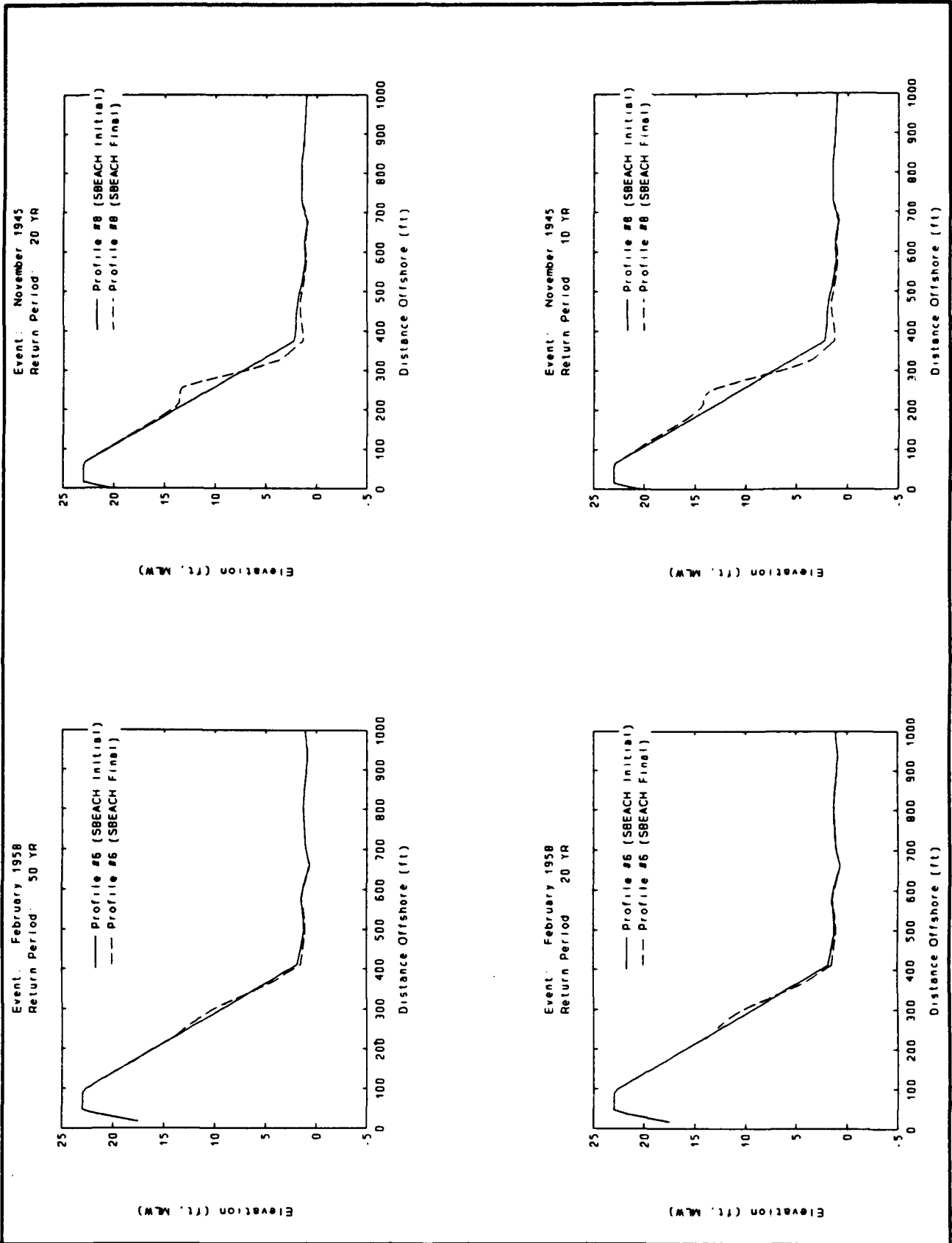


Event: November 1945
Return Period: 50 YR

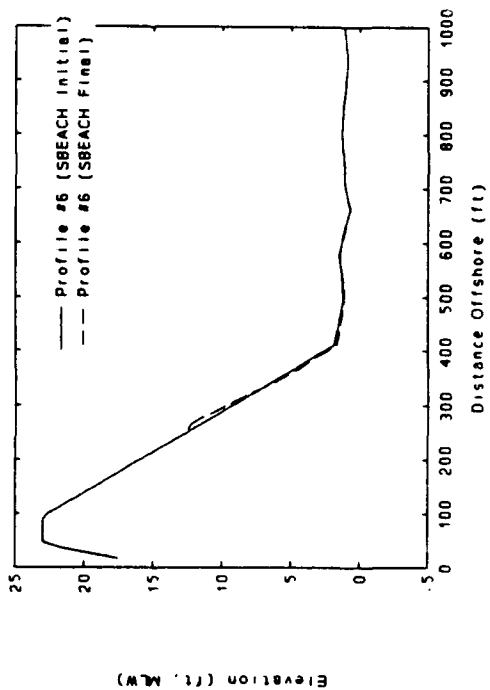


Event: November 1945
Return Period: 500 YR

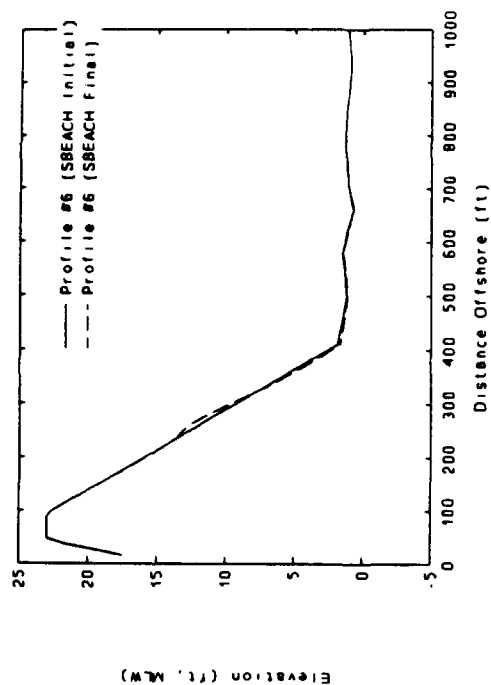




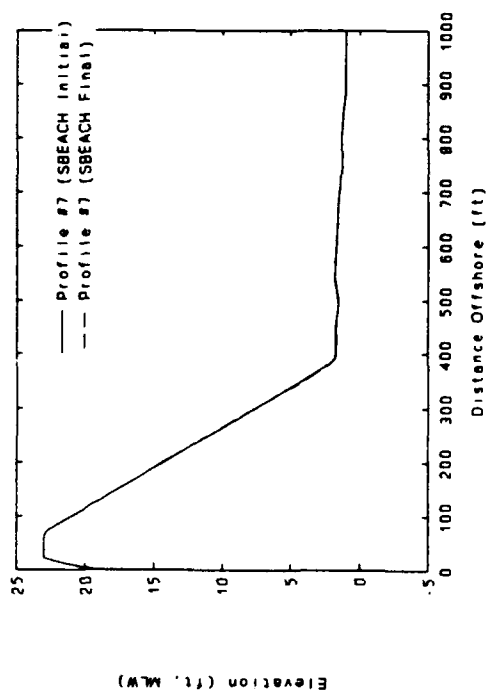
Event: February 1958
Return Period: 2 YR



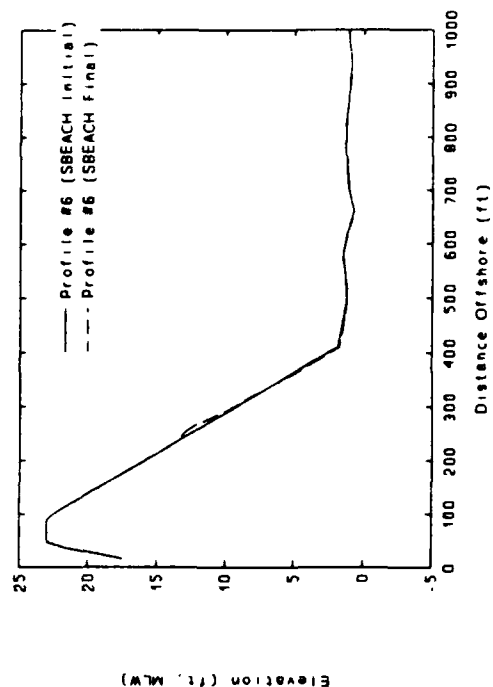
Event: February 1958
Return Period: 10 YR

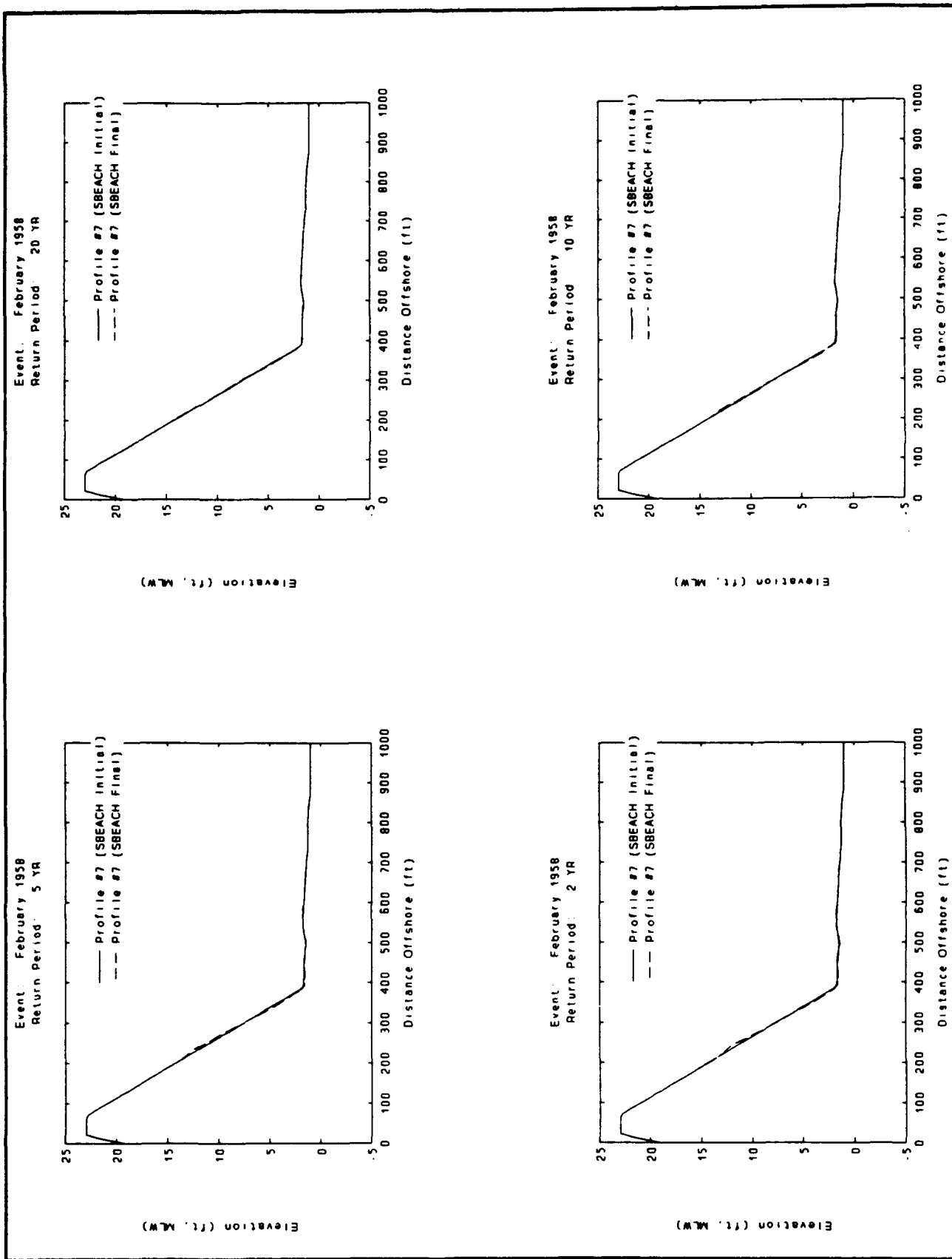


Event: February 1958
Return Period: 50 YR

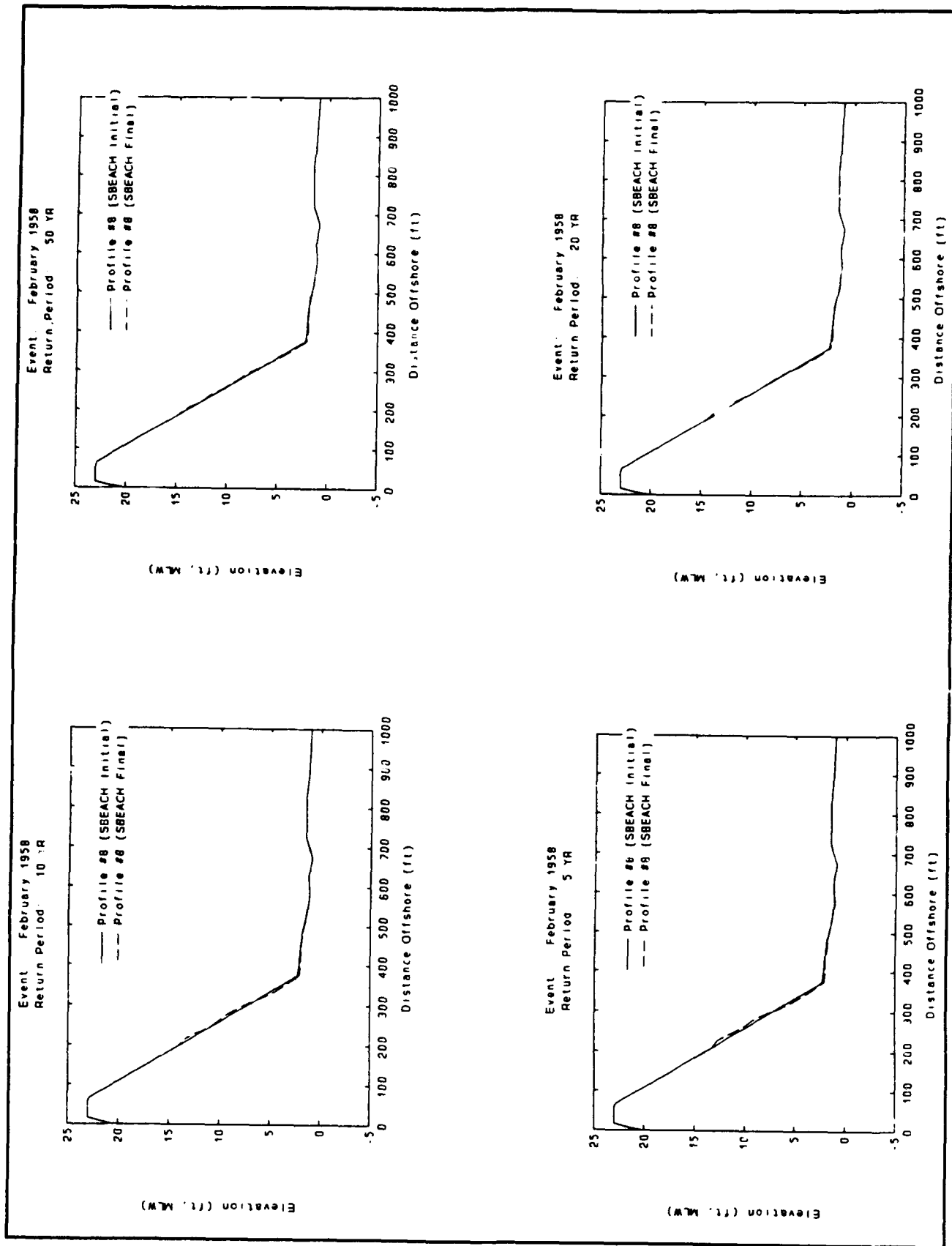


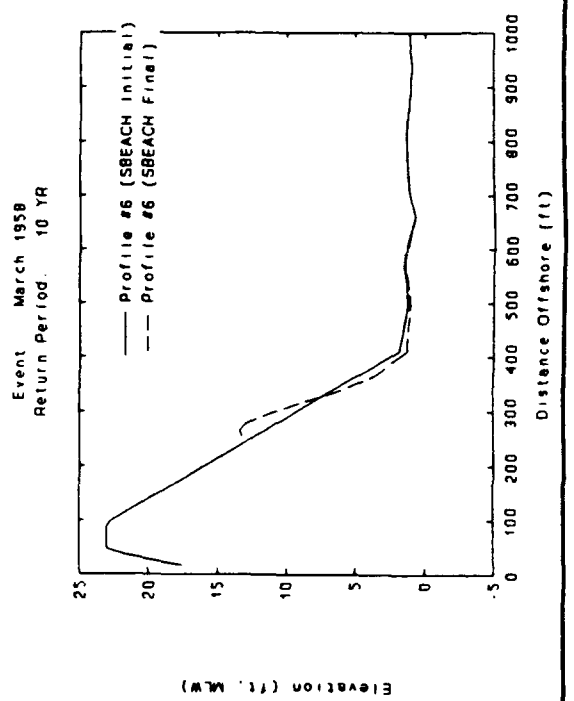
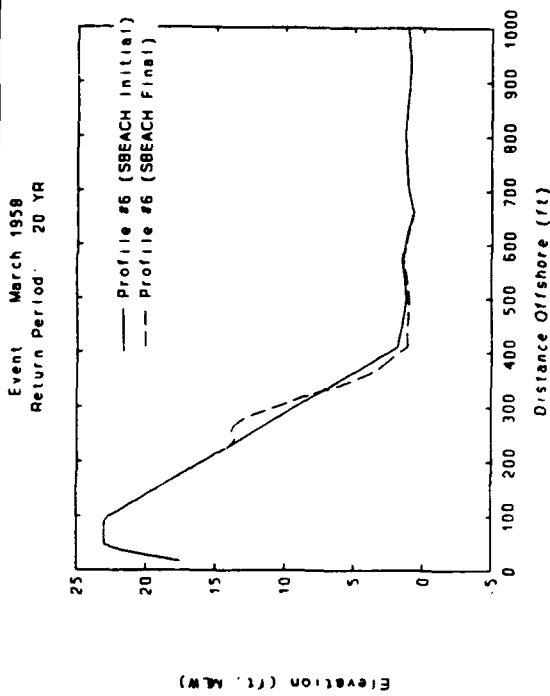
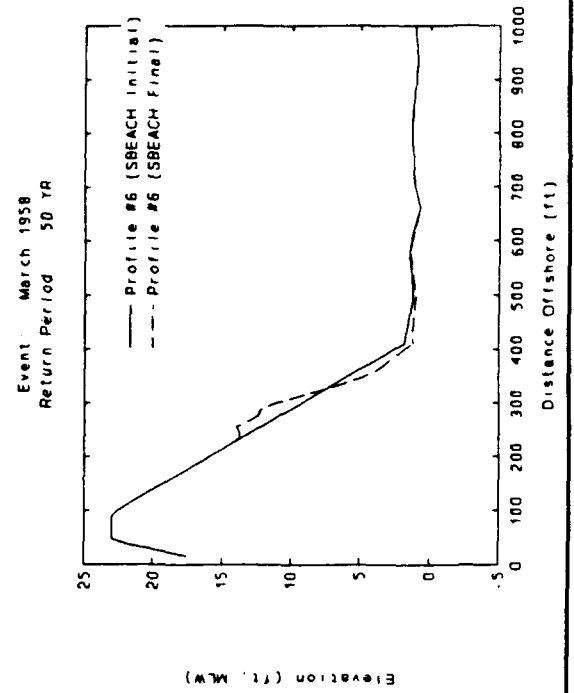
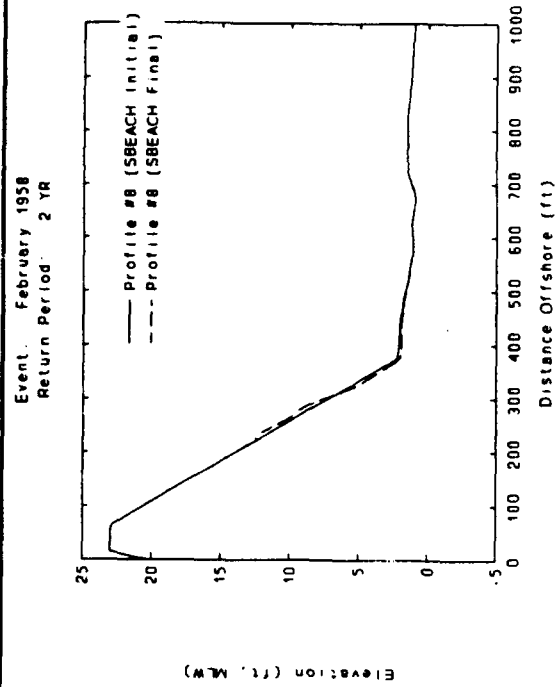
Event: February 1958
Return Period: 5 YR



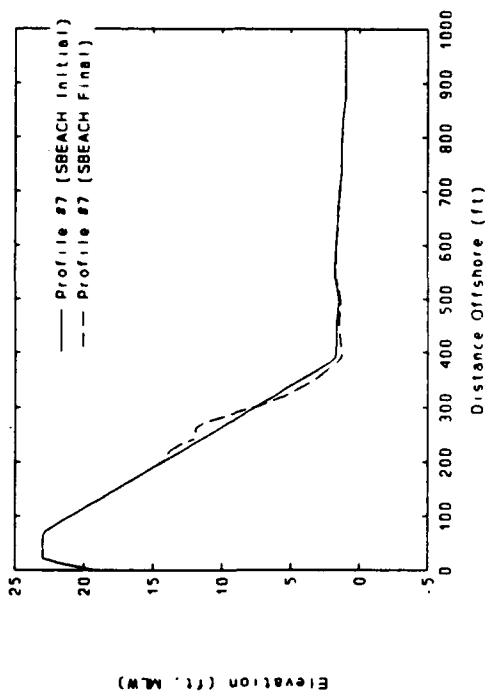


Appendix F Profile Response Simulations

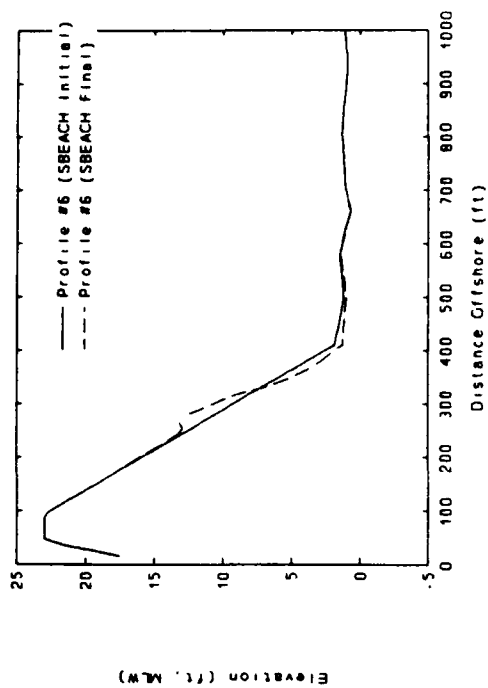




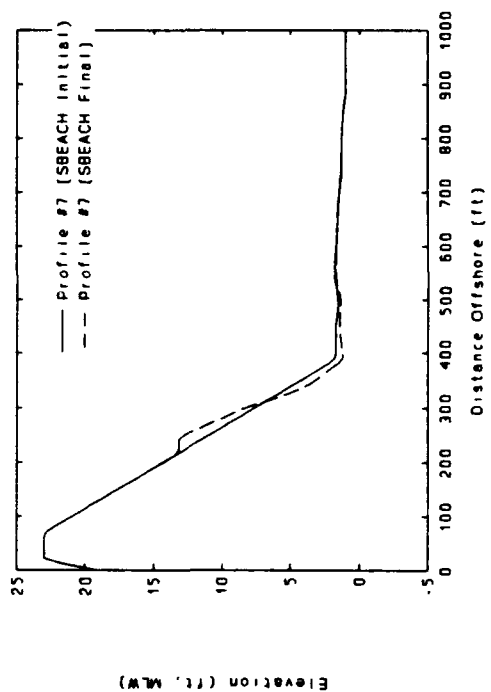
Event: March 1958
Return Period: 50 YR



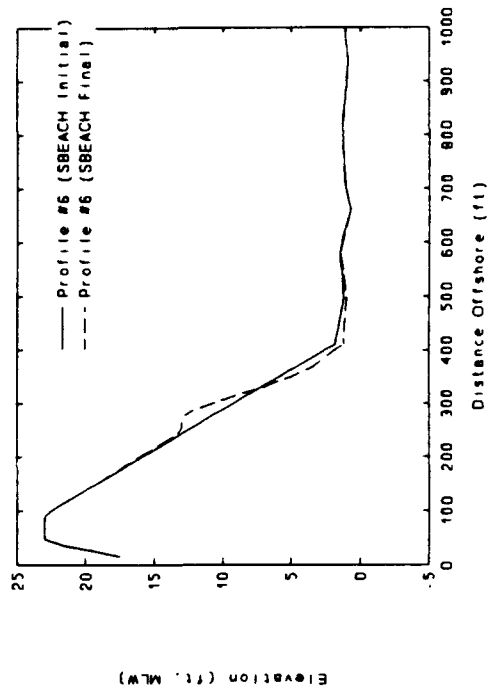
Event: March 1958
Return Period: 5 YR

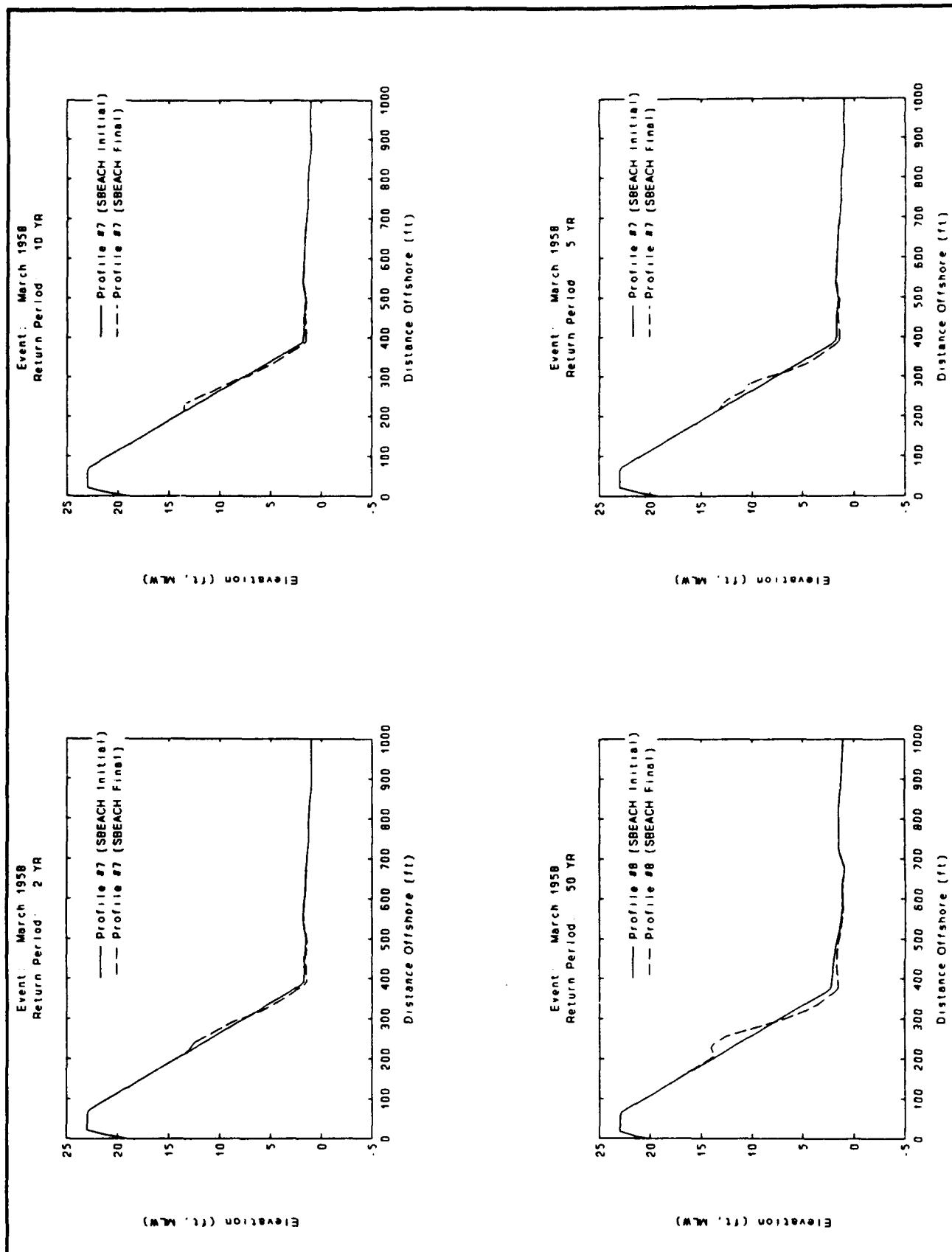


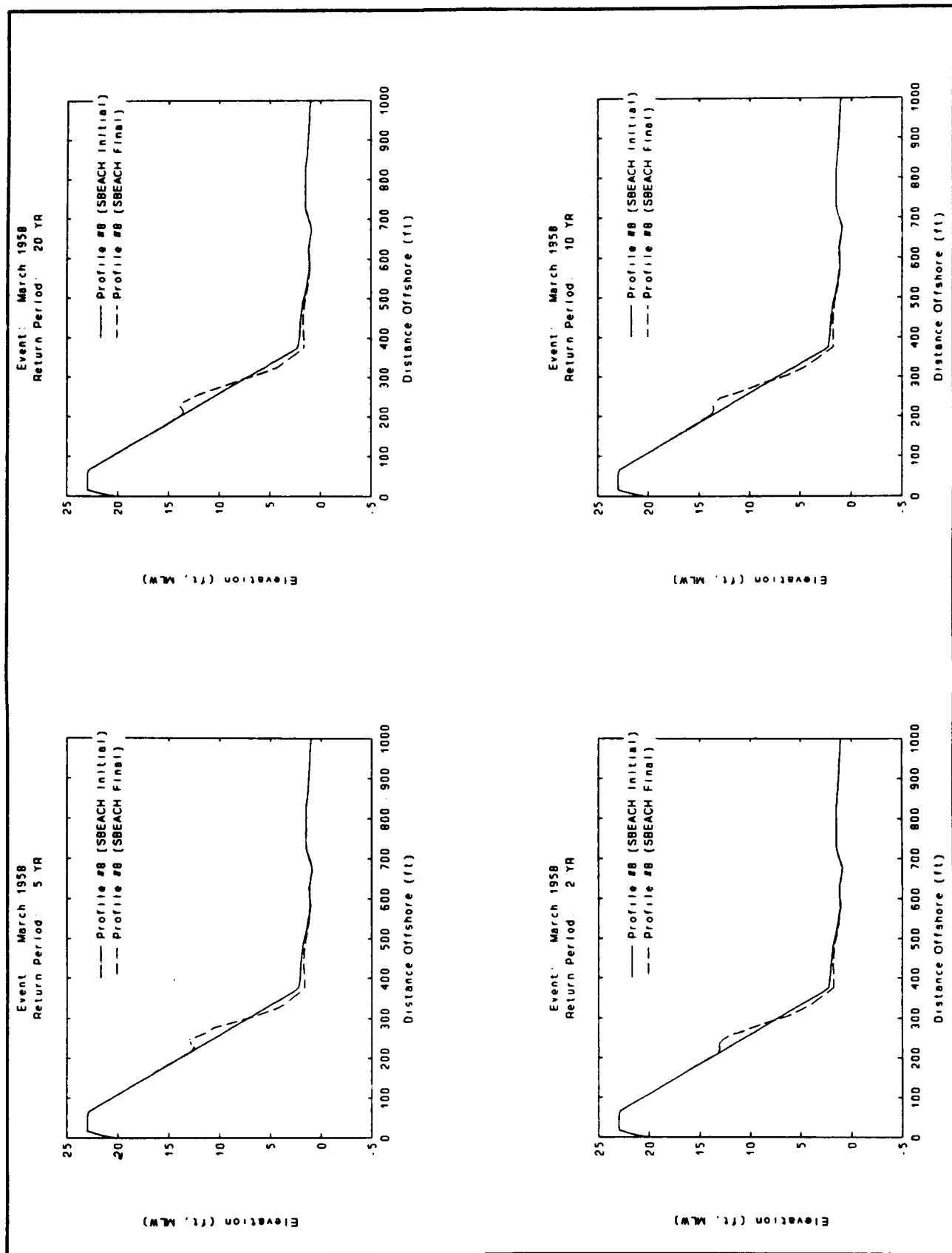
Event: March 1958
Return Period: 20 YR

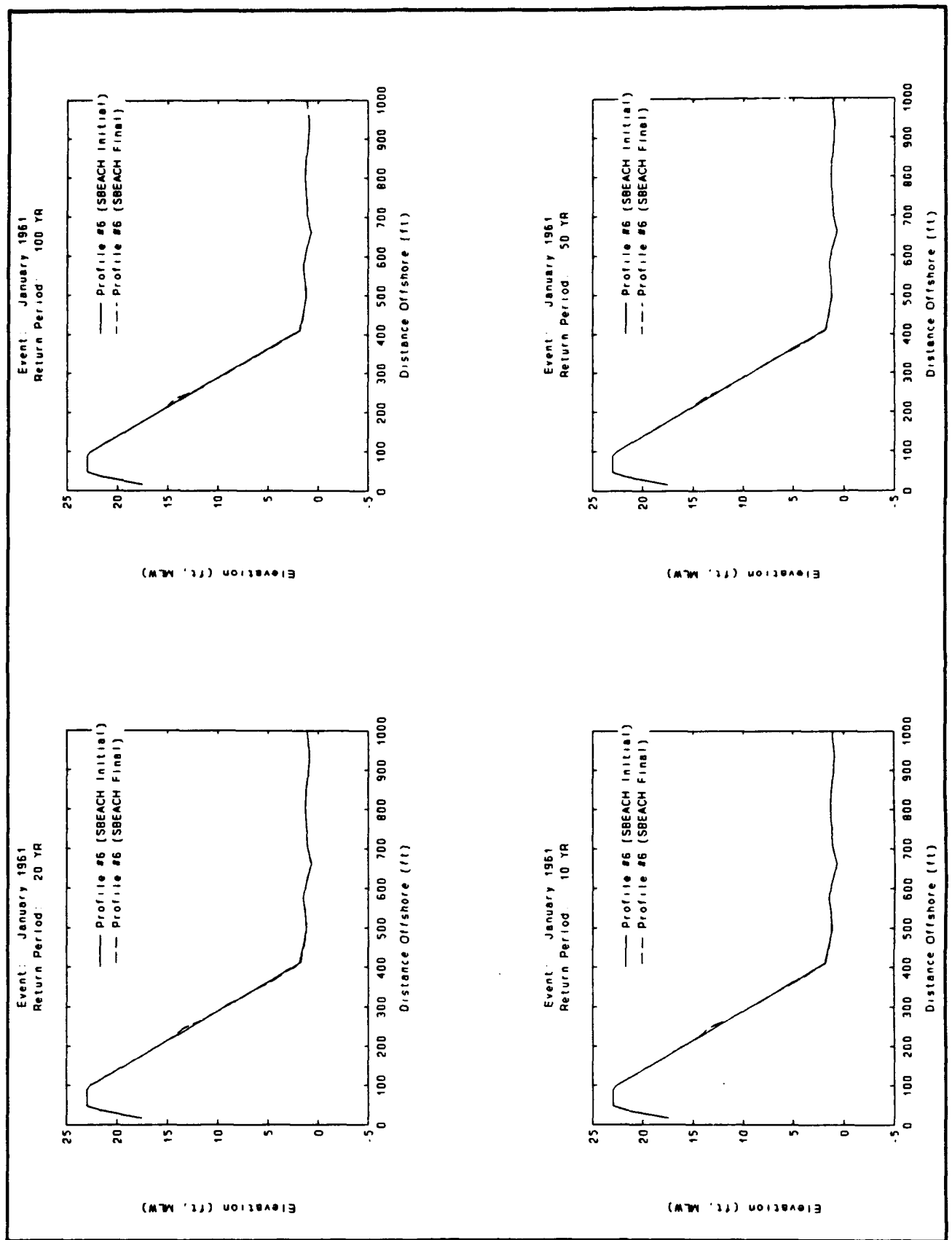


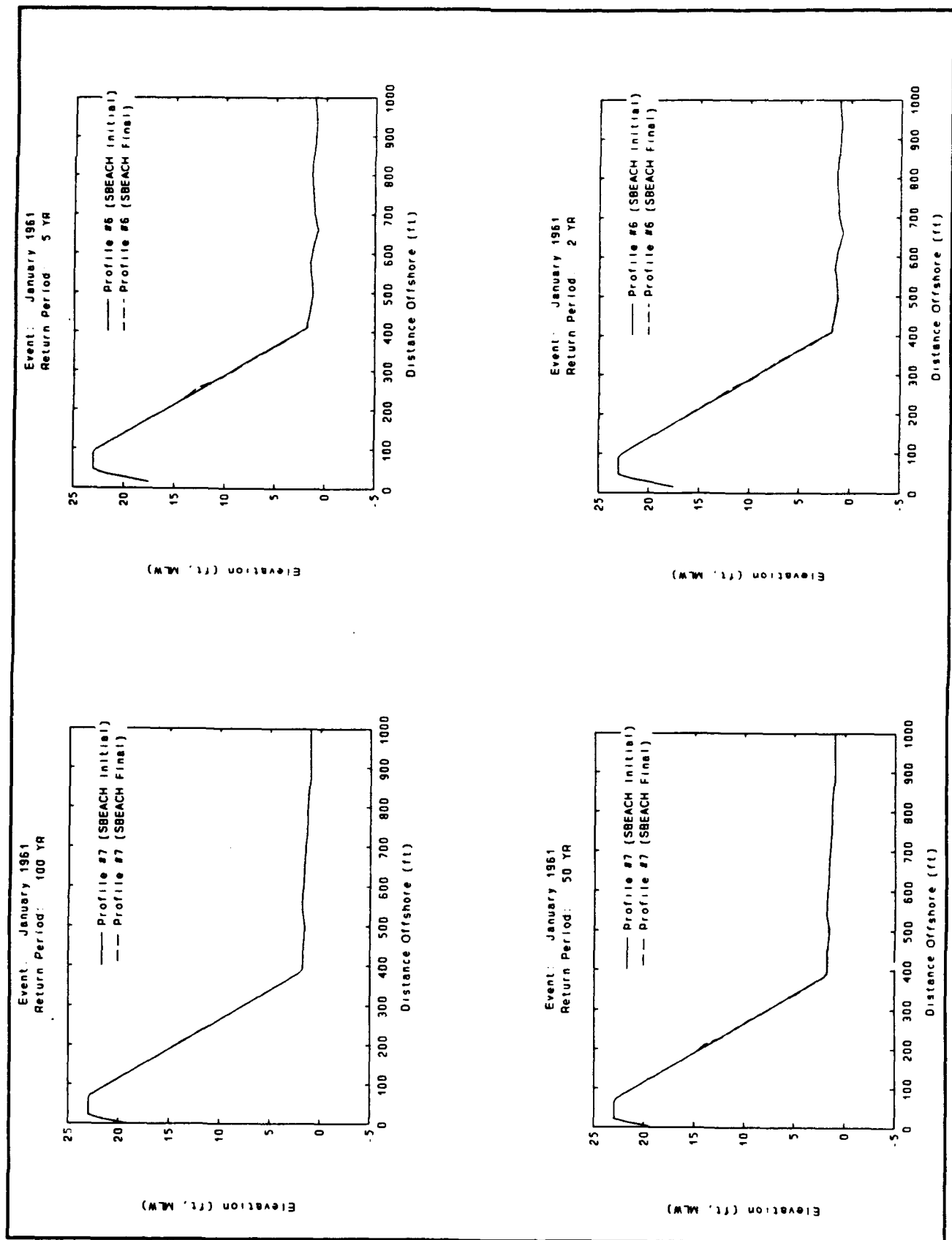
Event: March 1958
Return Period: 2 YR

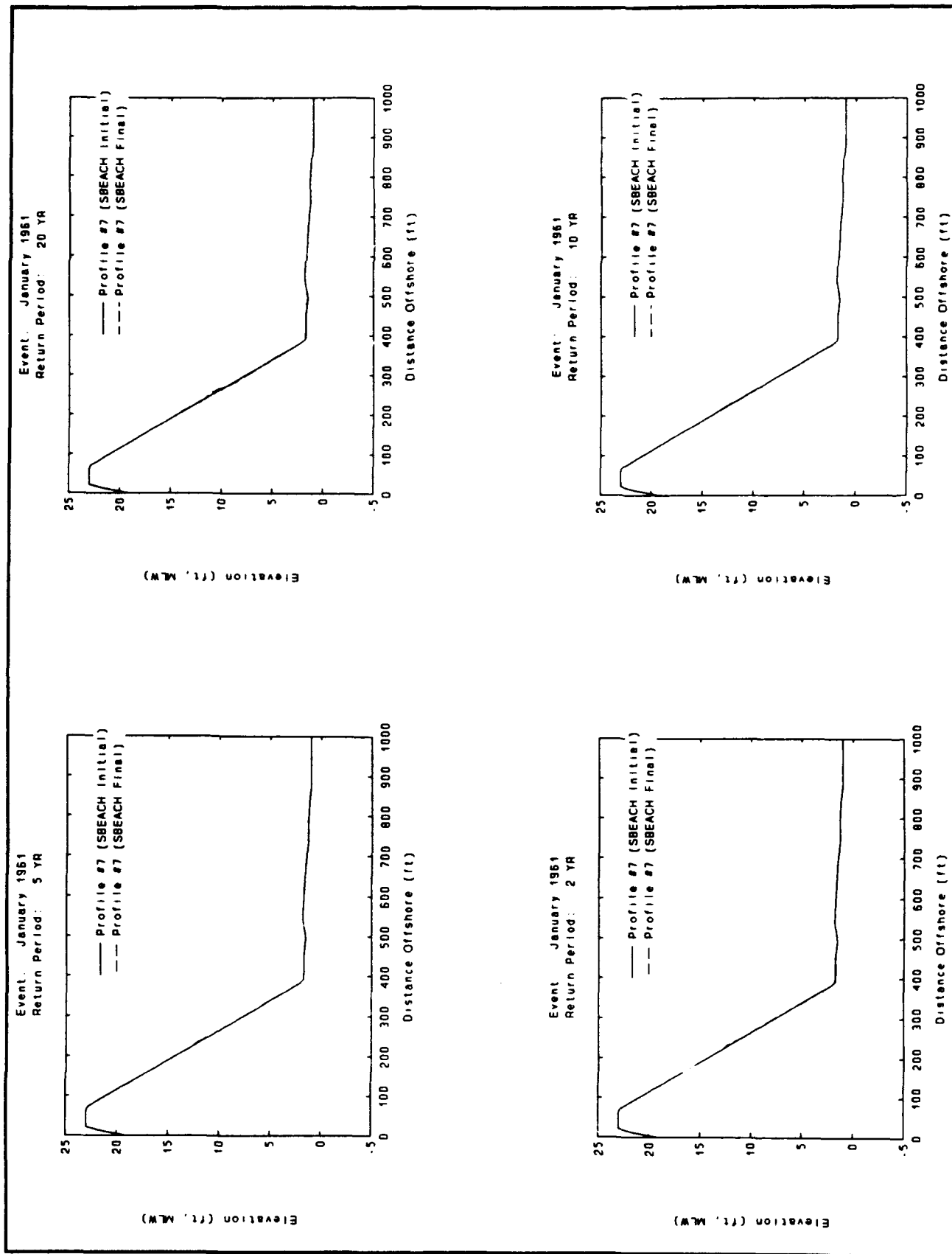




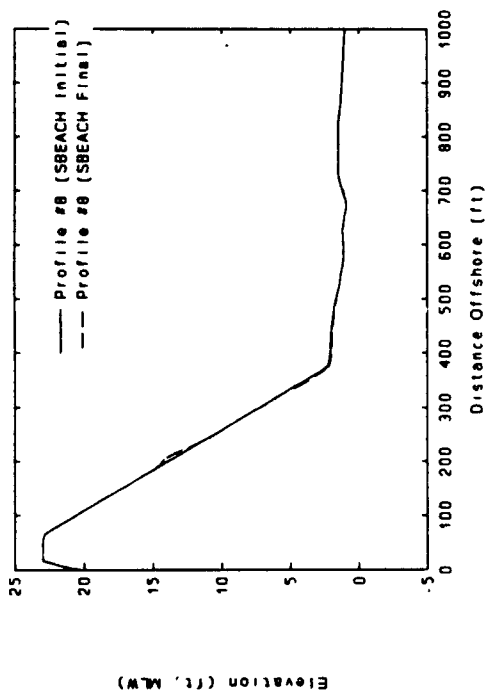




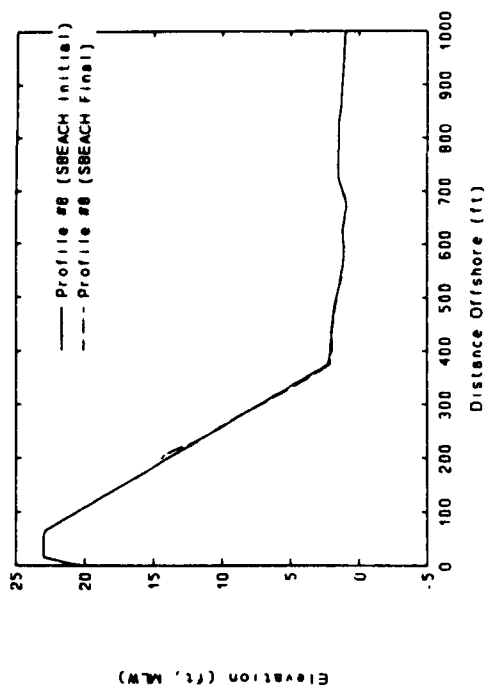




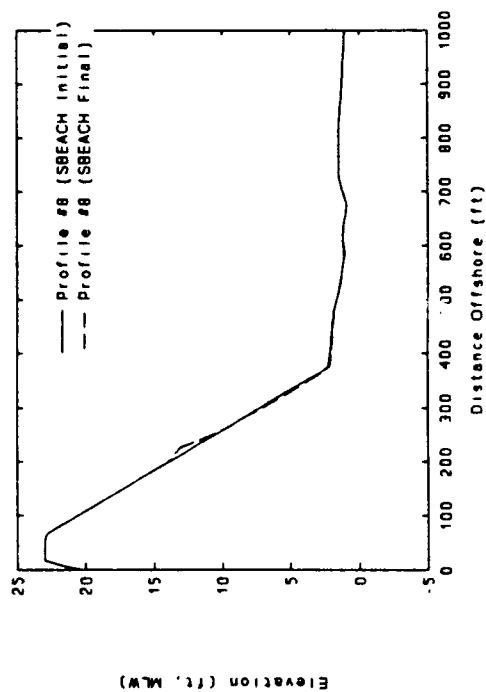
Event: January 1961
Return Period: 20 YR



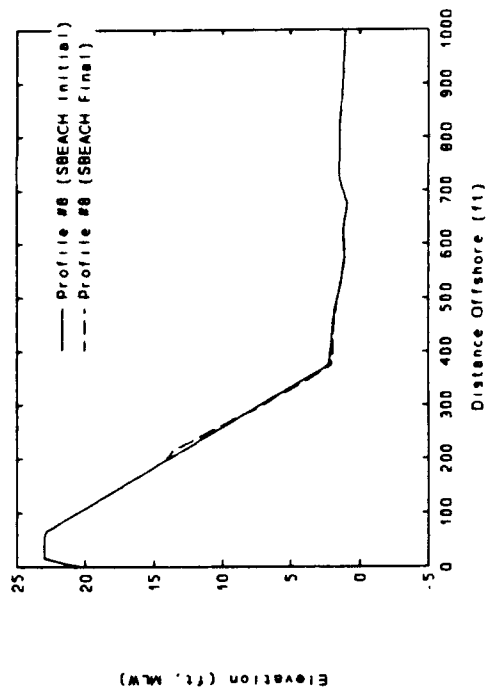
Event: January 1961
Return Period: 100 YR

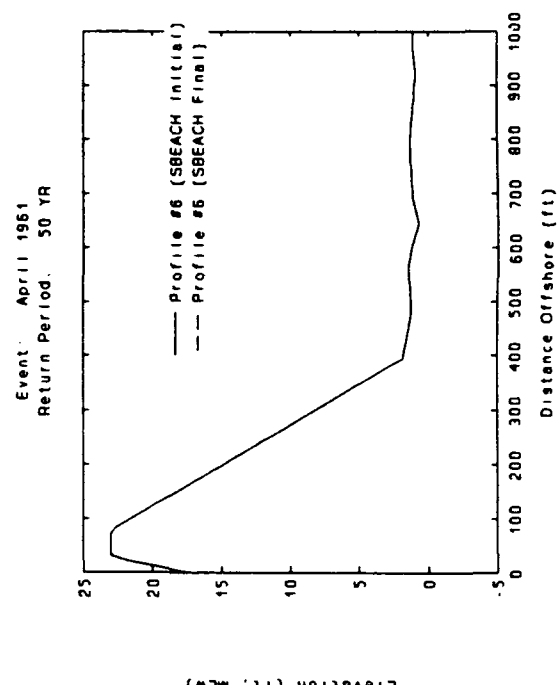
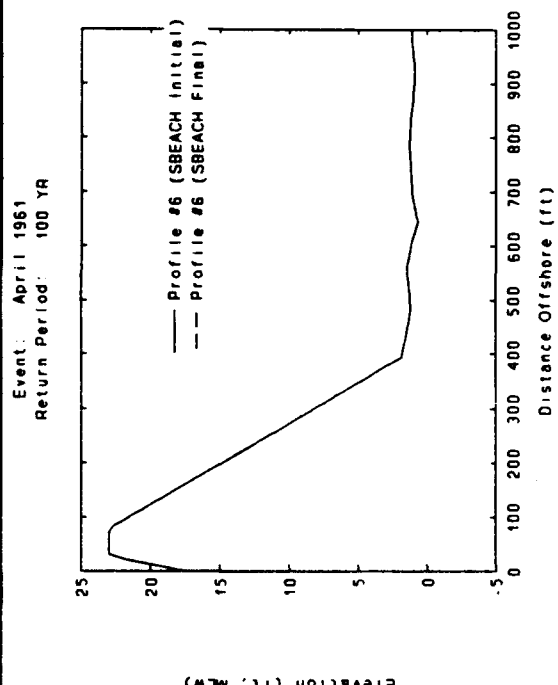
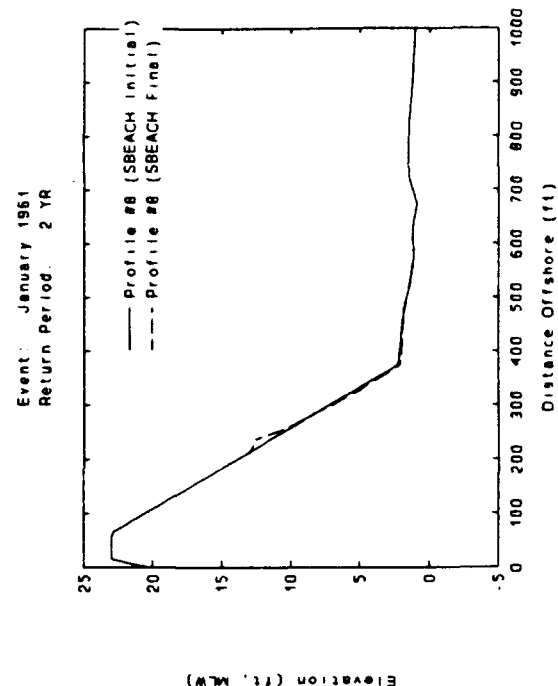
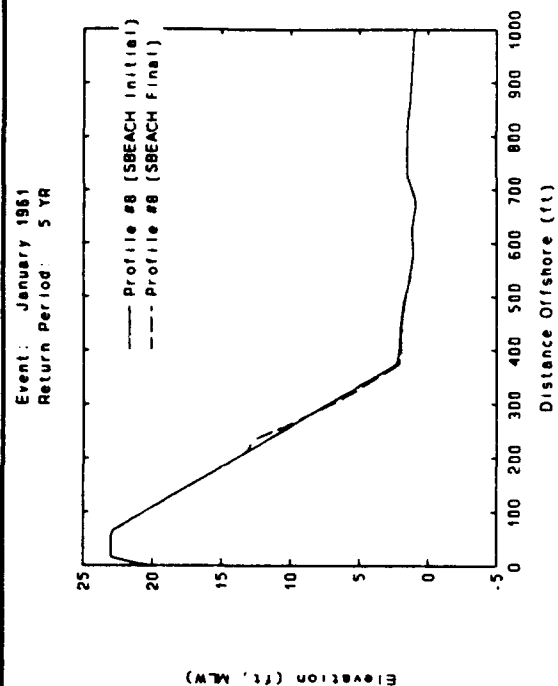


Event: January 1961
Return Period: 10 YR

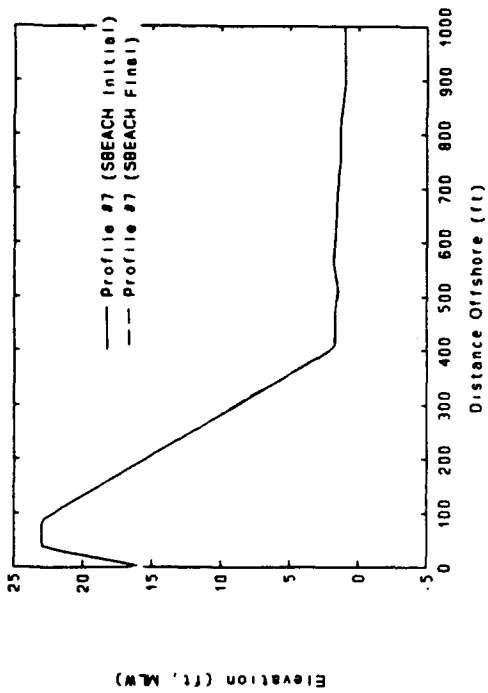


Event: January 1961
Return Period: 50 YR

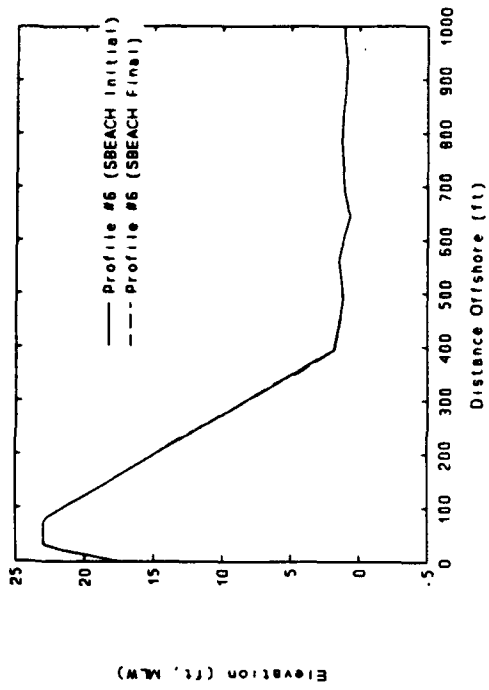




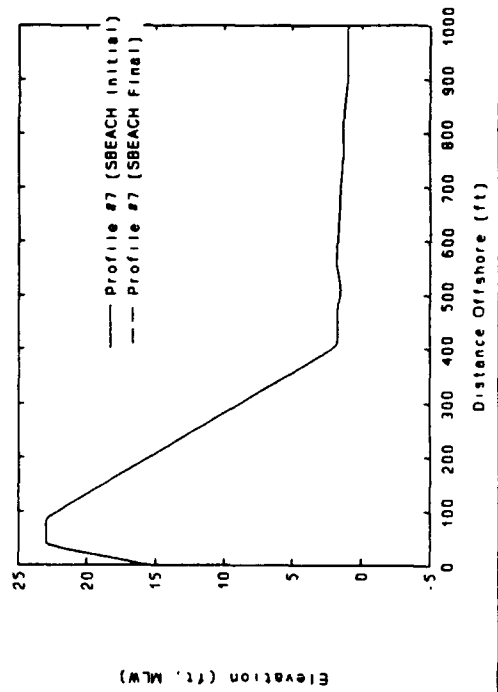
Event: April 1961
Return Period: 100 YR



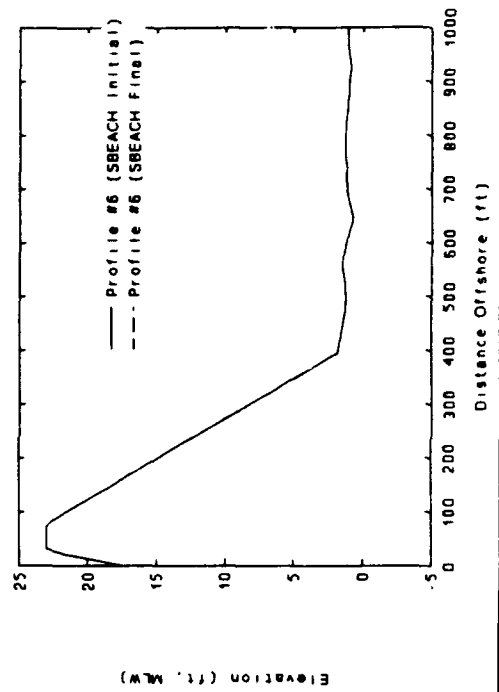
Event: April 1961
Return Period: 20 YR

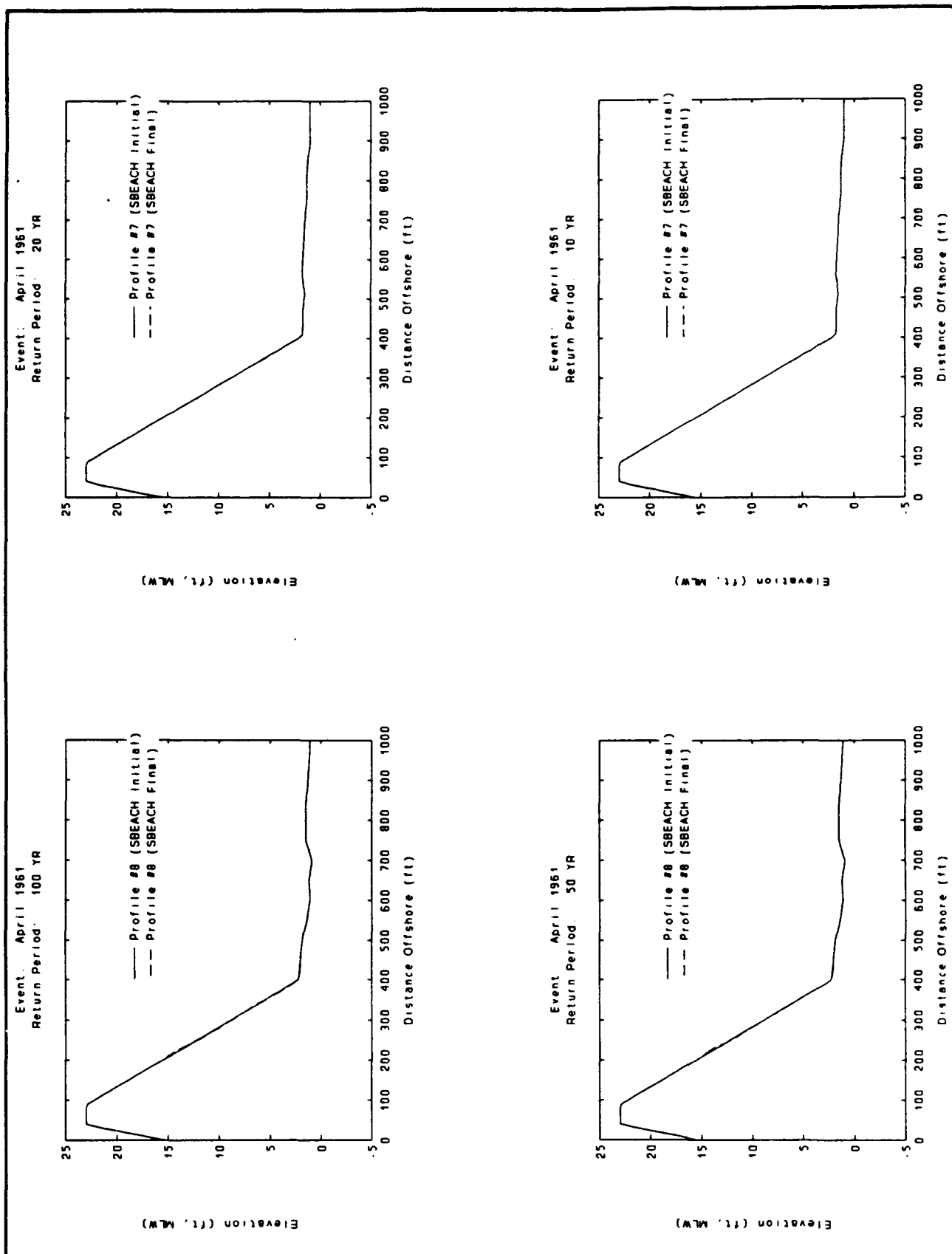


Event: April 1961
Return Period: 50 YR

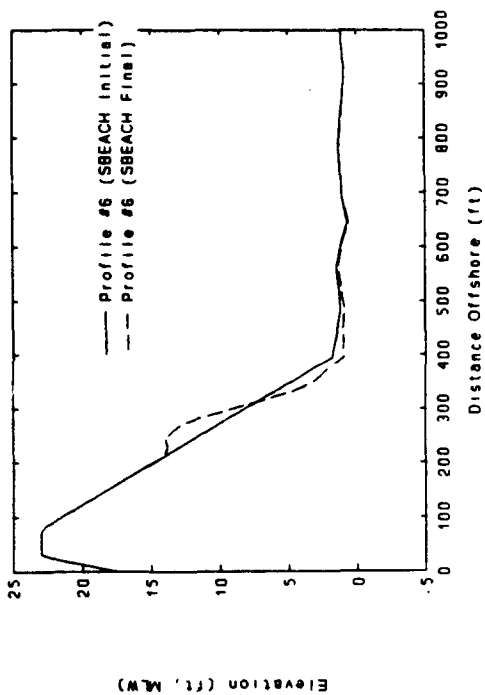


Event: April 1961
Return Period: 10 YR

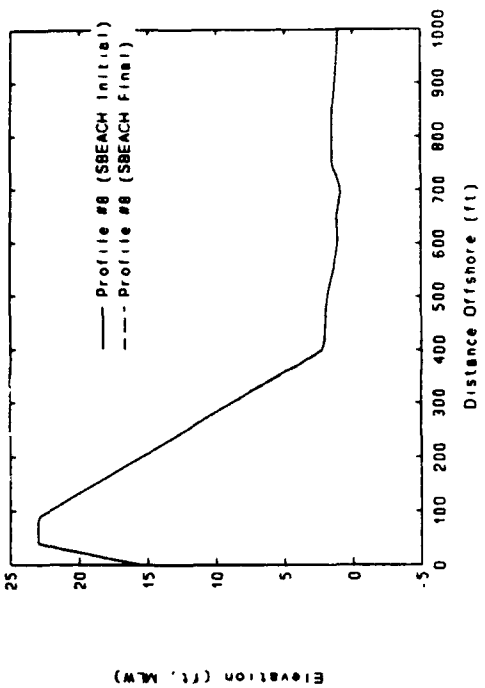




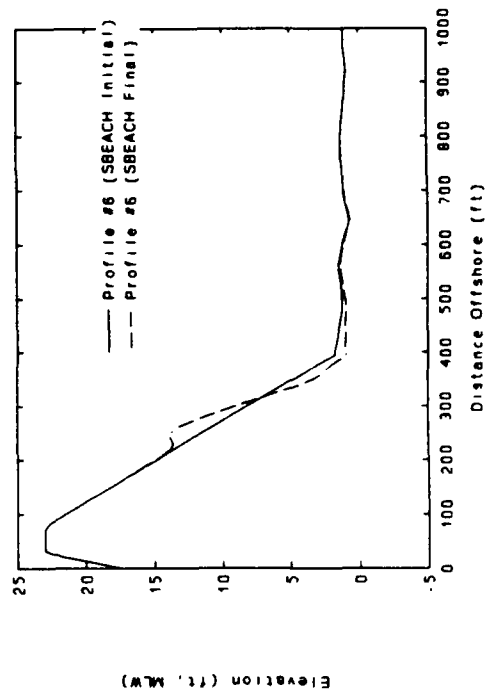
Event: December 1962
Return Period: 50 YR



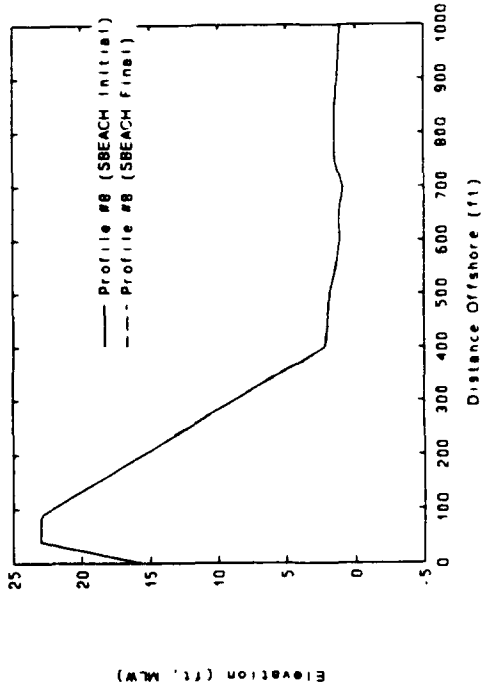
Event: April 1961
Return Period: 20 YR



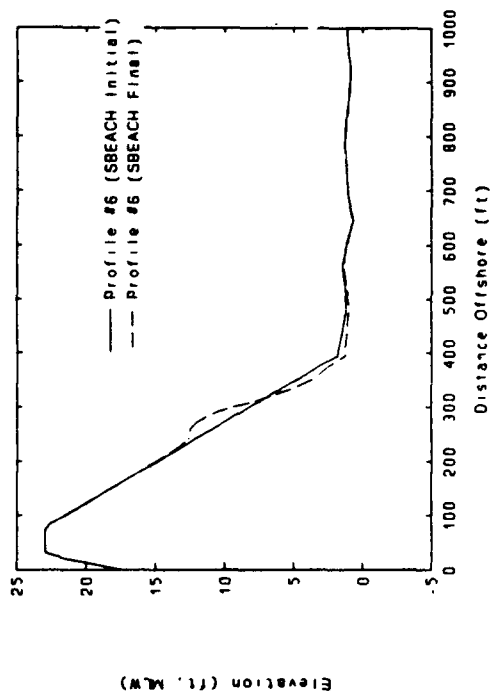
Event: December 1962
Return Period: 20 YR



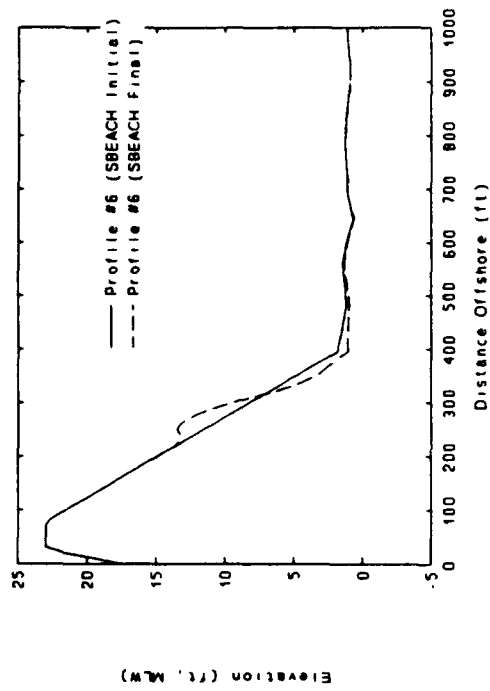
Event: April 1961
Return Period: 10 YR



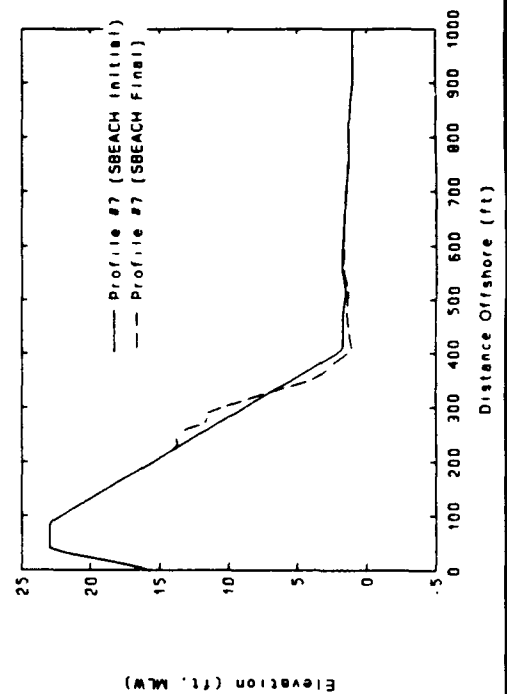
Event: December 1962
Return Period: 2 YR



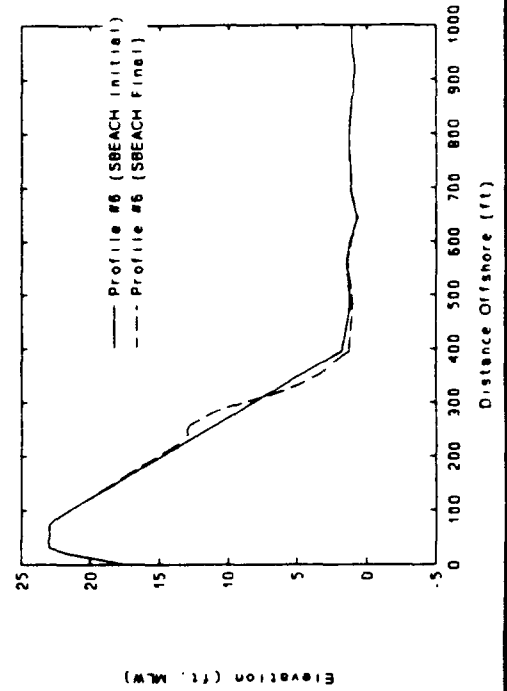
Event: December 1962
Return Period: 10 YR

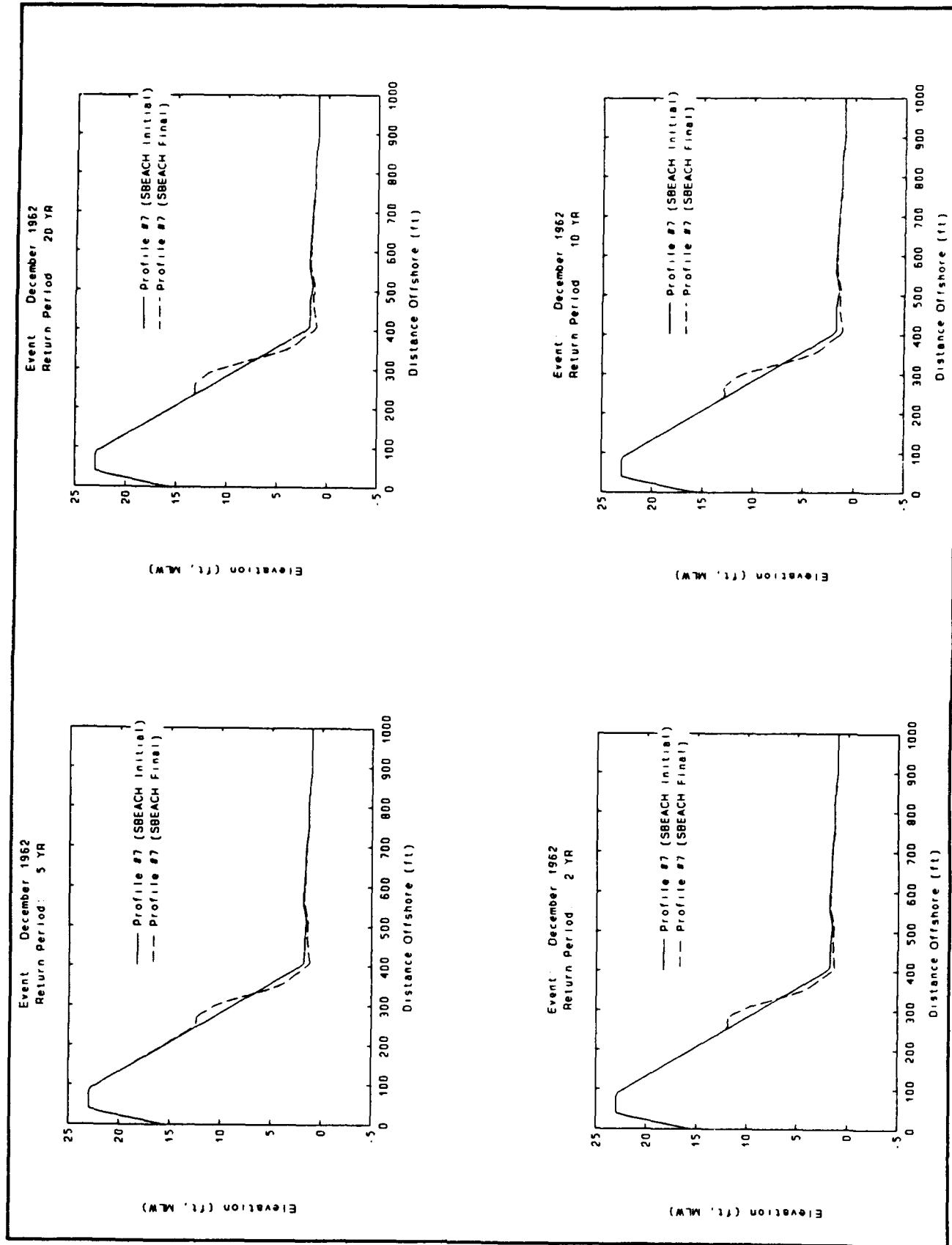


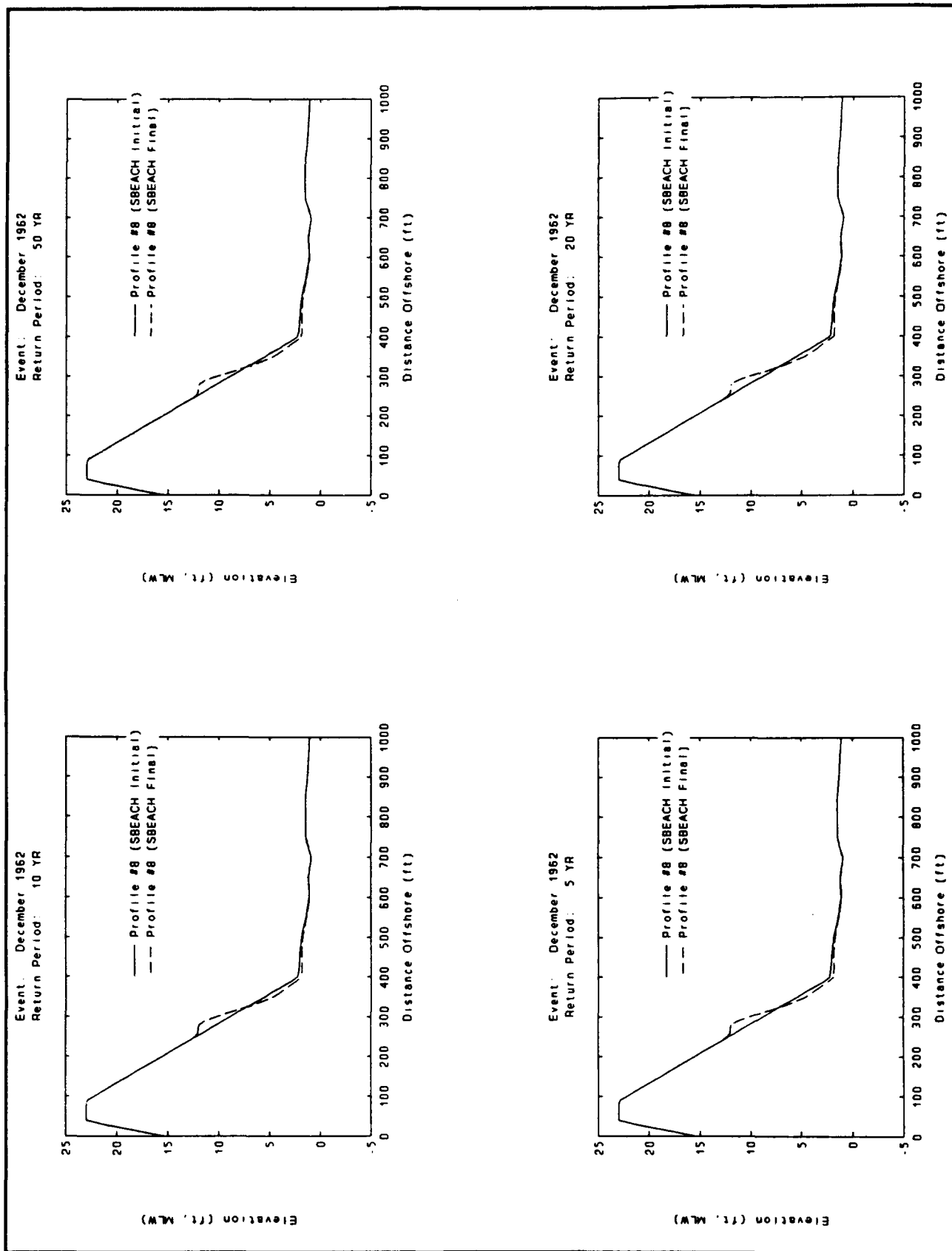
Event: December 1962
Return Period: 50 YR

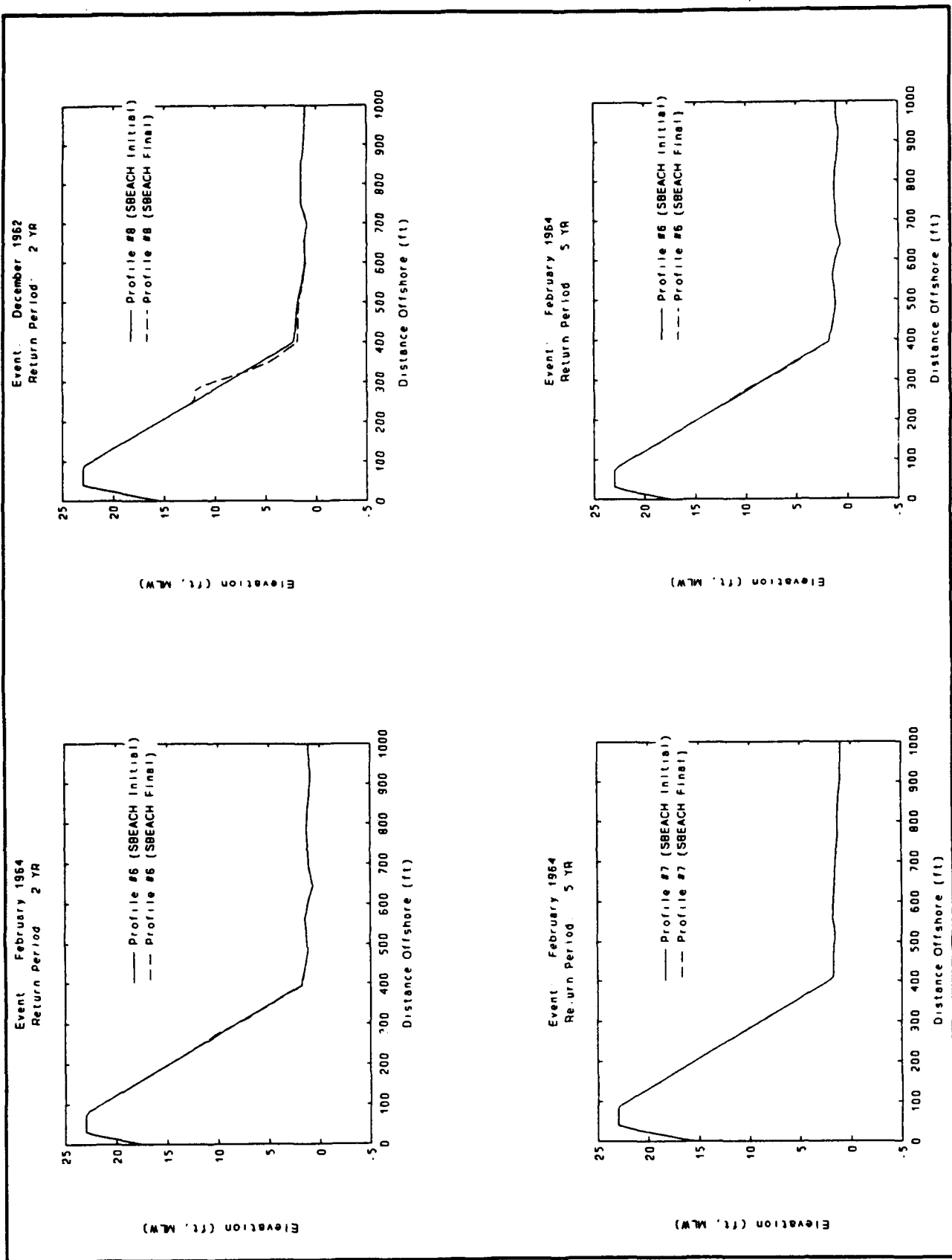


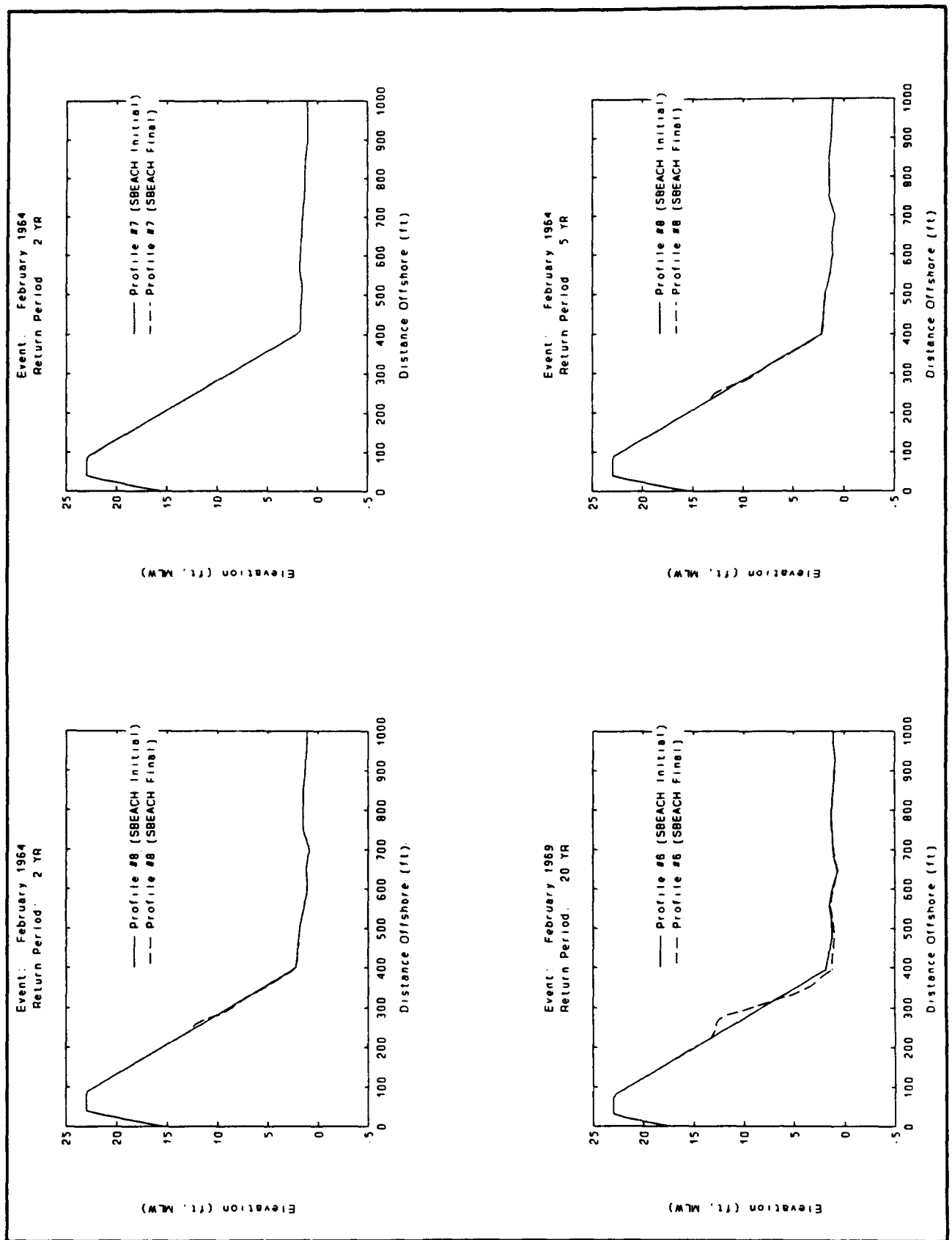
Event: December 1962
Return Period: 5 YR



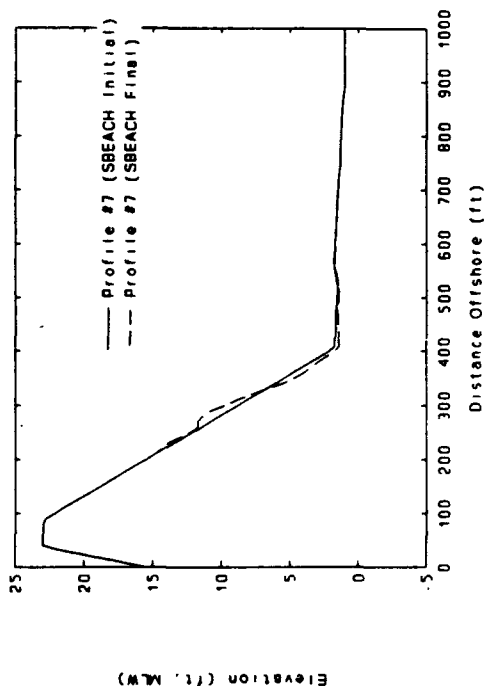




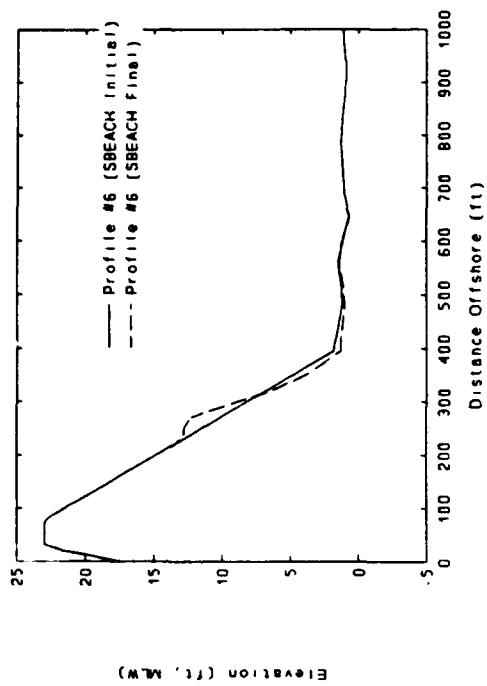




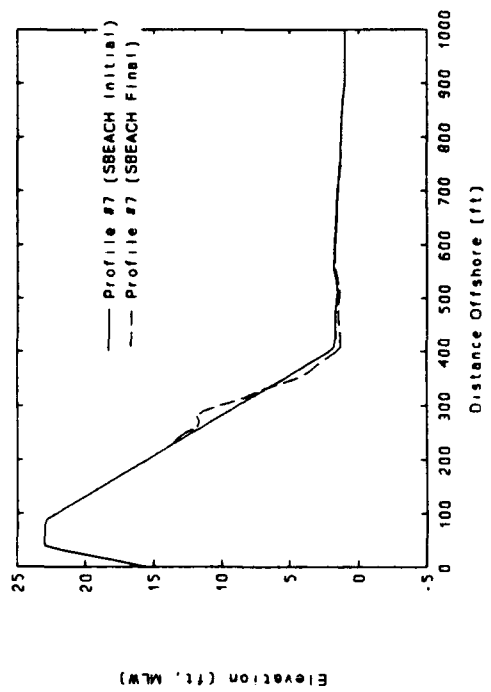
Event: February 1969
Return Period: 20 YR



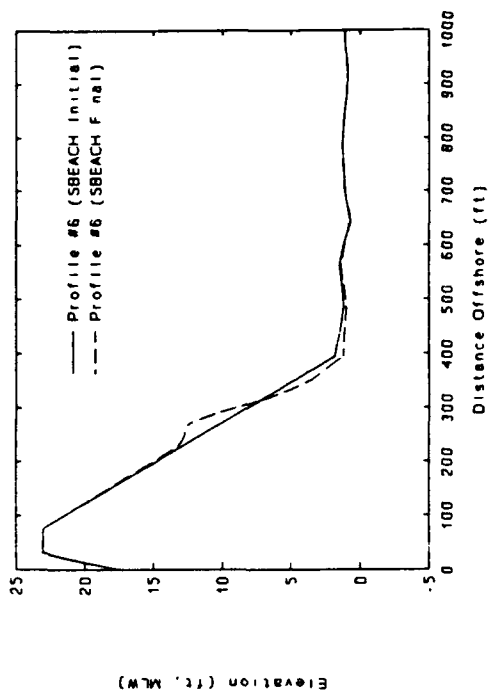
Event: February 1969
Return Period: 10 YR

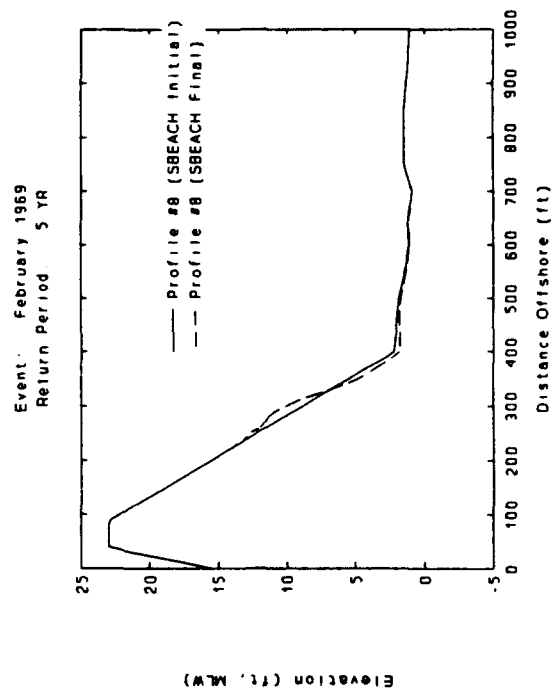
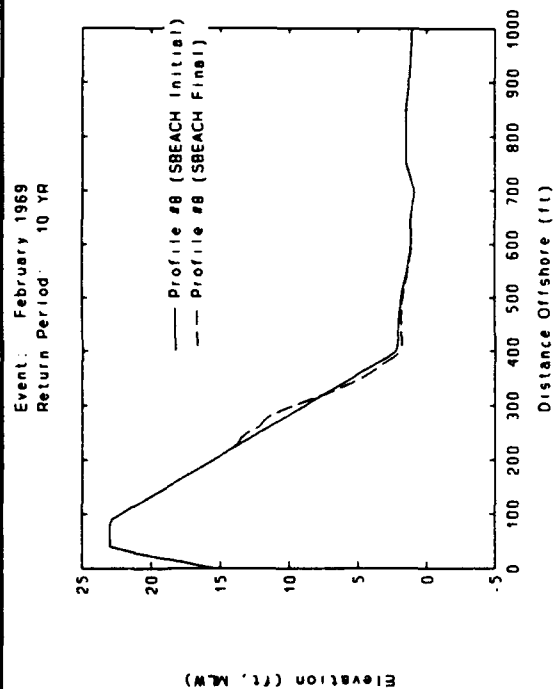
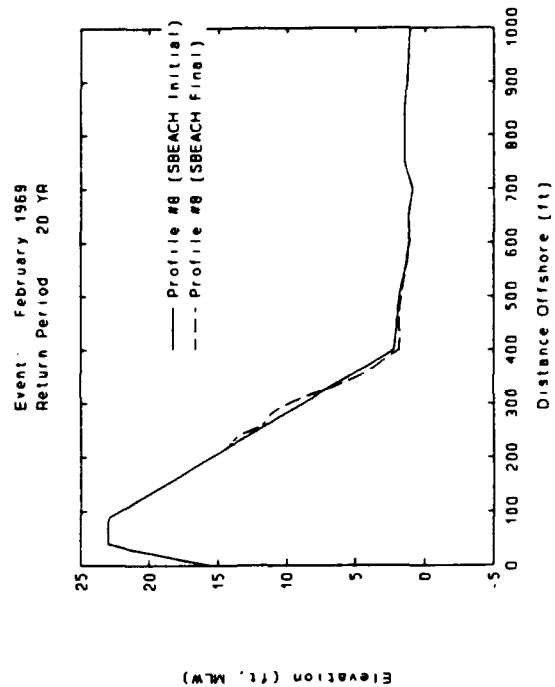
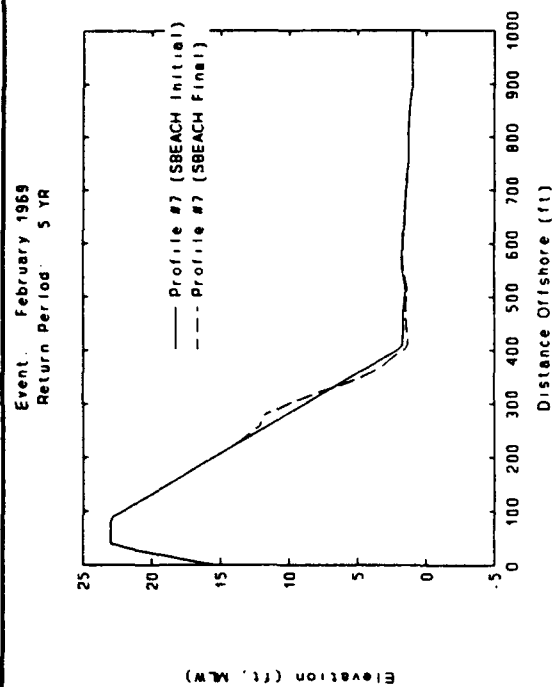


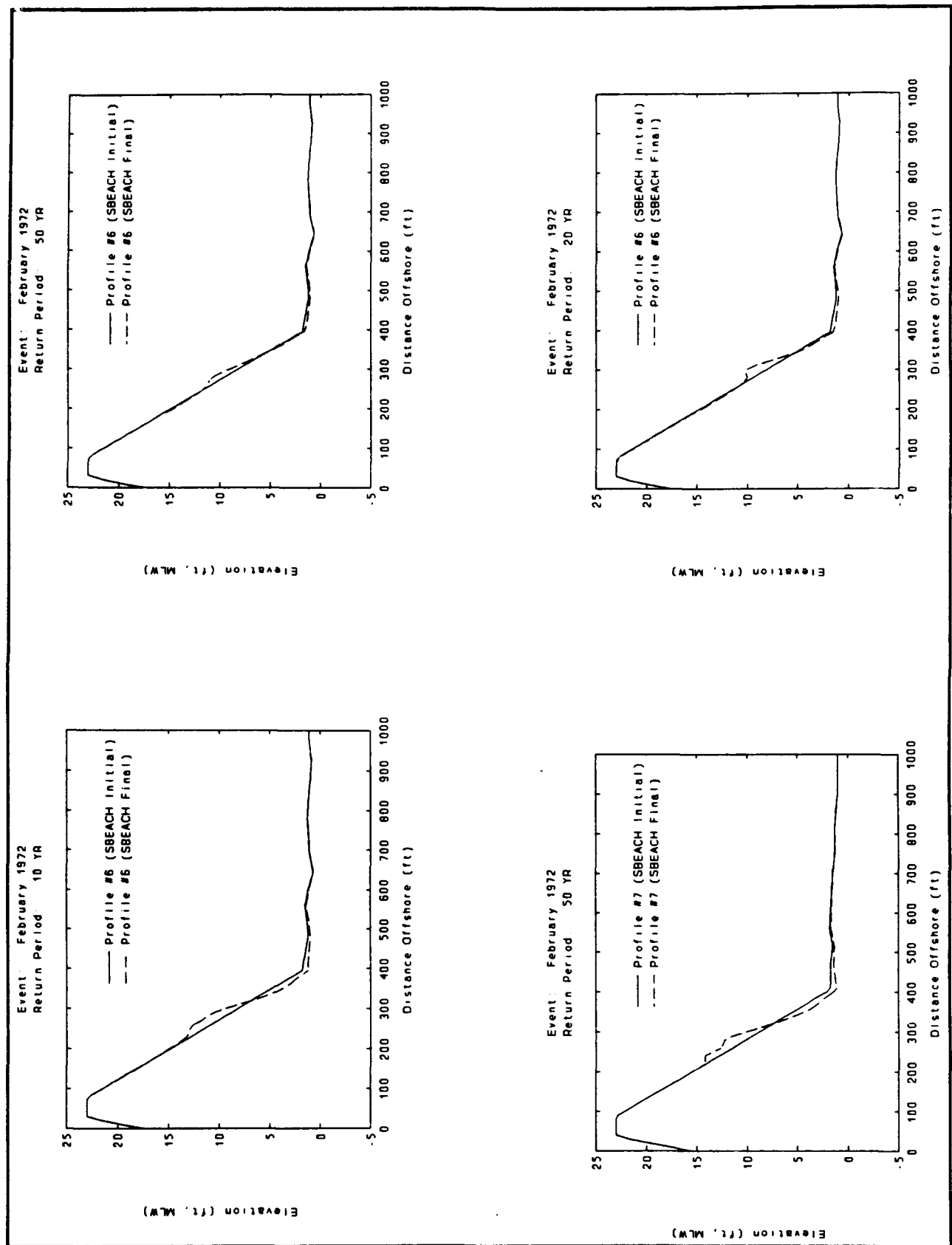
Event: February 1969
Return Period: 10 YR



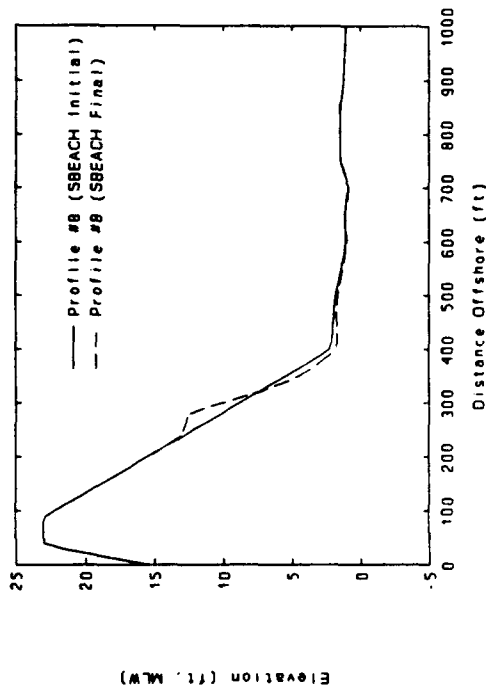
Event: February 1969
Return Period: 5 YR



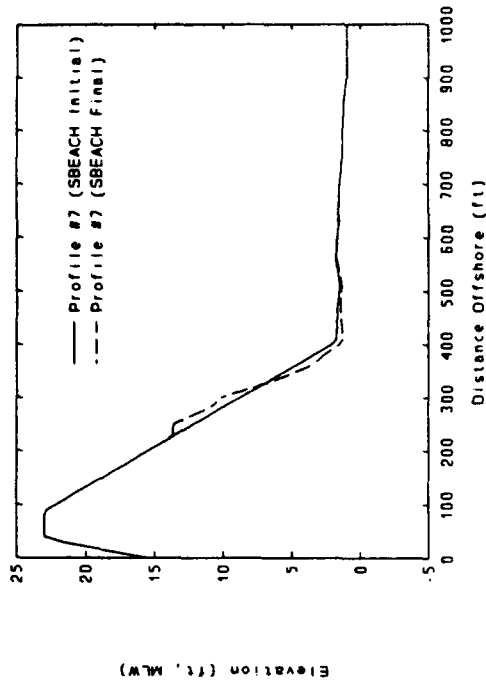




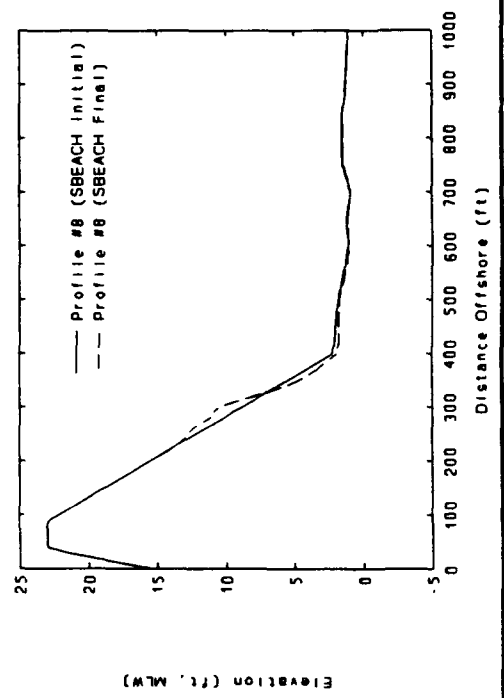
Event: February 1972
Return Period: 50 YR



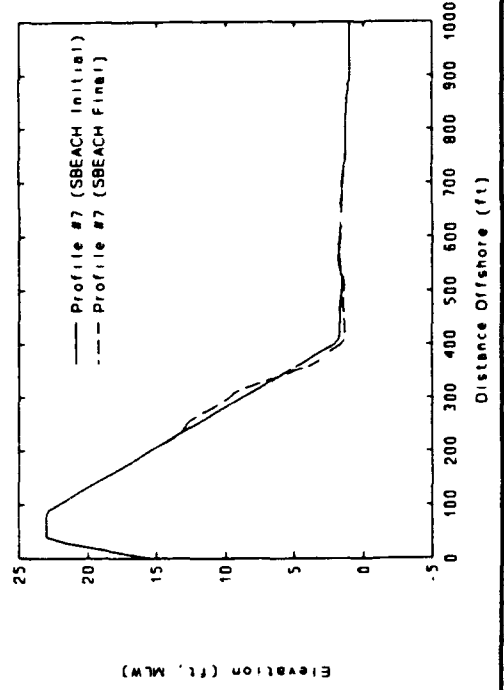
Event: February 1972
Return Period: 20 YR



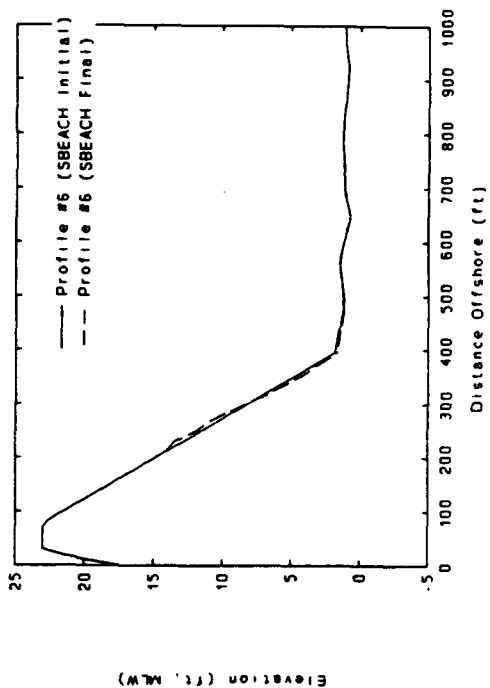
Event: February 1972
Return Period: 20 YR



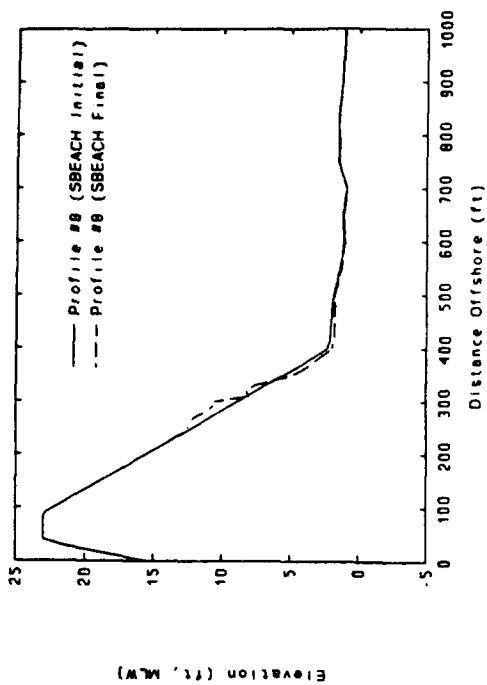
Event: February 1972
Return Period: 10 YR



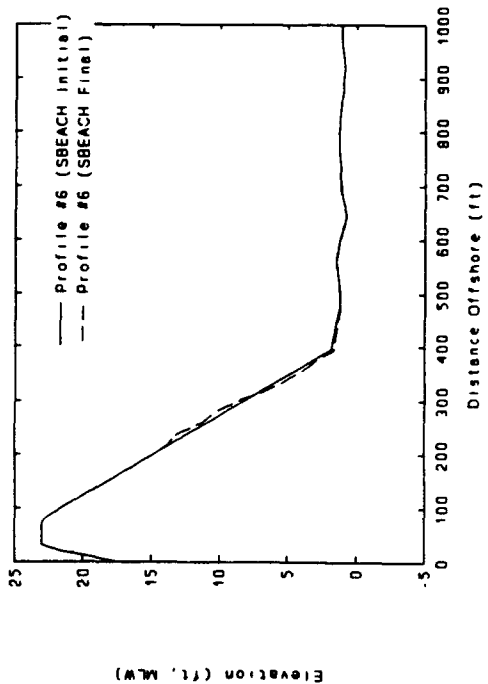
Event: November 1972
Return Period: 20 YR



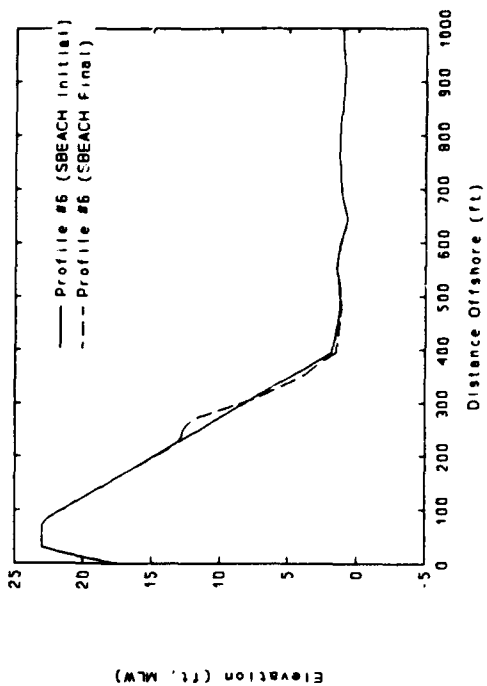
Event: February 1972
Return Period: 10 YR



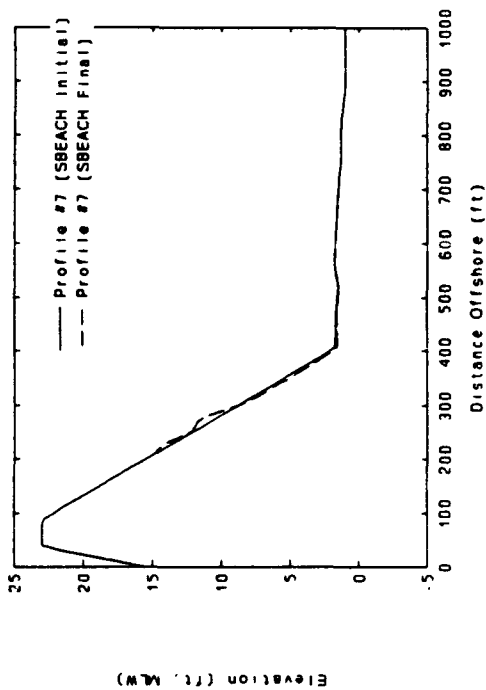
Event: November 1972
Return Period: 10 YR



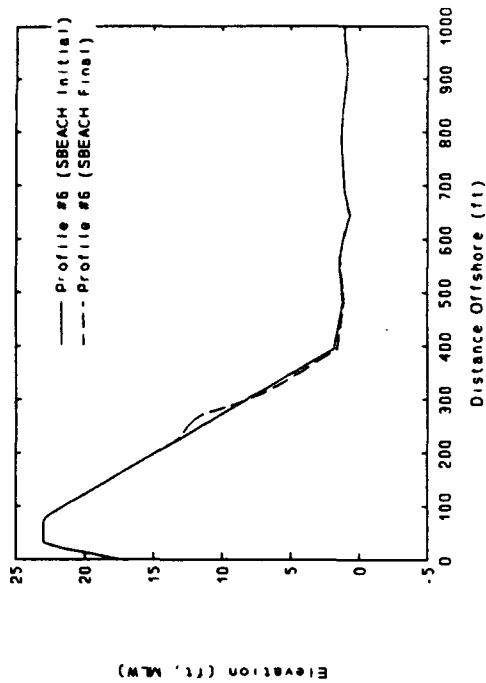
Event: November 1972
Return Period: 50 YR



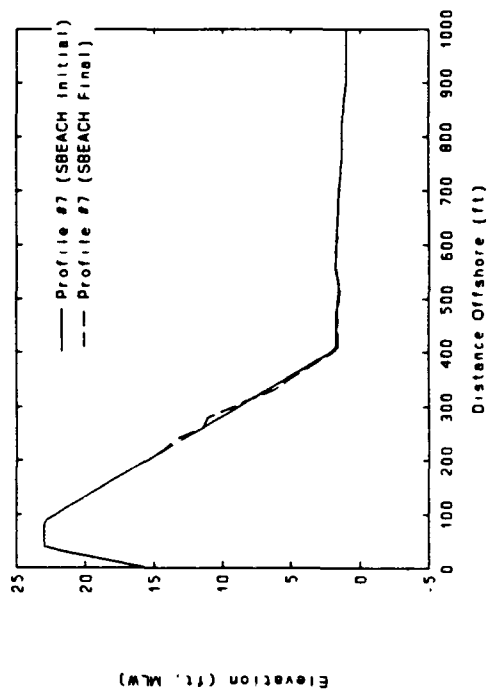
Event: November 1972
Return Period: 50 YR



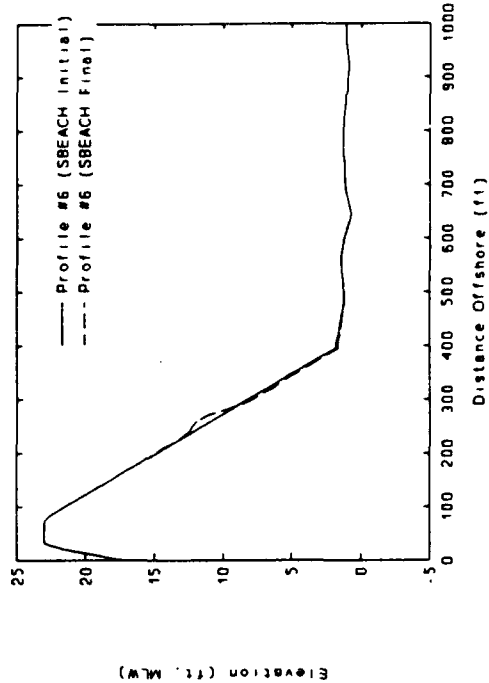
Event: November 1972
Return Period: 5 YR



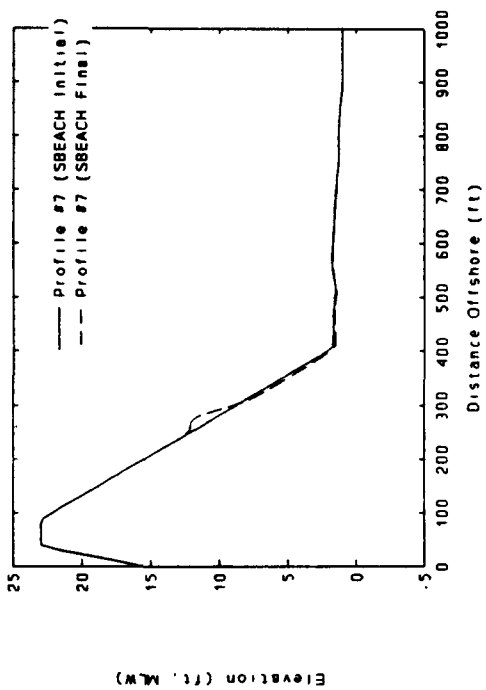
Event: November 1972
Return Period: 20 YR



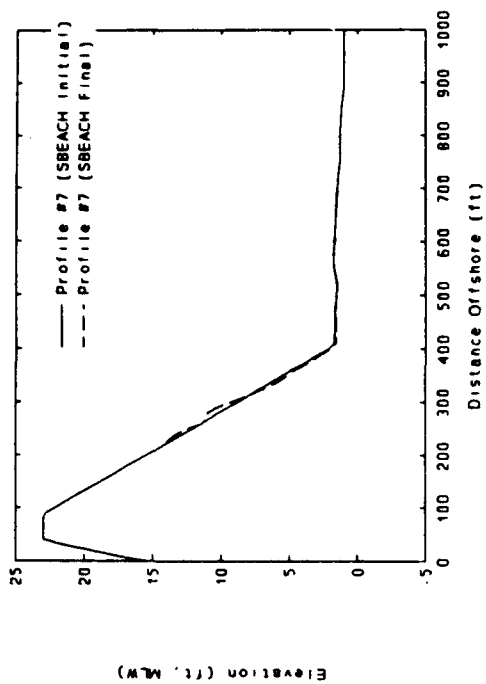
Event: November 1972
Return Period: 2 YR



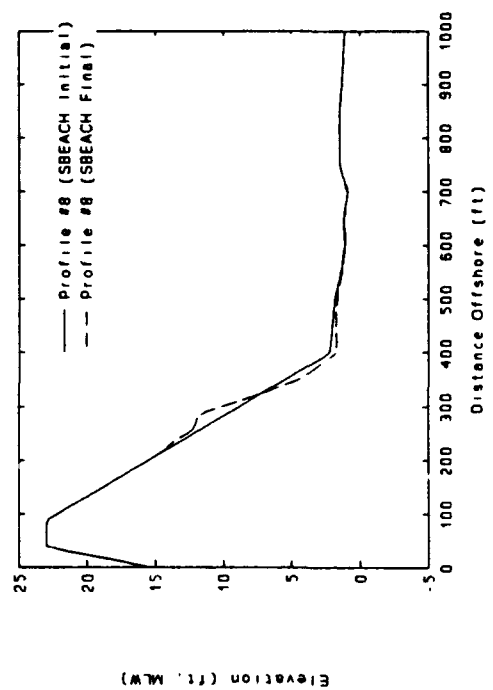
Event November 1972
Return Period 2 YR



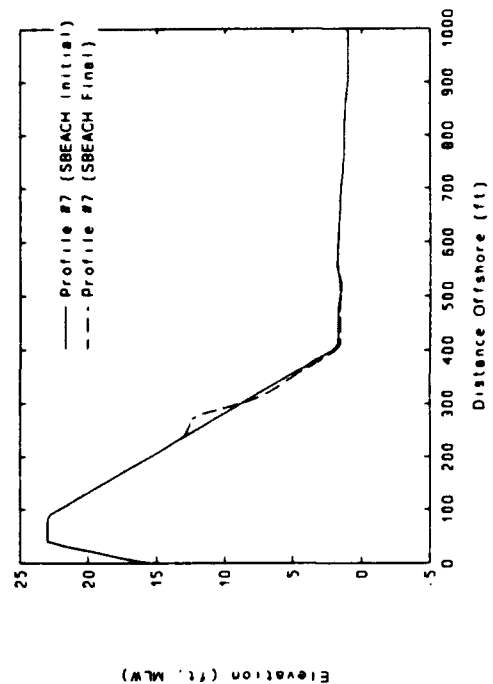
Event November 1972
Return Period 10 YR



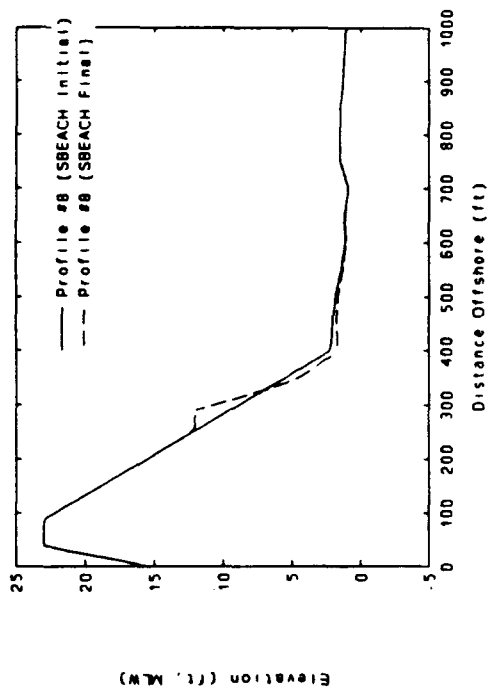
Event November 1972
Return Period 50 YR



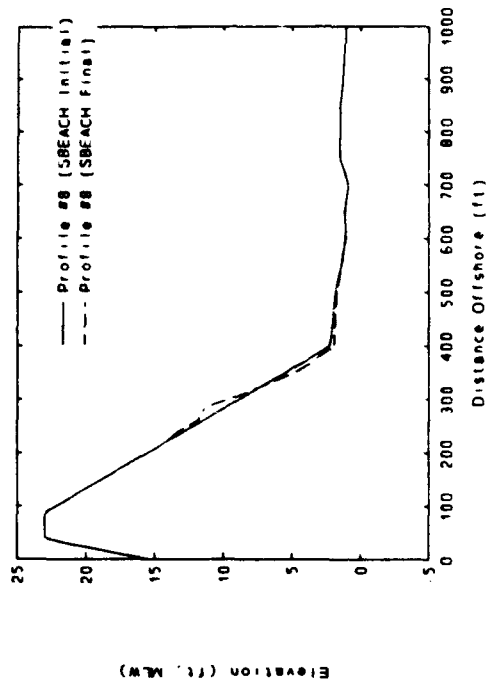
Event November 1972
Return Period 5 YR



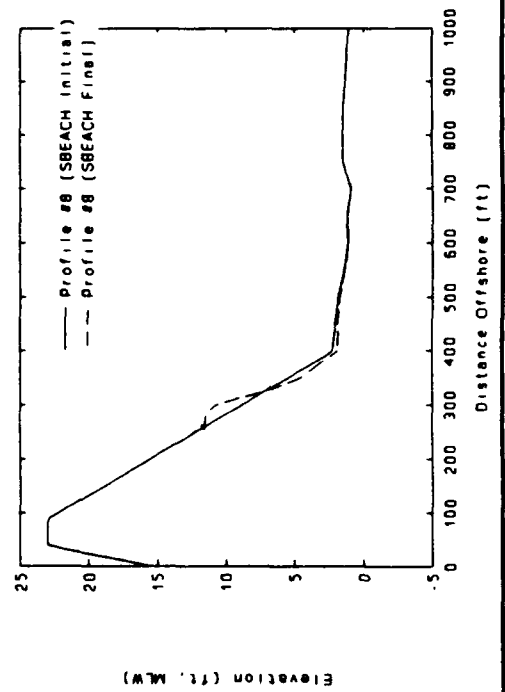
Event: November 1972
Return Period: 5 YR



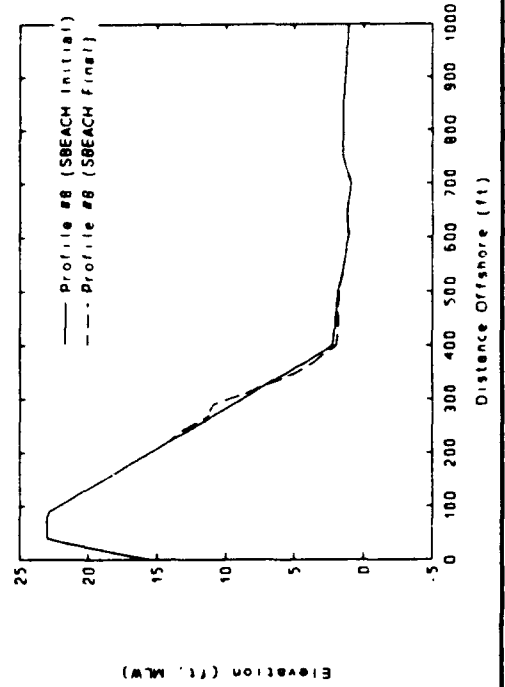
Event: November 1972
Return Period: 20 YR

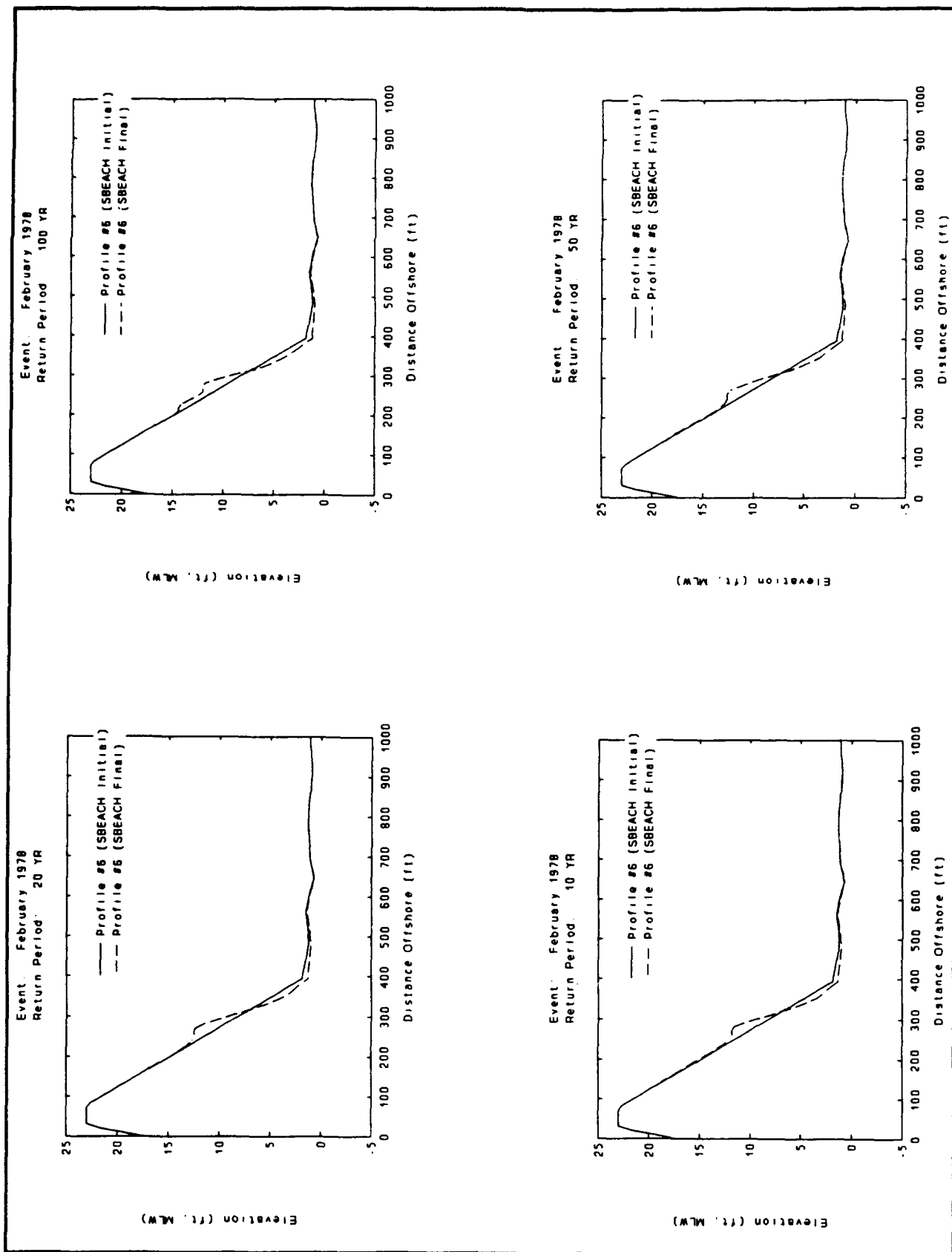


Event: November 1972
Return Period: 2 YR

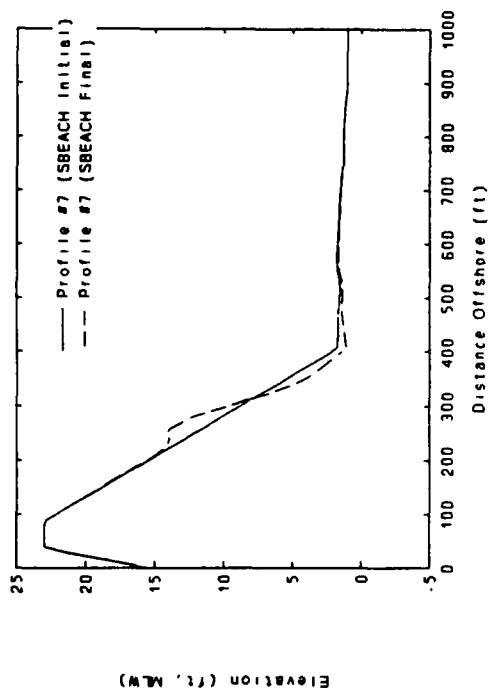


Event: November 1972
Return Period: 10 YR

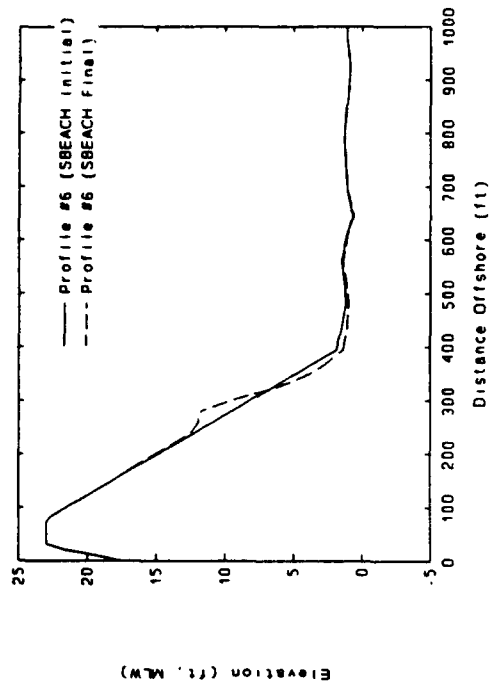




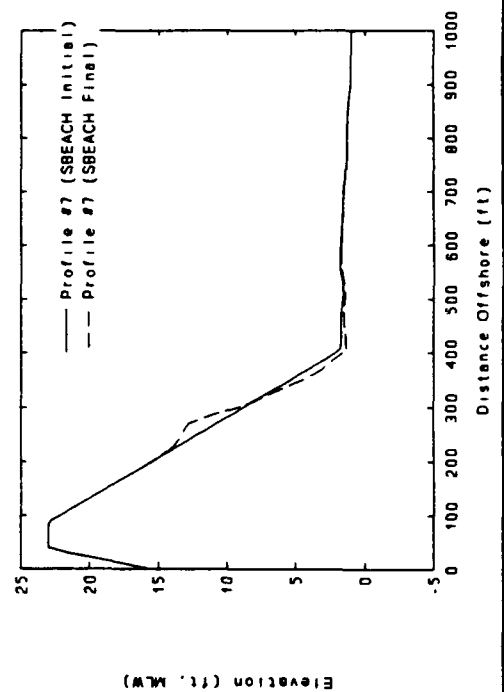
Event: February 1978
Return Period: 100 YR



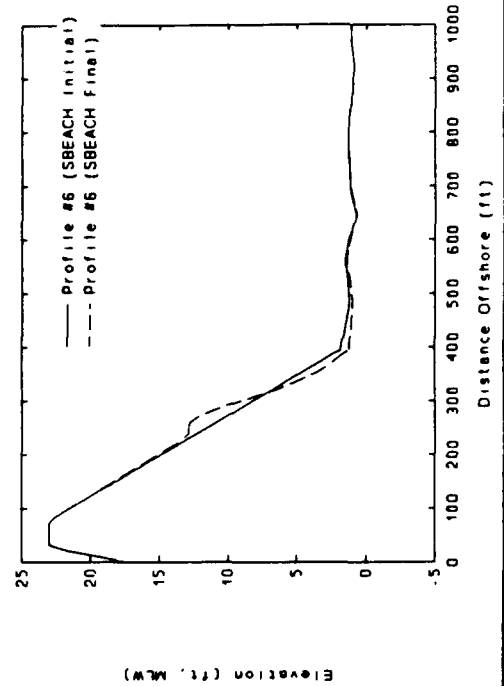
Event: February 1978
Return Period: 5 YR



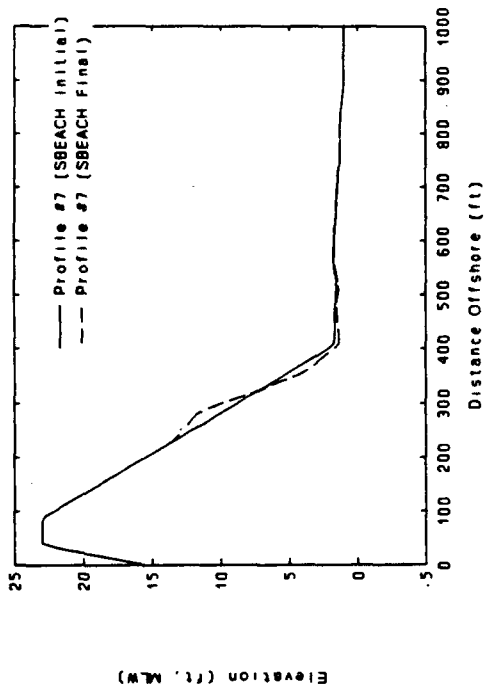
Event: February 1978
Return Period: 50 YR



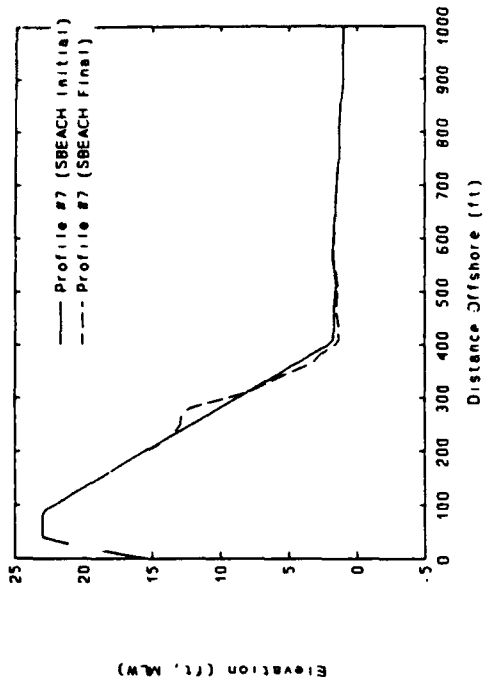
Event: February 1978
Return Period: 2 YR



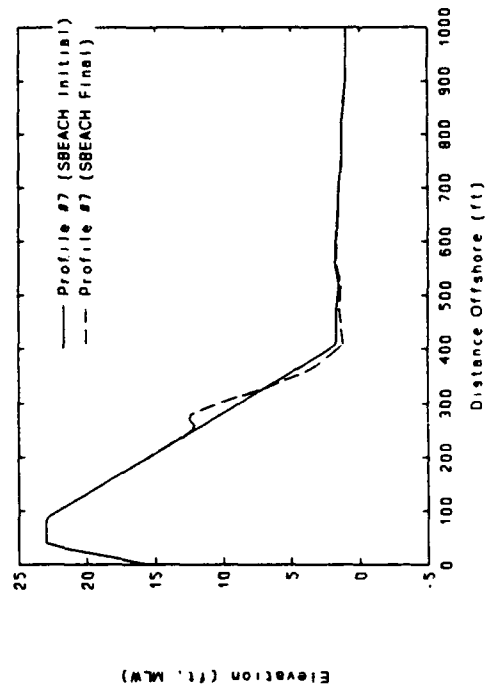
Event: February 1978
Return Period: 5 YR



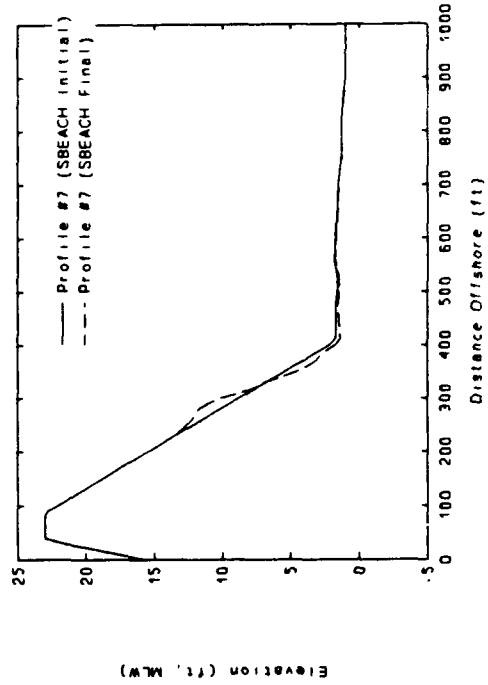
Event: February 1978
Return Period: 20 YR

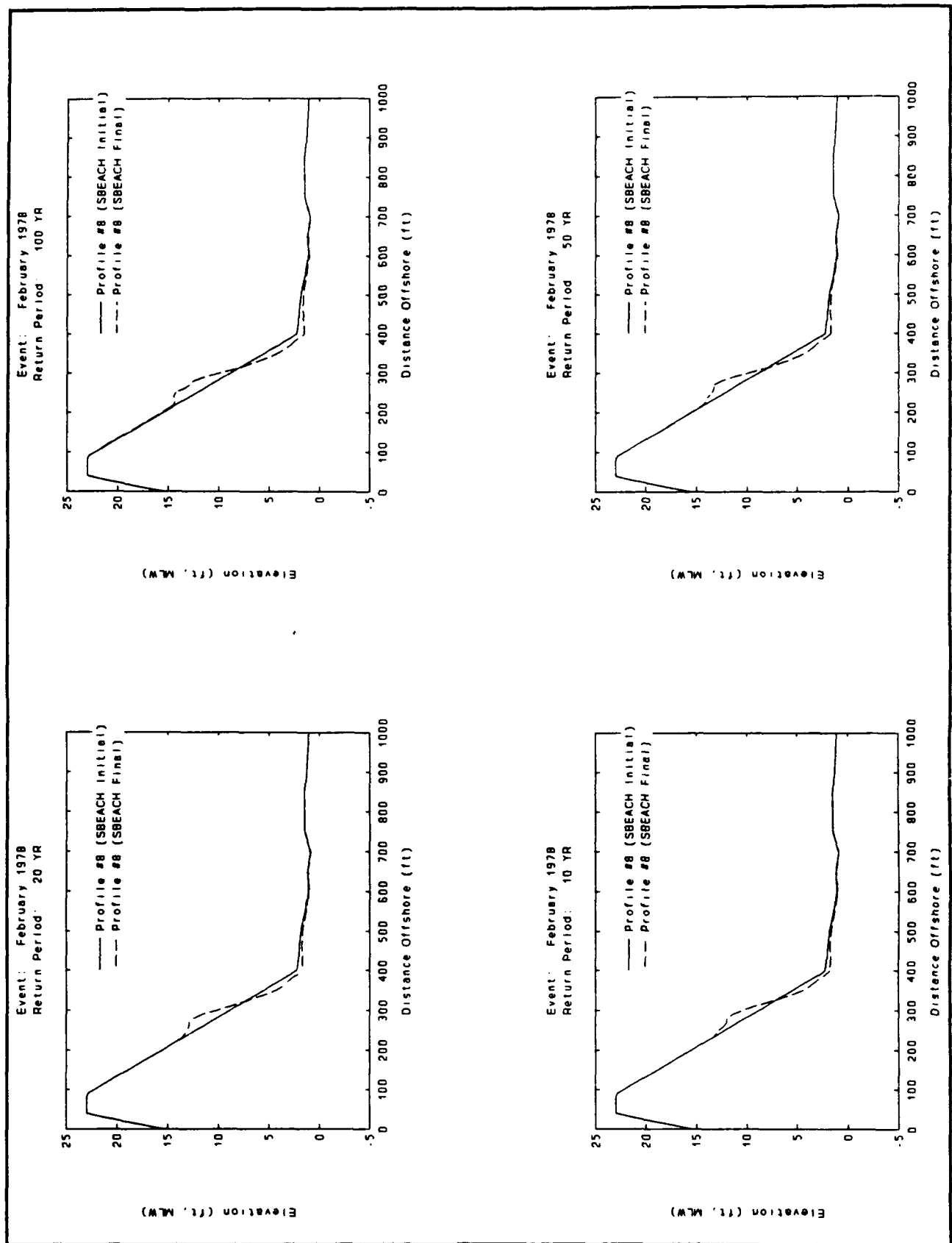


Event: February 1978
Return Period: 2 YR

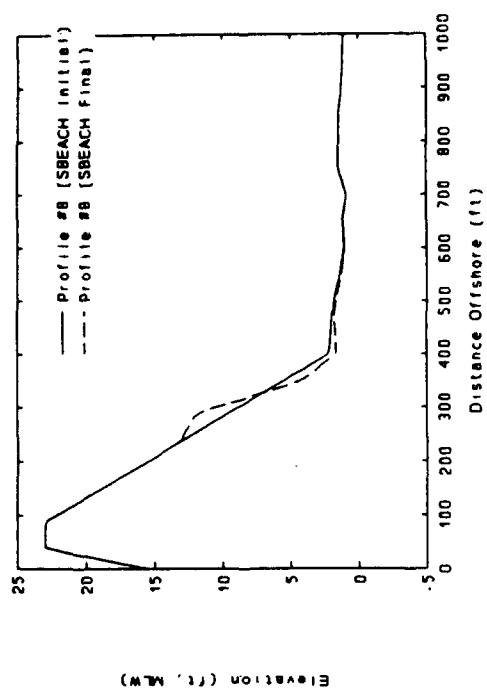


Event: February 1978
Return Period: 10 YR

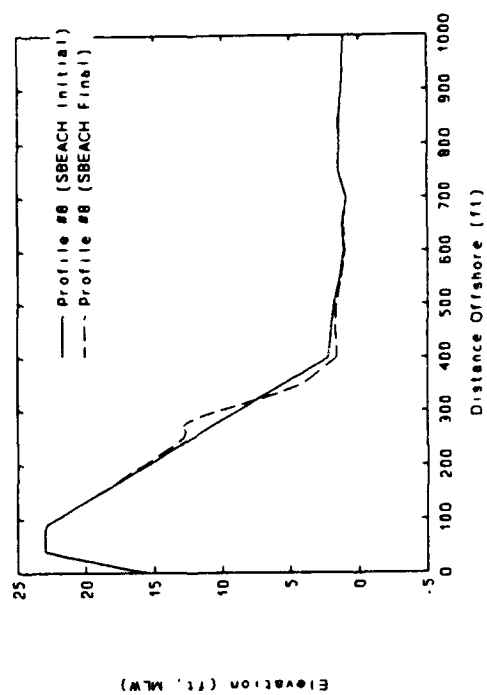




Event: February 1978
Return Period: 5 YR



Event: February 1978
Return Period: 2 YR



Appendix G

Maximum Wave Parameters at the Seaward Terminus of Each Profile

Appendix G presents a table of maximum wave height and corresponding wave period at the seaward terminus of each profile (see Figure 5 in main text for terminus locations). Wave parameters are listed for each storm used in the study.

Table G1
Maximum Wave Parameters at Seaward Terminus of Each Profile

Storm	Maximum Wave Height (ft), Corresponding Wave Period (sec) at Profiles*				
	1&3	2	4 and 5	6	7, 7a, and 8
November 1945 SPN	24.7, 15.9	28.1, 15.9	17.4, 15.9	13.7, 15.9	7.1, 15.9
November 1945 500-year	24.7, 15.9	28.1, 15.9	17.4, 15.9	13.7, 15.9	7.1, 15.9
November 1945 100-year	24.7, 15.9	28.1, 15.9	17.4, 15.9	13.7, 15.9	7.1, 15.9
November 1945 50-year	24.1, 15.9	27.7, 15.9	17.1, 15.9	13.2, 15.9	7.7, 15.9
November 1945 20-year	23.9, 15.9	27.1, 15.9	16.7, 15.9	13.1, 15.9	6.9, 15.9
November 1945 10-year	24.0, 15.9	27.5, 15.9	17.0, 15.9	13.0, 15.9	6.4, 15.9
February 1958 50-year	10.3, 11.0	13.4, 11.0	7.6, 11.0	5.7, 11.0	2.8, 11.0
February 1958 20-year	10.3, 11.0	13.4, 11.0	7.6, 11.0	5.4, 11.0	3.0, 11.0
February 1958 10-year	10.5, 11.0	13.6, 11.0	7.6, 11.0	5.7, 11.0	2.9, 11.0
February 1958 5-year	10.5, 11.0	13.6, 11.0	7.6, 11.0	5.8, 11.0	3.4, 11.0
February 1958 2-year	10.5, 11.0	13.6, 11.0	7.6, 11.0	5.8, 11.0	3.3, 11.0
March 1958 50-year	9.4, 13.0	11.1, 13.0	6.1, 13.0	4.9, 13.0	4.0, 13.0
March 1958 20-year	9.2, 13.0	11.2, 13.0	6.3, 13.0	4.9, 13.0	3.9, 13.0
March 1958 10-year	9.3, 13.0	11.1, 13.0	6.3, 13.0	5.1, 13.0	3.9, 13.0
March 1958 5-year	9.2, 13.0	11.0, 13.0	6.5, 13.0	5.0, 13.0	3.2, 13.0
March 1958 2-year	9.2, 13.0	10.9, 13.0	6.3, 13.0	5.0, 13.0	3.2, 13.0
January 1961 100-year	7.0, 9.0	7.4, 9.0	4.2, 9.0	3.2, 9.0	1.8, 9.0
January 1961 50-year	6.8, 9.0	7.5, 9.0	4.1, 9.0	3.2, 9.0	2.4, 9.0
January 1961 20-year	6.8, 9.0	7.4, 9.0	4.1, 9.0	3.1, 9.0	1.8, 9.0
January 1961 10-year	6.9, 9.0	7.4, 9.0	4.2, 9.0	3.2, 9.0	1.8, 9.0
January 1961 5-year	6.9, 9.0	7.4, 9.0	4.2, 9.0	3.2, 9.0	1.8, 9.0
January 1961 2-year	6.9, 9.0	7.4, 9.0	4.2, 9.0	3.2, 9.0	2.0, 9.0
April 1961 100-year	4.7, 9.0	5.6, 9.0	3.6, 9.0	2.7, 9.0	1.1, 9.0
April 1961 50-year	4.9, 9.0	5.6, 9.0	3.6, 9.0	2.7, 9.0	1.3, 9.0
April 1961 20-year	5.0, 9.0	5.8, 9.0	3.6, 9.0	2.7, 9.0	1.3, 9.0
April 1961 10-year	4.8, 9.0	5.7, 9.0	3.6, 9.0	2.7, 9.0	1.3, 9.0

(Continued)

* Approximate depths relative to MLW at seaward terminus of each profile are as follows: Profiles 1&3, 26 ft; Profile 2, 25 ft; Profiles 4 and 5, 28 ft; Profile 6, 30 ft; Profiles 7, 7a, and 8, 21 ft.

Table G1 (Concluded)**Maximum Wave Parameters at Seaward Terminus of Each Profile**

Storm	Maximum Wave Height (ft) and Corresponding Wave Period (sec) at Profiles*				
	1&3	2	4 and 5	6	7, 7a, and 8
December 1962 50-year	11.6, 14.1	13.7, 14.1	7.8, 14.1	6.2, 14.1	4.1, 14.1
December 1962 20-year	11.7, 14.1	13.8, 14.1	7.9, 14.1	6.3, 14.1	5.1, 14.1
December 1962 10-year	11.6, 14.1	13.8, 14.1	7.8, 14.1	6.2, 14.1	4.4, 14.1
December 1962 5-year	11.7, 14.1	13.8, 14.1	8.0, 14.1	6.1, 14.1	4.6, 14.1
December 1962 2-year	11.7, 14.1	13.8, 14.1	7.7, 14.1	6.2, 14.1	5.3, 14.1
February 1964 5-year	4.7, 9.0	5.9, 9.0	3.5, 9.0	2.8, 9.0	2.3, 9.0
February 1964 2-year	4.7, 9.0	5.9, 9.0	3.5, 9.0	2.8, 9.0	2.1, 9.0
February 1969 20-year	10.8, 13.0	13.7, 13.0	7.4, 13.0	5.7, 13.0	4.6, 13.0
February 1969 10-year	11.0, 13.0	13.7, 13.0	7.3, 13.0	5.8, 13.0	4.3, 13.0
February 1969 5-year	10.9, 13.0	13.7, 13.0	7.4, 13.0	5.8, 13.0	4.8, 13.0
February 1972 50-year	14.2, 14.1	17.3, 14.1	9.8, 14.1	7.3, 14.1	5.1, 14.1
February 1972 20-year	14.2, 14.1	17.3, 14.1	9.8, 14.1	7.4, 14.1	4.5, 14.1
February 1972 10-year	14.2, 14.1	17.4, 14.1	9.8, 14.1	7.5, 14.1	4.5, 14.1
November 1972 50-year	7.3, 9.0	8.7, 9.0	5.2, 9.0	4.1, 9.0	2.6, 9.0
November 1972 20-year	7.3, 9.0	8.7, 9.0	5.2, 9.0	4.1, 9.0	2.6, 9.0
November 1972 10-year	7.3, 9.0	8.7, 9.0	5.3, 9.0	4.1, 9.0	2.5, 9.0
November 1972 5-year	7.3, 9.0	8.7, 9.0	5.2, 9.0	4.1, 9.0	2.5, 9.0
November 1972 2-year	7.3, 9.0	8.7, 9.0	5.2, 9.0	4.0, 9.0	2.5, 9.0
February 1978 100-year	12.4, 13.0	15.6, 13.0	8.8, 13.0	6.8, 13.0	3.9, 13.0
February 1978 50-year	11.2, 13.0	14.8, 13.0	8.3, 13.0	6.7, 13.0	4.9, 13.0
February 1978 20-year	11.1, 13.0	14.8, 13.0	8.3, 13.0	6.7, 13.0	5.1, 13.0
February 1978 10-year	11.2, 13.0	14.8, 13.0	8.3, 13.0	6.7, 13.0	4.8, 13.0
February 1978 5-year	11.1, 13.0	14.8, 13.0	8.4, 13.0	6.8, 13.0	5.2, 13.0
February 1978 2-year	11.1, 13.0	14.8, 13.0	8.5, 13.0	6.7, 13.0	4.9, 13.0
October 1991 ("Halloween Storm")	18.5, 20.0	21.0, 20.0	12.0, 20.0	9.5, 20.0	6.0, 20.0

* Approximate depths relative to MLW at seaward terminus of each profile are as follows: Profiles 1&3, 26 ft; Profile 2, 25 ft; Profiles 4 and 5, 28 ft; Profile 6, 30 ft; Profiles 7, 7a, and 8, 21 ft.

REPORT DOCUMENTATION PAGE

Form Approved
OMB No. 0704-0188

Public reporting burden for this collection of information is estimated to average 1 hour per response, including the time for reviewing instructions, searching existing data sources, gathering and maintaining the data needed, and completing and reviewing the collection of information. Send comments regarding this burden estimate or any other aspect of this collection of information, including suggestions for reducing this burden, to Washington Headquarters Services, Directorate for Information Operations and Reports, 1215 Jefferson Davis Highway, Suite 1204, Arlington, VA 22202-4302, and to the Office of Management and Budget, Paperwork Reduction Project (0704-0188), Washington, DC 20503.

1. AGENCY USE ONLY (Leave blank)		2. REPORT DATE January 1994		3. REPORT TYPE AND DATES COVERED Final report	
4. TITLE AND SUBTITLE Revere Beach and Point of Pines, Massachusetts, Shore Front Study				5. FUNDING NUMBERS	
6. AUTHOR(S) W. Gray Smith, Julie D. Rosati, Stephen A. Bratos, John McCormick					
7. PERFORMING ORGANIZATION NAME(S) AND ADDRESS(ES) U.S. Army Engineer Waterways Experiment Station Coastal Engineering Research Center 3909 Halls Ferry Road, Vicksburg, MS 39180-6199				8. PERFORMING ORGANIZATION REPORT NUMBER Miscellaneous Paper CERC-94-1	
9. SPONSORING/MONITORING AGENCY NAME(S) AND ADDRESS(ES) U.S. Army Engineer Division, New England 424 Trapelo Road, Waltham, MA 02254-9149				10. SPONSORING/MONITORING AGENCY REPORT NUMBER	
11. SUPPLEMENTARY NOTES Available from National Technical Information Service, 5285 Port Royal Road, Springfield, VA 22161.					
12a. DISTRIBUTION/AVAILABILITY STATEMENT Approved for public release; distribution is unlimited.				12b. DISTRIBUTION CODE	
13. ABSTRACT (Maximum 200 words) The U.S. Army Engineer Division, New England (CENED) requested assistance from the U.S. Army Engineer Waterways Experiment Station, Coastal Engineering Research Center in quantifying storm-induced coastal processes, including beach erosion and overtopping along the Revere Beach and Point of Pines (POP) coastal reach. Specifically, CERC was asked by CENED to evaluate the degree of protection provided by a coarse-grained beach fill at Revere Beach, as well as to assess the benefits and optimize the design of a revetment and/or beach fill and dune system at POP. Wave and water level conditions associated with a set of 50 storms were defined using measured water level data and hindcast wave data. The cross-shore profile response model Storm-Induced BEach CHange (SBEACH) was applied to evaluate beach profile change. A runup and overtopping module was developed during the study, and a set of physical modeling tests were conducted to further test and improve the module. Each of the 50 storms was used as input to the runup and overtopping module. The study was conducted in two parts. In Part I, CERC developed a nearshore wave and water level database using hindcast wind and wave data for 11 historical northeaster storms from which a suite of 50 synthetic storms was created. Simulations with SBEACH using this storm database indicated that the existing coarse-grained beach fill at Revere Beach might provide unexpected flood protection due to its greater erosive resistance relative to the native material. This result was substantiated (Continued)					
14. SUBJECT TERMS Beach fill Cross-shore sediment transport Numerical modeling Overtopping Physical modeling Revere Beach and Point of Pines, Massachusetts Runup Wave transformation				15. NUMBER OF PAGES 306 16. PRICE CODE	
17. SECURITY CLASSIFICATION OF REPORT UNCLASSIFIED	18. SECURITY CLASSIFICATION OF THIS PAGE UNCLASSIFIED	19. SECURITY CLASSIFICATION OF ABSTRACT	20. LIMITATION OF ABSTRACT		

13. (Concluded).

with observations of beach response and overtopping rates during the 1991 "Halloween" storm, which impacted the area from 27 October - 1 November 1991. Additionally, Part I indicated that a sand dune/berm system might provide sufficient flood protection at POP.

Part II used pre- and post-Halloween storm data to (a) validate application of SBEACH to the project site; (b) test sensitivity of SBEACH to variations in median grain size, and wave height and angle; (c) develop a runup and overtopping module, which used SBEACH output to predict overtopping volumes, and (d) predict profile response and overtopping volumes due to the nearshore wave and water level database developed in Part I. Based on interim results of Part II, a physical model study of overtopping was added to provide data with which to further refine the runup and overtopping module.

Results indicated that the existing coarse-grained beach fill at Revere Beach, and proposed coarse-grained fill at POP provide significant storm-induced flood protection benefits over the existing condition or a native-sized beach fill. Observations of stability and minimal overtopping at Revere Beach during the Halloween storm, as compared to other historical storms, substantiated these results. Dune and profile response simulations at POP indicate that a coarse-grained dune/berm or combination revetment and beach fill project would provide the required level of storm-induced erosion and flood protection.